

Sinosenecio yangii (Asteraceae), a new species from Guizhou, China

Jing-Yi Peng¹, Dai-Gui Zhang^{1,2}, Tao Deng³, Xian-Han Huang³,
Jun-Tong Chen³, Ying Meng^{1,2}, Yi Wang¹, Qiang Zhou^{1,2}

1 College of Biology and Environmental Sciences, Jishou University, Jishou 416000, Hunan, China **2** Key Laboratory of Plant Resources Conservation and Utilization, Jishou University, College of Hunan Province, Jishou, Hunan 416000, China **3** CAS Key Laboratory for Plant Diversity and Biogeography of East Asia, Kunming Institute of Botany, Chinese Academy of Sciences, Kunming 650201, Yunnan, China

Corresponding author: Qiang Zhou (zhouqiang@jsu.edu.cn)

Academic editor: Alexander Sennikov | Received 26 June 2022 | Accepted 11 September 2022 | Published 27 September 2022

Citation: Peng J-Y, Zhang D-G, Deng T, Huang X-H, Chen J-T, Meng Y, Wang Y, Zhou Q (2022) *Sinosenecio yangii* (Asteraceae), a new species from Guizhou, China. *PhytoKeys* 210: 1–13. <https://doi.org/10.3897/phytokeys.210.89480>

Abstract

A new species *Sinosenecio yangii* D.G. Zhang & Q. Zhou (Asteraceae, Senecioneae) from Guizhou Province, China, is described and illustrated based on its morphological characteristics and molecular evidence. It closely resembles *S. confervifer* and *S. guangxiensis*, the former in the scapigerous habit and smooth and glabrous achene surface, the latter in the calyculate involucre and purple abaxial leaf surface, and both in the shape and indumentum of leaf lamina, but differs markedly from the latter two in having fewer capitula and epappose achenes. Phylogenetic analysis based on nrITS and *ndhC-trnV* sequences shows that this new species belongs to the *S. latouchei* clade and is sister to *S. guangxiensis* with moderate support.

Keywords

molecular evidence, morphology, pappus

Introduction

Sinosenecio B. Nordenstam (1978) (Senecioneae, Asteraceae) contains 45 species mainly distributed in central and southwestern parts of China (Chen et al. 2011; Liu and Yang 2012; Liu et al. 2019; Zou et al. 2020; Chen et al. 2022). This genus is

characterized by subscapiform or leafy stems, palmately or rarely pinnately veined leaf lamina, solitary to numerous capitula, and ecalyculate or sometimes calyculate involucre, etc. (Jeffrey and Chen 1984). *Sinosenecio* encompasses two species assemblages, i.e. the *Sinosenecio s.s.* group and the *S. oldhamianus* group, with different chromosome number ($x = 30$ vs. 24 or 13), patterns of endothelial cell wall thickenings (strictly polarized vs. polarized and radial), and phylogenetic affiliation (subtrib. Tussilaginatae s.s. vs. subtrib. Tephrosoidinae) (Liu 2010; Liu and Yang 2011a, b; Gong et al. 2016). These two groups also differ in geographical distribution. The former is restricted to mountainous regions around Sichuan Basin, southwestern China, and the latter is widely distributed in central and southern China, with two species extending to Indochina (Gong et al. 2016). However, a formal taxonomic adjustment is not yet proposed as phylogenetic relationships in subtrib. Tephrosoidinae need to be further clarified (Nordenstam and Pelsner 2011).

Libo County (Guizhou Province, China) belongs to the slope zone of transition from Guizhou Plateau to Guangxi Hilly Basin with typical karst topography and complex and diverse ecological environment (Tan 2010). In the past few years, some new species have been reported in this area, such as *Strobilanthes hongii* (Chen et al. 2019) and *Petrocodon luteoflorus* (Fan et al. 2020). During our field investigation at Lihua Town, Libo County in March 2021, we found several unusual *Sinosenecio* populations that morphologically resemble two members of the *S. oldhamianus* group, namely *S. confervifer* (H. Léveillé) Y. Liu & Q. E. Yang and *S. guangxiensis* C. Jeffrey & Y. L. Chen, but differs markedly from them in several morphological features, respectively. After examining herbarium specimens and relevant literature, we verified that it represents an undescribed species. Here, we described it as *S. yangii* D. G. Zhang & Q. Zhou with report on its chromosome number and phylogenetic position.

Materials and methods

Morphological observation

Morphological examination and comparison of the new species with *S. confervifer* and *S. guangxiensis* were based on fresh materials and herbarium specimens. Chromosome observation was conducted according to Meng et al. (2010).

Molecular analyses

To test the phylogenetic affiliation of *S. yangii*, we carried out phylogenetic analysis based on combined matrix of ITS and *ndhC-trnV* sequences. The matrix contained 23 accessions from 20 species, including the new species, 16 species of *S. oldhamianus* group, two of *Nemosenecio*, and an outgroup *Tephrosia flammea* (Turcz. ex DC.) Holub. The ITS and *ndhC-trnV* of *S. yangii* were sequenced in this study and the

Table 1. Primers used in this study.

Region	Name	Primer sequence (5'–3')
<i>nrITS</i>	ITS1	AGAAGTCGTAACAAGGTTCCGTAGG
	ITS4	TCCTCCGCTTATTGATATGC
<i>ndhC-trnV</i>	ndhCretF	AAGTTTCTCCGGTCCCTTGC
	trnVretR	TCTACGGTTCCAGTCCGTATAG

rest were downloaded from GenBank. The GenBank accession numbers are listed in Appendix 1. Total DNA was extracted from dried leaves using Plant Genomic DNA Kit DP305 (Beijing, China) and used as the template for polymerase chain reaction (PCR). The primers used in this study are listed in Table 1. Sequences obtained were edited using Sequencher-5.4.5 and then combined by Sequence Matrix-1.9 (Vaidya et al. 2011). Multi-sequence alignment and manual adjustment were conducted using programme CLUSTAL_W in Mega-X64 (Rédei 2008) and gaps were treated as missing data.

Phylogenetic trees were constructed using Bayesian Inference (BI) and Maximum Likelihood (ML) in CIPRES Portal (<https://www.phylo.org/portal2>). BI and ML analyses were performed using MrBayes version-3.2 (Ronquist et al. 2012) and RAxML-8.2.10 (Stamatakis 2014), respectively. For BI analysis, GTR+G was selected as best-fitting model using Akaike information criterion (AIC) in JmodelTest 2-2.1.6 (Posada 2008). The Markov chain Monte Carlo analyses were run with four simultaneous chains of 10,000,000 generations sampling one tree every 1,000 generations. After the first 25% of trees were discarded as burn-in, the remaining trees were used to construct a majority-rule consensus tree with Bayesian posterior probabilities. ML analysis was performed with GTRCAT model, support values was calculated with 1,000 bootstrap replicates using a fast bootstrapping algorithm (Stamatakis et al. 2008).

Results

Morphology and taxonomy

Morphological observation (Fig. 1) showed that *S. yangii*, *S. confervifer*, and *S. guangxiensis* share obvious resemblance in the leaf blade shallowly undulate and suborbicular, adaxially densely to sparsely villous and abaxially sparsely pubescent or nearly glabrous (Table 2). In addition, *S. yangii* is similar to *S. confervifer* in the stem leafless or with 1–2 bract-like leaf and smooth achene surface, and to *S. guangxiensis* in the calyculate involucre. Nevertheless, *S. yangii* differs from both species in having fewer capitula (usually 1–3) and epappose achenes. The metaphase chromosomes of this species were counted to be $2n = 48$ (Fig. 2A). The achene surface was glabrous and smooth (Fig. 2B) and the anther endothelial cell wall thickenings were polarized and radial (Fig. 2C).

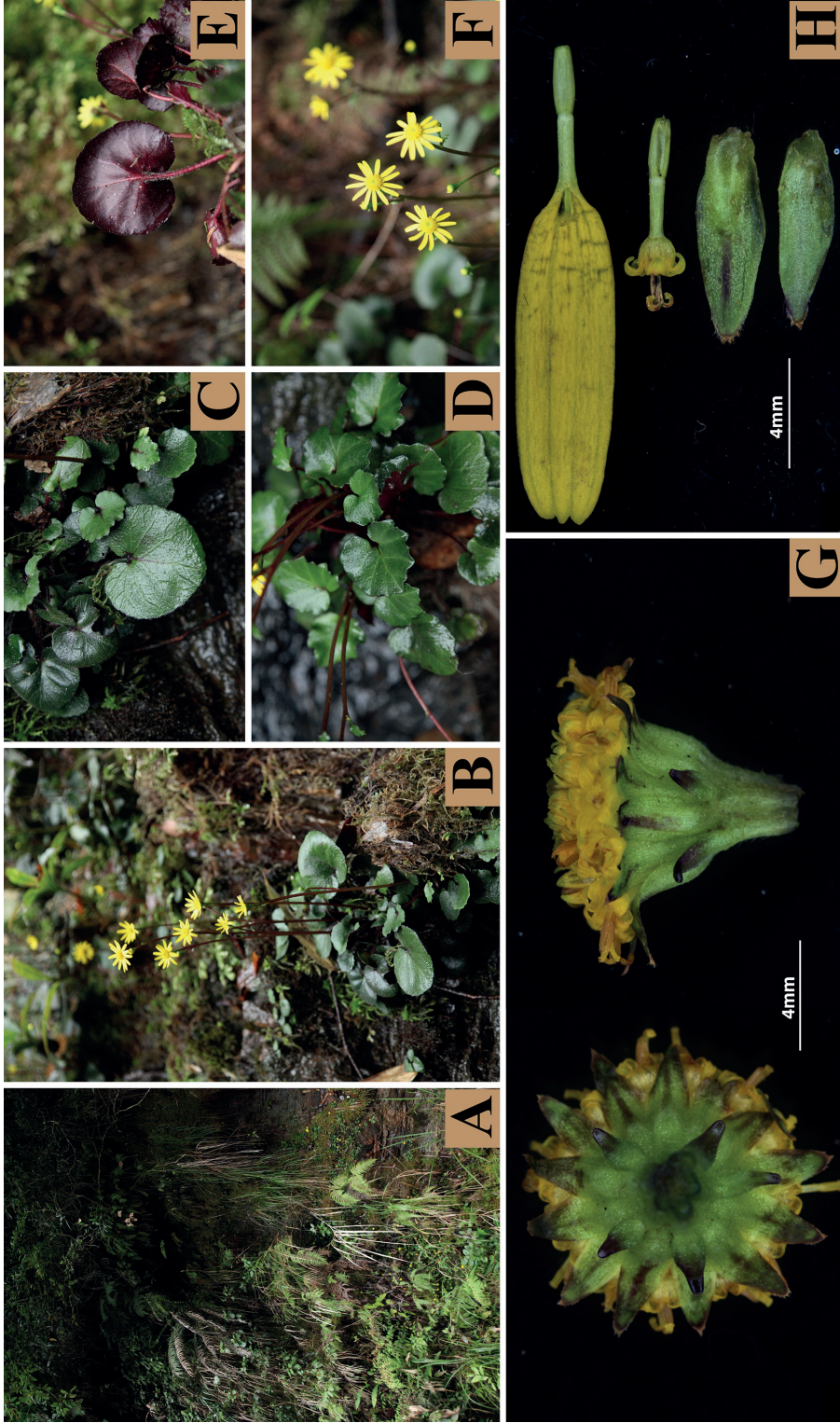
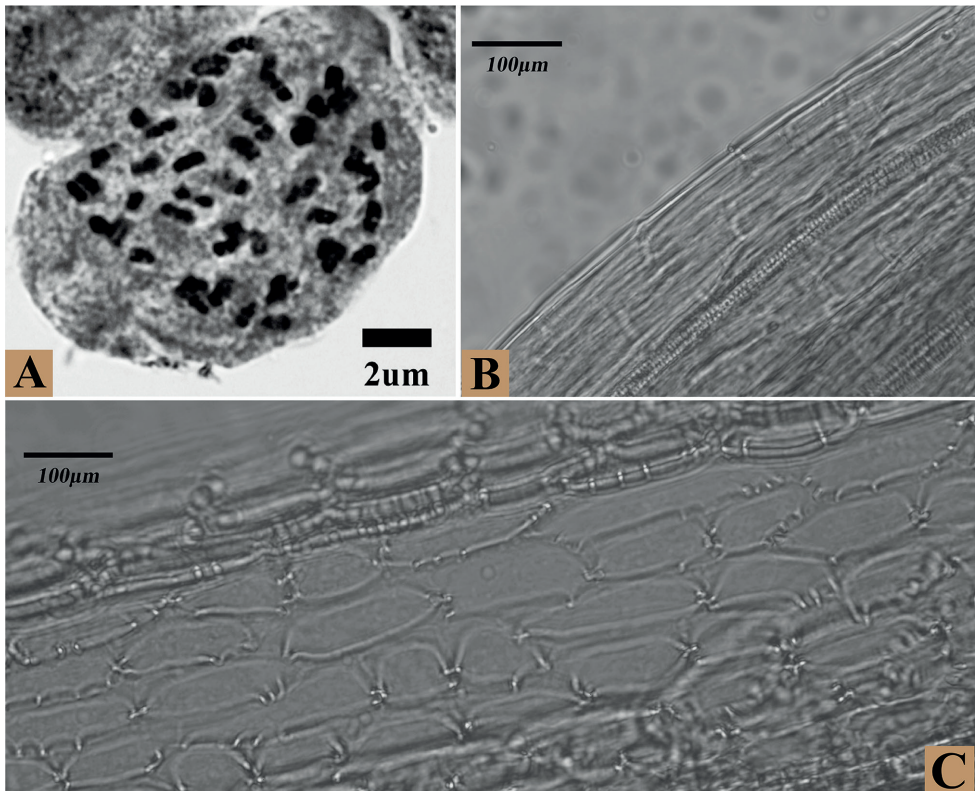


Figure 1. *Sinosenecio yangii* **A** habitat **B** habit **C–E** leaves **F** capitulum **G** bottom and side of involucre **H** ray floret, disc floret and phyllary (from top to bottom).

Table 2. Comparison of morphological characteristics among *Sinosenecio yangii*, *S. guangxiensis* and *S. confervifer*.

	<i>S. yangii</i>	<i>S. guangxiensis</i>	<i>S. confervifer</i>
Height (cm)	15–25	10–30	10–65
Leaf shape	Suborbicular or reniform, margin irregularly deltoid or rounded dentate, shallowly undulate or nearly entire	Suborbicular or reniform, margin coarsely repand or dentate with ovate-deltoid teeth	Orbicular or suborbicular, margin repand or lobed, with rounded or broadly deltoid mucronulate or obscurely mucronulate shallow teeth or lobes
Leaf size (cm)	2.5–4.5 × 2.5–6.5	2–6 × 2.5–7	1.5–6 × 2–6
Adaxial surface of leaf lamina	Green, densely or sparsely pubescent	Green or dark green, sparsely to densely villous or glabrous	Lustrous, green or deep green, densely or sparsely villous or glabrous
Abaxial surface of leaf lamina	Pale green or purplish red, sparsely arachnoid or nearly glabrous	Deep purplish red, densely white tomentose, sparsely villous or glabrescent	Pale green or slightly purple with sparsely arachnoid, veins villous or pubescent
Cauline leaves	1–2, bract-like	1–5, similar to radical ones	1–2, bract-like
Petiole base of cauline leaves	Expanded, not auriculate	Slightly expanded, not auriculate	Expanded, not auriculate
Number of capitula	Usually 1, sometimes 2 or 3	2–7 or more, rarely 1	1–7 (–10) or more
Involucre	Calyculate	Calyculate	Not calyculate
Phyllaries	13	13	13
Chromosome number 2x	48	48	48
Achene surface	Smooth, glabrous	Papillate, pubescent	Smooth, glabrous
Pappus	Absent	Present	Present
Geographical distribution	Guizhou	Guangxi, southwestern Hunan	Hunan, Sichuan, Chongqing, Guizhou, Yunnan

**Figure 2.** *Sinosenecio yangii* **A** metaphase chromosomes ($2x = 48$) **B** smooth and glabrous achene surface **C** polarized and radial endothelial cell wall thickenings.

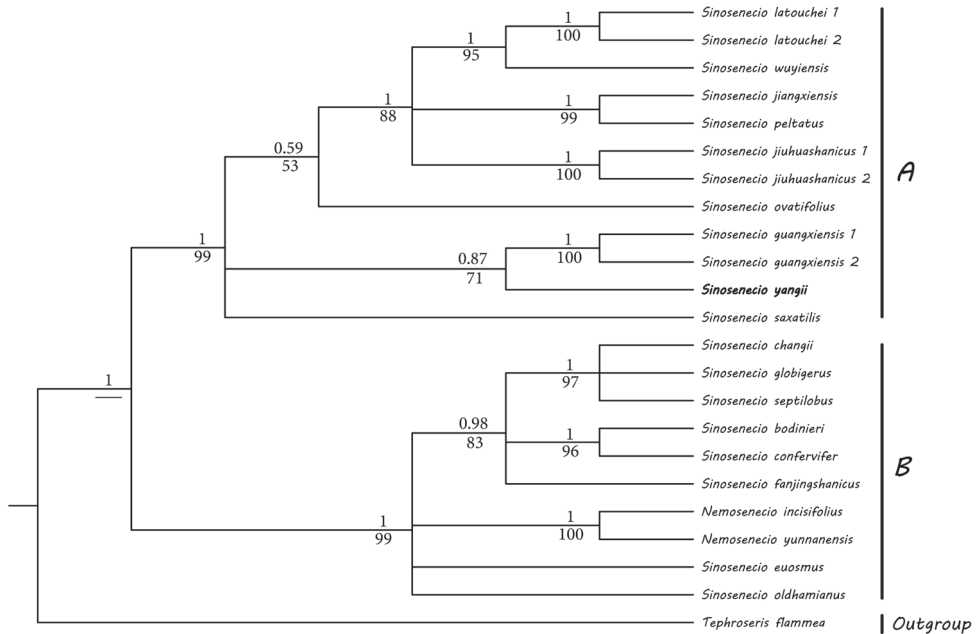


Figure 3. Bayesian phylogenetic tree based on the combined data of ITS and *ndhC-trnV* sequences. Numbers above and below branches are Bayesian posterior probabilities and ML bootstrap values, respectively. A and B represent the *S. latouchei* clade and *S. oldhamianus*-*Nemosenecio* clade. *Sinosenecio yangii* is noted in bold.

Phylogenetic analyses

The combined matrix of ITS and *ndhC-trnV* sequences contained 1,324 aligned bp. Bayesian (BI) and Maximum likelihood (ML) trees had similar topologies. The BI tree was presented in Fig. 3 with BI posterior probability (BP) and ML bootstrap support values (LP) labelled on the branches. Ingroups were resolved into two clades, viz. the *S. latouchei* clade (BP = 1, LP = 99) and the *S. oldhamianus*-*Nemosenecio* clade (BP = 1, LP = 99). *Sinosenecio yangii* was resolved as sister to *S. guangxiensis* (BP = 0.87, LP = 71) in the former clade, while *S. confervifer* was recovered as a member in the latter clade.

Discussion

Several lines of evidence demonstrated that *S. yangii* is a member of the *S. oldhamianus* group. *Sinosenecio yangii* has a base chromosome number of $x = 24$ (Fig. 2A) and polarized and radial anther endothelial cell wall thickenings (Fig. 2C), which are typical of the *S. oldhamianus* group. Analyses of ITS and *ndhC-trnV* sequences also corroborated its phylogenetic affiliation, resolving it as sister to *S. guangxiensis* in the *S. latouchei* clade of *S. oldhamianus* group.

Sinosenecio yangii was morphologically and phylogenetically close to *S. guangxiensis* in the *S. latouchei* clade. However, there are differences in morphology, distribution and ecology between the two species. *S. yangii* is easily distinguished from *S. guangxiensis* in the stem leafless or with 1–2 bract-like leaf (vs. 1–5 cauline leaves), fewer capitula (vs. 2–7 or more), smooth and glabrous achene surface (vs. papillate and pubescent), and epappose achenes (vs. present pappus). From the perspective of distribution area, the former is restricted to Libo County in Guizhou, appearing on the wet rock cliff, and the geographical location is adjacent to the border with Guangxi province. The latter is distributed in the Guangxi and southwestern Hunan, growing on the damp, shady places or rocky places at mountain summits. To some extent, the close relationship between these two species may also be related to their distributional ranges adjacent to each other. Additionally, it is worth noting that the epappose achenes of *S. yangii* is a character previously never recorded in the *S. latouchei* clade.

Taxonomic treatment

Sinosenecio yangii D. G. Zhang & Q. Zhou, sp. nov.

urn:lsid:ipni.org:names:77305747-1

Figs 4, 5

Type. CHINA. Guizhou: Libo County, Lihua Town, 25°36'53"N, 108°12'63"E, on rock cliff by the side of a rural road, elev. 347 m, 16 March 2021, D. G. Zhang & T. Deng 14231. (holotype: JIU!; isotype: JIU!).

Description. Scapigerous herbs. Rhizomes short and stout with many fibrous roots. Stems slender, scapiform, erect or declining, solitary or several, 13–22 cm long, basally reddish-brown and sparsely white villous, almost smooth in upper part. Radical leaves several; petiole ca. 3–6.5 cm long, densely villous or glabrescent, basally expanded, not auriculate; lamina suborbicular or reniform, ca. 2.5–4.5 × 2.5–6.5 cm, base cordate, margin irregularly triangular dentate, shallowly undulate or entire, apex slightly acute; adaxially green, densely or sparsely pubescent, abaxially pale green or purplish red, sparsely arachnoid or nearly glabrous. Upper leaves 1 or 2, bract-like, shortly petiolate, lanceolate. Capitula usually 1–3, peduncles slender, ca. 2–3.5 cm long, with a basal linear bracteole, or with 1–2 small linear bracteoles in the upper part. Involucres campanulate, calyculate with 2–3 bracteoles or more; phyllaries ca. 13, lanceolate, ca. 6 mm long, with ciliate margin, apically acute or obtuse and sometimes purplish. Ray florets ca. 13, corolla tube 3 mm long, glabrous; ray yellow, oblong, ca. 12 mm long, 4-veined, apically 3-denticulate. Disc florets numerous; corolla yellow, 4 mm, with ca. 1.5 mm glabrous tube and 0.85 mm limb. Anthers oblong, 5, ca. 1.2 mm long, basally obtuse. Style branches ca. 0.5 mm long, puberulent. Achenes ca. 1 mm long, smooth and glabrous. Pappus absent.

Phenology. Flowering from March to May, fruiting from April to June.



Figure 4. Holotype sheet of *Sinosenecio yangii* D. G. Zhang & Q. Zhou.

Etymology. The species was named after Professor Qin-er Yang, an expert in the field of *Asteraceae* at the Chinese Academy of Sciences. The Chinese name is given as “亲二蒲儿根” (qīn èr pú ér gēn).

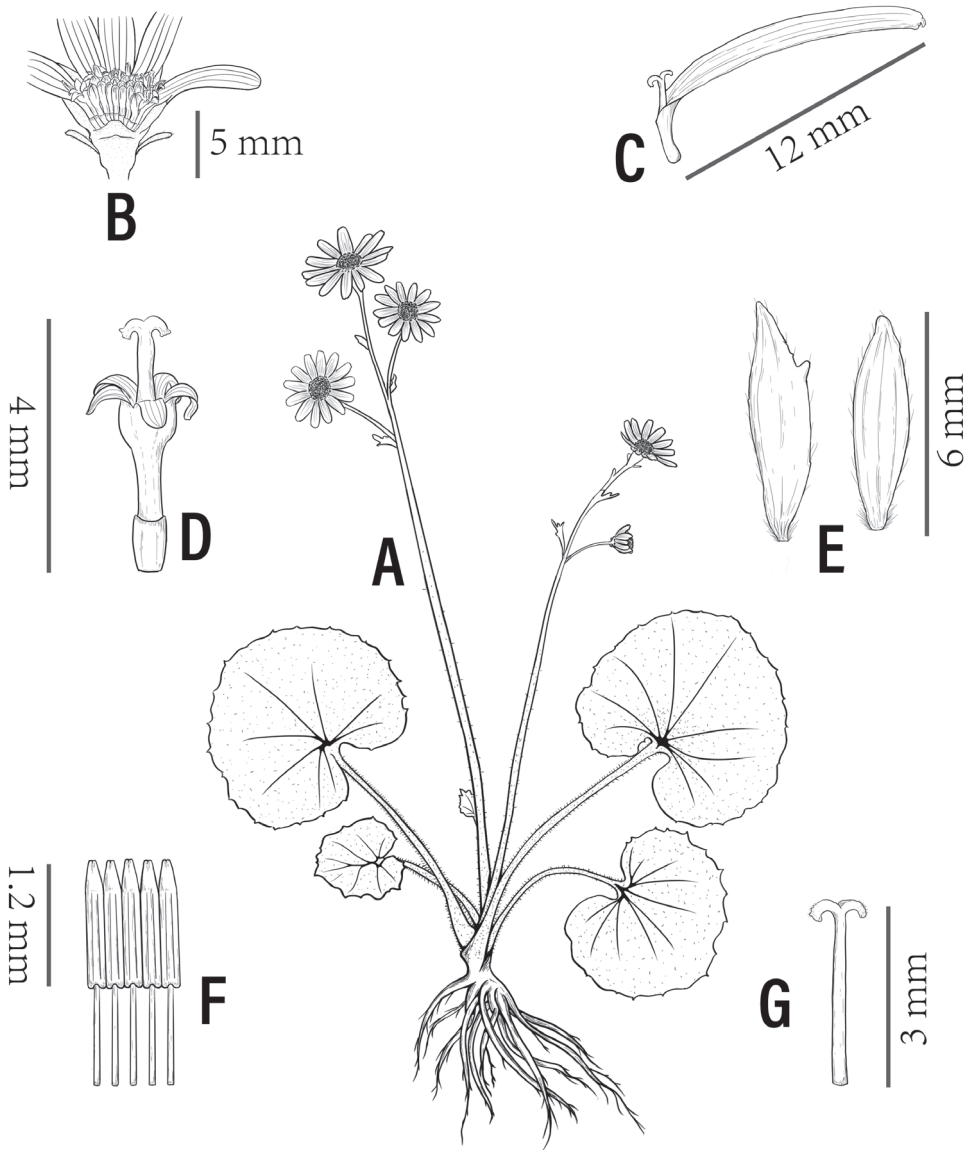


Figure 5. *Sinosenecio yangii* **A** habit **B** capitulum **C** ray floret **D** disk floret **E** phyllary **F** stamens **G** style (drawing by Chu-miao Xie).

Distribution and habitat. *Sinosenecio yangii* is known from Lihua Town, Libo County, Guizhou Province, China (Fig. 6). It was collected from a rock cliff by the side of a rural road in this town, at an altitude of 347 m.

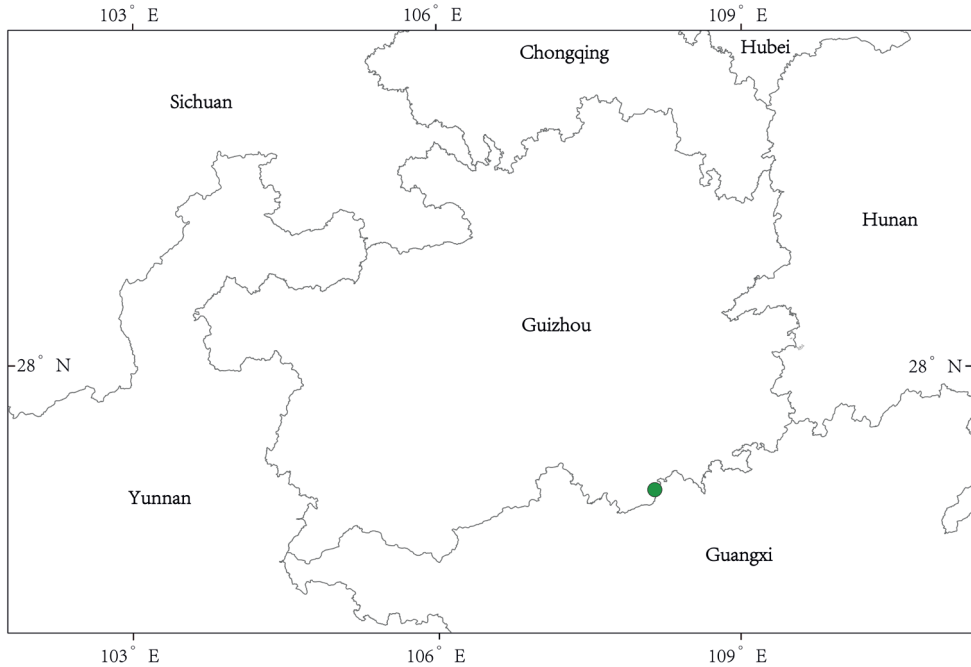


Figure 6. Distribution of *Sinosenecio yangii*.

Key to species of the *S. latouchei* clade

- 1 Pappus absent *S. yangii*
- Pappus present..... 2
- 2 Leaf lamina peltate..... *S. peltatus*
- Leaf lamina not peltate 3
- 3 Involucres calyculate 4
- Involucres ecalyculate..... 5
- 4 Cauline leaf absent or 1 and bract-like; base of petiole of cauline leaf slightly auriculate; capitula solitary, rarely 2 or 3 *S. jiangxiensis*
- Cauline leaves 1–5, similar to radical ones; base of petiole of cauline leaves never auriculate; capitula 1–5 or more *S. guangxiensis*
- 5 Ovaries and achenes glabrous..... 6
- Ovaries and achenes pubescent. 7
- 6 Leaf lamina broadly flabellate or suborbicular, dentate or palmately lobed to 1/2, lobes apically 2 or 3-denticulate, both surfaces glabrous *S. wuyiensis*
- Leaf lamina reniform or suborbicular, regularly 5–7-palmatilobed, lobes ovate-triangular, both surfaces glabrous or sometimes white tomentose abaxially and later glabrescent *S. saxatilis*
- Leaf lamina ovate, broadly ovate, rarely ovate-orbicular, inconspicuously undulate-dentate, adaxial surface villous, sometimes sparsely arachnoid, and abaxial surface villous and densely white arachnoid..... *S. ovatifolius*

- 7 Stem erect or flexuous; cauline leaves 1–3; leaf lamina adaxially villous with spreading hairs; leaf auricles 4–10 mm in diameter *S. latouchei*
- Stem erect; cauline leaves 3–7; leaf lamina adaxially pubescent with appressed hairs or sparsely or densely white tomentose; leaf auricles 7–30 mm in diameter *S. jiuwuashanicus*

Acknowledgements

We thank Chu-miao Xie and Xin-yuan Kuai for preparing the line drawing and illustration. We are very grateful to Wen-guang Sun (Yunnan Normal University) for his help in the experimental part of the manuscript. This work was supported by the Ecological Adaptability of Four Narrow Endemic *Sinosenecio* Species in Wuling Mountain Region (31860117), National Natural Science Foundation of China.

References

- Chen YL, Liu Y, Yang QE, Nordenstam B, Jeffrey C (2011) *Sinosenecio* B. Nord. In: Wu ZY, Raven PH (Eds) Flora of China (vol. 20–21). Science Press and Missouri Botanical Garden Press, 464–48.
- Chen FL, Deng YF, Xiong ZB, Ran JC (2019) *Strobilanthes hongii*, a new species of Acanthaceae from Guizhou, China. *Phytotaxa* 388(1): 135–144. <https://doi.org/10.11646/phytotaxa.388.1.7>
- Chen B, Liu Y, Luo JX, Wang Q, Yang QE (2022) *Sinosenecio jiuwuashanicus* (Asteraceae, Senecioneae), a new species from Sichuan, China. *Phytotaxa* 544(3): 289–294. <https://doi.org/10.11646/phytotaxa.544.3.3>
- Fan ZW, Cai L, Yang JW, Tang SH, Wen F (2020) *Petrocodon luteoflorus* (Gesneriaceae), a new species from karst region in Guizhou, China. *PhytoKeys* 157: 167–173. <https://doi.org/10.3897/phytokeys.157.32316>
- Gong W, Liu Y, Chen J, Hong Y, Kong HH (2016) DNA barcodes identify Chinese medicinal plants and detect geographical patterns of *Sinosenecio* (Asteraceae). *Journal of Systematics and Evolution* 54(1): 83–91. <https://doi.org/10.1111/jse.12166>
- Jeffrey C, Chen YL (1984) Taxonomic studies on the tribe Senecioneae (Compositae) of Eastern Asia. *Kew Bulletin* 39(2): 205–446. <https://doi.org/10.2307/4110124>
- Liu Y (2010) A systematic study of the genus *Sinosenecio* B. Nord. (Compositae). PhD Thesis, Institute of Botany, Chinese Academy of Sciences, Beijing.
- Liu Y, Yang QE (2011a) Floral micromorphology and its systematic implications in the genus *Sinosenecio* (Senecioneae-Asteraceae). *Plant Systematics and Evolution* 291(3–4): 243–256. <https://doi.org/10.1007/s00606-010-0385-z>
- Liu Y, Yang QE (2011b) *Hainanecio*, a new genus of the Senecioneae, Asteraceae from China. *Botanical Studies (Taipei, Taiwan)* 52: 115–120.
- Liu Y, Yang QE (2012) *Sinosenecio jiangxiensis* (Asteraceae), a new species from Jiangxi, China. *Botanical Studies (Taipei, Taiwan)* 53: 401–414.

- Liu Y, Xu Y, Yang QE (2019) *Sinosenecio peltatus* (Asteraceae, Senecioneae), a remarkably distinctive new species from Guangdong, China. *Phytotaxa* 406(3): 206–212. <https://doi.org/10.11646/phytotaxa.406.3.7>
- Meng Y, Sun H, Yang YP, Nie ZL (2010) Polyploidy and new chromosome counts in *Anaphalis* (Asteraceae: Gnaphalieae) from the Qinghai-Tibet Plateau of China. *Journal of Systematics and Evolution* 48(1): 58–64. <https://doi.org/10.1111/j.1759-6831.2009.00061.x>
- Nordenstam B (1978) Taxonomic studies on the tribe Senecioneae (Compositae). *Opera Botanica* 44: 1–84.
- Nordenstam B, Pelsner PB (2011) Notes on the generic limits of *Sinosenecio* and *Tephrosieris* (Compositae-Senecioneae). *Compositae Newsletter* 49: 1–7.
- Posada D (2008) jModelTest: Phylogenetic Model Averaging. *Molecular Biology and Evolution* 25(7): 1253–1256. <https://doi.org/10.1093/molbev/msn083>
- Rédei GP (2008) CLUSTAL W (improving the sensitivity of progressive multiple sequence alignment through sequence weighting, position-specific gap penalties and weight matrix choice). Springer Netherlands, 4673–4680. https://doi.org/10.1007/978-1-4020-6754-9_3188
- Ronquist F, Teslenko M, van der Mark P, Ayres DL, Darling A, Höhna S, Huelsenbeck JP (2012) MrBayes 3.2: Efficient Bayesian phylogenetic inference and model choice across a large model space. *Systematic Biology* 61(3): 539–542. <https://doi.org/10.1093/sysbio/sys029>
- Stamatakis A (2014) RAxML version 8: A tool for phylogenetic analysis and post-analysis of large phylogenies. *Bioinformatics* 30(9): 1312–1313. <https://doi.org/10.1093/bioinformatics/btu033>
- Stamatakis A, Hoover P, Rougemont J (2008) A rapid bootstrap algorithm for the RAxML web servers. *Systematic Biology* 57(5): 758–771. <https://doi.org/10.1080/10635150802429642>
- Tan CJ (2010) Protection and Sustainable Development of Forest Eco-environment in Libo County of Guizhou Province. *Anhui Nongye Kexue* 38(34): 19468–19470.
- Vaidya G, Lohman DJ, Meier R (2011) Sequence Matrix: Concatenation software for the fast assembly of multi-gene datasets with character set and codon information. *Cladistics* 27(2): 171–180. <https://doi.org/10.1111/j.1096-0031.2010.00329.x>
- Zou CY, Liu Y, Liu Y (2020) *Sinosenecio ovatifolius* (Asteraceae), a new species from Guangxi, China. *Phytotaxa* 460: 149–159. <https://doi.org/10.11646/phytotaxa.460.2.5>

Appendix I

Table AI. GenBank accessions of species used in this study.

Species	GenBank accession number of ITS / <i>ndhC-trnV</i>
<i>Tephrosia flammea</i>	KU696137 / KU750769
<i>Nemosenecio yunnanensis</i>	KU696047 / KU750695
<i>Nemosenecio incisifolius</i>	KU696045 / KU750694
<i>Sinosenecio latouchei</i>	JQ797428 / KU750748
<i>Sinosenecio latouchei</i>	JQ797429 / KU750749
<i>Sinosenecio wuyiensis</i>	JQ797431 / KU750764
<i>Sinosenecio jiangxiensis</i>	KT149879 / KU750743
<i>Sinosenecio peltatus</i>	MK818500 / –
<i>Sinosenecio jiuhuashanicus</i>	JQ797426 / KU750746
<i>Sinosenecio jiuhuashanicus</i>	JQ797425 / KU750745
<i>Sinosenecio ovatifolius</i>	MT522620 / –
<i>Sinosenecio guangxiensis</i>	JQ797432 / KU750738
<i>Sinosenecio guangxiensis</i>	JF978599 / KU750739
<i>Sinosenecio yangii</i>	OM413747 / OM371331
<i>Sinosenecio saxatilis</i>	JQ797430 / KU750757
<i>Sinosenecio changii</i>	AY176164 / KU750721
<i>Sinosenecio globigerus</i>	AY176159 / KU750736
<i>Sinosenecio septilobus</i>	AY176161 / KU750758
<i>Sinosenecio bodinieri</i>	KT149888 / KU750720
<i>Sinosenecio confervifer</i>	KT149891 / KU750723
<i>Sinosenecio fanjingshanicus</i>	KT149886 / KU750732
<i>Sinosenecio euosmus</i>	JF978589 / KU750730
<i>Sinosenecio oldhamianus</i>	JF978616 / KU750753

Monopyle glutinosa (Gesneriaceae), a new species from the western slopes of the Ecuadorian Andes

John L. Clark^{1,2}, Franciso Tobar^{3,4}, Jeremy Keene⁵

1 Science Department, The Lawrenceville School, Lawrenceville, NJ 08648, USA **2** Marie Selby Botanical Gardens, 811 South Palm Avenue, Sarasota, FL 34236, USA **3** Área de Investigación y Monitoreo de Avifauna, Aves y Conservación – BirdLife International, Quito, Ecuador **4** Instituto Nacional de Biodiversidad, Herbario Nacional del Ecuador, Quito, Ecuador **5** Science and Mathematics Department, Glenville State University, Glenville, WV 26351, USA

Corresponding author: John L. Clark (jclark@lawrenceville.org)

Academic editor: Michael Moeller | Received 26 June 2022 | Accepted 9 September 2022 | Published 28 September 2022

Citation: Clark JL, Tobar F, Keene J (2022) *Monopyle glutinosa* (Gesneriaceae), a new species from the western slopes of the Ecuadorian Andes. *PhytoKeys* 210: 15–21. <https://doi.org/10.3897/phytokeys.210.89520>

Abstract

Exploratory field expeditions to the western slopes of the Ecuadorian Andes resulted in the discovery of a new species of *Monopyle* (Gesneriaceae). *Monopyle glutinosa* J.L.Clark & Keene, **sp. nov.** is described as a narrow endemic from lowland forests along the border of the Reserva Ecológica Los Illinizas in the Province of Cotopaxi. The new species is unique for the presence of glutinous or sticky trichomes on the calyx lobes and outer surface of the inferior ovary. Based on IUCN guidelines, a preliminary conservation status is assigned as Critically Endangered (CR).

Resumen

Las expediciones a los bosques de las laderas noroccidentales de los Andes de Ecuador dieron como resultado el descubrimiento de una nueva especie: *Monopyle glutinosa* J.L.Clark & Keene, **sp. nov.**, la cual es endémica de una reducida área en el borde de la Reserva Ecológica Los Illinizas en la provincia de Cotopaxi. La nueva especie es única por la presencia de tricomas glutinosos o pegajosos en los lóbulos del cáliz y la superficie externa del ovario infero. Basados en los criterios de la UICN, se asigna un estado de conservación preliminar de En Peligro Crítico (CR).

Keywords

Ecuador, Gesneriaceae, *Monopyle*, taxonomy

Introduction

The flowering plant family Gesneriaceae is in the order Lamiales and comprises 3400+ species in 150+ genera (Weber 2004; Weber et al. 2013). The family is divided into three strongly-supported monophyletic subfamilies (Ogutcen et al. 2021) and seven tribes (Weber et al. 2013, 2020). The majority of New World members are in the subfamily Gesnerioideae and are represented by 1200+ species and 77 genera (Clark et al. 2020). *Monopyle* Moritz ex Benth. & Hook.f. is classified in the tribe Gesnerieae and subtribe Gloxiniinae (Weber et al. 2013, 2020).

Monopyle is a genus of terrestrial understory or epiphytic herbs distributed from Guatemala to northern South America. There are 11 described species of *Monopyle* in Ecuador (Keene 2013). The genus currently comprises 22 recognized species (Clark et al. 2020). The addition of *Monopyle glutinosa* brings the total species diversity to 23. The actual number of species is probably double what is currently recognized, based on preliminary estimates from ongoing monographic work by Keene (2013). Additionally, recent exploratory expeditions have yielded numerous new or undescribed species poorly represented in herbaria. Here, we describe a new species that was collected in 2022 during a research expedition to the western Andean foothills.

Monopyle is morphologically complex and has had little attention since Morton's monographic revision (Morton 1945). The genus is traditionally characterized by strongly anisophyllous opposite leaves, campanulate corollas, and the presence of uncinately trichomes (Keene 2013). Additional diagnostic characters that define *Monopyle* include variably swollen internodes, a nodal ridge, and the presence of an osmophore (floral fragrance gland) at the base of the corolla. Many *Monopyle* species are presumably local endemics and appear to be restricted to a specific watershed. Narrow distributions are likely the result of the minute seeds limited by a splash-cup seed dispersal mechanism.

Materials and methods

Plants were vouchered and photographed during a 2022 field expedition to Ecuador (Clark 2022). Specimens were deposited at the Pontificia Universidad Católica del Ecuador (**QCA**), Marie Selby Botanical Gardens (**SEL**), United States National Herbarium (**US**), New York Botanical Garden (**NY**), and Missouri Botanical Garden (**MO**). Digital images were taken of live specimens in the field using a Nikon D100 DSLR with a Nikon 105 mm lens and a Nikon SB-29s ring flash. Morphological observations and measurements were made from live collections, alcohol-preserved material, and digital images using the program ImageJ (<https://imagej.nih.gov/ij/>).

We assessed the extinction risk of *Monopyle glutinosa* following the IUCN Red List Categories and Criteria (2022) and guidelines of the IUCN Standards and Petitions Committee (2022). We considered observations, collection localities and population estimates from fieldwork. Species extent of occurrence (**EOO**) and area of occupancy (**AOO**) were calculated using *GeoCAT* (Bachman et al. 2011; <http://geocat.kew.org/>) with the default setting of 2 km² grid.

Taxonomic treatment

Monopyle glutinosa J.L.Clark & Keene, sp. nov.

urn:lsid:ipni.org:names:77305891-1

Fig. 1

Type. ECUADOR. Cotopaxi: cantón Pujuli, western lowland border of Reserva Ecológica Los Illinizas, trail towards finca of Narcisssa Castellano, trailhead accessed via road Guayacán-Pucayacu, 0°48'44"S, 79°5'37.5"W, 1014 m alt., 11 Mar 2022, *J.L. Clark, C. Restrepo & F. Tobar 16489* (holotype: US; isotypes: MO, NY, QCA, SEL).

Diagnosis. Similar to *Monopyle ecuadorensis*, differing in larger calyx lobes that reach 1.5 cm in length (*vs.* 0.5–1.0 cm long in *M. ecuadorensis*), larger campanulate corolla tube that exceeds 3.0 cm in length (*vs.* corolla tube less than 3 cm in *M. ecuadorensis*), and a uniformly dark purple corolla tube (*vs.* broad range of corolla tube colors from uniformly white to white suffused with blue in *M. ecuadorensis*).

Description. Terrestrial herb; roots fibrous, shoots dorsiventral, usually light green, occasionally green suffused with red, 20–60 cm tall, 2.5–5 mm diam., glabrous. Leaves opposite, strongly anisophyllous, interstipular scar present; the larger leaf of pair with petioles (4–) 7–17 mm long, uniformly green or green suffused with red, glabrous, blade asymmetrical ovate to elliptic, base oblique, to 10 mm between bases, apex acuminate, (5–) 8.5–23.3 × 3.0–5.8 (–8) cm, subentire to serrate, adaxially light green, sparsely pilose, abaxially green, puberulent to pilose with uncinata trichomes (more so on veins); the smaller leaf of a pair with petioles to 5 mm (some appearing sessile), glabrous, blade ovate to orbicular, base oblique (appearing equilateral), apex acuminate to cuspidate, 0.9–2.4 × 0.5–1.2 cm, entire to serrate towards the apex, adaxially and abaxially similar to larger leaf. Inflorescence a terminal, erect, compound cyme (appearing paniculate); peduncle 5–10 cm, glabrous, bracts in pairs 3–5 × 0.5–1 mm, persistent, opposite, adaxially and abaxially glabrous; rachis to 10 cm long, 3–10 nodes, with 2 cymules per node; pedicel 6–9 mm long. Calyx uniformly light green to uniformly wine red, lobes five, broadly ovate at base and acuminate at apex, 11–14 × 3–5 mm, connate at base, outer surface with dense sticky trichomes, inner surface nearly glabrous. Corolla campanulate, uniformly dark purple, base sometimes white suffused with purple, 30–45 × 15–20 mm, sparsely pilose, minute gland-tipped trichomes on the inner dorsal surface of the tube (inserted above androecium), osmophore present; corolla lobes with minute glandular trichomes along margin of the lobes, lateral and dorsal lobes 7–9 × 4–6 mm, ventral lobe 9–11 × 6–7 mm. Androecium with four stamens, 4–5 mm long, didynamous, included, filaments 3–5 mm long, adnate to corolla, anthers 0.8–1.1 × 0.5–0.7 mm, connivent for up to 1 mm; nectary absent. Gynoecium with inferior ovary, to 2 mm wide, densely pilose with glandular trichomes that extend to the calyx lobes, style to 5.6 mm long, glabrous, stigma stomatomorphic. Fruits not observed.

Phenology. Flowering in March. Fruits not observed.

Etymology. The trichomes on the calyx lobes and inferior ovary allow the flower to cling to an upside-down finger (Fig. 1C). This specific epithet reflects the sticky trichomes on the outer surface of the inferior ovary and calyx lobes.

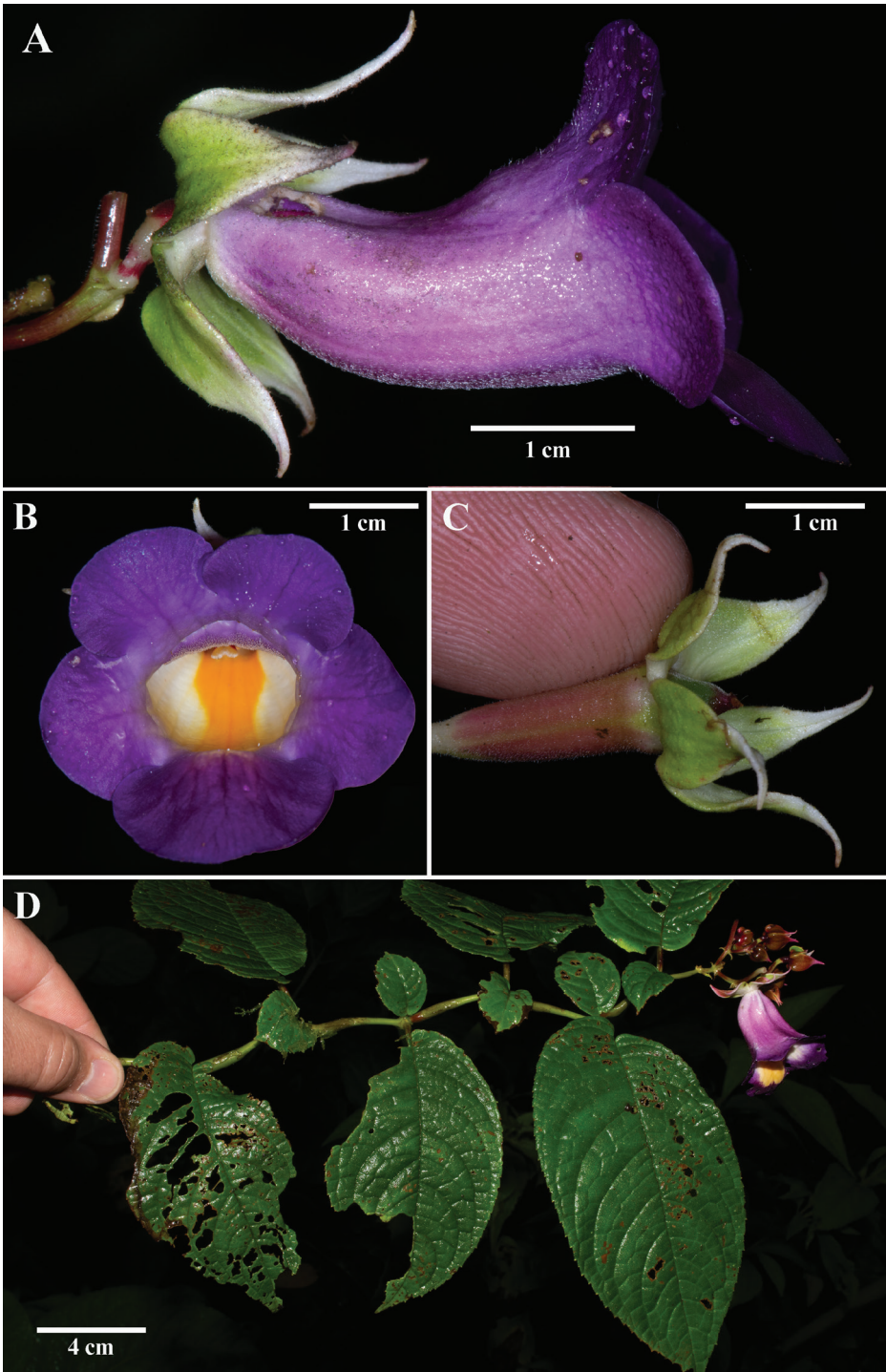


Figure 1. *Monopyle glutinosa* J.L.Clark & J.Keene **A** lateral view of flower **B** front view of flower **C** inferior ovary and calyx lobes adhering to a finger from the sticky trichomes **D** dorsiventral habit (**A–D** from *J.L. Clark 16489*). Photos by J.L. Clark.

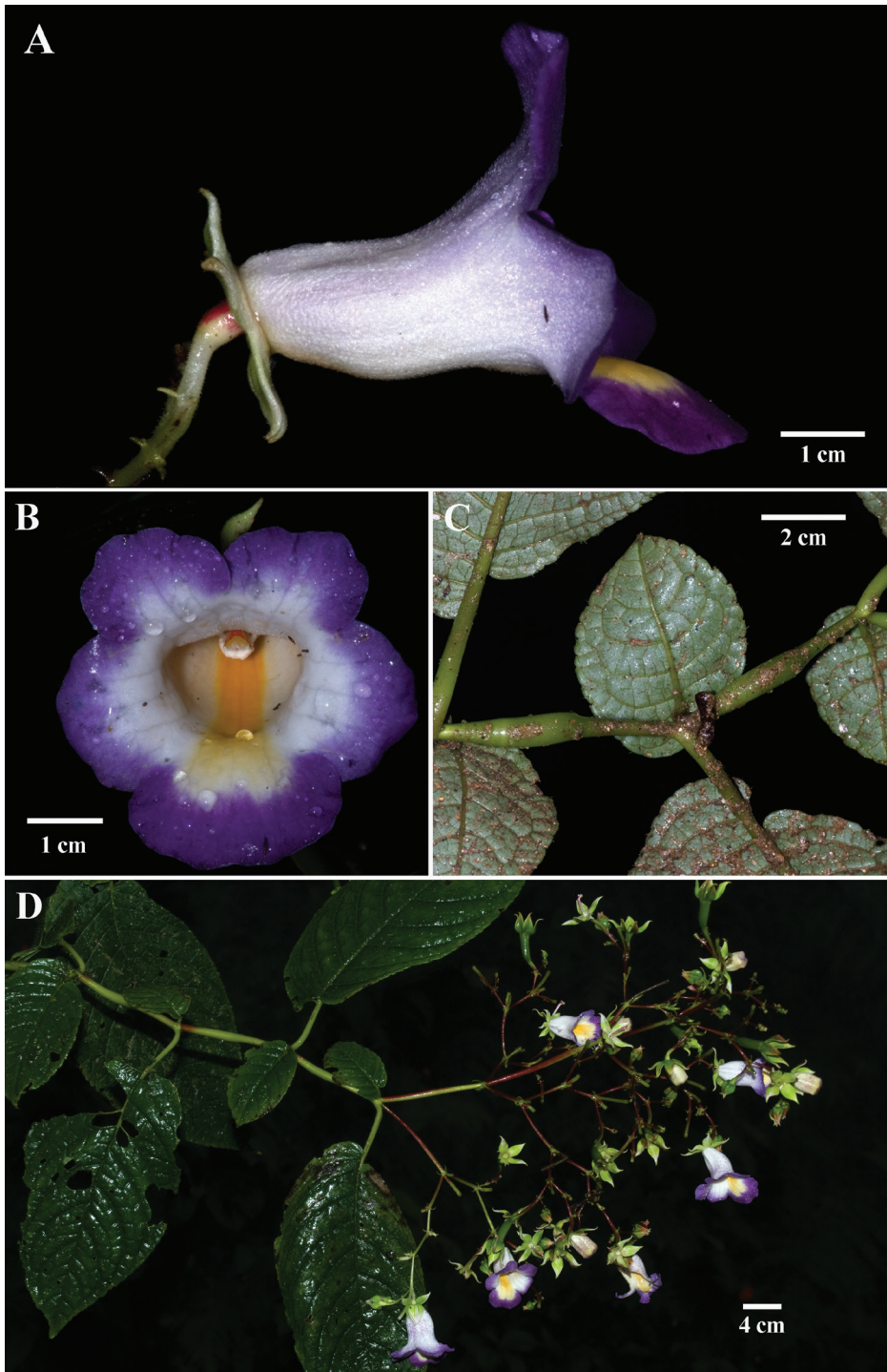


Figure 2. *Monopyle ecuadorensis* C.V.Morton **A** lateral view of flower **B** front view of flower **C** swollen region between nodes **D** dorsiventral habit with terminal inflorescence (**A, D** from *J.L. Clark 12301*, **B, C** *J.L. Clark 12294*). Photos by J.L. Clark.

Distribution and preliminary assessment of conservation status. *Monopyle glutinosa* is endemic to the western Andean slopes of Ecuador. The three known collections are located in the buffer zone and the southern region of Reserva Ecológica Los Illinizas, from disturbed primary forests. GeoCAT calculated the following values for EOO = 46.31 km² and AOO = 12 km². Based on the available information and according to the IUCN Red List Criteria and Guidelines (IUCN 2022; IUCN Standards and Petitions Committee 2022), *M. glutinosa* is preliminarily assessed as Critically Endangered (CR, B1a,biii), based on its limited geographic range (EOO < 100 km²) and the uncertain future of habitat conservation of western Andean forests as exemplified by the deforestation for agriculture throughout the buffer zone and inside the park.

Comments. *Monopyle glutinosa* differs from all other *Monopyle* by the presence of sticky glandular trichomes intermixed with similarly-sized uncinata trichomes on the outer surface of the inferior ovary and calyx lobes. *Monopyle glutinosa* and *M. ecuadorensis* share a similar terrestrial dorsiventral habit with a terminal inflorescence, swollen regions along the stem between nodes (Fig. 2C), and similar shapes of calyx and corolla. The inflorescence on *M. glutinosa* has shorter peduncles and appears more compact (< 10 cm). The inflorescence on *M. ecuadorensis* has more inflorescence branching and appears broader from longer peduncles, often exceeding 10 cm in length and width (Fig. 2D). The campanulate flowers and broadly ovate calyx lobes are similar to *M. ecuadorensis*. The campanulate corolla tube in *M. glutinosa* exceeds 3 cm (Fig. 1A), in contrast to the smaller corolla tube in *M. ecuadorensis* that rarely exceeds 3 cm in length (Fig. 2A) and 1 cm in width (Fig. 2B). The broadly ovate calyx lobes with acuminate, reflexed apices are longer (ca. 1.5 cm long) in *M. glutinosa* (Fig. 1B) relative to the shorter (ca. 0.5–1.0 cm long) calyx lobes in *M. ecuadorensis* (Fig. 2B). Corolla tube coloration ranges in *M. ecuadorensis* from uniformly white to white suffused with blue (Fig. 2A). In contrast, the corolla tube of *M. glutinosa* is uniformly dark purple (Fig. 1A). *Monopyle ecuadorensis* is distributed throughout western Ecuador (usually above 1200 meters). In contrast, *M. glutinosa* is locally endemic and restricted to altitudes below 1200 meters.

Additional specimens examined. ECUADOR. **Cotopaxi:** 20 km NW of El Corazón, 19–24 Jun 1967, *B. Sparre 17294* (MO, S); cantón Pujilí, Reserva Ecológica Los Illinizas, sector Paloseco, west of Choasillí, 0°58'34"S, 79°6'58"W, 1700 m alt., 12 Aug 2003, *P. Silverstone-Sopkin et al. 10064* (COL, MO, US).

Acknowledgements

We thank the Ministry of the Environment of Ecuador for providing specimen collection and transportation permits (Research permit Aves y Conservación N° 007-2018-IC-FLO-FAU and mobilization permit Aves y Conservación 005-FLO-2019-DPAP-MA). Peter Moonlight from the Royal Botanic Garden Edinburgh is acknowledged for suggesting the specific epithet of *glutinosa*. We thank Alain Chautems, Laura Clavijo, and Eric H. Roalson for providing valuable feedback on an earlier version of the manuscript.

References

- Bachman S, Moat J, Hill A, de la Torre J, Scott B (2011) Supporting Red List threat assessments with GeoCAT: Geospatial conservation assessment tool. *ZooKeys* 150: 117–126. <https://doi.org/10.3897/zookeys.150.2109>
- Clark JL (2022) Post-pandemic research expedition to Ecuador: Cognitive dissonance and discoveries. *Gesneriads* (72): 4–15.
- Clark JL, Skog LE, Boggan JK, Ginzburg S (2020) Index to names of New World members of the Gesneriaceae (Subfamilies Sanangoideae and Gesnerioideae). *Rheedea* 30: 190–256. <https://doi.org/10.22244/rheedea.2020.30.01.14>
- IUCN (2022) The IUCN Red List of Threatened Species. Version 2022–1. <https://www.iucn-redlist.org> [Accessed on 26 August 2022]
- IUCN Standards and Petitions Committee (2022) Guidelines for using the IUCN Red List Categories and Criteria. Version 15.1. <https://www.iucnredlist.org/resources/redlistguidelines>
- Keene J (2013) A reassessment of *Monopyle* (Gloxinieae: Gesneriaceae). Ph.D. thesis, Ohio University, Athens, OH, 1–134.
- Morton CV (1945) Las especies Sudamericanas del genero *Monopyle*. *Revista Universitaria (Cuzco)* 33(87): 98–116.
- Ogutcen E, Christe D, Nishii K, Salamin N, Möller M, Perret M (2021) Phylogenomics of Gesneriaceae using targeted capture of nuclear genes. *Molecular Phylogenetics and Evolution* 157: 107068. <https://doi.org/10.1016/j.ympev.2021.107068>
- Weber A (2004) Gesneriaceae. In: Kadereit J (Ed.) *The Families and Genera of Vascular Plants*. Vol. 7. Flowering Plants. Dicotyledons. Lamiales (Except Acanthaceae Including Avicenniaceae). Springer, Berlin, 63–158. https://doi.org/10.1007/978-3-642-18617-2_8
- Weber A, Clark JL, Möller M (2013) A new formal classification of Gesneriaceae. *Selbyana* 31(2): 68–94.
- Weber A, Middleton DJ, Clark JL, Möller M (2020) Keys to the infrafamilial taxa and genera of Gesneriaceae. *Rheedea* 30: 5–47. <https://doi.org/10.22244/rheedea.2020.30.01.02>

A new marine epipsammic diatom species, *Ambo dajingensis* sp. nov. (Bacillariophyceae), from the coast of Southeast China

Honghan Liu¹, Zhen Wang¹, Weiwei Wu¹, Chenhong Li¹,
Jiawei Zhang¹, Yahui Gao^{1,2}, Xuesong Li¹, Lin Sun²,
Junrong Liang¹, Jun Zhang¹, Changping Chen¹

1 Key Laboratory of Ministry of Education for Coastal and Wetland Ecosystems and School of Life Sciences, Xiamen University, Xiamen 361102, China **2** State Key Laboratory of Marine Environmental Science, Xiamen University, Xiamen 361102, China

Corresponding authors: Yahui Gao (gaoyh@xmu.edu.cn), Changping Chen (chencp@xmu.edu.cn)

Academic editor: Dmitry Kapustin | Received 26 July 2022 | Accepted 9 September 2022 | Published 28 September 2022

Citation: Liu H, Wang Z, Wu W, Li C, Zhang J, Gao Y, Li X, Sun L, Liang J, Zhang J, Chen C (2022) A new marine epipsammic diatom species, *Ambo dajingensis* sp. nov. (Bacillariophyceae), from the coast of Southeast China. *PhytoKeys* 210: 23–34. <https://doi.org/10.3897/phytokeys.210.90876>

Abstract

Ambo dajingensis HH Liu, Z Wang, YH Gao & CP Chen, **sp. nov.** is described as a new species in samples collected from sand grains at Dajing Beach, Ningde City, Fujian Province, China. Morphological details of the new species with respect to valve shape, size and valve ultrastructure are presented based on light microscopy (LM) and scanning electron microscopy (SEM). The main features of *Ambo dajingensis* under a light microscope are elongated elliptic valves with rounded apices, two internal costae on the valve and rectangular in girdle views. SEM observation showed that externally, the frustules are comprised of two valves with a relatively deep mantle and a transition between the valve faces. Small, flabelliform spines are present along the valve margin. Internally, the valves are divided into three sectors by robust costae, which penetrate the whole valve lumen and are thickest at the mantle interior and thinner toward the center. The sternum is narrow and linear, visible only in the valve apex, set off by costae. The striae are comprised of small, round areolae and they are parallel in the middle to slightly radiate at the apices. The new species is compared with other species in the genus *Ambo*.

Keywords

Ambo, China, Fujian Province, intertidal zone, new species

Introduction

The genus *Ambo* Witkowski, Ashworth, Lange-Bertalot & G. Klein is a recently established genus, with three species transferred and one species newly described by Witkowski et al. (2020). Witkowski et al. (2020) made new combinations for *Anaulus balticus*, *Anaulus simonsenii*, and *Plagiogramma tenuissimum* and added a new species for *A. galaeciae*. The type species selected for the new genus was *Ambo tenuissimum*, based on material from Lago de Maracaibo (Venezuela), the western Indian Ocean and the east coast of South Africa, and later also found to occur in the western Pacific margin. The genus *Ambo* is comprised of small taxa with internal costae across the valves. By scanning electron microscopy (SEM) observations, the unique features of the genus *Ambo* were revealed: hyaline valve center and areolated apices and the absence of rimoportulae.

Observations of the valve structure in *Ambo* species indicated that the costae across the valves were distinct under light microscopy (LM). However, in some small diatoms, with the exception of costae, a few features resolvable with LM could cause confusion in the identification and classification of these diatoms. In nonpennates and araphid diatoms, the genera *Eunotogramma* (Ashworth et al. 2015), *Anaulus* (Odebrecht et al. 2014; Franco et al. 2018) and *Plagiogramma* (Kaczmarska et al. 2017; Li et al. 2021) bear internal transverse costae. With the re-examination of some small species, i.e., *Anaulus balticus*, *Anaulus simonsenii* and *Plagiogramma tenuissimum*, in these genera through the use of the scanning electron microscope, the valve ultrastructures in these species were revealed, including symmetric valves without rimoportula, a hyaline area in the central part of the valve and unperforated girdle bands (Witkowski et al. 2020). Therefore, the new genus *Ambo* was described by Witkowski et al. (2020) to accommodate these species. Unlike *Ambo*, the genus *Eunotogramma* has an asymmetric valve, rimoportula, variable costae and parallel striae (Ross and Sims 1972; Amspoker 2016). Moreover, both *Anaulus* and *Eunotogramma* have broad girdles comprised of numerous perforated bands (Drebes and Schulz 1989) compared to plain girdle bands in the genus *Ambo*.

Here, we describe a new species, *Ambo dajingensis*, with few features resolvable with light microscopy (LM) other than internal costae across the valves. The cultured material also allowed us to examine the internal costa-bearing taxa using molecular tools, such as DNA sequence phylogenetics, to investigate the evolutionary relationship with other related species and their relationships. The molecular data, in combination with ultrastructural evidence provided by SEM, also allowed us to determine the classification of the new species.

Materials and methods

The samples were collected from the intertidal zone on Dajing Beach, Ningde City, Fujian Province, China (26°42'34"N, 120°7'17"E) (Fig. 1) in May 2018. The sample site is located in a subtropical monsoon humid climate zone. The beach covers an area of approximately 0.6 km². The average annual temperature is 18.6 °C, and the average annual precipitation is 1100–1800 mm.

The sand grains were collected and stored at low temperature until brought back to the laboratory. The diatoms attached to the sand particles were treated by ultrasonic waves and cultured through the pore plate dilution method, and the single high-density diatom solution was gradually expanded (Zhang et al. 2020). The diatom solution was acidified and washed 8 to 10 times with distilled water until the pH of the sample was nearly neutral (Li et al. 2022). The cleaned material was air-dried onto coverslips, and these were mounted on glass slides using Naphrax for light microscopy (Al-Handal et al. 2021; Lobban and Prelosky 2022). The diatoms were examined and identified using a Leica DM48 microscope (Leica, Germany) with a Leica Application Suite X camera (100× objective) system. The cleaned material was air-dried onto membrane filters, mounted onto aluminum stubs and coated with gold palladium for scanning electron microscopy (SEM). SEM observations were made using a JSM-6390LV scanning electron microscope at an accelerating voltage of 10 kV (Lin et al. 2022). Other portions of the diatom sample were fixed by adding glutaraldehyde at a concentration of 2.5% for 30 min at 4 °C, then rinsed with distilled water and attached to a glass coverslip. They were then dehydrated through 30%, 50%, 70%, 80%, 90%, 95% and 100% alcohol series and critical point dried (Leica CPD300) for SEM observation (Majewska et al. 2017). Valve dimensions and density of the striae were measured using LM and SEM images of 30 valves. The diatom morphological terminology follows Ross and Sims (1972), Round et al. (1990), Witkowski et al. (2020) and Van de Vijver et al. (2021). Samples are housed in the Biology Department Herbarium, Xiamen University (AU), China.

DNA extraction and sequencing

DNA was extracted from the cultured materials. Diatom cells were pelleted in a Fresco17 refrigerated superspeed centrifuge (Thermo Fisher Scientific, USA) for 10 min at 7649× g from a culture in the late logarithmic phase of growth. The product instructions of the Steady Pure Plant Genomic DNA Kit were followed to extract genomic DNA from monoclonal diatom cells that had been cultured for two weeks. Gel electrophoresis (1% agarose gel) and microspectrophotometry were used to determine the purity and concentration of the extracted DNA. The DNA samples were stored at –20 °C before the polymerase chain reaction (PCR). PCR using eukaryotic primers R1F 5'-TTAAGGAGAAATAAATGTCTCAATCTG-3' and R1R 5'-GC-GAAATCAGCT GTATCTGTWG- 3' was performed on the total DNA extracts. Refer to the primers of Alverson et al. (2007) and Ruck and Theriot et al. (2011) to amplify the *rbcL* gene fragment.

Polymerase chain reaction was performed with the premixed mix PrimeSTAR to amplify the *rbcL* gene fragment. The amplification conditions of *rbcL* were: initial denaturation at 95 °C for 5 min, denaturation at 95 °C for 30 s, annealing at 55 °C for 30 s, and extension at 72 °C for 60 s, for a total of 36 cycles, and a final extension at 12 °C for 15 min. The PCR products were detected by 1% agarose gel, purified using a SanPrep column PCR product purification kit, and sent to Sangon Sequencing Company for sequencing.

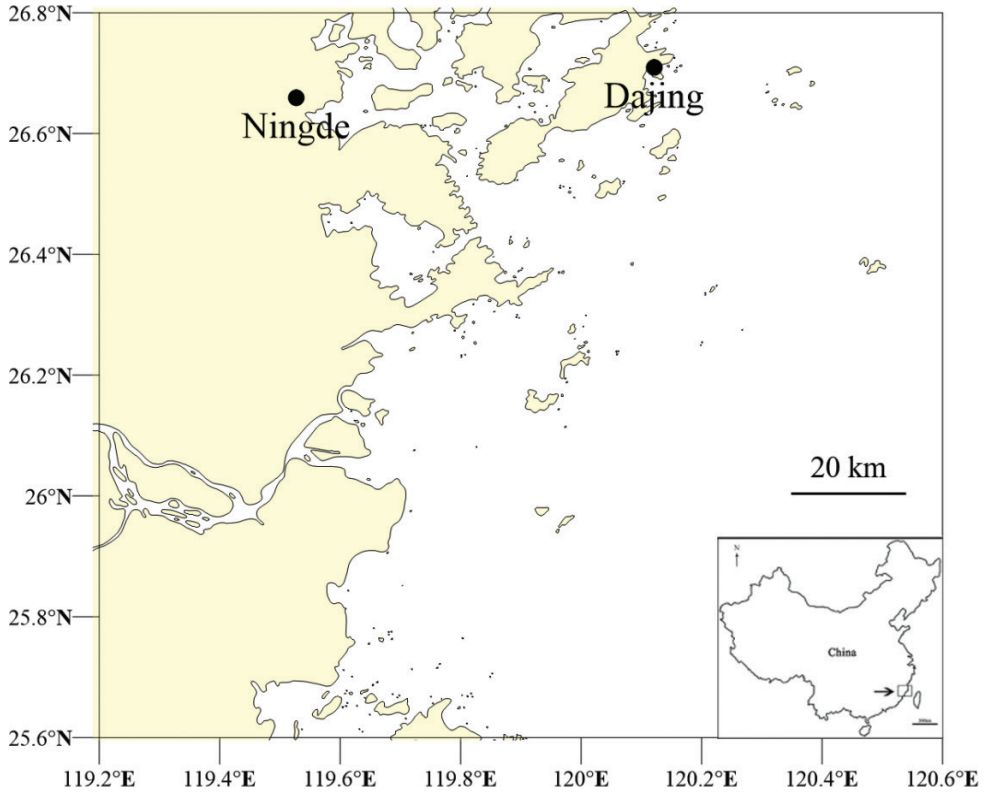


Figure 1. Maps with the geographic location of the study area.

Phylogenetic analysis

Phylogenetic analysis of the molecular data was conducted using the *rbcL* dataset. For DNA barcoding of diatoms, Hamsher et al. (2011) showed that the *rbcL* gene could be well selected based on its variance (Samanta and Bhadury 2018). Through BLAST in the GenBank database to compare the *rbcL* gene sequence obtained from this experiment, we downloaded 56 strains belonging to the araphid group in this study and the strain of *Bolidomonas pacifica* was chosen as the outgroup taxon. Then, the DNA sequence obtained from this experiment were merged with the sequence of the outgroup taxon. The resulting sequences were checked and first aligned using the mafft V7.110 online program (<http://mafft.cbrc.jp/alignment/server/>) and the default settings. We manually checked the alignment using BioEdit v.7.0.9 (Hall 1999). The maximum likelihood (ML) analysis was carried out by Raxml V7.2.6 (Stamatakis and Alachiotis 2010) using the Model GTRMM in T-rex web servers (Alix et al. 2012). The bootstrap values were obtained by making 1000 replicates of the ML analyses for each branch node of the phylogenetic tree (Guindon et al. 2010).

Results

Ambo dajingensis HH Liu, Z Wang, YH Gao & CP Chen, sp. nov.

Figs 2–4

Holotype (here designated): slide DJ1805 (AU, Biology Department Herbarium, Xiamen University). Fig. 2E represents holotype.

Type locality. Sand beach in Dajing County, Fujian Province, China, 26°42'34"N, 120°7'17"E, *leg.* Zhen Wang in May 2018

Etymology. The epithet “*dajingensis*” refers to the site where this specimen was collected.

Description. LM observations (Fig. 2A–I): The cells are connected to each other to form short chains and they live in groups. The girdle is comprised of several plain and open bands. The valves are linear elliptic with two costae that are straight or slightly curved to the outside and protrude deeply into the valve. The valve is 6–10 µm long and 2.4–3 µm wide.

SEM observations (Figs 3, 4): Through the observation of the samples treated by the critical point drying method, the cells on the girdle band valve are rectangular (Fig. 3A), with a wrapped layer of membrane. Several girdle bands (Fig. 3D) are connected between the epitheca and hypotheca valves. The girdle band has fine vertical lines (Fig. 3D) but no obvious spot pattern. Areolae can be observed at both ends of the valve, and the area of the areolae extends to the sternum, but there are no areolae or other cell structures in the middle of the cell (Fig. 3A, B). There is a circle of spines for cell connection at the edge of the valve (Fig. 3A–D). The single row of slightly radial striae is distributed at both ends of the cell (Fig. 3A). Observation of the samples processed by the acidification method showed striae at both ends of the cells and a narrow sternum in the center of the cells in the area of striae, but the sterna were not obvious. To the two ends of the valve, the striae at both ends of the valve extended from the valve in a single row, and the number of striae was 50–60 in 10 µm. The areolae on the valve are round, small, simple, and have no complex structure, such as a cribrum. A small circular area free of areolae is distinctly set off from the striae, and can be observed at the apical part of mantle area with several elongate areolae following the general pattern of the mantle (Fig. 3E, F). On the edge of the valve, there is a row of densely distributed small spines.

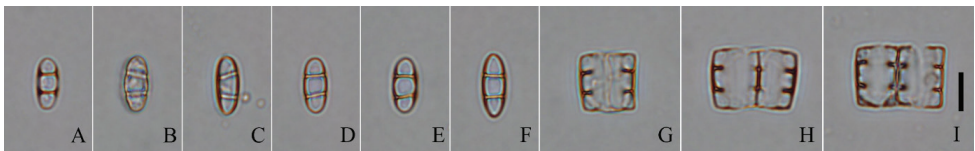


Figure 2. Light micrographs (LM) of *Ambo dajingensis* sp. nov. **A–F** valve showing the size and shape **G–I** girdle view. Scale bar: 5 µm.

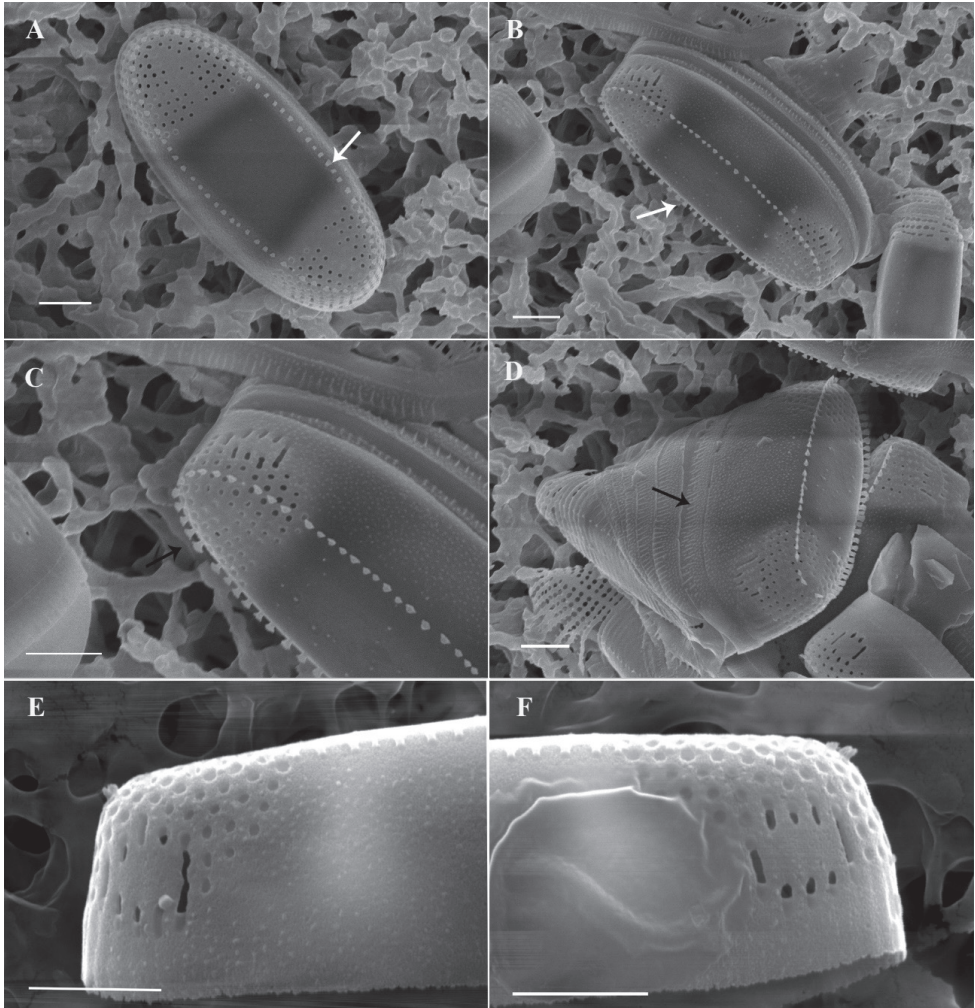


Figure 3. Scanning electron microscopy (SEM) images of *Ambo dajingensis* sp. nov. in an external view of the entire valve **A**, **B** external valve view of the whole specimen. There is a hyaline valve face over most of the length and transapical striae develop only at the valve apex, with a weakly expressed sternum at the apices **C**, **E**, **F** fan-shaped spines (arrows) are arranged along the valve margin, there is striation, a strongly expressed sternum on the valve apical part, a small circular striated area structure on the mantle apex **D** the girdle bands. Scale bar: 1 μ m.

Internally, the valves are divided into three sectors by robust costae (Fig. 4A, C). The interior of the valve face is flat, the transition from the valve face to the mantle is abrupt (Fig. 4A). The transapical striae are composed internally of small, round areolae, and they are parallel in the middle to slightly radiate at the apices. The sternum is narrow and linear, set off by costae (Fig. 4A).

Distribution. Marine, coastal. Collected from Dajing beach on sandy shores. Changchun Town, Xiapu, Ningde City, Fujian Province.

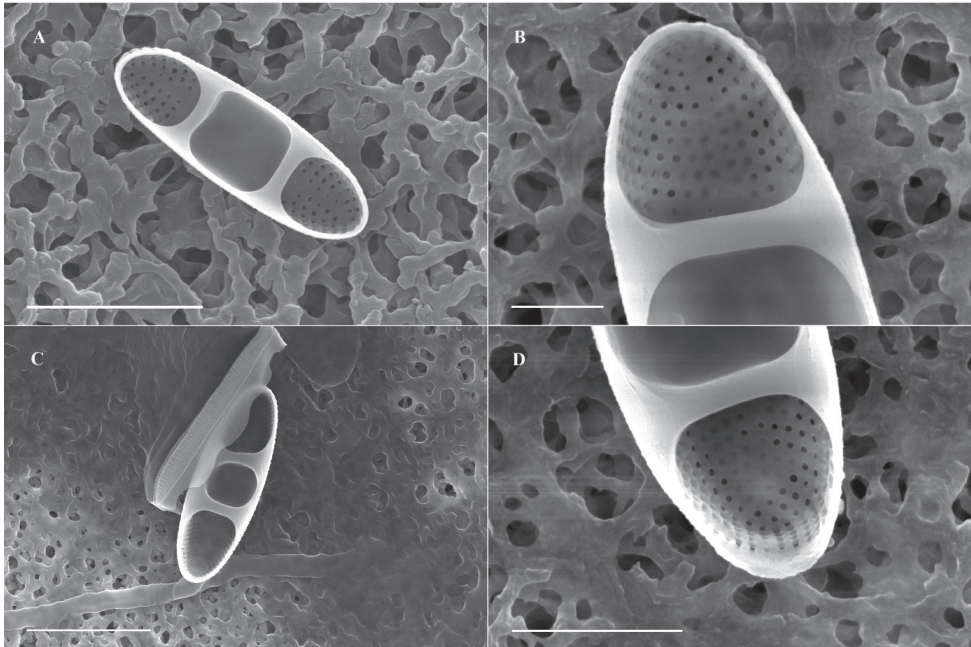


Figure 4. Scanning electron microscopy (SEM) images of *Ambo dajingensis* sp. nov. in an internal view of the entire valve **A**, **C** internal valve view of the whole specimen **B**, **D** the presence of costae (arrows) and the areolation. Scale bars: 3 μm (**A**); 1 μm (**B**); 5 μm (**C**); 2 μm (**D**).

Molecular phylogeny

Phylogenetic analysis of molecular data was conducted using a *rbcL*-gene dataset. The tree inferred from Maximum-Likelihood Phylogenies (MLP) analysis (Fig. 5) of the concatenated *rbcL*-gene dataset recovered the genus *Ambo* (represented by *A. tenuissimus*, *Ambo dajingensis* and *A. gallaeciae*) within the araphid diatoms, sister (bootstrap support [bs] = 100%) to a clade with *Diatoma moniliforma*, *Diatoma tenue*, and *Asterionella formosa*. *Ambo dajingensis* and *A. gallaeciae* were sister to a clade, but with low support. The phylogenetic relationships of the new species were sustained by genetic distance estimation. The sequences generated in the study were deposited in GenBank under access number OL457301.1.

Discussion

The characteristics of the genus *Ambo* were also observed in our samples. These features include 1) girdles consisting of several plain and open bands, 3) each costa near the apices, 4) areolae restricted to the ends of the valve face and absent at the central area, and 5) rimoportula absent.

Phylogenetic analysis of the *rbcL* sequences strongly supports our suggestion, based on morphological characteristics, that *A. dajingensis* is a new species for this

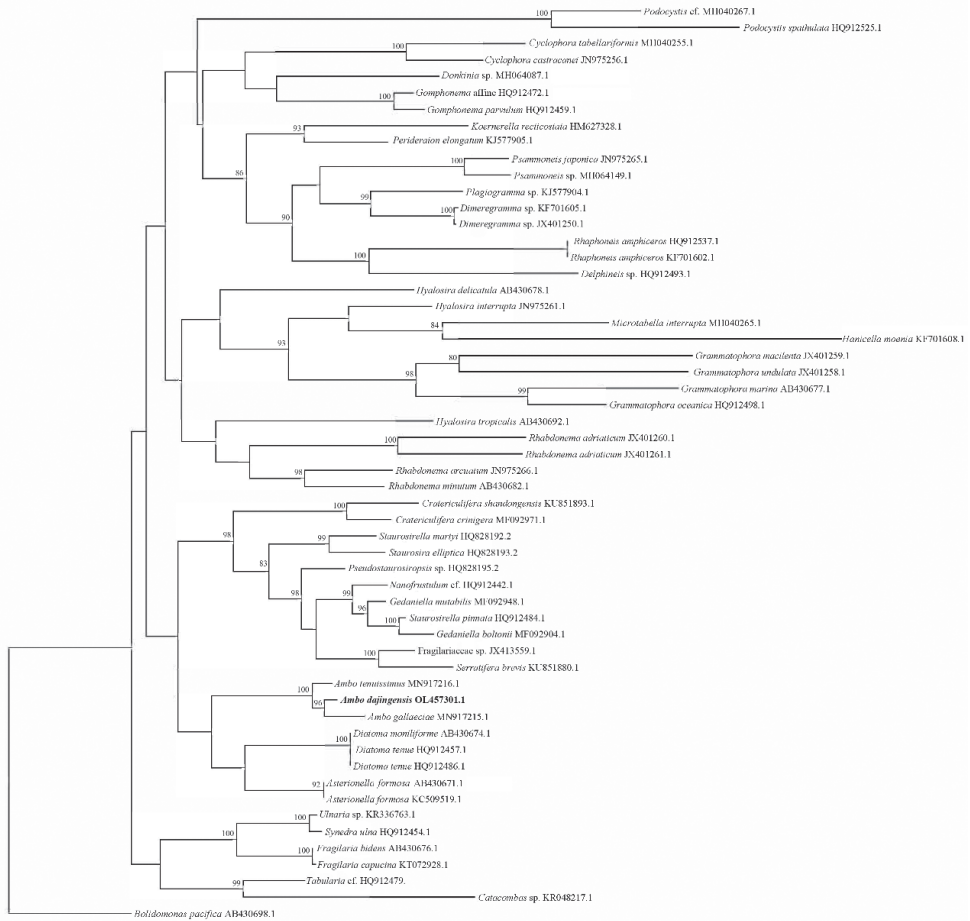


Figure 5. Maximum-Likelihood Phylogenies tree. Maximum-Likelihood Phylogenies (MLP) tree (based on analysis of the *rbcL* dataset) of mediophyccean strains related to *Ambo*.

genus. *A. dajingensis* and *A. gallaeciae* were positioned in a clade, which was sister to *A. tenuissimus* with a high support (bootstrap support = 100%). Our results revealed that the genus *Ambo* was sister to a clade with *Asterionella* and *Diatoma*. However, a much lower level of support (bootstrap support < 50) suggested that putting *Ambo* in Tabellariaceae could be difficult. Combining three-gene (nuclearencoded small subunit (SSU) rRNA, *rbcL* and plastid-encoded *psbC*) analysis, Witkowski et al. (2020) suggested that *Ambo* was sister to the Grammatophoraceae (*Hyalosira*, *Microtabella*, *Hanicella*, and *Grammatophora*) rather than Tabellariaceae (*Asterionella* and *Diatoma*). Lobban et al. (2021) also concluded that *Ambo* was sister to the Grammatophoraceae with high support (bootstrap support = 100%, posterior probability= 1.0).

A comparison of *Ambo dajingensis* with other morphologically similar species is shown in Table 1. The length and width of *A. dajingensis* are similar to those of

A. balticus. The valves of *Ambo dajingensis* are 6–10 μm long and 2.4–3 μm wide, and *Ambo balticus* valves are 5.5–14 μm long and 2.5–4 μm wide. However, *A. dajingensis* differs from *A. balticus* in several aspects: the general valve outline, which is more elliptical and narrower; the valve, which is symmetrical about the apical axis; and the number of striae, which is higher. Moreover, the presence of fan-shaped spines arranged along the valve margin and growing independently is another important feature for *A. dajingensis* (Fig. 3A–D), comparing with small and globular spines present along the valve margin, sometimes growing together into a ridge-like structure in *A. balticus* (Witkowski et al. 2020). Sternum in *A. dajingensis* is distinct and somewhat far from the apices (Fig. 3A), while Sternum in *A. balticus* is indistinct, and well expressed at apices. *A. dajingensis* shows some similarities to *A. tenuissimus*, which has comparable striation, a linear and narrow sternum, and an abrupt mantle with a small circular area free of areolae distinctly set off from the striae and surrounded by several elongate areolae.

However, they differ in many other features. The first is the valve outline, which is linear elliptic in *A. tenuissimus* but elliptic lanceolate in our new species. Moreover, in *A. dajingensis*, the spines are fan-shaped along the valve margin, not growing together into a continuous ridge (Fig. 3A–D), while in *A. tenuissimus*, the spines are small and globular along the valve margin, sometimes growing together into a continuous ridge (Witkowski et al. 2020). *A. dajingensis* is different from *A. tenuissimus* in areolae density (50–60 in 10 μm vs. 70–80 in 10 μm) (Table 1).

A. dajingensis is distinguished from *A. gallaeciae* by LM using size dimensions. *A. dajingensis* is 6–10 μm long and 2.4–3 μm wide with rounded apices, whereas *A. gallaeciae* is 6.5–8.0 μm long and 3.5–4.5 μm wide with broadly rounded apices. In SEM, a relatively deep mantle and an abrupt transition between the valve face and the mantle of *A. dajingensis* serve to distinguish this species from a relatively shallow mantle and a gradual transition between the valve face and the mantle of *A. gallaeciae*. Moreover, in *A. gallaeciae*, the spines are small, globular and irregularly distributed at the transition from the valve margin to the mantle, whereas in *A. dajingensis*, they are fan-shaped along the valve margin. The differences between *A. dajingensis* and *A. simonsenii* are based on the valve width (2.4–3 μm vs. 1–2.1 μm), stria density (50–60 in 10 μm vs. 80–100 in 10 μm) and areolae density (50–60 in 10 μm vs. 120 in 10 μm). Additionally, the presence *vs.* absence of spines on the valve surface also distinguish these species.

Table 1. Morphometric characteristics of *Ambo dajingensis* and comparison with other *Ambo* taxa (Witkowski et al. 2020).

Species	Valve outline	Valve apices	Spines	Valve length (μm)	Valve width (μm)	Striae (10 μm)	Areolae (10 μm)
<i>Ambo dajingensis</i>	elongated and elliptic	rounded	fan-shaped	6–10	2.4–3	50–60	50–60
<i>Ambo balticus</i>	linear to linear lanceolate	narrow and expressed	small, globular	5.5–14	2.5–4	50	60
<i>Ambo gallaeciae</i>	linear to linear elliptic	broadly rounded	small, irregularly distributed globular	6.5–8	3.5–4.5	55	70–80
<i>Ambo simonsenii</i>	narrowly linear-lanceolate with protracted	rounded	No data	4.5–15.5	1–2.1	80–100	120
<i>Ambo tenuissimus</i>	linear elliptic	rounded	small, globular	9–15	2	48–60	70–80

All the diatoms of *Ambo* genus had been found in the marine environment, and they are widely distributed in different regions of the world. *Ambo balticus* were observed in the Western Baltic Sea, Africa East coast, Sodwana Bay, Pacific Ocean, etc. *Ambo simonsenii* were in the western Baltic Sea, Disko Bay, North Sea, etc. *Ambo tenuissimus* was reported from Venezuela, the Indian Ocean, the Yellow Sea coast, China, etc. *Ambo gallaaciae* are known from the Atlantic coast of NW Spain. The samples of this genus were collected from Dajing Beach, Ningde City, Fujian Province. *Ambo dajingensis* sp. nov. is a marine epipsammic araphid diatom.

The newly documented species in the present study were collected from sand, suggesting that the diversity of tiny araphid taxa is understudied in these habitats and remains to be further explored. The diversity of small-celled diatoms is easily ignored when observed under LM, in which distinguishing characteristics are difficult to resolve. On the basis of our study, we suggest that among the small-celled taxa, the diversity in their ultrastructural morphology and genetic data reflect a great deal of taxonomic diversity, despite their small valves, overlapped size dimension and striae density. It is entirely possible that this taxonomic diversity also reflects a strong diversification across ecological habitats. When encountering small diatoms, it is necessary to focus on their ultramorphological (examined with SEM) or phylogenetic differences, which are likely diverged by some specific type of environment and should not be ignored.

Acknowledgements

This research was supported by National Natural Science Foundation of China under contract Nos: 41776124, 42076114, 41876146. We would like to thank Dr. Caiming Wu, Dr. Luming Yao and Ms. Jie Liu for their assistance with electron microscopy, and American Journal Experts for language editing.

References

- Al-Handal AY, Romero OE, Eggers SL, Angela Wulff A (2021) *Navithidium* gen. nov., a new monoraphid diatom (Bacillariophyceae) genus based on *Achnanthes delicatissima* Simonsen. *Diatom Research* 36(2): 133–141. <https://doi.org/10.1080/0269249X.2021.1921039>
- Alix B, Boubacar DA, Vladimir M (2012) T-REX: A web server for inferring, validating and visualizing phylogenetic trees and networks. *Nucleic Acids Research* 40(W1): W573–W579. <https://doi.org/10.1093/nar/gks485>
- Alverson AJ, Jansen RK, Theriot EC (2007) Bridging the Rubicon: Phylogenetic analysis reveals repeated colonizations of marine and fresh waters by thalassiosiroid diatoms. *Molecular Phylogenetics and Evolution* 45(1): 193–210. <https://doi.org/10.1016/j.ympev.2007.03.024>
- Amspoker MC (2016) *Eunotogramma litorale* sp. nov., a marine epipsammic diatom from Southern California, USA. *Diatom Research* 31(4): 389–395. <https://doi.org/10.1080/0269249X.2016.1256350>

- Ashworth MP, Ruck EC, Lobban CS, Romanovicz DK, Theriot A (2015) A revision of the genus *Cyclophora* and description of *Astrosyne* gen. nov. (Bacillariophyta), two genera with the pyrenoids contained within pseudosepta. *Phycologia* 51(6): 684–699. <https://doi.org/10.2216/12-004.1>
- Drebes G, Schulz D (1989) *Anaulus australis* sp. nov. (Centrales, Bacillariophyceae), a New Marine Surf Zone Diatom, Previously Assigned to *A. birostratus* (Grunow) Grunow. *Botanica Marina* 32(1): 53–64. <https://doi.org/10.1515/botm.1989.32.1.53>
- Franco AR, Marcelo D, Moreira MP (2018) Diatom accumulations on a tropical meso-tidal beach: environmental drivers on phytoplankton biomass. *Estuarine Coastal and Shelf Science* 207(JUL.31): 414–421. <https://doi.org/10.1016/j.ecss.2017.07.020>
- Guindon S, Dufayard JF, Lefort V, Anisimova M, Hordijk W, Gascuel O (2010) New Algorithms and Methods to Estimate Maximum-Likelihood Phylogenies: Assessing the Performance of PhyML 3.0. *Systematic Biology* 59(3): 307–321. <https://doi.org/10.1093/sysbio/syq010>
- Hall TA (1999) BioEdit: A User-Friendly Biological Sequence Alignment Editor and Analysis Program for Windows 95/98/NT. *Nucl Acids Symposium Series* 41(41): 95–98. <https://doi.org/10.1021/bk-1999-0734.ch008>
- Hamsher SE, Evans KM, Mann DG, Pouličková A, Saunders GW (2011) Barcoding Diatoms: Exploring Alternatives to COI-5P. *Protist* 162(3): 405–422. <https://doi.org/10.1016/j.protis.2010.09.005>
- Kaczmarek I, Gray BS, Ehrman JM, Thaler M (2017) Sexual reproduction in plagiogrammeacean diatoms: First insights into the early pennates. *PLoS ONE* 12(8): e0181413. <https://doi.org/10.1371/journal.pone.0181413>
- Li C, Ashworth MP, Mackiewicz P, Dabek P, Witkowski J, Gorecka E, Krzywda M, Witkowski A (2021) Morphology, phylogeny, and molecular dating in Plagiogrammeaceae family focused on *Plagiogramma-Dimeregramma* complex (Urneidophycidae, Bacillariophyceae). *Molecular Phylogenetics and Evolution* 148: 1–23. <https://doi.org/10.1016/j.ympev.2020.106808>
- Li C, Tan L, Gao Y, Li X, Sun L, Liang J, Zhang J, Huang L, Chen C (2022) Morphology of *Amphora lunulata* A.H. Wachnicka & E.E. Gaiser and its transfer to *Seminavis* D.G. Mann. *Diatom Research* 37(1): 63–69. <https://doi.org/10.1080/0269249X.2022.2041490>
- Lin H, Wu W, Sun L, Witkowski A, Li X, Patil V, Liang J, Li X, Gao Y, Chen C (2022) *Chinia* gen. nov.—The second diatom genus simonsenioid raphe from mangroves in Fujian, China. *Journal of Oceanology and Limnology* 40(3): 1220–1232. <https://doi.org/10.1007/s00343-021-1067-0>
- Lobban CS, Prelosky GH (2022) *Gomphotheca marciae* (Bacillariophyceae: Bacillariaceae), a new species in a rarely seen genus. *Diatom Research* 37(2): 119–126. <https://doi.org/10.1080/0269249X.2022.2064552>
- Lobban CS, Majewska R, Ashworth M, Bizsel N, Bosak S, Kooistra WHCF, Lam DW, Navarro JN, Pennesi C, Sato S, Vijver BV, Witkowski A (2021) Diatom Genus *Hyalosira* (Rhabdonematales emend.) and Resolution of its Polyphyly in Grammatophoraceae and Rhabdonemataceae with a New Genus, *Placosira*, and Five New *Hyalosira* Species. *Protist* 172(3): 125816. <https://doi.org/10.1016/j.protis.2021.125816>
- Majewska R, Vijver BVD, Nasrolahi A, Ehsanpour M, Afkhami M, Bolaños F, Iamunno F, Santoro M, Stefano MD (2017) Shared Epizoic Taxa and Differences in Diatom

- Community Structure Between Green Turtles (*Chelonia mydas*) from Distant Habitats. *Microbial Ecology* 74(4): 969–978. <https://doi.org/10.1007/s00248-017-0987-x>
- Odebrecht C, Preez D, Abreu PC, Campbell EE (2014) Surf zone diatoms: A review of the drivers, patterns and role in sandy beaches food chains. *Estuarine Coastal and Shelf Science* 150(pt.a): 24–35. <https://doi.org/10.1016/j.ecss.2013.07.011>
- Ross R, Sims PA (1972) The fine structure of the frustule in centric diatoms: A suggested terminology. *British Phycological Journal* 7(2): 139–163. <https://doi.org/10.1080/00071617200650171>
- Round FE, Crawford RM, Mann DG (1990) The diatoms. Biology and Morphology of the Genera. Cambridge University Press, Cambridge, 747 pp.
- Ruck EC, Theriot E (2011) Origin and Evolution of the Canal Raphe System in Diatoms. *Protist* 162(5): 723–737. <https://doi.org/10.1016/j.protis.2011.02.003>
- Samanta B, Bhadury P (2018) Study of diatom assemblages in Sundarbans mangrove water based on light microscopy and *rbcL* gene sequencing. *Heliyon* 4(6): e00663. <https://doi.org/10.1016/j.heliyon.2018.e00663>
- Stamatakis A, Alachiotis N (2010) Time and memory efficient likelihood-based tree searches on phylogenomic alignments with missing data. *Bioinformatics* 26(12): i132–i139. <https://doi.org/10.1093/bioinformatics/btq205>
- Vijver BVD, Hürlimann J, Williams DM, Levkov Z, Wetzel CE, Ector L (2021) *Fragilaria subreapitellata* (Fragilariaceae, Bacillariophyta), a new diatom species from Switzerland. *Diatom Research* 36(2): 119–131. <https://doi.org/10.1080/0269249X.2021.1942221>
- Witkowski A, Ashworth M, Li C, Sagna I, Manning SR (2020) Exploring diversity, taxonomy and phylogeny of diatoms (Bacillariophyta) from marine habitats. novel taxa with internal costae. *Protist* 171(2): 125713. <https://doi.org/10.1016/j.protis.2020.125713>
- Zhang J, Wang Z, Zhuo S, Gao Y, Li X, Zhang J, Sun L, Liang J, Li L, Chen C (2020) *Scoliolyra elliptica* gen. et sp. nov. (Bacillariophyceae), a new marine genus from sandy beach in Southern China. *Phytotaxa* 472(1): 1–12. <https://doi.org/10.11646/phytotaxa.472.1.1>

Two new endemic species, *Peucedanum miroense* and *P. tongkangense* (Apiaceae), from Korea

Kyeonghee Kim¹, Hwa-Jung Suh², Jun-Ho Song^{3,4}

1 Plant Resources Division, National Institute of Biological Resources, Incheon 22689, Republic of Korea **2** Department of Biology, Daejeon University, Daejeon 34520, Republic of Korea **3** Herbal Medicine Resources Research Center, Korea Institute of Oriental Medicine, Naju 58245, Republic of Korea **4** Department of Biology, Chungbuk National University, Cheongju 28644, Republic of Korea

Corresponding author: Jun-Ho Song (jhsong@chungbuk.ac.kr)

Academic editor: Leandro Giacomini | Received 2 May 2022 | Accepted 6 September 2022 | Published 29 September 2022

Citation: Kim K, Suh H-J, Song J-H (2022) Two new endemic species, *Peucedanum miroense* and *P. tongkangense* (Apiaceae), from Korea. *PhytoKeys* 210: 35–52. <https://doi.org/10.3897/phytokeys.210.86067>

Abstract

Two new species of *Peucedanum* (Apiaceae), *P. miroense* and *P. tongkangense*, from Gangwon Province, South Korea, are described. Both species are most similar to *P. elegans* and *P. hakuunense* because of their linear ultimate leaf segments. *Peucedanum miroense* was found on crevices of rocks in mountain summits and can be distinguished by its pubescent ovary, purple anthers, oblong schizocarp, and 1 or (2) vittae per vallecule and 4 on the commissural face. *Peucedanum tongkangense* was found in open areas on rocky cliffs along the Donggang River and can be distinguished by its glabrous ovary, whitish-yellow anthers, narrowly ellipsoid schizocarp, and 3 vittae per vallecule and 4 on the commissural face. Distinguishing characteristics, full descriptions, illustrations, photographs, taxonomic notes on geographical distribution, ecology, and phenology of the two species are presented. An identification key for all Korean species of *Peucedanum* is also provided. In addition, the mericarp surface of two new species and their close relatives are compared using micromorphological analysis.

Keywords

Apiaceae, FE-SEM, Korea, new species, *Peucedanum*, taxonomy

Introduction

Peucedanum L. (Apiaceae), represented by 100–120 species, is broadly distributed in the Old World (Hiroe 1979; Pimenov and Leonov 1993; Ostroumova and Pimenov 1997a, b; Shneyer et al. 2003). *Peucedanum* is distinguished from other genera by its

dorsally compressed mericarps with narrowly winged marginal ribs and filiform dorsal ribs (Drude 1898; Sheh and Watson 2005). The leaves are ternately or pinnately compound, and the leaflets are variously lobed and pinnatifid, pinnatisect, or sometimes simply toothed (Thellung 1926; Shishkin 1951; Shan and Sheh 1992). The ultimate leaf segments of *Peucedanum* are linear, lanceolate, oblong, or oblanceolate (Thellung 1926; Shishkin 1951; Shan and Sheh 1992).

Peucedanum is a complex and heterogeneous genus because many species present a complicated morphological variation of key characters, such as composition of leaves and ribs of mericarps (Pimenov and Leonov 1993; Shneyer et al. 2003). Therefore, many authors have tried to divide the genus *Peucedanum* into several genera, according to the species morphology. For example, Pimenov (1986) newly defined a genus *Kitagawia* Pimenov based on the shapes of mericarps, ribs on mericarps, apex of petals, and morphology of the base of the leaves. Other than genus *Kitagawia*, there are several segregate genera part of *Peucedanum* s.l.; these are *Imperatoria* L., *Thysselium* Adans., *Cervaria* Wolf, *Holandrea* Reduron, Charpin & Pimenov, and *Leutea* Pimenov (Spalik et al. 2004). However, the generic delimitation and synapomorphy of each group is not clear. Therefore, a comprehensive study including further molecular phylogenetic research with more various species is necessary to understand the phylogenetic relationships among groups of *Peucedanum* s.l.

Some species of *Peucedanum* have been used in traditional medicine for the treatment of various conditions, including coughs, cramps, pain, rheumatism, asthma, angina, and headaches (Morioka et al. 2004; Sarkhail, 2014). The most representative phytochemicals isolated from *Peucedanum* are coumarin compounds called pyranocoumarins and furanocoumarins, which have pharmacological effects in ailments including asthma, rheumatism, and gastrointestinal disorders (Sarkhail 2014; Gurbuz et al. 2018). For example, *P. praeruptorum* Dunn, which is distributed in China, is regarded as an effective medicinal plant with anti-inflammatory, anti-asthmatic, and anti-osteoclastogenic properties (Lee et al. 2015; Song et al. 2015).

To date, nine taxa, including three endemic species, in four sections of *Peucedanum* have been reported in Korea (Chung 1957; Kitagawa 1972; Lee 1996; Park et al. 2017; Lee 2018; Kim et al. 2019). During recent fieldwork and as a part of comprehensive systematic studies of *Peucedanum* in South Korea, we identified two distinct undescribed species of *Peucedanum* that have not been reported previously. One species was on the top of mountains in Gangwon Province and the other was on rocky slopes near rivers in Gangwon and North Chungcheong provinces. After detailed morphological, anatomical, and carpological analysis, we concluded that these plants differed from all other species of *Peucedanum*, particularly from *P. elegans* Kom. and *P. hakuunense* Nakai, which have similar ultimate leaf segments. We therefore propose the name *P. miroense* K. Kim, H.J.Suh & J.H.Song for the plants from the top of the mountains and *P. tongkangense* K. Kim, H.J.Suh & J.H.Song for those from the rocky slopes near the rivers and describe them here. We also present illustrations, a taxonomic key to all species of *Peucedanum* in Korea, images and a map of their distribution.

Materials and methods

Morphological description

The morphological descriptions of the two new species were based on observation of living plants and specimens collected from the type localities in 2021. We also examined specimens in the herbaria KB, KH, KIOM, and SNU (Thiers 2022) to compare them with related species. Type and voucher specimens were deposited in the Korean Herbarium of Standard Resources, Korean Institute of Oriental Medicine (KIOM). Measurements of morphological structures were performed using a digital vernier caliper (CD-15CP; Mitutoyo, Kawasaki, Japan). Digital images of floral parts were captured by using an Olympus SZX16 stereomicroscope (SM: Olympus, Tokyo, Japan), equipped with an attached Olympus DP21 digital camera (Olympus, Tokyo, Japan). Quantitative data of floral structures obtained from SM images were determined using Digimizer software (version 5.4.3; MedCalc Software, Mariakerke, Belgium).

Micromorphological observation

We also observed and compared micromorphological details of the mericarp surface of *Peucedanum miroense* and *P. tongkangense* and their close relatives, *P. hakuunense* and *P. elegans*. The dried mericarps of the four species were rehydrated overnight in a wetting agent (Agepon: distilled water, 1:200) (Agfa Gevaert, Leverkusen, Germany). Rehydrated materials were dehydrated through an ethanol series (50%, 70%, 90%, 95%, and 100%) at room temperature for one hour each. The dehydrated material was immersed in liquid CO₂ for CPD (SPI-13200JE-AB; SPI Supplies, West Chester, PA, USA) and subsequently mounted on aluminum stubs using a double-sided adhesive conductive carbon disk (05073-BA; SPI Supplies, West Chester, PA, USA). All samples were gold-coated using an ion-sputtering device (208HR; Cressington Scientific Instruments Ltd., Watford, UK) and observed using a low-voltage field-emission scanning electron microscope (FE-SEM: JSM-7600F; JEOL, Tokyo, Japan) at an accelerating voltage of 3–5 kV and a working distance of 8 mm.

Taxonomy

Peucedanum miroense K. Kim, H.J.Suh & J.H.Song, sp. nov.

urn:lsid:ipni.org:names:77305892-1

Figs 1, 2, 6A

Type. KOREA. Gangwon Province: Samcheok-si, Miro-myeon, Naemiro-ri, Swinŭmsan, crevices of rocks on mountain summits, 37°26'37.7"N, 129°01'49.4"E, alt. 540 m, 7 September 2021, *J.H.Song* & *S. Yang*, *KIOM-2021-646-1* [Holotype: KIOM! (Fig. 6A); Isotype KB!].

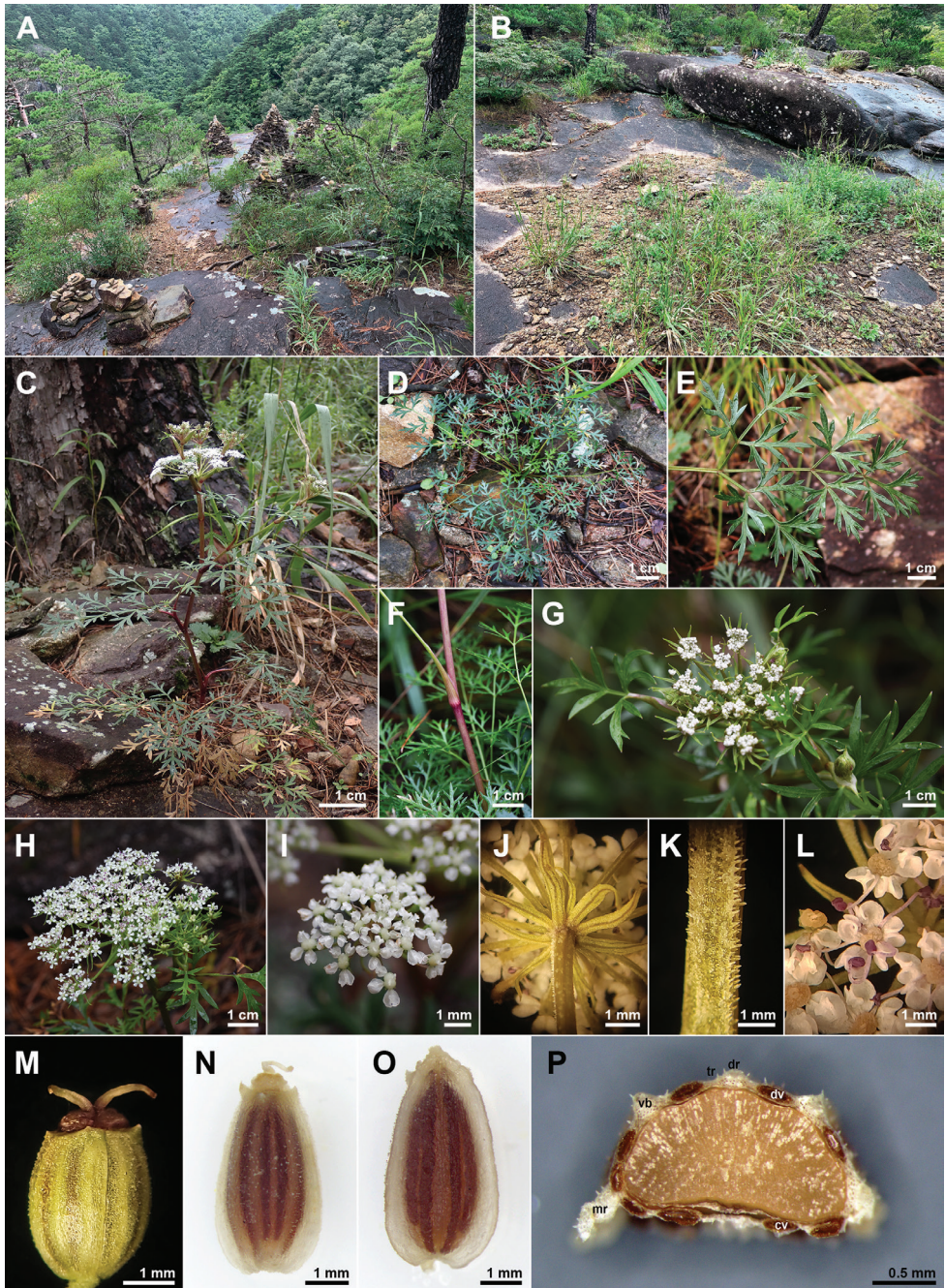


Figure 1. Photographs of *Peucedanum miroense* K. Kim, H.J.Suh & J.H.Song **A–C** habitat **D** basal leaves **E** cauline leaf **F** sheath **G** compound umbel (early flowering stage) **H** compound umbel (mature flowering stage) **I** umbellet (after anthesis) **J** bractlets **K** rays **L** flowers **M** calyx teeth and stylopodium (mature fruiting stage) **N** dorsal side of mericarp **O** commissural side of mericarp **P** transverse plane of mericarp. cv, commissure vittae; dr, dorsal ribs; dv, vallecule vitta; mr, marginal ribs; tr, trichomes; vb, vascular bundles.

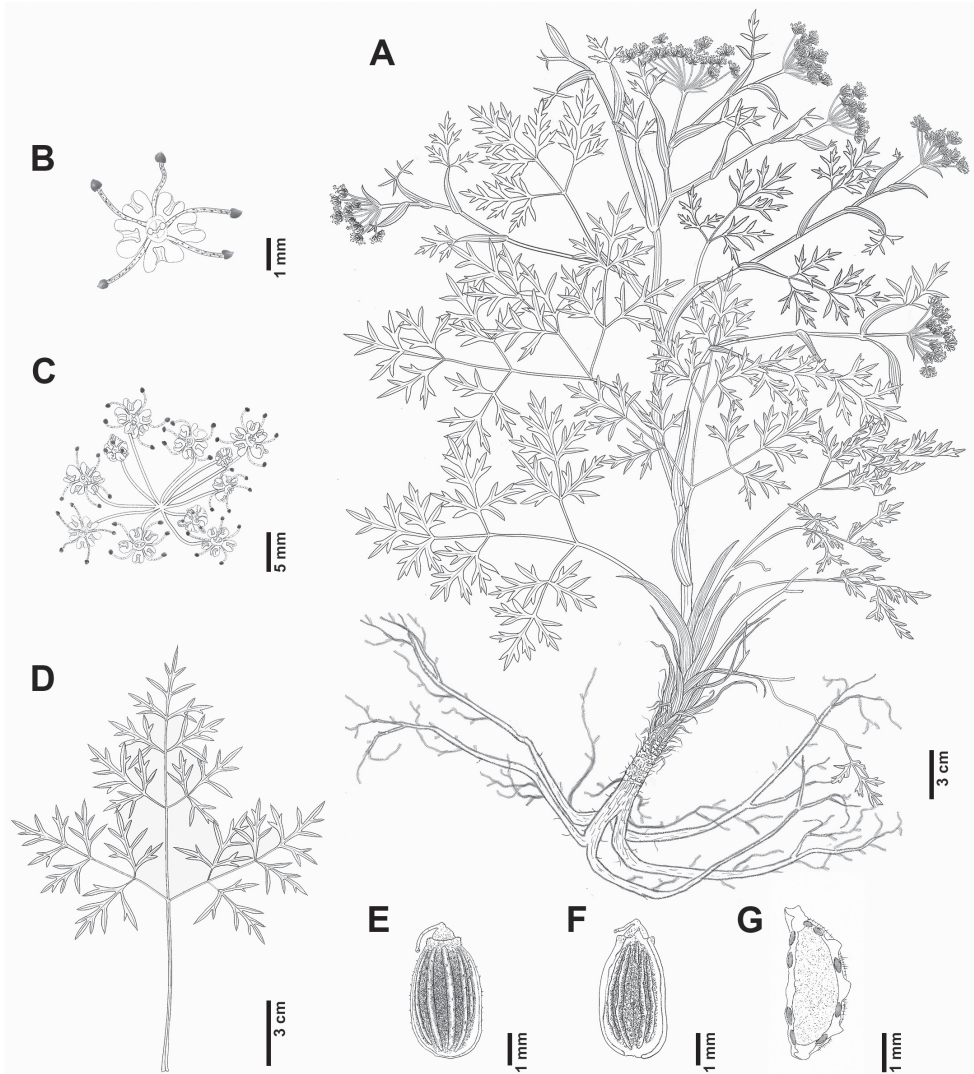


Figure 2. *Peucedanum miroense* K. Kim, H.J.Suh & J.H.Song **A** habit **B** flower **C** umbellet **D** basal cauline leaf **E** mericarp (dorsal side) **F** mericarp (commissural side) **G** mericarp (cross-section) (**A–F** J.H.Song & S. Yang, KIOM2021-646-2).

Diagnosis. *Peucedanum miroense* is similar to *P. elegans* but differs in its height at anthesis 37–50 cm tall (vs. 60–90 cm) and number of vittae, 8 or 9 vittae (vs. 6), 1 or (2) per vallecule (vs. 1 per vallecule), and 4 on commissure (2 on commissure). *Peucedanum miroense* is similar to *P. hakuunense* in ultimate leaf segments but has 2- or 3-pinnate leaves (vs. 1- or 2-ternate leaves) (Table 1).

Description. Herbs, perennial, hermaphroditic, 37–50 cm tall. Root a taproot, whitish to pale yellow, elongated, thickened, approximately 20 × 0.6–1.2 cm. Rhizomes erect or ascending, yellowish white, cylindrical, 0.3–1 cm in diameter, woody. Stems erect, pur-

Table 1. Comparison of major morphological characteristics of *Peucedanum miroense*, *P. tongkangense*, and their close relatives *P. bakuunense* and *P. elegans*.

	<i>P. miroense</i>	<i>P. tongkangense</i>	<i>P. bakuunense</i> *	<i>P. elegans</i> *
Habitat	crevices of rocks on mountain summits	open areas on rocky cliffs along the river	grassy places on mountain summits	mountain slopes
Height (cm)	37–50	60–120	30–75	60–90
Stems				
Pith	solid	solid	solid	hollow
Branch	branched	much branched	much branched	simple or branched in upper part
Basal leaves				
Division	2-pinnate	3-pinnate	2-ternate	3-pinnate
Persistence	usually deciduous	usually deciduous	persistent	persistent
Outline of blade	ovate to triangular	elliptic to rhombic	triangular to pentagonal	ovate or ovate-oblong
Central/terminal leaflet division	1- or 2-pinnatisect	2-pinnatisect	2-pinnatisect	1-pinnatisect
Central/terminal leaflet shape	triangular or ovate-rhombic	triangular or ovate-rhombic	ovate or rhombic	ovate-rhombic
Ultimate segments shape	narrowly oblong-lanceolate to linear	narrowly oblong-lanceolate to linear	narrowly lanceolate	linear
Ultimate segments apex	acute	acute	acute	cuspidate with spine 1–1.5 mm long
Cauline leaves				
Division	1-pinnatisect	1- or 2-pinnatisect	deeply 3-lobed	entire or 3-lobed
Uppermost one shape	ovate to rhombic	ovate to rhombic	ovate	linear or lanceolate
Inflorescences				
No. of flowers per umbellet	16–23	15–25	15–20	20–24
No. of rays	12–16	16–18	10–20	15–25
No. of bracts	1 or 2	1	usually absent, rarely 1 or 2	5–7
No. of bractlets	6–10	5–6	6 or 8, rarely 9	6–9
Flowers				
Petal color	white	white	white or pinkish	white or pinkish white
Petal shape	obcordate	obcordate	oblong to obovate	obovate-orbicular
Petal size (mm)	0.9–1.2 × 0.7–1.2	0.7–1.3 × 0.9–1.6	approximately 1 × 0.8	0.5–1 × 0.7–1
Anther color	purple	yellowish white	pale yellow	pale yellow
Anther size (mm)	0.3–0.5 × 0.4–0.5	0.5–1.1 × 0.8–1.2	0.2–0.3 × ca. 0.2	0.3–0.4 × 0.2–0.3
Fruit				
Carpophore length (mm)	3.4–4.5	2.1–2.4	2.5–4.5	2.9–3.8
Mericaip size (mm)	3.7–5 × 2.4–2.7	3.8–4.4 × 1.5–2	3.7–4 × 2.3–2.5	3–4 × 2–3
Pubescence on dorsal side	moderately to densely pubescent with short simple unicellular hairs	subglabrous to sparsely tuberculate	sparsely tuberculate [†]	moderately to densely pubescent with short simple unicellular hairs [†]
Marginal wings width (mm)	0.2–0.7	0.2–0.3	approximately 0.5	0.5–0.8
No. of vittae	8 or 9	13–16	18–28	6
No. of vittae per vallicula / on commissure	1 or (2) / 4	3 / 4	3 or 4 / 6–12	1 / 2

* Refer to the Park et al. (2017), Flora of Korea, Vol. 5c. Rosidae: Rhamnaceae to Apiaceae. † Newly updated description of mericaip surface in the present study.

plish below middle, purplish green apically, branched, 4–7 mm in diameter, terete, longitudinally grooved, solid, glabrous, with fibrous remnants of basal leaves. Leaves basal and cauline, alternate, pinnately compound, petiolate, petiole sheathing at base; stipules absent. Basal leaves many, 2-pinnate, usually deciduous; petiole 5.6–9.5 cm long, glabrous; sheath purplish or purplish green, cylindrical, not inflated, 1.1–1.8 cm × 5–7.5 mm, margins scarious, glabrous; blade ovate to triangular in outline, 6.5–11.5 × 7.3–10.6 cm, both surfaces green, glabrous; petiolule of terminal leaflet (0.8–)1.7(–3.5) cm long; terminal leaflet triangular or ovate-rhombic, 1- or 2-pinnatisect, 1.5–2.2 × 1.5–2.6 cm, apex acute, base cuneate, margins entire; petiolule of basal lateral leaflets 0.7–2.7 cm long; lateral leaflets elliptic-ovate to ovate, 1- or 2-pinnatisect, 1.8–5 × 1.3–3.7 cm, apex acute, base cuneate, margins entire, uppermost ones sessile; ultimate segments narrowly oblong-lanceolate to linear, 0.5–1.2 cm × 1.8–3.5 mm. Cauline leaves similar to basal ones and becoming smaller upward; petiole of lower cauline leaves (1.5–)4.8–8 cm long, reduced upward, glabrous; blade elliptic to ovate in outline; uppermost cauline leaves ovate to rhombic, 1-pinnatisect, 0.6–1 × 0.5–1.2 cm, sessile. Inflorescences terminal and lateral, with 2–10 compound umbels, more or less flat-topped, 6.5–7 cm in diameter; umbellets hermaphroditic, 16- to 23-flowered, 1.1–1.5 cm in diameter; peduncle 2.5–6 cm long, sparsely pubescent with short simple unicellular hairs, uppermost part densely pubescent; rays 12–16, spreading to ascending, 1–2.7 cm long, unequal in length, adaxial surface sparsely pubescent with short simple unicellular hairs; bracts 1 or 2, persistent or sometimes caducous, lanceolate, entire, 0.9–1.2 cm × 1–1.8 mm, apex acute, margins scarious, glabrous; pedicels 1.5–7 mm long, adaxial surface sparsely pubescent with simple unicellular hairs; bractlets 6–10, persistent, linear, entire, 2.6–6.7 × 0.4–0.6 mm, apex acute, glabrous. Flowers bisexual, actinomorphic, 1.8–2.1 mm in diameter; calyx 5-toothed; calyx teeth minute, narrowly triangular, 0.2–0.5 × 0.1–0.3 mm, adaxial surface glabrous, abaxial surface sparsely pubescent with short conical simple unicellular hairs; petals 5, white, obcordate, 0.9–1.2 × 0.7–1.2 mm, apex incurved, base cuneate to caudate, with greenish yellow line on abaxial surface, glabrous; stamens 5, alternating with petals, with purplish dots; filaments filiform, 1.2–2 mm long; anthers 2-locular, purple, introrse, versatile, dehiscent longitudinally, subglobose, 0.3–0.5 × 0.4–0.5 mm; pistil 1, 2-carpellate; ovary inferior, syncarpous, 2-locular, moderately to densely pubescent with short simple unicellular hairs; stylopodium conical; styles 2, free, ascending, 0.2–0.5 mm at anthesis, 1.0–1.5 mm in fruit, swollen at base to form a stylopodium, reflexed in fruit; ovule 1 per locule, anatropous, pendulous. Fruit a dry schizocarp composed of 2 mericarps, pale brown to brown at maturity, oblong; carpophore 3.4–4.5 mm long, 2-cleft; mericarps splitting apart at maturity, oblong, dorsally compressed, 3.7–5.0 × 2.4–2.7 mm, moderately to densely pubescent with short simple unicellular hairs on dorsal surface, glabrous on commissural surface; dorsal ribs 3, prominent, not winged; marginal ribs 2, slightly winged; wings 0.2–0.7 mm wide, scarious; secondary ribs absent; vittae (oil tubes) 8 or 9, 1 or (2) per vallecula and 4 on commissure; commissure 1.7–3.6 mm wide. Seed 1 per mericarp; narrowly oblong in cross-section; face plane.

Phenology. Flowering September to October. Fruiting October to November.

Etymology. The specific epithet '*miroense*' refers to Miro-myeon, Samcheok-si, where the type specimen was collected.

Vernacular name. Mi-ro-gi-reum-na-mul.

Distribution and ecology. *Peucedanum miroense* is restricted to only two populations on the summits of Swinŭm-san and Duta-san at Miro-myeon, Samcheok-si, Gangwon Province, South Korea. The two populations are connected to each other. The plants occur in rocky areas at the top of the mountains at an elevation of 540–680 m (Fig. 5). One population, at the type locality on Swinŭm-san, was growing with *Allium thunbergii* G. Don (Amaryllidaceae), *Dendranthema boreale* (Makino) Y. Ling ex Kitam. (Asteraceae), *Fraxinus sieboldiana* Blume (Oleaceae), *Lespedeza bicolor* Turcz., *L. maximowiczii* C.K. Schneid. (Fabaceae), *Peucedanum terebinthaceum* (Fischer ex Trevir.) Turcz. (Apiaceae), *Pinus densiflora* Siebold & Zucc. (Pinaceae), *Quercus mongolica* Fisch. ex Turcz. (Fagaceae), *Rhododendron mucronulatum* Turcz. (Ericaceae), *Sedum polytrichoides* Hemsl. (Crassulaceae), and *Spodiopogon sibiricus* Trin. (Poaceae). The other population of *P. miroense* on Duta-san was growing with *Aconogonon microcarpum* (Kitag.) H. Hara (Polygonaceae), *Chrysanthemum zawadskii* Herlich (Asteraceae), and *Geranium koreanum* Kom. (Geraniaceae). Each population of *P. miroense* comprised approximately 120 individuals.

Additional specimens examined (Paratypes). KOREA. Gangwon Province: Samcheok-si, Miro-myeon, Naemiro-ri, Swinŭm-san, 37°26'46.5"N, 129°01'41.0"E, alt. 535 m, 12 October 2014, K. Kim & H.-J. Suh, KK#4 (SNU).

Proposed IUCN conservation status. After conducting fieldwork throughout the country and examining specimens from several domestic herbaria, we found out that *Peucedanum miroense* is known only from Miro-myeon, Gangwon. Therefore, according to the IUCN criteria, *P. miroense* is classified as endangered (IUCN 2022; EN D) because the known number of individuals occurring at Swinŭm-san and Duta-san in Gangwon Province, South Korea, is less than 250.

Taxonomic notes. *Peucedanum miroense* is morphologically similar to *P. elegans* and *P. hakuunense* among species with linear ultimate leaf segments. *Peucedanum miroense* is clearly distinguishable from *P. elegans*, which is restricted to mountain slopes in North Korea, by the shape of the leaf apex, the number of bracts, pubescence of the mericarp, and the number of vittae per mericarp (non-overlapping character states). *Peucedanum miroense* has an acute leaf apex, 1 or 2 bracts, moderate to dense pubescence with short simple unicellular hairs on the dorsal surface of the mericarps, and 8 or 9 vittae [1 or (2) per vallecule and 4 per commissure] whereas *P. elegans* has spine-tipped ultimate leaf segments, 5–7 bracts, glabrous mericarps, and 6 vittae (1 per vallecule and 2 per commissure) (Table 1).

Additionally, *P. miroense* is easily distinguishable from *P. hakuunense*, which is only in the southern part of South Korea, on the basis of its 2-pinnate leaves, obcordate petals, purple anthers, 8 or 9 vittae [1 or (2) per vallecule and 4 per commissure]; *P. hakuunense* has 3-ternate leaves, persistent basal leaves, oblong to obovate petals, and 18–28 vittae (3 or 4 per vallecule and 6–12 per commissure) (Table 1).

The natural habitat of *P. miroense* on Swinŭm-san and Duta-san in Gangwon Province is one of the major limestone areas in Korea, with sedimentary rock outcrops consisting of calcium carbonate. *Peucedanum miroense* can be considered a calciphile and added to the limestone flora of Korea (Kim et al. 2021).

***Peucedanum tongkangense* K. Kim, H.J.Suh & J.H.Song, sp. nov.**

urn:lsid:ipni.org:names:77305893-1

Figs 3, 4, 6B

Type. KOREA. Gangwon Province: Jeongseon-gun, Sindong-eup, Unchi-ri, Donggang River, rocky cliffs along the riverside, 37°16'25.7"N, 128°36'33.8"E, alt. 264 m, 8 September 2021, *J.H.Song* & *S. Yang*, *KIOM-2021-802-1* [Holotype: KIOM! (Fig. 6B); Isotype KB!].

Diagnosis. *Peucedanum tongkangense* is similar to *P. miroense*, but differs in its subglabrous (vs. pubescent) ovary, yellowish white (vs. purple) anthers, narrowly ellipsoid (vs. oblong) schizocarp, 13–16 vittae (3 per vallecule, 4 on commissure) [vs. 8 or 9 vittae, 1 or (2) per vallecule, 4 on commissure] per mericarp. *Peucedanum tongkangense* is also similar to *P. elegans* and *P. hakuunense* but is distinct from both in the acute (vs. spine-tipped) apex of the ultimate leaf segments and 2-pinnate (vs. 1- or 2-ternate) leaves (Table 1).

Description. Herb, perennial, hermaphroditic, (60–)75–95(–120) cm tall. Root a taproot, whitish or pale yellow, elongated, thickened, 17–23 × 0.4–1.5 cm. Rhizomes erect or ascending, yellowish white, cylindrical, approximately 0.6–1.1 cm in diameter, woody. Stems erect, purplish green, much branched, 3–9 mm in diameter, terete, longitudinally grooved, solid, glabrous, with fibrous remnants of basal leaves. Leaves basal and cauline, alternate, pinnately compound, petiolate; petiole sheathing at base; stipules absent. Basal leaves many, 3-pinnate, usually deciduous; petiole 8.5–10.5 cm long, glabrous; sheath purplish or yellowish green, cylindrical, not inflated, 1.3–2 cm × 3.6–8.5 mm, margins scarios, glabrous; blade elliptic to rhombic in outline, 15–21.5 × 12–16.8 cm, both surfaces green, glabrous; petiolule of terminal leaflet 2.7–4.8 cm long; terminal leaflet triangular or ovate-rhombic, 2-pinnatisect, 3.5–5 × 2.8–4.1 cm, apex acute, base cuneate, margins entire; petiolule of basal lateral leaflets 1.8–3.8 cm long; lateral leaflets elliptic to elliptic-ovate, 3-pinnatisect, 7.1–9.9 × 4.7–5.4 cm, apex acute, base cuneate, margins entire, uppermost leaflets sessile; ultimate segments narrowly oblong-lanceolate to linear, 1.3–2 cm × 2.8–4.3 mm. Cauline leaves similar to basal ones and becoming smaller upward; petiole of lower cauline leaves (2–)2.8–4.5 cm long, reduced upward, glabrous; blade elliptic to ovate in outline; uppermost cauline leaves ovate to rhombic, 1- or 2-pinnatisect, 0.9–2.4 × 1.1–2.7 cm, sessile. Inflorescences terminal and lateral, with 15–48 compound umbels, more or less flat-topped, 3.5–8.8 cm in diameter; umbellets hermaphroditic, 15- to 25-flowered, 0.5–1.2 cm in diameter; peduncle 2.5–5 cm long, glabrous; rays 16–18, spreading to ascending, 1–2.5 cm long, unequal in length, adaxial surface sparsely pubescent with short simple unicellular hairs; bract 1, persistent or sometimes caducous, lanceolate, entire, 0.7–2 cm × 1–1.5 mm, apex acute, margins scarios, glabrous; pedicels 1.5–2.5(–5) mm long, adaxial surface sparsely pubescent with simple unicellular hairs; bractlets 5–6, persistent, linear, entire, 2.5–7 × 0.4–0.8 mm, apex acute, glabrous. Flowers bisexual, actinomorphic, 2.4–3.2 mm in diameter; calyx 5-toothed; calyx teeth minute, narrowly triangular, 0.2–0.4 × 0.1–0.2 mm, adaxial surface glabrous, abaxial surface sparsely pubescent with short

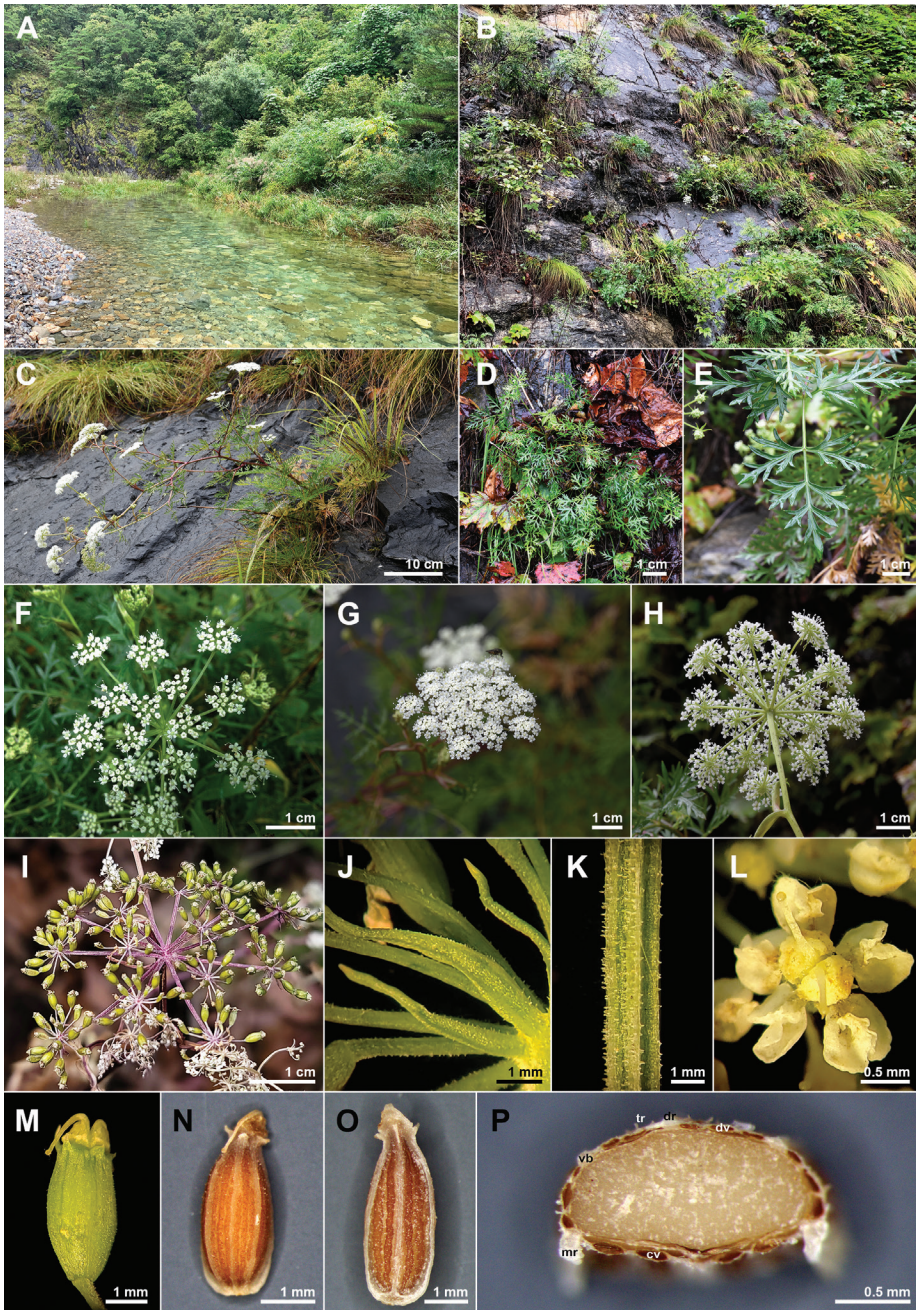


Figure 3. Photographs of *Peucedanum tongkangense* K. Kim, H.J.Suh & J.H.Song **A–C** habitat **D** basal leaves **E** cauline leaf **F** compound umbel (early flowering stage) **G–H** compound umbel (mature flowering stage) **I** compound umbel (fruiting stage) **J** bractlets **K** rays **L** flowers **M** calyx teeth and stylopodium (mature fruiting stage) **N** dorsal side of mericarp **O** commissural side of mericarp **P** transverse plane of mericarp. cv, commissure vittae; dr, dorsal ribs; dv, vallicula vittae; mr, marginal ribs; tr, trichomes; vb, vascular bundles.

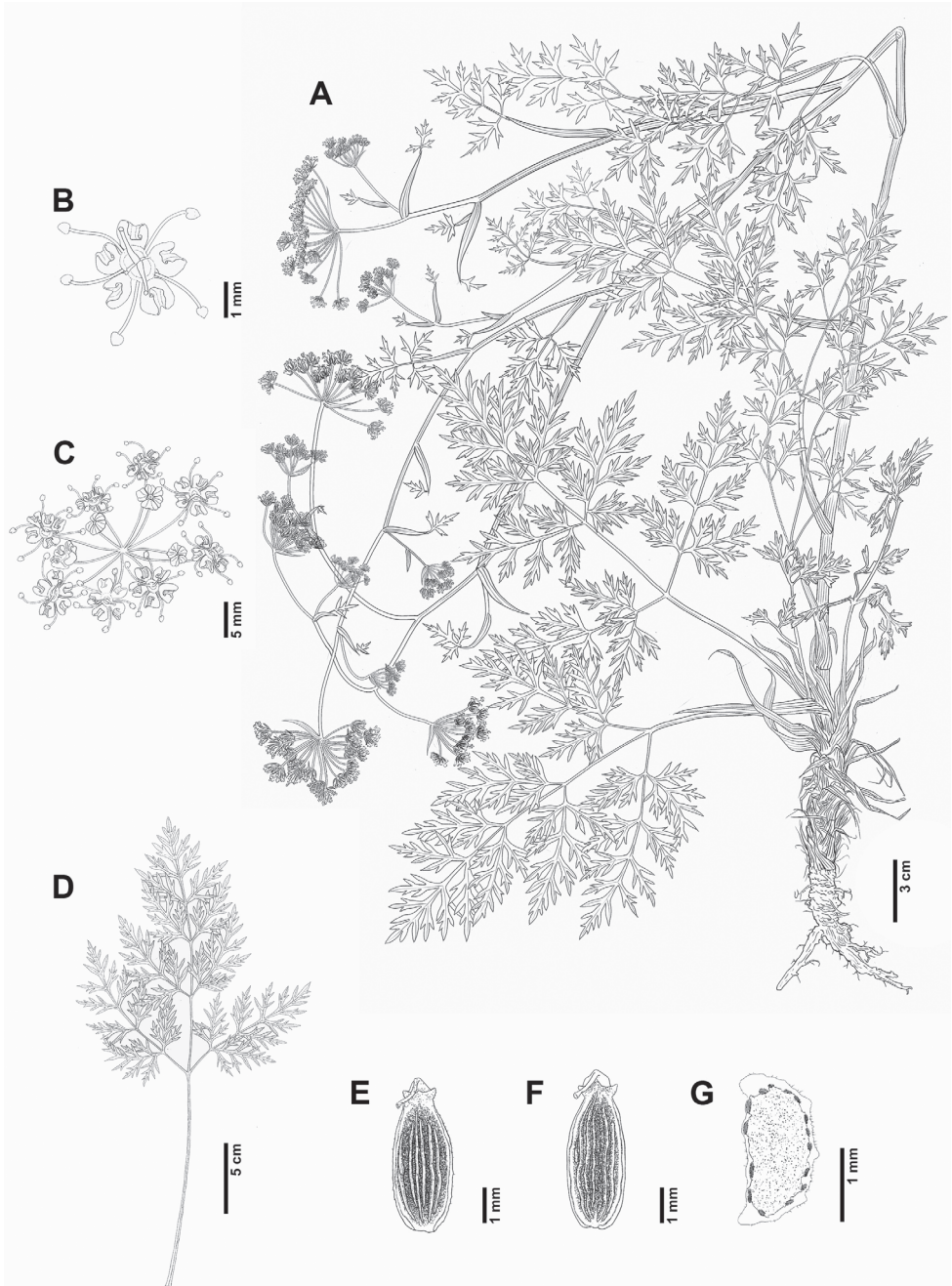


Figure 4. *Peucedanum tongkangense* K. Kim, H.J.Suh & J.H.Song **A** habit **B** flower **C** umbellet **D** basal cauline leaf **E** mericarp (dorsal side) **F** mericarp (commissural side) **G** mericarp (cross-section) (A–F J.H.Song & S. Yang, KIOM2021-729-1).

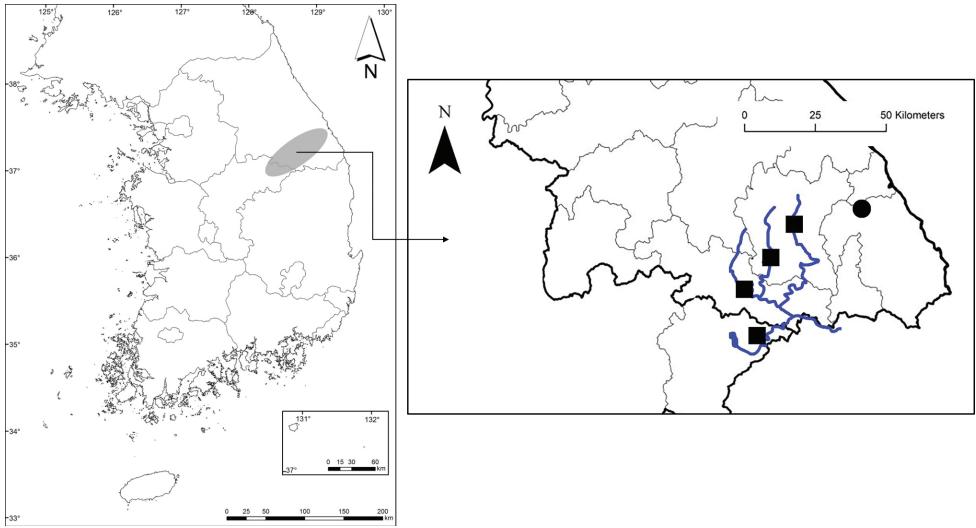


Figure 5. Distribution of *Peucedanum miroense* and *P. tongkangense* = gray ellipse. *P. miroense* = black circle. *P. tongkangense* = black squares. Blue lines: rivers.

conical simple unicellular hairs or glabrous; petals 5, white, obcordate, 0.7–1.3 × 0.9–1.6 mm, apex incurved, base cuneate to caudate, glabrous; stamens 5, alternating with petals; filaments filiform, 1.6–2.5 mm long; anthers 2-locular, yellowish white, introrse, versatile, dehiscing longitudinally, subglobose, 0.5–1.1 × 0.8–1.2 mm; pistil 1, 2-carpellate; ovary inferior, syncarpous, 2-locular, subglabrous; stylopodium conical; styles 2, free, ascending, 0.3–0.7 mm at anthesis, 1.0–1.7 mm in fruit, swollen at base to form a stylopodium, reflexed in fruit; ovule 1 per locule, anatropous, pendulous. Fruit a dry schizocarp composed of 2 mericarps, pale brown to brown at maturity, narrowly ellipsoid; carpophore 2.1–2.4 mm long, 2-cleft; mericarps splitting apart at maturity, narrowly ellipsoid, slightly dorsally compressed, 3.8–4.4 × 1.5–2 mm, subglabrous to sparsely tuberculate on dorsal side, glabrous on commissural side; dorsal ribs 3, filiform, not winged; marginal ribs 2, slightly winged; wings 0.2–0.3 mm wide, scarious; secondary ribs absent; vittae 13–16, 3 per vallecule and 4 on commissure; commissure 0.9–1.2 mm wide. Seed 1 per mericarp; oblong in cross-section; face plane.

Phenology. Flowering September to October. Fruiting October to November.

Etymology. The specific epithet '*tongkangense*' refers to the rocky cliffs along the Donggang River, where the type specimen was collected.

Vernacular name. Dong-gang-gi-reum-na-mul

Distribution and ecology. *Peucedanum tongkangense* grows in open areas on rocky cliffs near the Donggang River in Gangwon Province and the Namhangang River in North Chungcheong Province, South Korea. Five populations were found: the type locality and those at Unchi-ri, Sindong-eup, Jeongseon-gun, Gangwon Province, along the Dong-gang river at 150–400 m elevations (Fig. 5). The type locality was growing with *Artemisia sacrorum* Ledeb. var. *iwayomogi* (Kitam.) M.S. Park



Figure 6. Holotype of **A** *Peucedanum miroense* K. Kim, H.J.Suh & J.H.Song (*J.H.Song & S. Yang*, KIOM-2021-646-1) and **B** *P. tongkangense* K. Kim, H.J.Suh & J.H.Song (*J.H.Song & S. Yang*, KIOM-2021-802-1).

& G.Y. Chung, *Aster scaber* Thunb., *Galinsoga ciliata* (Raf.) S.F. Blake (Asteraceae), *Boehmeria spicata* (Thunb.) Thunb. (Urticaceae), *Calamagrostis purpurea* (Trin.) Trin. (Poaceae), *Carex siderosticta* Hance (Cyperaceae), *Humulus scandens* (Lour.) Merr. (Cannabaceae), *Isodon inflexus* (Thunb.) Kudô (Lamiaceae), *Parthenocissus tricuspidata* (Siebold & Zucc.) Planch. (Vitaceae), *Polystichum craspedosorum* (Maxim.) Diels (Dryopteridaceae), *Rubia argyi* (H. Lév. & Vaniot) H. Hara ex Lauener & D.K. Ferguson (Rubiaceae), *Scabiosa comosa* Fisch. ex Roem. & Schult. (Caprifoliaceae), and *Spiraea blumei* G. Don (Rosaceae). Three populations of *P. tongkangense* were also found along the Donggang River where they were growing with *Aster yomena* (Kitam.) Honda (Asteraceae), *Clematis serratifolia* Rehder (Ranunculaceae), and *Trichophorum dioicum* J. Jung & H.K. Choi (Cyperaceae). The fifth population was near the Namhangang River in North Chungcheong Province where it was growing with *Gypsophila oldhamiana* Miq. (Caryophyllaceae), *Mukdenia rossii* (Oliv.) Koidz. (Saxifragaceae), *Patrinia rupestris* (Pall.) Dufur. (Caprifoliaceae), *Potentilla dickinsii* Franch. & Sav. (Rosaceae), *Pyrrosia petiolosa* (Christ) Ching (Polypodiaceae), and *Selaginella stauntoniana* Spring (Selaginellaceae).

Additional specimens examined (Paratypes). KOREA. Gangwon Province: Yeongwol-gun, Seo-myeon, Ongjeong-ri, 37°13'5.3"N, 128°20'56.6"E, alt. 234 m, 13 Octo-

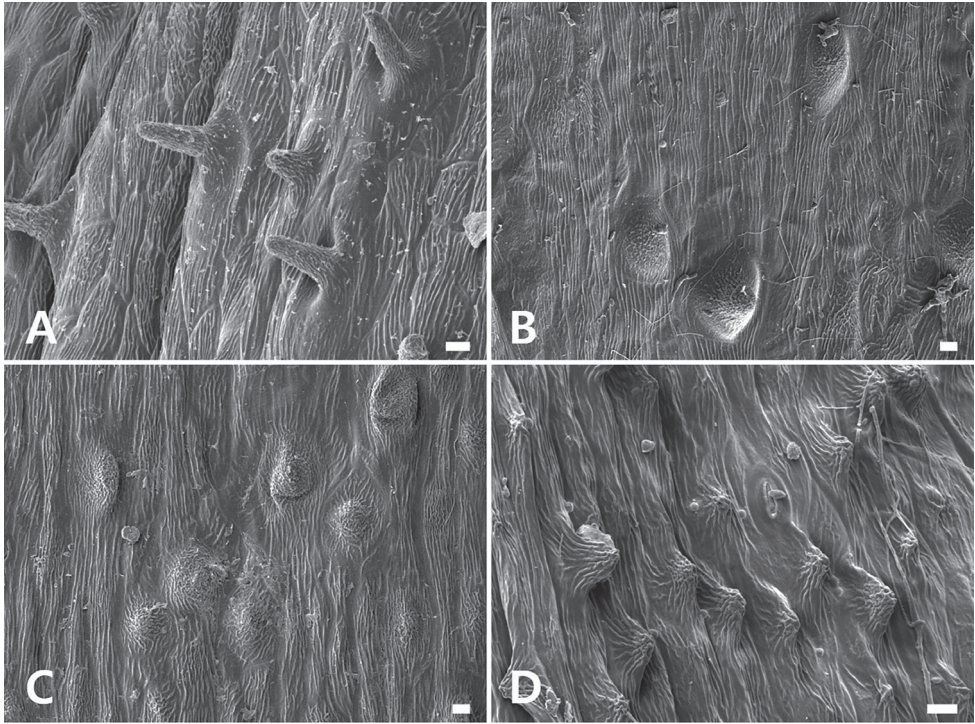


Figure 7. Scanning electron micrographs of mericarp surface of four species of *Peucedanum* **A** *P. miroense* **B** *P. tongkangense* **C** *P. hakuunense* **D** *P. elegans*. All scale bars: 10 μ m.

ber 2010, *B.-Y. Lee et al.*, SHY2322 (KB); Gangwon Province: Jeongseon-gun, Hwaam-myeon, Bukdong-ri, 37°22'4.78"N, 128°47'54.35"E, alt. 687 m, 25 September 2012, *G.-H. Nam & J.-H. Kim*, SHY3-2023 (KB); Jeongseon-eup, Yeotan-ri, 37°22'05.6"N, 128°43'41.9"E, alt. 30 October 2016, *K. Kim & H.-J. Suh*, KK3510 (SNU); Gangwon Province: Jeongseon-gun, Nam-myeon, Nakdong-ri, 37°18'38.47" N, 128°42'43.27"E, alt. 719 m, 01 September 2016, *J.-H. Kim & H.-J. Park*, Beaki161681 (KB).

Proposed IUCN conservation status. After conducting field surveys throughout the country and examining specimens from several domestic herbaria, three more populations along the Donggang River, Gangwon Province were documented for *Peucedanum tongkangense*. According to the IUCN criteria, *P. tongkangense* is classified as least concern (IUCN 2022; LC), because it is distributed widely and a considerable number of individuals is known.

Taxonomic notes. *Peucedanum tongkangense* is morphologically similar to *P. miroense* but it is clearly distinct due to its subglabrous ovary, yellowish white anthers, narrowly ellipsoid schizocarp, and 13–16 vittae (3 per vallecule and 4 on commissure) in mericarp; *P. miroense* has a pubescent ovary, purple anthers, oblong schizocarp, and 8–10 vittae [1 or (2) per vallecule and 4 on commissure]. Additionally, *P. tongkangense* is similar to *P. elegans* and *P. hakuunense* but is distinguished from *P. elegans* by the

acute apex of the ultimate leaf segments (vs. spine-tipped) and from *P. hakuunense* by its 2-pinnate leaves (vs. 1- or 2-ternate leaves) (Table 1).

North Chungcheong Province is also a major limestone area in Gangwon Province. Thus, it is necessary to add *P. tongkangense* to the limestone flora list for Korea (Kim et al. 2021).

Comparative mericarp micromorphology

Micromorphological characteristics of fruits using scanning electron microscopy (SEM) have provided valuable information in classifying and identifying taxa of Apiaceae (Ostroumova 2018 and references therein). Significantly, SEM micrographs helped to visualize trichome types and small rounded projections, such as tubercules (Ostroumova 2018; Lee et al. 2018).

In our study, we found that *P. miroense* and *P. elegans* have short, simple unicellular hairs with a striate surface. Hair length in *P. miroense* was up to 40 µm long, and up to 10 µm long in *P. elegans* (Fig. 7). *Peucedanum tongkangense* and *P. hakuunense* had tubercules 20–30 µm in diameter (Fig. 7). The micromorphological measurements of the mericarps of *P. miroense* and *P. tongkangense* differ from other species. *Peucedanum* has at least two types of mericarp surface.

Key to the species of *Peucedanum* in Korea

- 1 Basal and cauline leaves 1- to 3-pinnately compound..... 2
- 2 Ultimate segments of leaves linear..... 3
- 3 Umbellets 20- to 44-flowered. Vittae 6, 1 per vallecule and 2 on commissural face 4
- 4 Leaves 2-pinnately compound; blade triangular to broadly ovate in outline; ultimate segments linear-lanceolate, apex acute, not spine-tipped. Bracts 1 or 2 **1. *P. paishanense***
- 4' Leaves 2- or 3-pinnately compound; blade ovate in outline; ultimate segments linear, apex spine-tipped. Bracts 5–7..... **2. *P. elegans***
- 3' Umbellets 16- to 20-(to 27)-flowered. Vittae 8–18, 1–3 per vallecule, 4 or 6 on commissural face..... 5
- 5 Plants 10–20 cm tall. Bracts 2–7; bractlets 10–12..... **3. *P. coreanum***
- 5' Plants 50–80 cm tall. Bract 1 or absent; bractlets 6–10..... 6
- 6 Anthers purple. Mericarp pubescent with short simple hairs. Schizocarp oblong; vittae 8 or 9, 1 or (2) per vallecule, 4 on commissural face **4. *P. miroense***
- 6' Anthers yellowish white. Mericarp subglabrous to sparsely tuberculate. Schizocarp narrowly ellipsoid; vittae 13–16, 3 per vallecule, 4 on commissural face **5. *P. tongkangense***
- 2' Ultimate segments of leaves lanceolate to elliptic, not linear 7
- 7 Apex of ultimate leaf segments acute; vittae 6, 1 per vallecule and 2 on commissure **6. *P. terebinthaceum***

- 7' Apex of ultimate leaf segments rounded; vittae 20–38; 3 or 4 per vallecule and 8–12 on commissure..... **8**
- 8 Leaf blades ovate to triangular in outline, both surfaces glabrous. Bracts 1–4, lanceolate; bractlets 4–8, lanceolate to narrowly triangular.... **7. *P. chujaense***
- 8' Leaf blades triangular or broadly triangular in outline, both surfaces sparsely pubescent with short simple hairs along veins. Bracts 1, 2 or absent, lanceolate or narrowly triangular; bractlets 8–10, lanceolate to linear..... **8. *P. litorale***
- 1' Basal and cauline leaves 1- or 2-ternately compound **9**
- 9 Leaves coriaceous, both surfaces glaucous; ultimate leaf segments obovate or elliptic. Calyx teeth obsolete. Seed face slightly concave in cross-section **9. *P. japonicum***
- 9' Leaves not coriaceous, adaxial surface green, abaxial surface pale green; ultimate leaf segments linear. Calyx teeth prominent, triangular. Seed face plane in cross-section **10. *P. hakuunense***

Acknowledgements

We thank the directors of the herbaria (KB, KH, and SNU) for granting us permission to examine the specimens. This research was supported by the National Research Foundation of Korea (NRF) grant funded by the Korean government (MSIT) (NRF-2020R1A2C1100147) to J.H.Song. The corresponding author sincerely thanks Dr. Sungyu Yang (Korea Institute of Oriental Medicine) for his help with the field survey. Finally, we are grateful to the editor, Leandro Giacomini, and two anonymous reviewers for their suggestions regarding the manuscript.

References

- Chung TH (1957) Korean Flora, Vol. 2. Herbaceous Plants. Sinjisa, Seoul, 1025 pp.
- Drude CGO (1898) Umbelliferae. In: Engler A, Prantl A (Eds) Die Natürlichen Pflanzenfamilien, Vol. 3. Wilhelm Engelmann, Leipzig, 63–250.
- Gurbuz P, Baran MY, Demirezer LO, Guvenalp Z, Kuruuzum-Uz A (2018) Phenylacylated-flavonoids from *Peucedanum chryseum*. Revista Brasileira de Farmacognosia 28(2): 228–230. <https://doi.org/10.1016/j.bjpt.2018.01.003>
- Hiroe M (1979) Umbelliferae of World. Ariake Book Company, Tokyo, 2128 pp.
- IUCN (2022) Guidelines for using the IUCN red list categories and criteria, version 15. Prepared by the standards and petitions committee. <https://www.iucnredlist.org/documents/RedListGuidelines.pdf> [accessed 21.02.2022]
- Kim K, Kim CS, Oh SH, Park CW (2019) A new species of *Peucedanum* (Apiaceae) from Korea. Phytotaxa 393(1): 75–83. <https://doi.org/10.11646/phytotaxa.393.1.7>
- Kim JH, Nam GH, Lee SB, Shin S, Kim JS (2021) A checklist of vascular plants in limestone areas on the Korean Peninsula. Korean Journal of Plant Taxonomy 51(3): 250–293. <https://doi.org/10.11110/kjpt.2021.51.3.250>

- Kitagawa M (1972) *Peucedanum* L. In: Kitagawa M (Ed.) Neo-Lineamenta Florae Manshuri-cae. J. Cramer, Hirschberg, 486–487.
- Lee WT (1996) Lineamenta Florae Koreane. Academy Publishing Co., Seoul, 1688 pp.
- Lee BY (2018) *Peucedanum* L. In: Flora of Korea Editorial Committee (Eds) The Genera of Vascular Plants of Korea. Hongreung Publishing Co., Seoul, 1006–1007. [in Korean]
- Lee J, Lee YJ, Kim J, Bang OS (2015) Pyranocoumarins from root extracts of *Peucedanum praeruptorum* Dunn with multidrug resistance reversal and anti-inflammatory activities. *Molecules* (Basel, Switzerland) 20(12): 20967–20978. <https://doi.org/10.3390/molecules201219738>
- Lee C, Kim J, Darshetkar AM, Choudhary RK, Park SH, Lee J, Choi S (2018) Mericarp morphology of the tribe Selineae (Apiaceae, Apioideae) and its taxonomic implications in Korea. *Bangladesh Journal of Plant Taxonomy* 25(2): 175–186. <https://doi.org/10.3329/bjpt.v25i2.39524>
- Morioka T, Suzui M, Nabandith V, Inamine M, Aniya Y, Nakayama T, Ichiba T, Mori H, Yoshimi N (2004) Themodifying effect of *Peucedanum japonicum*, a herb in the Ryukyu Islands, on azoxymethane-induced colon preneoplastic lesions in male F344 rats. *Cancer Letters* 205(2): 133–141. <https://doi.org/10.1016/j.canlet.2003.10.002>
- Ostroumova TA (2018) Fruit micromorphology in the Umbelliferae of the Russian Far East. *Botanica Pacifica: Journal of Plant Science and Conservation* 7(1): 41–49. <https://doi.org/10.17581/bp.2018.07107>
- Ostroumova TA, Pimenov MG (1997a) Carpological diversity in African *Peucedanum* s.l. (Umbelliferae) I. The species of southern Africa. *Feddes Repertorium* 108(5–6): 299–318. <https://doi.org/10.1002/fedr.19971080503>
- Ostroumova TA, Pimenov MG (1997b) Carpological diversity in African *Peucedanum* s.l. (Umbelliferae) II. The species of Tropical Africa. *Feddes Repertorium* 108(7–8): 533–547. <https://doi.org/10.1002/fedr.19971080706>
- Park CW, Lee BY, Song JH, Kim K (2017) *Peucedanum* L. In: Flora of Korea Editorial Committee (Eds) Flora of Korea, Vol. 5c. Rosidae: Rhamnaceae to Apiaceae. Junghaengsa, Seoul, 141–146.
- Pimenov MG (1986) *Kitagawia* – A new Asiatic genus of the family Umbelliferae. *Botanicheskii Zhurnal* (Moscow & Leningrad) 71(7): 942–949.
- Pimenov MG, Leonov MV (1993) The Genera of the Umbelliferae: A Nomenclator. Royal Botanic Gardens, Kew, London, 156 pp.
- Sarkhail P (2014) Traditional uses, phytochemistry and pharmacological properties of the genus *Peucedanum*: A review. *Journal of Ethnopharmacology* 156: 235–270. <https://doi.org/10.1016/j.jep.2014.08.034>
- Shan RH, Sheh ML (1992) *Peucedanum* L. In: Shan RH, Sheh ML (Eds) Flora Reipublicae Popularis Sinicae, Vol. 55 (3). Science Press, Beijing, 123–160.
- Sheh ML, Watson MF (2005) *Peucedanum* Linnaeus In: Wu ZY, Raven PH, Hong DY (Eds) Flora of China, Vol. 14 (Apiaceae through Ericaceae). Science Press, Beijing, & Missouri Botanical Garden Press, St. Louis, 182–192.
- Shishkin BK (1951) *Peucedanum* L. In: Shishkin BK (Ed.) Flora of the USSR, Vol. 17. Izdatel'stvo Akademii Nauk SSSR, Moskva-Leningrad, 168–203. [English translation (1974) Israel Program for Scientific Translations, Jerusalem]
- Shneyer VS, Kut'yavina NG, Pimenov MG (2003) Systematic relationships within and between *Peucedanum* and *Angelica* (Umbelliferae-Peucedaneae) inferred from immunological

- studies of seed proteins. *Plant Systematics and Evolution* 236(3–4): 175–194. <https://doi.org/10.1007/s00606-002-0239-4>
- Song Y, Jing W, Yan R, Wang Y (2015) Research progress of the studies on the roots of *Peucedanum praeruptorum* Dunn (Peucedani radix). *Pakistan Journal of Pharmaceutical Sciences* 28(1): 71–81.
- Spalik K, Reduron JP, Downie SR (2004) The phylogenetic position of *Peucedanum* sensu lato and allied genera and their placement in tribe Selineae (Apiaceae, subfamily Apioideae). *Plant Systematics and Evolution* 243(3): 189–210. <https://doi.org/10.1007/s00606-003-0066-2>
- Thellung A (1926) *Peucedanum* L. In: Hegi G (Ed.) *Illustrierte Flora von Mitteleuropa*, Vol. 5. J.F. Lehmanns Verlag, Munich, 1363–1415.
- Thiers B (2022) [continuously updated] *Index Herbariorum: a global directory of public herbaria and associated staff*. New York Botanical Garden, Bronx. <http://sweetgum.nybg.org/ih/> [accessed 21.02.2022]

Smithia yehii (Leguminosae, Papilionoideae), a new species from Taiwan

Chiu-Mei Wang¹, Chih-Yi Chang², Yen-Hsueh Tseng^{2,3}

1 Department of Biology, National Museum of Natural Science, 1 Guancian Rd., Taichung 40453, Taiwan

2 Department of Forestry, National Chung-Hsing University, No. 145, Hsing-Ta Rd., Taichung 40227, Taiwan

3 Taiwan Forestry Research Institute, No. 53, Nanhai Rd., Zhongzheng Dist., Taipei City, 10066, Taiwan

Corresponding author: Yen-Hsueh Tseng (tseng2005@nchu.edu.tw)

Academic editor: Patrick Herendeen | Received 20 July 2022 | Accepted 8 September 2022 | Published 29 September 2022

Citation: Wang C-M, Chang C-Y, Tseng Y-H (2022) *Smithia yehii* (Leguminosae, Papilionoideae), a new species from Taiwan. *PhytoKeys* 210: 53–65. <https://doi.org/10.3897/phytokeys.210.90958>

Abstract

A new species of *Smithia* Aiton, *S. yehii* C.M.Wang, Chih Y.Chang & Y.H.Tseng, **sp. nov.** from the wetlands of Taiwan is reported in this article. This species was mistakenly identified as *S. sensitiva* Aiton, but can be distinguished by its pale yellow corolla (vs. vivid yellow), often smaller flowers and shorter style. There is also a color gradient on the adaxial surface of the leaflets between young and mature leaves. Surface sculpture of pollen of *S. yehii* has significantly larger perforations, and muri are wider than those of *S. sensitiva*. An identification key to the *Smithia* taxa of Taiwan and *S. sensitiva* is presented.

Keywords

endangered (EN), macro-morphology, pollen morphology, scanning electron microscopy (SEM), *Smithia ciliata* Royle, *S. sensitiva* Aiton

Introduction

The genus *Smithia* Aiton belongs to the tribe Aeschynomeneae (Benth.) Hutch., Papilionoideae DC., Leguminosae Juss. (LPWG 2017) and contains c. 20 species (Sa and Delgado-Salinas 2010). The genus is widely distributed in the tropics, chiefly in Asia and Madagascar (Huang and Huang 1987; Klitgaard and Lavin 2005). There are fourteen species in India (Balan and Predeep 2017), five species in China (Sa and Delgado-Salinas 2010), and two species in Taiwan (Huang and Ohashi 1977; Huang and Huang 1987, 1993).

The first record of Taiwanese *Smithia* was made by Forbes and Hemsley (1887), in which they recorded the species, *S. sensitiva* Aiton. Next, Hayata (1911) described a new species, *S. nagasawai* Hayata, based on its truncated or round apex of bracts, which differ from the acute apex of bracts in the similar *S. ciliata* Royle. Later, Hosokawa (1936) recorded *S. ciliata* in central Taiwan. Huang and Ohashi (1977) treated *S. nagasawai* as a synonym of *S. ciliata*. Since then, all authors have treated only two species of *Smithia* in Taiwan in subsequent papers (Huang and Ohashi 1977; Huang and Huang 1987, 1993): *S. sensitiva* and *S. ciliata*.

During a recent field and herbarium investigation, we noticed that the identity of *S. sensitiva* was somewhat controversial in Taiwan. Specimens initially identified in the field as *Smithia sensitiva* had vivid yellow flowers up to 1.5 cm long with styles up to 8 mm long (Aiton 1789; Efloraofindia 2007 onwards; Sa and Delgado-Salinas 2010; Balan and Predeep 2017). However, all specimens previously identified as *S. sensitiva* in Taiwan had smaller pale yellow flowers with shorter styles. Hence, it was suspected the Taiwanese population was likely an unknown taxon distinct from *S. sensitiva*. The aim of the present study was to elucidate the taxonomic status of this taxon by morphological and palynological approaches.

Materials and methods

Morphological comparison

We compared three *Smithia* taxa including Taiwanese taxa, viz. *S. ciliata* and the unknown taxon, together with its similar species, viz. *S. sensitiva*, which were collected from herbaria (see additional specimens examined). Morphological measurements were made on both fresh and dried materials. For the morphological description, the terminology followed the studies of Sa and Delgado-Salinas (2010) and Balan and Predeep (2017).

Herbarium resources

Herbarium acronyms followed Index Herbariorum (Thiers 2022, continuously updated). Voucher specimens collected for the current study were deposited in TCF and TNM. Physical or digital specimens from the following herbaria were examined: HAST, PH, TAI, TAIE, TAIF, TCF and TNM. Type information of *S. sensitiva* followed the study of Balan and Predeep (2017).

Pollen morphology

We compared the pollen morphology of the unknown taxon with that of its similar species, *S. sensitiva*, and information about the voucher specimens is provided in Table 1. Pollen materials were treated according to the methods of Schols et al. (2004) and

Table 1. Specimens referenced for *Smithia yehii* C.M.Wang, Chih Y.Chang & Y.H.Tseng and *S. sensitiva* Aiton pollen morphology.

Taxon	Location	Coordinate	Altitude	Date	Voucher
<i>S. yehii</i>	TAIWAN. Miaoli County Tunghsiao Township, Tunghsiao Township 14 th Cemetery	24.44718°N, 120.69563°E	81 m	17 Dec 2021	<i>Chih Y.Chang 3620</i> (TCF, TNM)
<i>S. sensitiva</i>	THAILAND. Chiang Mai Province Samoeng district, Samoeng Forest	18.87321°N, 98.78213°E	1100 m	24 Nov 2018	<i>C.M.Wang 17941</i> (TNM)
	CHINA. Guangdong Province Huidong County, Gutianshan Nature Reserve	23.19310°N, 114.78134°E	220 m	8 Sept 1984	<i>Huidong collector team 730</i> (TNM)

Halbritter (1998). Pollen grains were obtained from herbarium materials and isolated anthers were rehydrated overnight. Whole anthers were fixed in 2% glutaraldehyde overnight, then treated with DMP (2, 2-dimethoxypropane) for 30 minutes, and transferred to acetone for 30 minutes before critical-point drying (CPD). Dried pollen was mounted on a stub and sputter coated with gold for > 100 s (Quorum SC7620) and examined by scanning electron microscopy (Hitachi S-3400N). The terminology for pollen shape, size, and exine ornamentation followed the recommendations of Erdtman (1952) and Halbritter et al. (2018).

The quantitative palynological traits were measured and their means and standard deviations were calculated. For each quantitative character, the Shapiro-Wilks normality test was first used to check the distribution, then an independent sample *t*-test was performed after logarithmic transformation (Kim 2015). All analyses were done using the PASW Statistics ver. 18 software (Sarma and Vardhan 2018).

Distribution map

The occurrence data was based on herbarium specimens. A distribution map was generated by using the package of Lin (2018) for QGIS ver. 3.4.

Results and discussion

We compared the macro-morphology of the three *Smithia* taxa, *S. sensitiva*, *S. ciliata* and *S. yehii* (Fig. 1, Table 2) and the pollen morphology between *S. sensitiva* and *S. yehii* (Fig. 2, Table 3).

Macro-morphological differences

Smithia ciliata is distinctly different from other species in that its inflorescences often have more than twelve flowers (Fig. 1C), whereas those of *S. sensitiva* and *S. yehii* have fewer than seven flowers (Fig. 1 A, B). The calyx of *S. ciliata* is densely ciliate at the margin, and membranous with clearly reticulate veins, while *S. sensitiva* and *S. yehii* have entire margins and scarious parallel veins. The pods of *S. ciliata* are slightly orbicular and often more

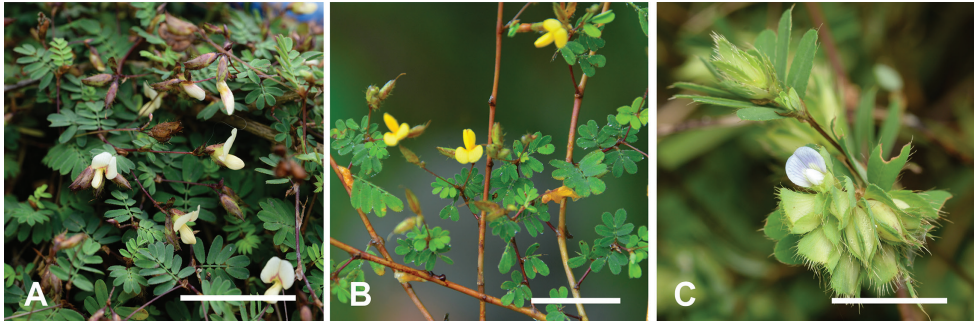


Figure 1. Comparison of *Smithia yehii* C.M.Wang, Chih Y.Chang & Y.H.Tseng and its similar species. Scale bars: 3 cm **A** *S. yehii* (photo by C.M.Wang, from Miaoli, Taiwan) **B** *S. sensitiva* Aiton (photo by Chih Y.Chang, from Chiang Mai, Thailand) **C** *S. ciliata* Royle (photo by C.M.Wang, from Chiayi, Taiwan).

Table 2. Summary of diagnostic characters of *Smithia yehii* C.M.Wang, Chih Y.Chang & Y.H.Tseng and its similar species.

Characters	<i>S. yehii</i>	<i>S. sensitiva</i> (Efloraofindia 2007; Sa and Delgado-Salinas 2010; Balan and Predeep 2017)	<i>S. ciliata</i> (Huang and Huang 1993; Sa and Delgado-Salinas 2010)
Leaflet pairs	(2)4–9	4–11	4–7
Leaflet size	3.5–7.0 × 1.2–2.3 mm	4–15 × 2–3 mm	6–12 × 2–4 mm
Leaflets, adaxial color	dark green at apex, light green at base when young and mature	same color between apex and base	same color between apex and base
Flowers, number per raceme	1–7	3–6	12 to many
Flowers	0.7–1.0 cm long	0.8–1.5 cm long	c. 1 cm long
Calyx	entire at margin, scarious, with parallel veins	entire at margin, scarious, with parallel veins	ciliate at margin, membranous, with reticulate veins
Corolla	pale yellow	vivid yellow	white or yellow
Style	3.4–4.1 mm long	c. 8 mm long	c. 2.5 mm long
Pod shape and size	more or less straight, 0.5–0.8 cm long	more or less straight, c. 0.4 cm long	slightly orbicular, 1–1.5 cm long
Jointed number of pod	(4)6–7	4–6	6–8
Distribution	endemic to Taiwan, in wetlands and open places, at elevations of < 300 m	widely distributed in Australia, India, Madagascar and Tropical Asia, in field margins, wetlands; at elevations of < 1000 m	widely distributed in Taiwan, China, Bhutan, India, Japan, Malaysia, Nepal, Philippines, Thailand and Vietnam. Taiwan, in margin of thickets, at elevation of 1,000–1,800 m

than 1.1 cm long, whereas both *S. sensitiva* and *S. yehii* are more or less straight and usually less than 1 cm long (Huang and Huang 1993; Sa and Delgado-Salinas 2010) (Table 2).

Compared with *S. sensitiva*, the corolla of *S. yehii* is pale yellow (Fig. 1A); whereas *S. sensitiva* has a vivid yellow corolla (Fig. 1B). *S. yehii* often has smaller flowers (0.7–1.0 cm long) than *S. sensitiva* (0.8–1.5 cm long). In addition, *S. yehii* has a shorter style

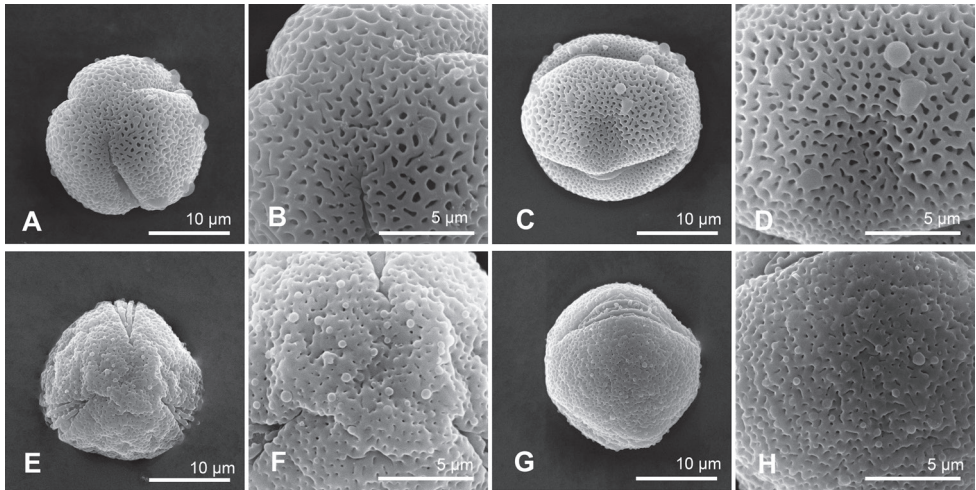


Figure 2. Comparison of the pollen morphology of *Smithia* Aiton **A–D** *Smithia yehii* C.M.Wang, Chih Y.Chang & Y.H.Tseng **E–H** *S. sensitiva* Aiton **A, E** polar view **B, F** exine ornamentation of polar view **C, G** equatorial view **D, H** exine ornamentation of equatorial view.

Table 3. Comparison of pollen characters of *Smithia yehii* C.M.Wang, Chih Y.Chang & Y.H.Tseng and *S. sensitiva* Aiton.

Taxon	Polar axis length (μm)	Equatorial axis length (μm)	P/E ratio	Exine ornamentation	Murus wide (μm)	Perforate size (μm)
<i>S. yehii</i>	21.2±1.0 (19.6–22.7)	19.5±1.6 (16.5–21.9)	1.1±0.1 (0.9–1.3)	perforate	0.5±0.1 (0.3–1.1)	0.4±0.1 (0.2–0.6)
<i>S. sensitiva</i>	21.0±1.4 (18.5–23.5)	18.4±1.6 (15.9–20.4)	1.1±0.1 (0.9–1.3)	perforate	0.4±0.1 (0.3–0.7)	0.2±0.1 (0.1–0.3)

(3.4–4.1 mm) than *S. sensitiva* (c. 8 mm) (Efloraofindia 2007; Sa and Delgado-Salinas 2010) (Table 2). Leaves of *S. yehii* are usually smaller (3.5–7.0 mm long) with fewer than nine pairs of leaflets, while *S. sensitiva* often has up to eleven pairs of leaflets and they are larger (up to 1.5 cm) (Efloraofindia 2007; Sa and Delgado-Salinas 2010) (Table 2). Furthermore, *S. yehii* has color variations on parts of the adaxial surface of the leaflets, with dark green at the apex and light green at the base (Figs 1A, 3B, F); older leaflets are consistently dark green. *S. sensitiva* leaflets remain consistently pale green (Fig. 1B).

Pollen morphological differences

The pollen grains of both *S. yehii* and *S. sensitiva* are small, tricolporate, and spheroidal with perforated exine ornamentation. *Smithia yehii* has significantly larger exine perforations (0.2–0.6 μm) than *S. sensitiva* (0.1–0.3 μm) ($p = 0.000^{***}$), and *S. yehii* has significantly larger muri (width of 0.3–1.1 μm) than *S. sensitiva* (0.3–0.7 μm) ($p = 0.044^*$) (Fig. 2, Tables 3, 4). The pollen characteristics also support the two taxa as distinct species.

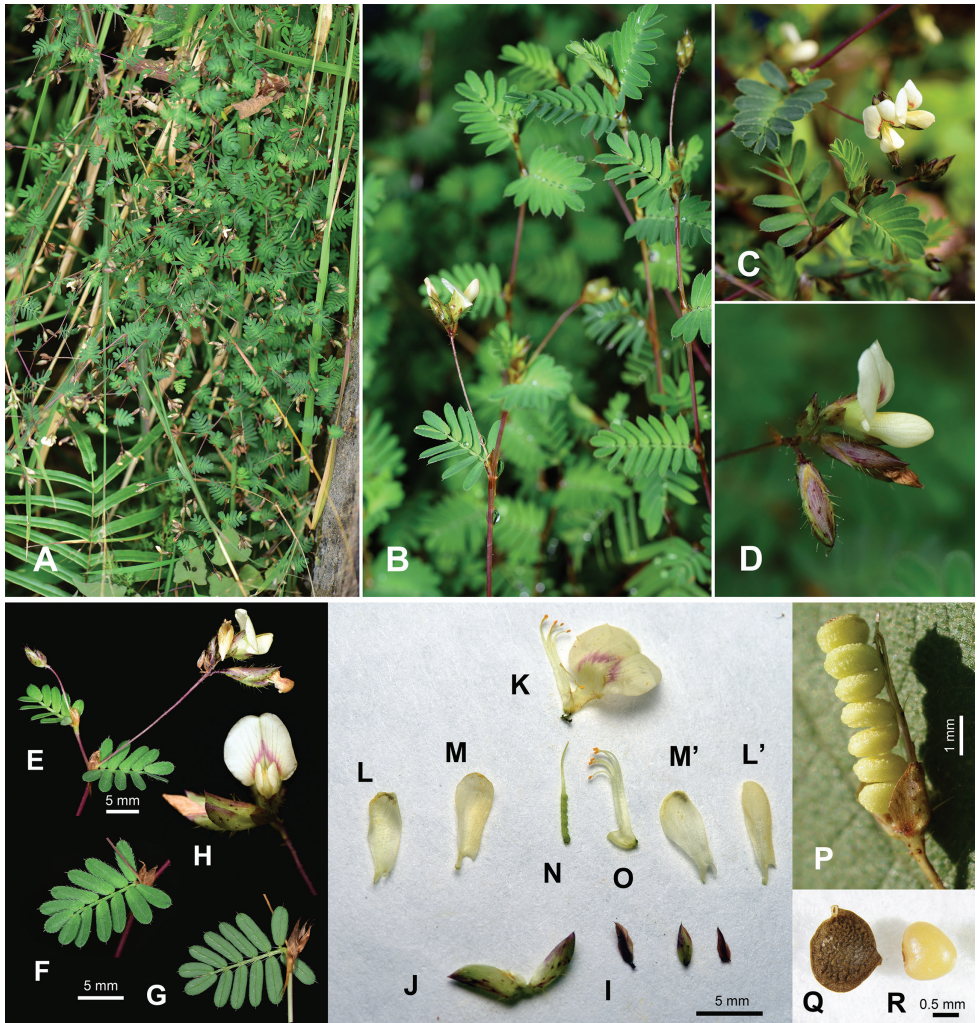


Figure 3. *Smithia yehii* C.M.Wang, Chih Y.Chang & Y.H.Tseng **A** habitat **B, C** habit **D, E** raceme **F** (leaf adaxial) **G** (leaf abaxial) **H** flowers **I** bracteoles **J** calyx **K** standard and part of diadelphous stamen **L** wing **M** keel **N** gynoeceum **O** diadelphous stamen **P** pod **Q** joint of pod **R** seed. Voucher **A, D–H** Chih Y.Chang 3620 (TCF) **B, L–R** C.M.Wang 17247 (TNM).

Key to *Smithia yehii* and its similar species (modified from Huang and Huang (1993), and Sa and Delgado-Salinas (2010))

- 1 Inflorescences often with more than 12 flowers, calyx ciliate at margin, membranous, with reticulate veins; pods slightly orbicular, more than 1.1 cm long *S. ciliata*
- Inflorescences with fewer than 7 flowers, calyx entire at margin, scarious, with parallel veins; pods more or less straight, less than 1 cm 2

- 2 Corolla pale yellow, flowers often less than 1 cm long (0.7–1.0 cm), style less than 5 mm long (3.4–4.1 mm); leaflets adaxial dark green at apex and light green at base between young and mature *S. yebii*
- Corolla vivid yellow, flowers up to 1.5 cm long (0.8–1.5 cm), style longer than 6 mm (c. 8 mm); adaxial surface of leaflets same color between apex and base..... *S. sensitiva*

Taxonomic treatment

***Smithia yebii* C.M.Wang, Chih Y.Chang & Y.H.Tseng, sp. nov.**

urn:lsid:ipni.org:names:77305894-1

Figs 1A, 2A–D, 3–6

S. sensitiva sensu acut. Forbes and Hemsley, J. Linn. Soc., Bot. 23: 170, 1887; Henry, List 32, 1896; Matsumura, Bot. Mag. (Tokyo) 16: 73, 1902; Hayata, Icon. Pl. Formosan. 1: 180, 1911; Hosokawa in Masamune, Short. Fl. Formosa 106, 1936; Chuang and Huang, Leg. Taiwan Past. 93, 1965; Huang and Ohashi in Li, Fl. Taiwan 3: 381, 1977; Huang and Huang, Taiwania 32(1): 88, 1987; Huang and Huang, Flora of Taiwan, 2nd edition 3: 364, 1993, *non* Aiton.

Diagnosis. The new species is similar to *S. sensitiva*, but can be distinguished by its pale yellow corolla (vs. vivid yellow), often smaller flower and shorter style, and color variation on adaxial surface of leaflets when young and mature, viz. dark green at apex and light green at base.

Type. TAIWAN. Miaoli County: Tunghsiao Township, Tunghsiao Township 14th Cemetery, 81 m alt., 24.44718°N, 120.69563°E, 17 Dec 2021, *C.M.Wang 19231* (holotype: TNM) (Fig. 6).

Description. Diffuse annual herb, 25–50 cm long; stem slender, sparsely bristly. Stipules 2.7–5.5 × 1.0–1.6 mm, ovate, striate, scarious, persistent; appendage to the stipules 1.9–3.6 mm long, bilobed. Leaf rachis bristly; petioles 0.9–1.6 mm long; leaflets (2)4–9 pairs, 3.5–7.0 × 1.2–2.3 mm, linear-oblong, obtuse at apex, mucronate, oblique and truncate at base, bristly beneath along the midvein and margins; adaxial surface dark green at apex, light green at base; older leaflets consistently dark green. Racemes axillary, 1.1–3.4 cm long, 1–7-flowered; peduncles filiform, sparsely bristly.

Table 4. Students’ *t* scores and *p* values for quantitative characters of pollen grains.

Characters	t score	p value
Polar axis long	-1.753	0.095
Equatorial axis long	-1.687	0.107
P/E ratio	0.227	0.823
Interval between perforations	-2.076	0.044*
Perforation size	-7.361	0.000***

Note: *p* value significance: **p* < 0.05, ***p* < 0.01, ****p* < 0.001

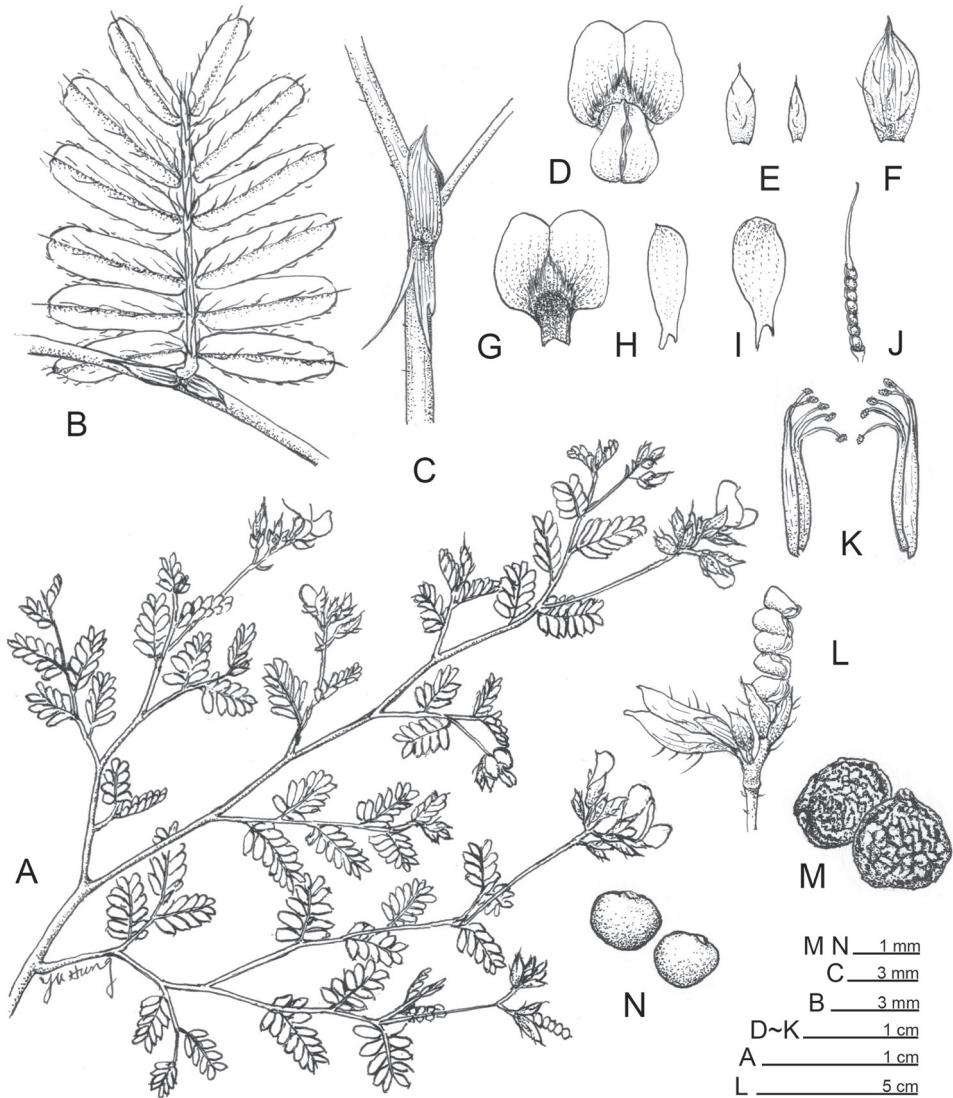


Figure 4. Line drawings of *Smithia yehii* C.M.Wang, Chih Y.Chang & Y.H.Tseng **A** habit **B** leaf (abaxial) **C** stipule **D** flower **E** bracteoles **F** calyx **G** standard **H** wing **I** keel **J** gynoecium **K** diadelphous stamen **L** pod **M** joint of pod **N** seeds.

Flowers 0.7–1.0 cm long; pedicels 1.0–3.1 mm long; bracteoles 2.3–4.0 × 0.9–2.4 mm, ovate, striate, persistent. Calyx parallel-veined, lips 4.5–8.2 mm long, equal, ovate, acute at apex, with a few scattered bristles. Corolla pale yellow, standard (5.2)6.2–9.0 × 5.7–8.0 mm, obovate, pale yellow with red circle pattern in centre; wings 4.0–6.9 × 1.8–2.6 mm, oblong, auricled; keels 4.8–7.5 × 1.9–2.5 mm, oblanceolate. Stamens diadelphous; filaments 5.1–6.4 mm long; anthers 0.2–0.3 mm long, ovoid. Ovary

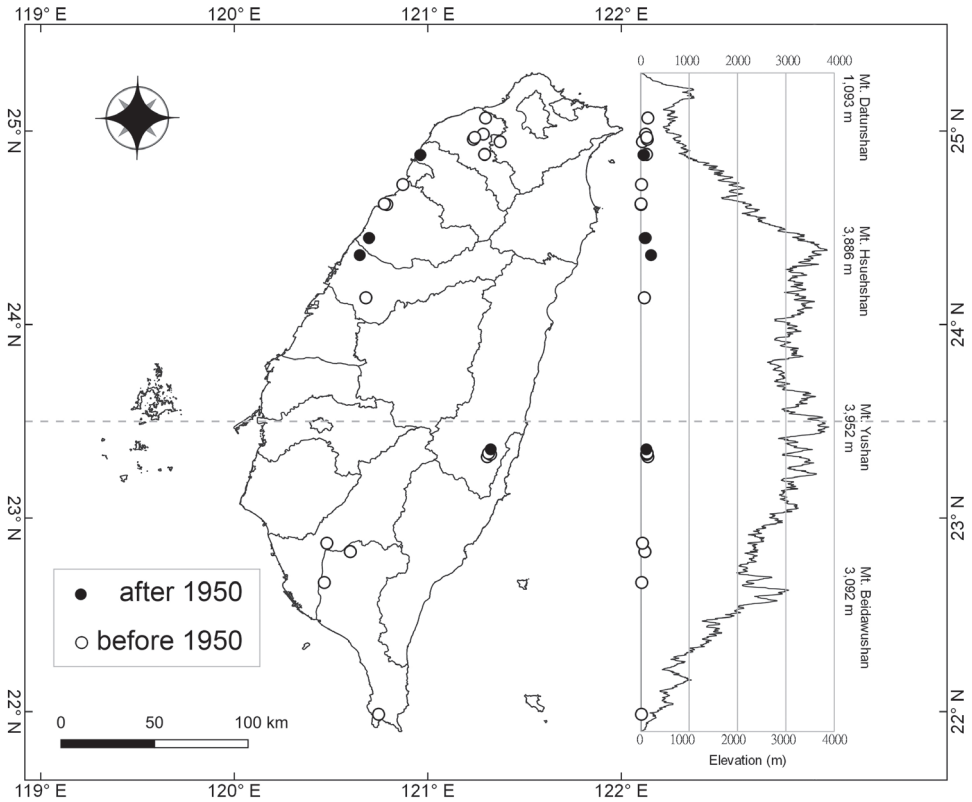


Figure 5. Distribution map of *Smithia yehii* C.M.Wang, Chih Y.Chang & Y.H.Tseng.

stipitate, 2.2–2.9 mm long, linear, (4)6–7-ovuled; style 3.4–4.1 mm long; stigma pointed. Pods more or less straight, 4.5–8.0 mm long, included, (4)6–7-jointed; joints 1.4–1.6 × 1.2–1.4 mm, papillose. Seeds 1.1–1.3 × 0.9–1.2 mm, reniform.

Phenology. Flowering was observed from November to February and fruiting from December to March.

Distribution and habitat. Endemic species of Taiwan. *Smithia yehii* grows in wetlands and open places, at elevations of < 300 m (Fig. 5). Common companion species are *Cirsium lineare* (Thunb.) Sch. Bip. (Compositae), *Apluda mutica* L. (Poaceae), *Eriochloa villosa* (Thunb.) Kunth (Poaceae), *Hydrocotyle batrachium* Hance (Araliaceae), and *Ampelopteris prolifera* (Retz.) Copel. (Thelypteridaceae).

Chinese name. yè-shih-po-yóu-gan (葉氏坡油甘).

Etymology. The species epithet “*yehii*” was chosen to honor Prof. Mau-Shing Yeh (葉茂生), Department of Agronomy, National Chung-Hsing University, for his contributions to research into the legumes of Taiwan.

Palynology. Pollen grains are small, tricolporate, and spheroidal, perforate in surface sculpture, and 19.6–22.7 × 16.5–21.9 μm, P/E ratio 0.9–1.3, perforations 0.2–0.6 μm in diam., and murus width 0.3–1.1 μm (Fig. 2A–D).



Figure 6. Holotype of *Smithia yehii* C.M. Wang, Chih Y. Chang & Y.H. Tseng.

Conservation status. *Smithia yehii* was evaluated as least concern (LC) by the Editorial Committee of the Red List of Taiwan Plants (2017) as *S. sensitiva*, because there were many records in the herbarium. However, many populations are probably extinct now. *Smithia yehii* is known after 1950 from only four sites (Fig. 5), each of which had only a few individuals (c. < 30) because of human disturbances and habitat fragmentation. Therefore, following the criteria of IUCN (2019), we regard this species as endangered (EN B2ab(ii, iii); C2a(i); D), and recommend that it urgently needs to be protected against extinction.

Specimens examined. *Smithia yehii* C.M.Wang, Chih Y.Chang & Y.H.Tseng TAIWAN. **New Taipei City:** Sanxia District, “Ryoenpo” [Lungpuli], 24 Nov. 1910, 36 m alt., *T.Kawakami s. n.* (TAI!); **Taoyuan City:** “Toen” [Toyen], 25 May 1930, 134 m alt., *S.Suzuki 2627* (PH, TAI!); same loc., 17 Dec. 1933, 125 m alt., *S.Suzuki 4041* (TAI!); Daxi District, “Taikei” [Tahsi], 31 Mar. 1940, 119 m alt., *T.Nakamura 4311* (TAI!); Luzhu District, “Toen-Nankan” [Taoyuan-Nankan], 23 Nov. 1931, 147 m alt., *T.Suzuki 7876* (TAI!); **Hsinchu County:** Chupei City, Lienhua Temple, 19 June 1986, 63 m alt., *T.C.Huang 12692* (TAI!); same loc., 24 Oct. 1996, 57 m alt., *C.C.Huang 1619* (TAIE!); same loc., 30 Aug. 1996, 56 m alt., *K.C.Yang 4969* (HAST!); same loc., 16 Oct. 1997, 56 m alt., *Y.C.Kao 93* (HAST!); same loc., 29 Nov. 1997, 56 m alt., *W.C.Leong 667* (HAST!); same loc., 15 Sept. 1998, 68 m alt., *S.C.Liu 84* (TAIF!); same loc., 23 Aug. 1999, 56 m alt., *C.IPeng 17683* (HAST!); same loc., 30 Aug. 1996, 57 m alt., *K.C.Yang 4969* (TNM!); same loc., 15 Sept. 1998, 57 m alt., *S.C.Liu 84* (TNM!); **Miaoli County:** Houlong Township, “Koryu” [Houlung], 1 Nov. 1924, 6 m alt., *Y.Simada 1337* (HAST!, TAI!); Tunghsiao Township, Tunghsiao Township 14th Cemetery, 27 Oct. 2016, 93 m alt., *T.C.Hsu 8660* (TAIF!); same loc., 21 Oct. 2017, 103 m alt., *L.H.Yang 908* (TAIE!); same loc., 2 Dec. 2017, 103 m alt., *R.P.Hsieh 49* (TAIE!); same loc., 26 Sept. 2019, 93 m alt., *T.C.Hsu 12070* (TAIF!); same loc., 20 Oct. 2021, 103 m alt., *Z.X.Chang 2666* (TAIF!); same loc., 11 Dec. 2017, 81 m alt., *C.M.Wang 17247* (TNM); same loc., 21 Oct. 2017, 81 m alt., *L.H.Yang 910* (TAIE!); same loc., 1 Mar. 2018, 81 m alt., *M.Y.Shen 5542* (TAIE!); same loc., 13 Oct. 2021, 81 m alt., *M.Y.Shen 6841* (TAIE!); same loc., 17 Dec 2021, *Chih Y.Chang 3620, 3621, 3622* (TCF); Zhunan Township, “Kityo” [Chiting], 3 Aug. 1940, 16 m alt., *Fukuya s. n.* (TAI!); **Taichung City:** “Taityushi” [Taichung], Oct. 1905, 75 m alt., *G.Nakahara s. n.* (PH); same loc., 27 Aug. 1931, 75 m alt., *S.Suzuki 8217* (TAI!); Dajia District, Mt. Tiehchen, 12 Oct. 1997, 213 m alt., *S.Y.Lu s. n.* (TAIF!); **Kaohsiung City:** Cishan District, “Banshoryo” [Chishan], 1 Nov. 1934, 36 m alt., *S.Suzuki 5825* (TAI!); **Pingtung County:** Gaoshu Township, “Takagi” [Kaoshu], 8 Nov. 1931, 86 m alt., *T.Hosokawa 3377* (TAI!); same loc., 8 Nov. 1931, 86 m alt., *T.Hosokawa s. n.* (TAI!); Hengchun Township, “Koshun” [Hengchun], Aug. 1915, 15 m alt., *E.Matuda 1083* (TAI!); Pingtung City, “Rokkwaiseki” [Liukueitsu], 31 Oct. 1934, 21 m alt., *S.Suzuki 5713* (TAI!); **Hualien County:** Yuli Township, “Tamazatosyo Nodyo” [Yuli], 28 Aug. 1933, 147 m alt., *Y.Yamamoto 3099* (TAI!); Hualien County, Yuli Township, “Tamazato” [Yuli], 29 Aug. 1933, 123 m alt., *Y.Yamamoto 3082* (TAI!); same loc., 29 Aug. 1933, 133 m alt., *Y.Yamamoto 3087* (TAI!); Yuli, 11 Feb. 1975, 116 m alt., *S.Y.Lu 3440* (TAIF!).

Additional specimens examined. *Smithia sensitiva* Aiton Type: INDIA. “India Orientalis” [Bengal], 1875, *Koenig s.n.*, (holotype: BM, photo!) CHINA. **Fujian Province:** Wuping Country, Mt. Cuiye, 16 Oct. 2017, *T.W.Hsu 21882* (TAIE!); **Guangdong Province:** Huidong County, Gutianshan Nature Reserve, 220 m alt., 23.19310°N, 114.78134°E, 8 Sept. 1984, *Huidong collector team 730* (TNM!); Lianshan County, Shangshuai Town, Lungshuangshan, 150 m alt., 21 Oct. 1999, *F.Y.Zeng 2252* (TNM!); Lianshan County, Shangshuai Town, Lianguan Village, 500 m alt., 13 Oct. 2000, *H.G.Ye 5117* (TNM!); THAILAND. **Chiang Mai Province:** Samoeng district, Samoeng Forest, 1100 m alt., 18.87321°N, 98.78213°E, 24 Nov. 2018, *Chih Y.Chang 2139* (TNM); same loc., 24 Nov. 2018, *C.M.Wang 17941* (TNM); VIETNAM. **Lâm Đông Province:** Lac Duong District, Cong Troi Waterfall, Lat commune., 28 Oct. 2019, *T.C.Hsu 12222* (TAIF).

Acknowledgements

We thank Dr. Hsy-Yu Tzeng (曾喜育), Dr. Chien-Ti Chao (趙建棟) and Ms. Yu-Ting He (何郁庭) for providing useful suggestions. This manuscript was edited by Dr. Gary Bentley, an editor with Peerwith. This study was supported by the grant of National Science and Technology Council no. 110-2313-B-005-033-MY3 to Yen-Hsieh Tseng (曾彥學).

References

- Aiton W (1789) *Hortus Kewensis, or, a Catalogue of the Plants Cultivated in the Royal Botanic Garden at Kew*, vo. Printed for George Nicol, Bookseller to his Majesty, London. <https://doi.org/10.5962/bhl.title.104529>
- LPWG (2017) A new subfamily classification of the Leguminosae based on a taxonomically comprehensive phylogeny. *Taxon* 66(1): 44–77. <https://doi.org/10.12705/661.3>
- Balan AP, Predeep SV (2017) A taxonomic revision of the genus *Smithia* Ait. (Fabaceae) in South India. *Taiwania* 62(2): 175–204. <https://doi.org/10.6165/tai.2017.62.175>
- Editorial Committee of the Red List of Taiwan Plants (2017) *The Red List of Vascular Plants of Taiwan, 2017*. Endemic Species Research Institute, Forestry Bureau, Council of Agriculture, Executive Yuan and Taiwan Society of Plant Systematics, Nantou, Taiwan, 194 pp. https://www.tesri.gov.tw/Uploads/userfile/A6_2/2019-02-25_1315069780.pdf
- Efloraofindia (2007) *Smithia sensitiva*. <https://efloraofindia.com/2011/03/30/smithia-sensitiva/> [Accessed: 9 June 2022]
- Erdtman G (1952) *Pollen Morphology and Taxonomy*. Stockholm Almqvist and Wiksell, Sweden. <https://doi.org/10.1080/11035895209453507>
- Forbes FB, Hemsley WB (1887) An enumeration of all the plant known from China proper, Formosa, Hainan, the Corea, The Luchu archipelago, and the island of Hongkong;

- together with their distribution and synonymy. *Journal of the Linnean Society of London, Botany* 23(150): 1–489. <https://doi.org/10.1111/j.1095-8339.1886.tb00530.x>
- Halbritter H (1998) Preparing living pollen material for scanning electron microscopy using 2,2-dimethoxypropane (DMP) and critical-point drying. *Biotechnic & Histochemistry* 73(3): 137–143. <https://doi.org/10.3109/10520299809140519>
- Halbritter H, Ulrich S, Grímsson F, Weber M, Zetter R, Hesse M, Bruchner R, Svojtka M, Frosch-Radivo A (2018) *Illustrated Pollen Terminology 2nd Edn.* Springer International Publishing, 483 pp. <https://doi.org/10.1007/978-3-319-71365-6>
- Hayata B (1911) *Materials for a Flora of Formosa.* Journal of Science Imperial University, Tokyo, Japan.
- Hosokawa T (1936) *Smithia.* In: Masamune G (Ed.) *Short Flora of Formosa.* Kudoa, Taihoku, 106 pp.
- Huang SF, Huang TC (1987) Taxonomic treatment of the Papilionoideae (Leguminosae) of Taiwan. *Taiwania* 32(1): 11–118. <https://doi.org/10.6165/tai.1987.32.11>
- Huang SF, Huang TC (1993) *Smithia* Ait. In: Editorial Committee of the Flora of Taiwan (Eds) *Flora of Taiwan. 2nd Edn., vol. 3.* Editorial Committee, Dept. Bot., NTU, Taipei, 362–366.
- Huang TC, Ohashi H (1977) *Smithia* Ait. In: Li HL (Ed.) *Flora of Taiwan 1st vol. 3.* Epoch publishing company, Taipei, 378–383.
- IUCN (2019) *Guidelines for Using the IUCN Red List Categories and Criteria. Version 14.* Prepared by the Standards and Petitions Committee. <http://www.iucnredlist.org/documents/RedListGuidelines.pdf> [Access: 25 August 2021]
- Kim TK (2015) T test as a parametric statistic. *Korean Journal of Anesthesiology* 68(6): 540–546. <https://doi.org/10.4097/kjae.2015.68.6.540>
- Klitgaard BB, Lavin M (2005) Tribe Dalbergieae. In: Lewis G, Schrire B, Mackinder B, Lock M (Eds) *Legumes of the World.* Royal Botanic Gardens, Kew, 330 pp.
- Lin CT (2018) QGIS template for displaying species distribution by horizontal and vertical view in Taiwan. <https://doi.org/10.5281/zenodo.1493690> [Access: 21 March 2019]
- Sa R, Delgado-Salinas A (2010) *Smithia* Aiton. In: Editorial Committee of the Flora of China (Eds) *Flora of China vol. 10.* Science Press (Beijing) & Missouri Botanical Garden Press (St. Louis), 133–135.
- Sarma KVS, Vardhan RV (2018) *Multivariate Statistics Made Simple: A Practical Approach.* CRC Press, Boca Raton, 258 pp. <https://doi.org/10.1201/9780429465185>
- Schols P, Es K, D’hondt C, Merckx V, Smets E, Huysmans S (2004) A new enzyme-based method for the treatment of fragile pollen grains collected from herbarium material. *Taxon* 53(3): 777–782. <https://doi.org/10.2307/4135450>
- Thiers B (2022, continuously updated) *Index Herbariorum: A global directory of public herbaria and associated staff.* New York Botanical Garden’s Virtual Herbarium. <http://sweetgum.nybg.org/science/ih/> [Access: 10 June 2022]

Liparis macrosepala (Orchidaceae), a new species from southwest China with its phylogenetic position

Zhengwei Wang¹, Yi Zhang², Ze Zhang², Xiaochen Li¹, Zhijin Wu¹, Lan Yan²,
Aixian Lu^{1,3}, Chengzhi Xie^{1,4}, Chao Hu¹, Weichang Huang^{1,3}

1 Eastern China Conservation Centre for Wild Endangered Plant Resources, Shanghai Chenshan Botanical Garden, Shanghai 201602, China **2** Yunnan Yelantang Biological Technology Co., Ltd., Kunming 650114, China **3** College of Art and Landscape Architecture, Fujian Agriculture and Forestry University, Fuzhou 350002, China **4** Key Laboratory of Genetics and Germplasm Innovation of Tropical Special Forest Trees and Ornamental Plants, Ministry of Education, College of Forestry, Hainan University, Haikou 570228, China

Corresponding authors: Chao Hu (hc320320@163.com), Weichang Huang (hwc_zx@126.com)

Academic editor: Timothée Le Péchon | Received 2 June 2022 | Accepted 20 September 2022 | Published 4 October 2022

Citation: Wang Z, Zhang Y, Zhang Z, Li X, Wu Z, Yan L, Lu A, Xie C, Hu C, Huang W (2022) *Liparis macrosepala* (Orchidaceae), a new species from southwest China with its phylogenetic position. *PhytoKeys* 210: 67–77. <https://doi.org/10.3897/phytokeys.210.87033>

Abstract

A new orchid species, *Liparis macrosepala*, is illustrated and described from Yunnan Province, China, based on morphological and molecular analyses. This plant is characterised by the ovoid-fusiform, slightly compressed pseudobulbs with 4 or 5 leaves with slightly crisped margins on their apical half, dorsal sepal heart-shaped, lip with a bituberculate basal callus and a thickened folded lateral lobe on each side, centrally with one cavity with slightly raised margins, the column with a single pair of broadly triangular, obtuse wings. Maximum Likelihood and Bayesian Inference analyses of combined nrITS and plastid *matK* DNA sequences place this species in section *Cestichis*.

Keywords

Liparis section *Cestichis*, molecular phylogeny, morphology, *matK*, nrITS

Introduction

The genus *Liparis* Rich. (Epidendroideae, Malaxideae, Malaxidinae) comprises about 320 species distributed worldwide with more than 70 species in China (Pridgeon et al. 1999; Chen et al. 2009; Tian et al. 2015; Huang et al. 2018; Ya et al. 2021). Species

from this genus are terrestrial, lithophytic, epiphytic and rarely mycoheterotrophic, with inflorescences laxly or densely many-flowered, lip often reflexed and usually with a basal callus, lacking a spur, column winged at apex and sometimes at base and four pollinia in two pairs (Chen et al. 2009).

During our field surveys in Xishuangbanna, Yunnan, China, an unknown species was found. In this paper, we analysed the morphological differences of the newly-found species and its allied species and the phylogenetic position of the new entity is also discussed, based on molecular evidence from nrITS and plastid *matK*. After careful morphological comparison and phylogenetic analyses, we concluded that this species is new to science.

Material and method

Morphological observations

Materials of the new species were collected from Xishuangbanna, Yunnan, China during a field expedition. Morphological characters were observed, measured and photographed based on five living individuals under a stereomicroscope (SZX16-6151, Olympus, Japan) and photographed with a digital camera (D750, Nikon, Japan). A voucher specimen, designated as the holotype, was deposited at Shanghai Chenshan Herbarium (CSH). Conservation assessment has been conducted following IUCN guidelines (IUCN 2019).

Taxonomic sampling

DNA sequences of nrDNA ITS and plastid *matK* of the new species were sequenced and sequences of the same markers for 82 related species were downloaded from GenBank, including five outgroup species from other subtribes (Table 1).

Phylogenetic analyses

DNA sequences were aligned using the MAFFT programme in Geneious v. 2020.2.4 (<https://www.geneious.com>, accessed on 10 March 2021). Phylogenetic analyses were conducted using Maximum Likelihood (ML) and Bayesian Inference (BI) in RAxML v.7.0.4 (Stamatakis 2006) and MrBayes v.3.2.6 (Huelsenbeck and Ronquist 2001; Ronquist et al. 2012), respectively. The appropriate DNA substitution model under AIC criteria was estimated using jModelTest 2.1.10 (Posada 2008). ML analyses were conducted with bootstrap values calculated by running 1,000 replicates. For BI analysis, four chains were run with random initial trees, each for 1,000,000 generations, until the average standard deviation of the split frequency values was less than 0.01 to ensure convergence, sampling trees every 1,000 generations. After the first 20% of samples were discarded as burn-in, the remaining replicates were used to estimate the posterior probabilities.

Table 1. Taxon sampling in this study.

	Species Name	nrITS	matK
1	<i>Acanthophippium mantinianum</i> L.Linden & Cogn.	AF521081	AF263618
2	<i>Collabium simplex</i> Rchb.f.	EF670387	AY557200
3	<i>Crepidium acuminatum</i> (D.Don) Szlach.	KJ459274	KJ459304
4	<i>Crepidium babanense</i> (Hand.-Mazz.) S.C.Chen & J.J.Wood	MH116611	MH117500
5	<i>Crepidium bancanoides</i> (Ames) Szlach.	AB290885	AB290893
6	<i>Crepidium brevidentatum</i> (Schweinf.) M.A.Clem. & D.L.Jones	AB290886	AB290894
7	<i>Crepidium resupinatum</i> (G.Forst.) Szlach.	JN114483	JN004403
8	<i>Dendrobium dixanthum</i> Rchb.f.	KY966535	KY966825
9	<i>Dienia cylindrostachya</i> Lindl.	JN114491	JN004422
10	<i>Eria ferruginea</i> Lindl.	AF521071	AF263660
11	<i>Eulophia graminea</i> Lindl.	MH768269	MH767976
12	<i>Liparis macrosepala</i> Z.W. Wang, Y. Zhang & W.C. Huang	ON642332	ON642331
13	<i>Liparis anopheles</i> J.J.Wood	AY907075	AY907139
14	<i>Liparis assamica</i> King & Pantl.	KJ459276	KJ459306
15	<i>Liparis aureolabella</i> J.D. Ya & Z.D. Han	MN065679	MN065733
16	<i>Liparis auriculata</i> Blume ex Miq.	AB289458	KF262076
17	<i>Liparis balansae</i> Gagnep.-1	KF589874	KF589880
18	<i>Liparis balansae</i> Gagnep.-2	KJ459277	KJ459307
19	<i>Liparis bingzhongluensis</i> X.H. Jin	MW169041	MW169042
20	<i>Liparis bistriata</i> E.C.Parish & Rchb.f.	KJ459279	KJ459309
21	<i>Liparis bootanensis</i> Griff	KJ459280	KJ459310
22	<i>Liparis bracteata</i> T.E.Hunt	AY907076	AY907140
23	<i>Liparis brunnescens</i> Schltr.	AY907098	AY907165
24	<i>Liparis condylobulbon</i> Rchb.f.	AY907080	AY907144
25	<i>Liparis cordifolia</i> Hook.f.	KJ459282	KJ459312
26	<i>Liparis delicatula</i> Hook.f.	KJ459283	KJ459313
27	<i>Liparis distans</i> C.B.Clarke	KJ459284	KJ459314
28	<i>Liparis disticha</i> (Thouars) Lindl.	AY907081	AY907145
29	<i>Liparis elliptica</i> Wight	KJ459285	KJ459315
30	<i>Liparis fissilabris</i> Tang & F.T.Wang	KJ459286	KJ459316
31	<i>Liparis fissipetala</i> Finet	KJ459287	KJ459317
32	<i>Liparis formosana</i> Rchb.f.	AY907082	AY907147
33	<i>Liparis fujisanensis</i> F.Maek. ex Konta & S.Matsumoto	EU024936	EU024937
34	<i>Liparis gibbosa</i> Finet-1	AY907083	AY907148
35	<i>Liparis gibbosa</i> Finet-2	AY907084	AY907149
36	<i>Liparis glossula</i> Rchb.f.	KJ459289	KJ459319
37	<i>Liparis guangxiensis</i> C.L.Feng & X.H.Jin	KF589875	KF589881
38	<i>Liparis japonica</i> (Miq.) Maxim.	AY907086	AY907151
39	<i>Liparis koreana</i> (Nakai) Nakai	EU017422	EU017444
40	<i>Liparis kumokiri</i> F.Maek.	AY907087	AY907152
41	<i>Liparis latifolia</i> Lindl.	AY907088	AY907153
42	<i>Liparis latilabris</i> Rolfe	KJ459291	KJ459321
43	<i>Liparis liliifolia</i> (L.) Rich. ex Lindl.	AY907090	AY907156
44	<i>Liparis loeselii</i> (L.) Rich.	AY907091	AY907157
45	<i>Liparis makinoana</i> Schltr.	EU017405	EU017428
46	<i>Liparis mannii</i> Rchb.f.	KJ459293	KJ459323
47	<i>Liparis meihuashanensis</i> S.M.Fan	MF959772	MF959773
48	<i>Liparis mengziensis</i> J.D. Ya & Lei Cai	MN065734	MN065678
49	<i>Liparis nanlingensis</i> H.Z.Tian & F.W.Xing	AB701346	/
50	<i>Liparis napoensis</i> L.Li, H.F.Yan & S.J. Li-1	MT012899	MT019986
51	<i>Liparis napoensis</i> L.Li, H.F.Yan & S.J. Li -2	MT012900	MT019987
52	<i>Liparis nervosa</i> (Thunb.) Lindl.	AY907092	AY907158
53	<i>Liparis nugentiae</i> F.M.Bailey	AY907093	AY907159
54	<i>Liparis odorata</i> (Willd.) Lindl.	KJ021033	KJ021029
55	<i>Liparis pandurata</i> Ames	AY907094	AY907160
56	<i>Liparis pauliana</i> Hand.-Mazz.	AY907096	AY907163

	Species Name	nrITS	matK
57	<i>Liparis petiolata</i> (D.Don) P.F.Hunt & Summerh.	MW186826	MW187482
58	<i>Liparis resupinata</i> Ridl.	KJ459297	KJ459327
59	<i>Liparis somae</i> Hayata-1	MT012898	MT019985
60	<i>Liparis somae</i> Hayata-2	MT012897	MT019984
61	<i>Liparis sootenzanensis</i> Fukuy.	KJ021034	KJ021030
62	<i>Liparis stricklandiana</i> Rchb.f.-1	MT012903	MT019990
63	<i>Liparis stricklandiana</i> Rchb.f.-2	KJ459298	KJ459328
64	<i>Liparis sula</i> N.Hallé	AY907104	AY907171
65	<i>Liparis terrestris</i> J.B.Comber	AY907105	AY907172
66	<i>Liparis truncicola</i> Schltr.	AY907106	AY907173
67	<i>Liparis viridiflora</i> (Blume) Lindl.-1	MT012902	MT019989
68	<i>Liparis viridiflora</i> (Blume) Lindl.-2	MT012901	MT019988
69	<i>Malaxis brachypoda</i> (A.Gray) Fernald	AY907108	AY907175
70	<i>Malaxis monophyllos</i> (L.) Sw.	MW181626	MW187483
71	<i>Malaxis soulei</i> L.O.Williams	AY907119	AY907186
72	<i>Malaxis abieticola</i> Salazar & Soto Arenas	AY907129	AY907196
73	<i>Oberonia acaulis</i> Griff.	KY242066	KY241943
74	<i>Oberonia brunoniana</i> Wight	JN114623	JN004516
75	<i>Oberonia equitans</i> (G.Forst.) Mutel	AY907130	AY907198
76	<i>Oberonia heliophila</i> Rchb.f.	AY907131	AY907199
77	<i>Oberonia iridifolia</i> Roxb. ex Lindl.	AY907132	AY907200
78	<i>Oberonia mucronata</i> (D.Don) Ormerod & Seidenf	JN114640	JN004534
79	<i>Oberonia neocaledonica</i> Schltr.-1	AY907133	AY907201
80	<i>Oberonia neocaledonica</i> Schltr.-2	AY907134	AY907202
81	<i>Oberonia padangensis</i> Schltr.	AY907135	AY907203
82	<i>Oberonia wappeana</i> J.J.Sm.	AY907138	AY907206
83	<i>Oberonioides pusillus</i> (Rolfé) Marg. & Szlach.	KJ527610	KJ459302

Results

Phylogenetic analyses

The length of nrITS matrix was 792 bp including 262 parsimony-informative sites and for *matK*, the length and parsimony-informative sites were 1443 bp and 120, respectively. Both analyses (MP and BI) recovered similar relationships. The ML tree with bootstrap percentages, on which the posterior probabilities from the BI analysis were also indicated, is shown in Fig. 1.

The phylogenetic analyses indicate that *Liparis* is not monophyletic, being mingled with species of other genera of Malaxideae. This result agrees with what was found in previous studies (Cameron 2005; Margońska et al. 2012; Tang et al. 2015; Li et al. 2020; Kumar et al. 2022). The new species, henceforth referred to as *Liparis macrosepala* Z.W. Wang, Y. Zhang & W.C. Huang, is grouped with species in *Liparis* sect. *Cestichis* Thouars ex Pfitzer as the sister of a clade consisting of *L. delicatula* Hook.f., *L. fissipetala* Finet, *L. assamica* King & Pantl. and *L. resupinata* Ridl.

Morphological comparisons

Liparis is defined as species with racemose inflorescences, resupinate lip lacking a spur, column without a conspicuous foot and four pollinia in two pairs with small viscidium, but no caudicle. The morphology of *Liparis macrosepala* is in

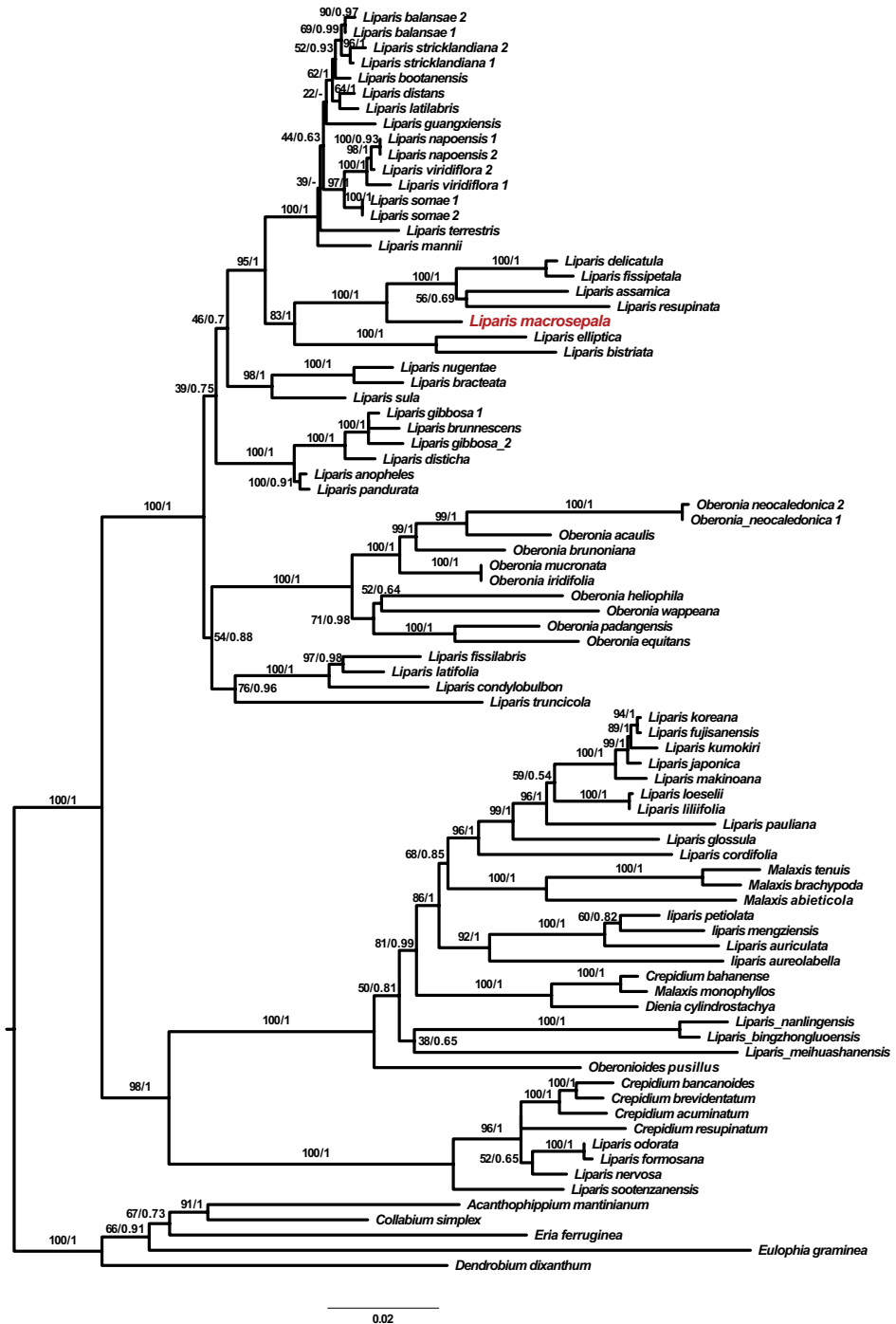


Figure 1. Maximum Likelihood tree of *Liparis* and its allied genera in subtribe Malaxidinae inferred from the combined analysis of nrITS and *matK*. ML bootstrap values (ML_{BP})/Bayesian posterior probabilities (PP) are indicated above the branches, respectively. The sectional taxonomy of *Liparis* follows Garay and Romero-Gonzalez (1999) and Li et al. (2020).

accordance with the characteristics of sect. *Cestichis* like the slightly flattened, narrowly winged rachis with alternating bracts. The morphological characters can distinguish *Liparis macrosepala* from its close relatives *L. delicatula*, *L. fissipetala*, *L. assamica* and *L. resupinata*.

Taxonomic treatment

***Liparis macrosepala* Z.W. Wang, Y. Zhang & W.C. Huang, sp. nov.**

urn:lsid:ipni.org:names:77306143-1

Figs 2, 3

Chinese name: 大萼羊耳蒜

Type. CHINA. Yunnan Province (云南), Xishuangbanna (西双版纳), Mengla County (勐腊县) epiphyte on the tree trunk, 1620 m elev., 23Nov 2021, Zhengwei Wang, Xiaochen Li, Yu Zhang & Zhijin Wu, WZW04247 (holotype: CSH!)

Diagnosis. *Liparis macrosepala* is characterised by the ovoid-fusiform, slightly compressed pseudobulbs with 4 or 5 alternate leaves on their apical half, these with slightly crispate margins, dorsal sepal ovate with cordate base, broadly elliptic, ca. 4 mm long, 2 callus-shaped and thickened folds, base with 2 oblong lobes on both sides, centrally with 1 thickened, concave callus, column with a single pair of arcuate wings.

Epiphytic herbs. Roots slender, flexuose. Pseudobulbs clustered, ovoid-fusiform, slightly compressed laterally, 1–2 × 0.5–1 cm, upper half with 4–5 widely spaced leaves. Leaf blade ovate-oblong, 1.8–2.3 × 0.8–1.2 cm, apex acuminate, base contracted into a short petiole, articulate, margins of their apical half slightly crispate. Peduncle 7–10 cm long, with several sterile bracts 2–5 mm long; raceme with 7–10 flowers arranged in zigzag manner. Floral bracts broadly ovate with cordate base, 2–3 × 1–1.5 mm, acute. Flowers greenish-orange; pedicel and ovary ca. 7 mm long. Dorsal sepal broadly ovate with cordate base, 3.2–5 × 3–3.6 mm, 1-veined, abaxially carinate, apex acute; lateral sepal oblong-ovate or ovate-lanceolate, 5–6 × ca. 0.6 mm long, abaxially slightly carinate. Petals narrowly linear, 3–4 × ca. 0.2 mm; lip elliptic, 2–3 × ca. 1 mm, apex apiculate, base bearing a bituberculate callus, then expanded on each side into a thickened, folded, rounded lobe, with 1 excavation with raised margins between the lobes. Column straight, ca. 2 mm long, with a pair of subtriangular, obtuse wings on each side near the middle and a ridge on the back of the column. Anther cap hemispherical, pale yellow; pollinia 4 in 2 pairs with one pollinium of each pair smaller than the other, waxy, brownish, with minute apical viscidium.

Phenology: Flowering in November–December.

Distribution and habitat. It is found on tree trunks on a limestone ridge-top evergreen broad-leaved forest at an elevation of 1500–1700 m in Mengna County, Xishuangbanna Autonomous Prefecture, Yunnan Province, People's Republic of China. The habitat presents a tropical monsoon climate.

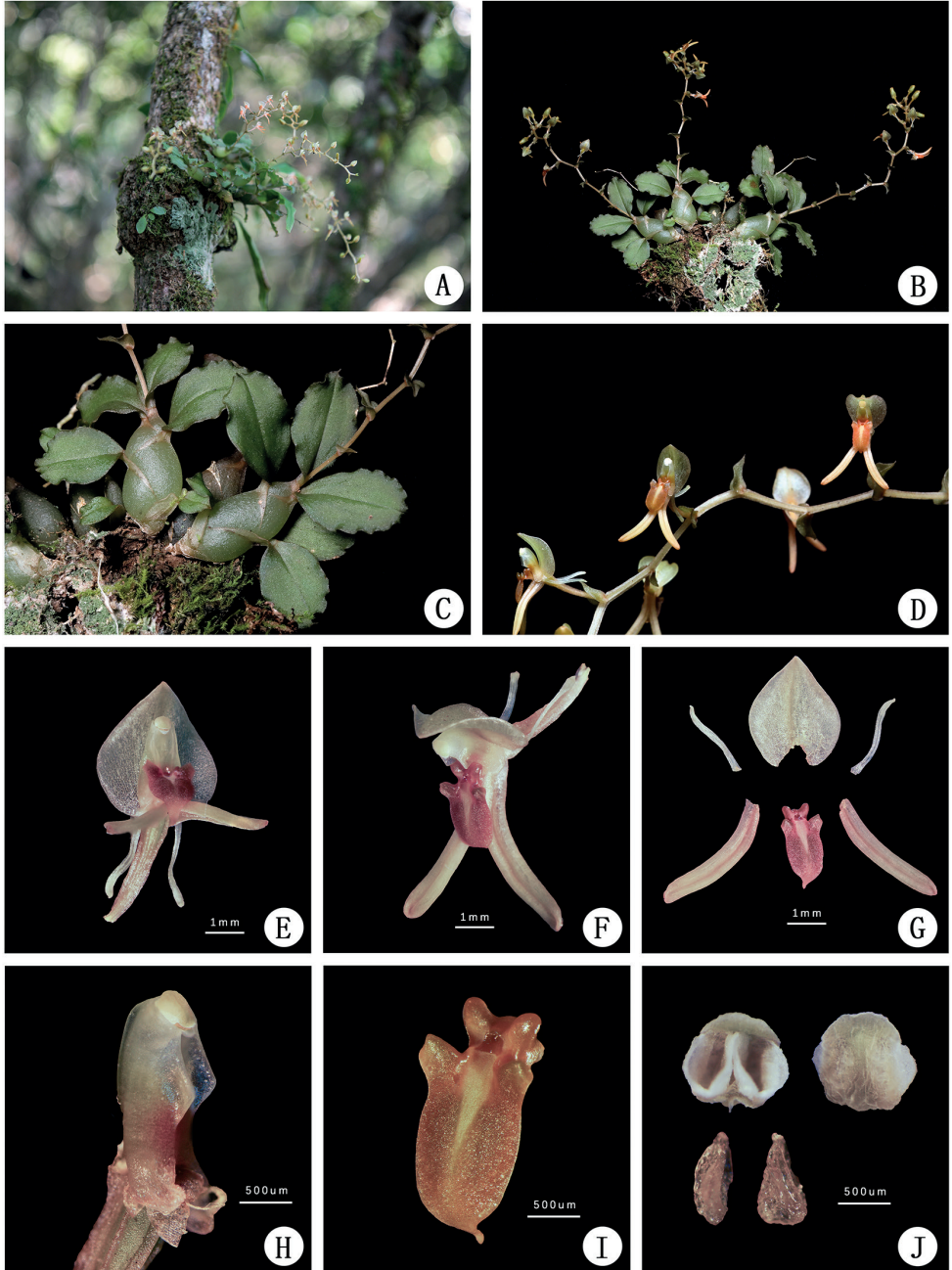


Figure 2. Morphology of *Liparis macrosepala*. **A** plants in situ **B** flowering plant **C** pseudobulbs and leaves **D** inflorescence **E** flowers, front view **F** flowers, side view **G** perianth dissection **H** column from side **I** lip in oblique view **J** anther cap and pollinia. Photographs by Weichang Huang.

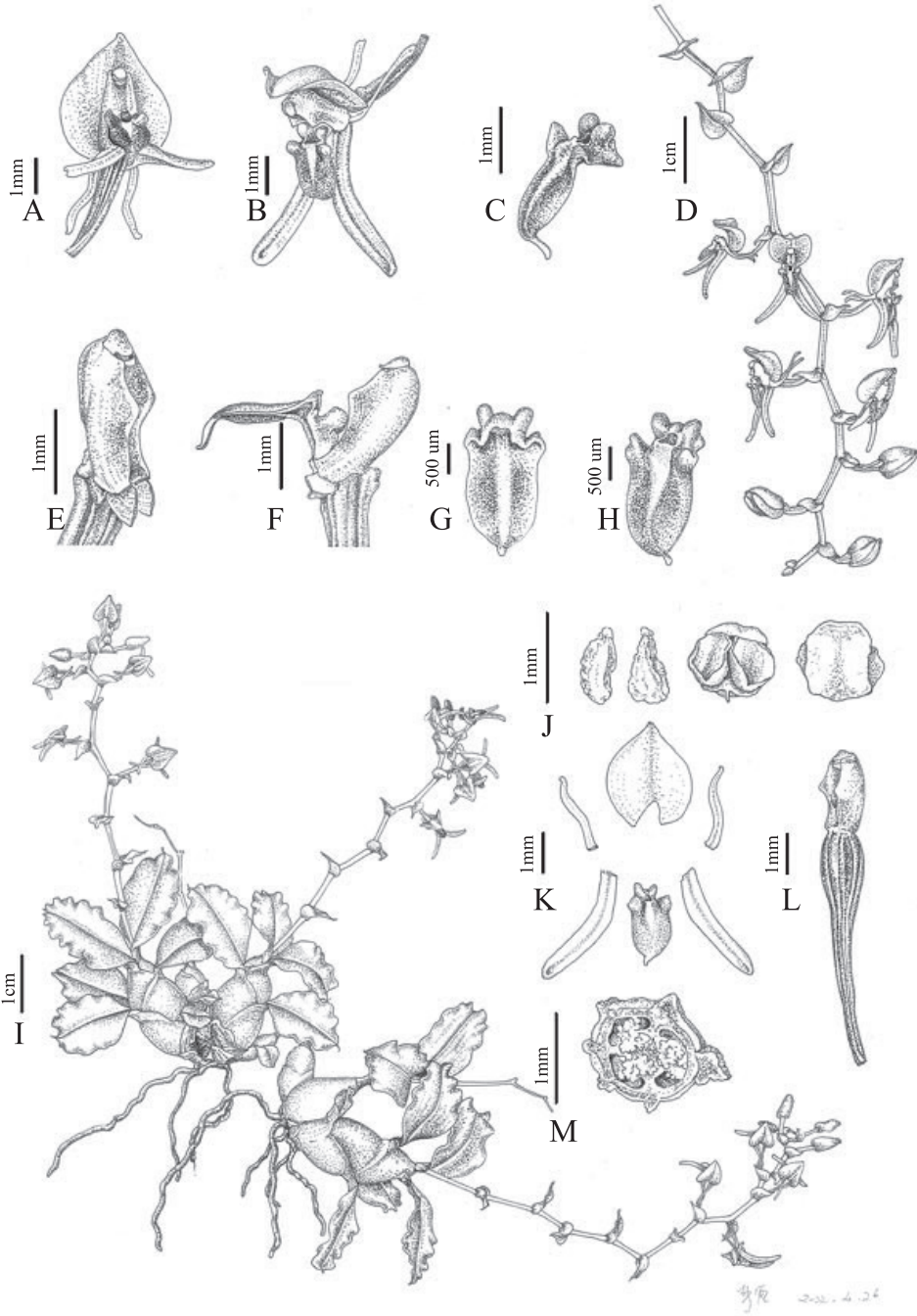


Figure 3. *Liparis macrosepala* **A** flower, front view **B** flower, side view **C** lip, side view **D** inflorescence **E** column, side view **F** lip and column, side view **G** lip, back view **H** lip, front view **I** flowering plant **J** pollinia and anther cap **K** perianth dissection **L** column and ovary, oblique view **M** ovary, transection. Drawn by Lan Yan.

Etymology. The species epithet refers to the large and conspicuous dorsal sepal of the flower.

Taxonomic notes. *Liparis macrosepala* differs from *L. delicatula* in its 4 to 5 leaves with slightly crispate margins on their apical half and single pair of wings on the column. Its entire, not Y-shaped petals and sessile lip (i.e. without a claw) easily distinguish *L. macrosepala* from *L. fissipetala*. The dorsal sepal of *L. assamica* is narrowly ovate-oblong, in contrast with the heart-shaped dorsal sepal of *Liparis macrosepala*. *Liparis resupinata* is distinguished from *L. macrosepala* by its 10–50-flowered raceme and the column with a single pair of broad wings, each with a retrorse thread. The main differences between these closely-related species, according to our phylogenetic analyses, are summarised in Table 2.

Conservation assessment. The new species was found in a ridge-top evergreen broad-leaved forest on a limestone mountain. Despite numerous surveys in the areas, only six mature individuals were found without fruits or evidence of cross-pollination.

This extremely small effective population occurs in a touristic zone which is a serious threat to the survival of the species. Consequently, the species can be assessed as Critically Endangered (CR, D), based on current information and following IUCN guidelines (IUCN 2019).

Table 2. Comparison of *L. macrosepala* and related species.

Characters	<i>L. delicatula</i>	<i>L. fissipetala</i>	<i>L. assamica</i>	<i>L. resupinata</i>	<i>L. macrosepala</i>
Pseudobulbs	oblong or cylindrical-fusiform 5–9 3–5 mm	ovoid, 8–10 mm long	ovoid-fusiform, slightly compressed 1.5–2.5 cm × 6–10 mm	subcylindrical or ± spindle-shaped, 1.8–5 cm × 3–6 mm	ovoid-fusiform, slightly compressed, 1–2 cm × 0.5–1 cm
Leaf	2 or 3, margin flat	3 or 4, strongly crisped-margined	3 or 4, apical half slightly crisped-margined	3 or 4, margin slightly serrate	4 or 5, apical half slightly crisped-margined
Scape	2–5 cm, several to 10-flowered, flowers white	5–10 cm long, with 10–15 flowers, flowers yellow,	10–13 cm, more than 10-flowered, flowers orange	7–18 cm, 10–50-flowered, flowers pale green or greenish-yellow	7–10 cm, more than 10-flowered, flowers greenish-orange
Bracts	ovate-lanceolate, 2–3 mm	ovate-lanceolate, 1.5–3.5 mm	lanceolate, 2–3 mm	lanceolate, 3–5 mm	broadly ovate, 2–3 mm
Dorsal sepal	ovate-oblong, 2.5–3 × 1.5–1.8 mm	oblong-lanceolate, 3–4 × 0.8–1 mm	narrowly ovate-oblong, 4.8–5.8 × ca. 1.6 mm	oblong or elliptic-oblong, ca. 4 × 1.8 mm	broadly ovate, ca. 3.2–5 × 3–3.6 mm
Petals	narrowly linear-lanceolate, 2.5–3 × ca. 0.5 mm, entire	narrow linear, 4–5 mm long, Y-shaped	narrowly linear, 5–5.5 × ca. 0.7 mm, entire	narrowly linear, ca. 3.5 × 0.3 mm, entire	narrowly linear, 3–4 × ca. 0.2 mm, entire
Lip	broadly elliptic or orbicular, ca. 2.5 mm, base with an orbicular, auriculate, callus-shaped fold on either side, with a concave callus near base	epichile broadly oblong or subsquare, 1.5–2 × 1–1.5 mm, base with two auricles on both sides; claw short, with a fleshy callus centrally near base	broadly obovate-oblong, ca. 4 × 2.7 mm, with two callus-shaped thickened folds, two suborbicular lobes on both sides, centrally with one concave callus near base	broadly elliptic-oblong or broadly ovate-oblong, 2.5–3 mm, with two lateral splits below middle; two suborbicular lobes, centrally with one bilobed callus near base	broadly elliptic, ca. 2–3 mm long, two callus-shaped and thickened folds, base with two oblong lobes on both sides, centrally with one bituberculate callus near base
Column	ca. 2.2 mm, two pairs of wings	ca. 1.5 mm, broadly winged with two horn-like appendages	ca. 2 mm, two pairs of wings	ca. 2.8 mm, a pair of wings, each with a retrorse thread	ca. 2 mm, a single pair of subtriangular wings

Acknowledgements

This study was supported by grants from the National Wild Plant Germplasm Resource Centre for Shanghai Chenshan Botanical Garden (ZWX2102), the Science and Technology Commission, Shanghai Municipality (19390743600) and the project of Shanghai Landscaping and City Appearance Administrative Bureau (G192424, G202401). We are grateful to Mingzhong Huang for his help with the literature and Hongjin Wei for his fieldwork. We are grateful to Dr. Pankaj Kumar for his help in improving the language and describing the conservation status. We are also grateful to the reviewers for their valuable views in improving this article.

References

- Cameron KM (2005) Leave it to the leaves: A molecular phylogenetic study of Malaxideae (Epidendroideae, Orchidaceae). *American Journal of Botany* 92(6): 1025–1032. <https://doi.org/10.3732/ajb.92.6.1025>
- Chen S, Liu Z, Zhu G, Lang K, Ji K, Luo Y, Jin X, Cribb PJ, Wood JJ, Gale SW, Ormerod P, Vermeulen J, Wood HP, Clayton DB (2009) Orchidaceae. In: Wu Z, Raven PH, Hong D (Eds) *Flora of China* (Vol. 25). Science Press, Beijing & Missouri Botanical Garden Press, St. Louis.
- Garay LA, Romero-Gonzalez GA (1999) *Schedulae orchidum* II. *Harvard Papers in Botany* 4(2): 475–488.
- Huang HX, Chen LJ, Liu ZJ, Li MH (2018) *Liparis vivipara* (Orchidaceae: Malaxideae), a new species from China: evidence from morphological and molecular analyses. *Phytotaxa* 351(4): 289–295. <https://doi.org/10.11646/phytotaxa.351.4.5>
- Huelsenbeck JP, Ronquist F (2001) MRBAYES: Bayesian inference of phylogenetic trees. *Bioinformatics* 17(8): 754–755. <https://doi.org/10.1093/bioinformatics/17.8.754>
- IUCN (2019) *Guidelines for Using the IUCN Red List Categories and Criteria*, version 14. Prepared by the Standards and Petitions Committee. <http://www.iucnredlist.org/> [accessed 5 September 2022]
- Kumar P, Li J, Gale SW (2022) Integrative analyses of *Crepidium* (Orchidaceae, Epidendroideae, Malaxideae) shed more light on its relationships with *Dienia*, *Liparis* and *Malaxis* and justify reinstatement of narrow endemic *C. allanii*. *Botanical Journal of the Linnean Society* 198(3): 285–305. <https://doi.org/10.1093/botlinnean/boab048>
- Li L, Chung SW, Li B, Zeng SJ, Yan HF, Li SJ (2020) New insight into the molecular phylogeny of the genus *Liparis* s.l. (Orchidaceae: Malaxideae) with a new generic segregate: *Blepharoglossum*. *Plant Systematics and Evolution* 306(54): 1–10. <https://doi.org/10.1007/s00606-020-01679-3>
- Margońska H, Kowalkowska A, Górniak M, Rutkowski P (2012) Taxonomic redefinition of the subtribe Malaxidinae (Orchidales, Malaxideae). Koeltz Scientific Books, Koenigstein.
- Posada D (2008) jModelTest: Phylogenetic model averaging. *Molecular Biology and Evolution* 25(7): 1253–1256. <https://doi.org/10.1093/molbev/msn083>

- Pridgeon AM, Cribb PJ, Chase MW, Rasmussen FN (1999) *Genera orchidacearum*. vol. 4: Epidendroideae, part 1. Oxford University Press, New York and Oxford.
- Ronquist F, Teslenko M, van der Mark P, Ayres DL, Darling A, Höhna S, Larget B, Liu L, Suchard MA, Huelsenbeck JP (2012) MrBayes 3.2: Efficient bayesian phylogenetic inference and model choice across a large lodel lpace. *Systematic Biology* 61(3): 539–542. <https://doi.org/10.1093/sysbio/sys029>
- Stamatakis A (2006) RAxML-VI-HPC: Maximum likelihood-based phylogenetic analyses with thousands of taxa and mixed models. *Bioinformatics (Oxford, England)* 22(21): 2688–2690. <https://doi.org/10.1093/bioinformatics/btl446>
- Tang GD, Zhang GQ, Hong WJ (2015) Phylogenetic analysis of Malaxideae (Orchidaceae: Epidendroideae): two new species based on the combined nrDNA ITS and chloroplast matK sequences. *Guangxi Zhi Wu* 35(4): 447–463.
- Tian HZ, Hu AQ, Liu QX, Zhou XX, Hu C, Chung SW, Xing FW (2015) *Liparis tsii*: a new species of Orchidaceae (tribe-Malaxideae) from Guangdong, China with its phylogenetic position. *Plant Biosystems-An International Journal Dealing with all Aspects of Plant Biology* 150(6): 1225–1232. <https://doi.org/10.1080/11263504.2015.1014445>
- Ya JD, Lin DL, Han ZD, Cai L, Zhang ZR, He DM, Jin XH, Yu WB (2021) Three new species of *Liparis* s.l. (Orchidaceae: Malaxideae) from Southwest China based on morphological characters and phylogenetic evidence. *Plant Diversity* 43(5): 401–408. <https://doi.org/10.1016/j.pld.2021.01.006>

Phylogenomic and morphological evidence reveal a new species of spider lily, *Lycoris longifolia* (Amaryllidaceae) from China

Yi-Lei Lou^{1,2*}, Dai-Kun Ma^{3*}, Ze-Tao Jin^{3,4*}, Hui Wang⁵, Lu-Huan Lou⁵,
Shui-Hu Jin⁵, Kun Liu⁶, Bin-Bin Liu³

1 College of Landscape Architecture, Zhejiang Agriculture and Forestry University, Hangzhou 311300, China **2** College of Landscape Architecture, Beijing Forestry University, Beijing 100083, China **3** State Key Laboratory of Systematic and Evolutionary Botany, Institute of Botany, Chinese Academy of Sciences, Beijing 100093, China **4** Centre of Pear Engineering Technology Research, State Key Laboratory of Crop Genetics and Germplasm Enhancement, Nanjing Agricultural University, Nanjing 210095, China **5** College of Forestry and Biotechnology, Zhejiang Agriculture and Forestry University, Hangzhou 311300, China **6** Anhui Provincial Key Laboratory of the Conservation and Exploitation of Biological Resources, College of Life Sciences, Anhui Normal University, Wuhu 241000, China

Corresponding author: Bin-Bin Liu (liubinbin@ibcas.ac.cn), Kun Liu (hudixiao@126.com)

Academic editor: Lorenzo Peruzzi | Received 15 July 2022 | Accepted 29 August 2022 | Published 5 October 2022

Citation: Lou Y-L, Ma D-K, Jin Z-T, Wang H, Lou L-H, Jin S-H, Liu K, Liu B-B (2022) Phylogenomic and morphological evidence reveal a new species of spider lily, *Lycoris longifolia* (Amaryllidaceae) from China. *PhytoKeys* 210: 79–92. <https://doi.org/10.3897/phytokeys.210.90391>

Abstract

Lycoris longifolia, a new species from China, was described and illustrated here. Our phylogenomic evidence based on whole plastomes strongly supported the separate phylogenetic position of this new species, and morphologically it could also be distinguished by its long leaves with a distinct purplish-red midrib on the abaxial surface.

Keywords

Lycoris, morphological, phylogenomics, whole plastome

* Contributed equally as the first authors.

Introduction

The genus *Lycoris* Herb., including ca. 13–20 species of flowering plants in the family Amaryllidaceae, subfamily Amaryllidoideae, is native to eastern and southern Asia. Herbert described the first species in 1820, *L. aurea* (L'Hér.) Herb., which has important ornamental and medicinal values (Hsu et al. 1994). In the mid-20th century, an American horticulturist, Hayward, did much work on introducing and cultivating *Lycoris* species. Given the easily distinguished habit of the populations of *Lycoris aurea* distributed in northern Taiwan and southernmost Japan, i.e., the leaves appear in autumn, about a month later than *L. aurea*, and no remains of leaf bases (Hsu et al. 1994), Hayward described these populations as a new species, *L. traubii* W.Hayw. (Hayward 1957; Hsu et al. 1994; Kurita 1987). Having narrower perianth lobes and long-exserted stamens (Hsu et al. 1994; Ji and Meerow 2000), the populations from South Gansu (Kang Xian) and Northwest Hubei (Feng Xian) were described as a variety of *Lycoris aurea*, as *L. aurea* var. *angustitepala* P.S.Hsu, Kurita, Z.Z.Yu & J.Z.Lin (Hsu et al. 1994). In the last decades, numerous new species or hybrids of *Lycoris* have been published in its diversity center, i.e. mainland China, such as *L. hunanensis* M.H.Quan, L.J.Ou & C.W.She (Quan et al. 2013), *L. × hubeiensis* KunLiu (Meng et al. 2018), *L. tsinlingensis* P.C.Zhang, YiJunLu & TingWang (Lu et al. 2020), and *L. wulingensis* S.Y.Zhang (Zhang et al. 2021). Nowadays, more than 30 species and varieties have been recognized in the genus (Hsu et al. 1994; Ji and Meerow 2000; Kim 2004; Quan et al. 2013; Meng et al. 2018; Lu et al. 2020; Zhang et al. 2021), and nearly 20 of them are from China.

During our recent field explorations in Sichuan Province, China, we collected a wild flowering plant of *Lycoris*, which resembles *L. aurea* with yellow flowers. However, it could be easily distinguished from *L. aurea* by markedly long leaves with a distinct purplish-red midrib on the abaxial surface. Our morphological and molecular evidence strongly supported this population as a new *Lycoris* species.

Materials and methods

Total genomic DNAs were extracted from 15mg of silica gel dried leaves using a modified CTAB method (Li et al. 2013). The library was prepared at the Molecular Biology Experiment Center, Germplasm Bank of Wild Species in Southwest China using a NEBNext Ultra™ II DNA Library Prep Kit (New England Biolabs, Ipswich, MA, USA). The paired-end (150 bp) reads have been generated on the HiSeq 2500 (Illumina, Inc., San Diego, CA, USA) platform in Beijing Genomics Institution (BGI) (Shenzhen, China), ca. 8 GB of raw data for this new species. The raw reads have been deposited in the NCBI Sequence Read Archive in the BioProject (PRJNA857321) with the Run number SRR20072320.

The raw data generated from the Illumina platform was trimmed by Trimmomatic v.0.40 (Bolger et al. 2014) with the default parameters. The clean data was

checked by FastQC (Andrews 2010) for quality control. We used the successive assembly approach (Zhang et al. 2015), combining the reference-based and the de novo assembly methods to assemble the chloroplast genome; this method has been performed well in various angiosperm lineages (e.g., Liu et al. 2019, 2020a, 2020b, 2021, 2022; Wang et al. 2020). We annotated the assembled chloroplast genome with two reference genomes (MK353216 and MH118290) downloaded from GenBank, and checked the start and stop codons carefully by translating the coding sequences of plastome into proteins in Geneious Prime (Kearse et al. 2012). We also verified the boundary of two reverse complementary repeats in the plastome using Find Repeats embedded in Geneious Prime (Kearse et al. 2012). The assembled chloroplast genome has been submitted to GenBank with the accession number ON960856. The gene map of the new species *Lycoris longifolia* chloroplast genome was drawn by OrganellarGenomeDRAW (OGDRAW) version 1.3.1 (Greiner et al. 2019).

We downloaded 24 chloroplast genomes from GenBank as the ingroup and *Narcissus poeticus* L. as the outgroup for phylogenomic analysis. Given the potential effect of the missing data for the accurate phylogenetic inference, we used the whole plastome (WP) and 78 coding sequences (CDS) to estimate the phylogeny, respectively. Because of the nearly identical sequence of two inverted repeats (IR) in plastomes, we only included one repeat of IR region for downstream WP analyses. Each CDS sequence was extracted separately by Geneious Prime; the WP matrix was aligned with MAFFT v. 7.480 (Nakamura et al. 2018) with default parameters. The WP matrix was trimmed using trimAL v1.2 (Capella-Gutiérrez et al. 2009) with a heuristic method to decide on the best-automated method. All 78 CDS sequences of each plastome were concatenated by AMAS (Borowiec 2016). The best-fit partitioning schemes and/or nucleotide substitution models for the 78 CDS sequences were estimated using PartitionFinder2 (Stamatakis 2006; Lanfear et al. 2016), under the corrected Akaike information criterion (AICc) and linked branch lengths, as well as with rcluster (Lanfear et al. 2014) algorithm options. The resulting optimal partitioning schemes and evolutionary model for each CDS sequence were applied for the following tree inference. We used IQ-TREE2 v. 2.1.3 (Minh et al. 2020) with 1000 SH-aLRT and the ultrafast bootstrap replicates and RAxML 8.2.12 (Stamatakis 2014) with GTRGAMMA model for each partition and clade support assessed with 200 rapid BS replicates for the Maximum Likelihood (ML) analysis. The BI was performed with MrBayes 3.2.7 (Ronquist et al. 2012). The Markov Chain Monte Carlo (MCMC) analyses were run for 10,000,000 generations. The stationarity was regarded to be reached when the average standard deviation of split frequencies remained below 0.01. Trees were sampled every 1,000 generations, and the first 25% of samples were discarded as burn-in. The remaining trees were used to build a 50% majority-rule consensus tree. Considering the possible different evolutionary forces in the chloroplast genome, we also used ASTRAL-III (Zhang et al. 2018) for estimating a coalescent-based species tree based on the 78 CDS sequences.

Results

The chloroplast genome of *Lycoris longifolia* was 158,413 bp in length, with a typical quadripartite structure consisting of a large single copy region and a small single copy region separated by two long inverted repeats (Fig. 1B). And this structure has been nearly similar to other *Lycoris* chloroplast genomes released in GenBank. They contained the same number of coding sequences (78), tRNAs (30), and rRNAs (4).

The WP matrix was 131,649 bp in length, with the poor sites trimmed by trimAL (Capella-Gutiérrez et al. 2009); the concatenated CDSs were 67,953 bp in length. These two matrices generated seven trees (Fig. 1A, Suppl. material 1–6). The four ML trees (Fig. 1A, Suppl. material 1, 3, 4), two Bayesian trees (Suppl. material 2, 5), and the species tree (Suppl. material 6) resulted in a consistent phylogenetic position, and this new species, *Lycoris longifolia*, formed a separate clade (Fig. 1A). This result showed that this new species has been distant from other species in *Lycoris*. The examined morphological characters, long leaves and purplish-red midrib abaxially, also supported its distinguished status.

Taxonomy

Lycoris longifolia L.H.Lou, sp. nov.

urn:lsid:ipni.org:names:77306298-1

Chinese name: 长叶石蒜

Figs 2, 3

Diagnosis. Most similar to *L. aurea* but differs from it by markedly longer leaves, abaxially with a distinct purplish-red midrib.

Type. CHINA. Sichuan: Ya'an, Yucheng, Bifengxia, Houyancun, Yanjiashan, under the shrub along the stream, elevation ca. 950 m, 10 May 2021, *L.H. Lou* & *Y.L. Lou* 8765 (holotype PE [barcode 02347459]!; isotypes KUN!, PE [barcode 02347457]!).

Additional Specimens examined. CHINA. Sichuan: Ya'an, Yucheng, Bifengxia, Houyancun, Yanjiashan, under the shrub along the stream, elevation ca. 950 m, 30 July 2021, *L.H. Lou* & *Y.L. Lou* 8766 (paratype PE [barcode 02347458]!).

Description. Bulbous perennial. Bulbs subglobose, 3–6 cm diam., tunics membranous, dark brown. Leaves ligulate, acute at the apex, ca. 80–120 × 1.5–2 cm, absent at the flowering time and appearing in autumn, dark green, with a prominent midrib on the abaxial surface, abaxial midrib distinctly purplish-red. Inflorescence scapose, umbellate; scape solid, 70–75 cm long, ca. 2.0 cm diam. at base, light green with purplish-red base; involucre bracts 2, lanceolate, 5.0–9.0 cm long by 1.8 cm wide at base, membranous, light green; bracteoles membranous, lanceolate, 1.0–4.0 cm long. Flowers 5–7 per umbel; pedicels 2–2.5 cm long; perianth with 6 tepals; tube ca. 1.5 cm; lobes yellow, abaxially with white mid-vein, strongly recurved, narrowly oblanceolate, ca. 7 × 0.8–1.0 cm, margin strongly undulate. Stamen filaments 6, creamy-yellow, slightly longer than perianth; anther light purplish, dorsifixed, 8–10 mm long before

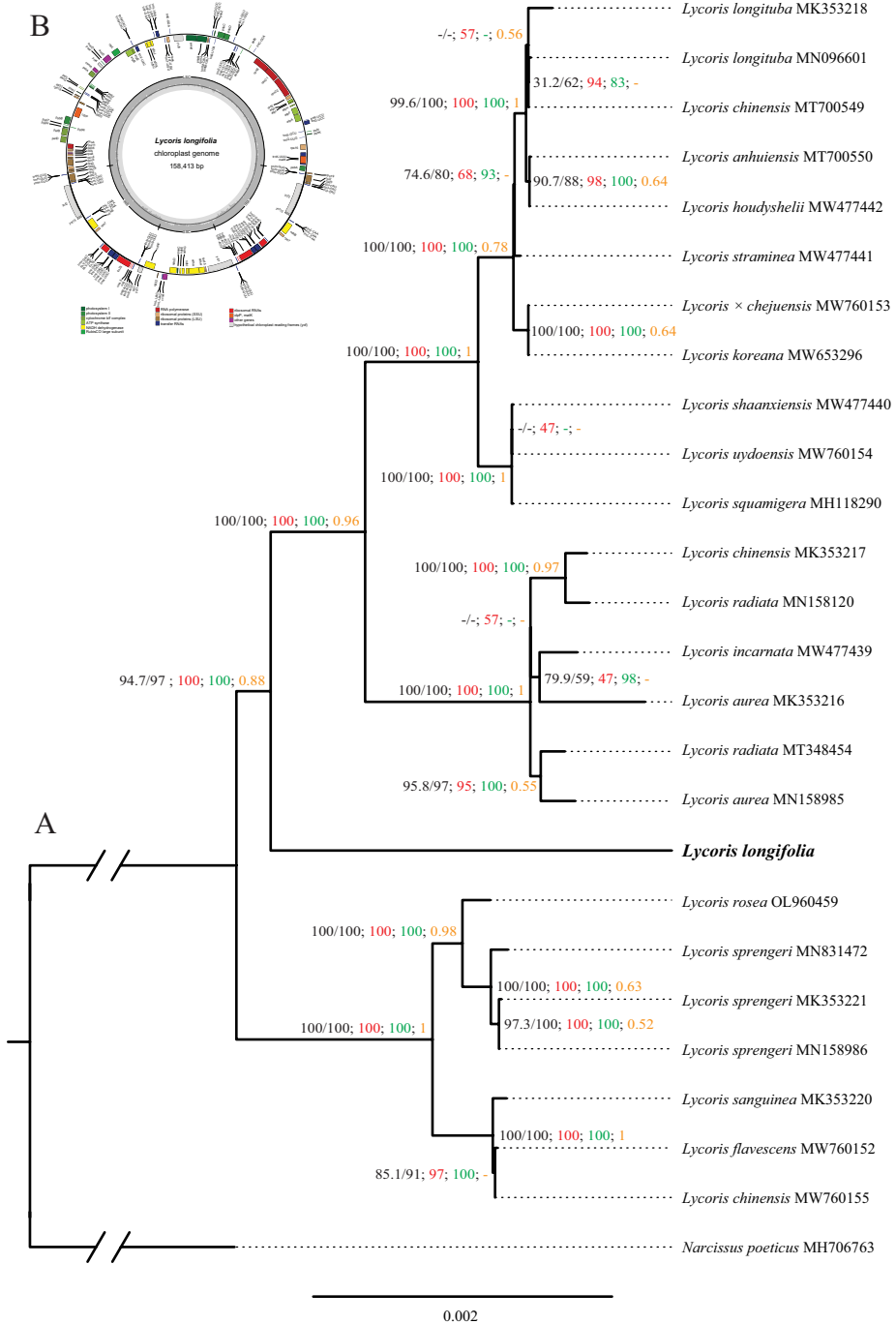


Figure 1. Maximum likelihood phylogeny of *Lycoris* inferred from RAxML analysis of the whole plastome data **A** numbers above the branches indicate the SH-aLRT support and Ultrafast Bootstrap support (black) by IQ-TREE2, the bootstrap support (red) by RAxML, the posterior probabilities (green) by MrBayes, and the local posterior possibility (orange) by ASTRAL-III. The upper-left inset was a gene map of the new species *Lycoris longifolia* chloroplast genome **B**.

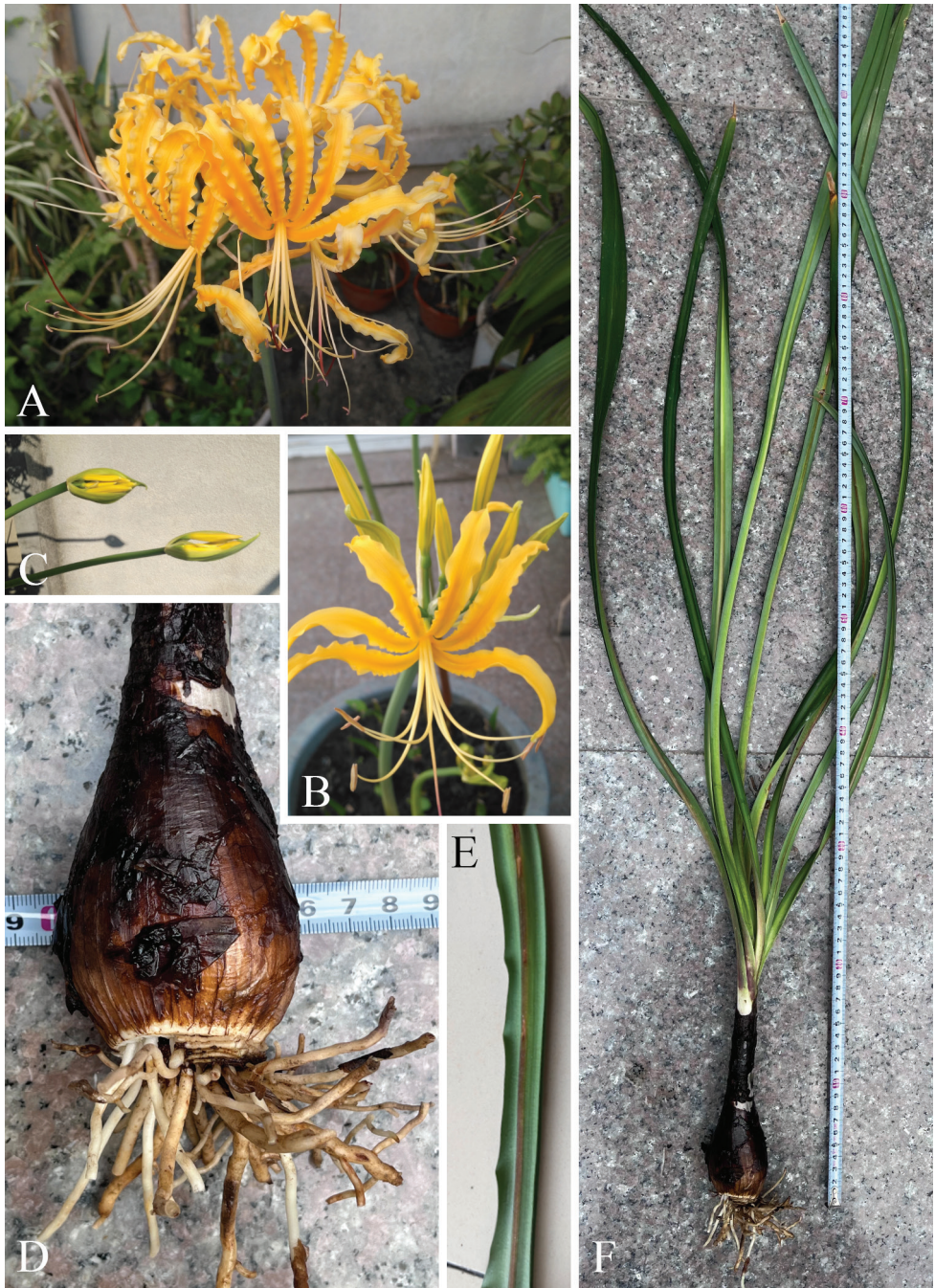


Figure 2. Field photos of *Lycoris longifolia* **A-C** flowers **D** bulb **E** the distinct purplish-red midrib abaxially **F** vegetative growth period, showing the long leaves.



Figure 3. Illustration of *Lycoris longifolia*, drawn by Ai-Li Li (PE).

anthesis. Style creamy-yellow but rose-red at apex, slightly exceeding filaments; stigma purplish-red; ovary green, ovoid, ca. 5 mm long.

Phenology. Scape produced from July to August, and vegetative growth from September to May next year. This new species grows along the forest edge near the riverside, and *Quercus glauca* Thunb. and *Pinus massoniana* Lamb. are the dominant associated species.

Etymology. The specific epithet alludes to length of leaf blades, a diagnostic character.

Distribution. This new species has been narrowly discovered in Ya'an, Sichuan, China. Some localities of Southwestern China have been poorly discovered, and a comprehensive floristic investigation will help elucidate the germplasm resources.

Key to the species of *Lycoris* in China

- | | | |
|----|--|------------------------|
| 1 | Flowers actinomorphic..... | 2 |
| – | Flowers zygomorphic..... | 6 |
| 2 | Margin of perianth lobes not undulate..... | 3 |
| – | Margin of perianth lobes basally minutely undulate..... | 4 |
| 3 | Perianth pale purple but apically blue | <i>L. sprengeri</i> |
| – | Perianth white or yellow | <i>L. longituba</i> |
| 4 | Perianth purple..... | <i>L. squamigera</i> |
| – | Perianth not purple..... | 5 |
| 5 | Perianth yellow..... | <i>L. anhuiensis</i> |
| – | Perianth white, abaxially with purple midvein..... | <i>L. incarnata</i> |
| 6 | Leaves appearing in autumn..... | 7 |
| – | Leaves appearing in spring..... | 15 |
| 7 | Perianth yellow or ocher-yellow | 8 |
| – | Perianth bright red, deep red, rose-red, or white | 11 |
| 8 | Perianth yellow; leaves 1.5–5 cm wide | 9 |
| – | Perianth ocher-yellow; leaves 1.0–1.5 cm wide..... | 10 |
| 9 | Leaves ensiform, ca. 60 × 2–5 cm | <i>L. aurea</i> |
| – | Leaves ligulate, ca. 100 × 1.5–2 cm..... | <i>L. longifolia</i> |
| 10 | Leaves ensiform, apex acuminate | <i>L. straminea</i> |
| – | Leaves ligulate, apex obtuse..... | <i>L. hunanensis</i> |
| 11 | Perianth bright red, deep red, or rose-red..... | 12 |
| – | Perianth white..... | <i>L. houdyshelii</i> |
| 12 | Perianth bright red or deep red, lobes strongly recurved..... | 13 |
| – | Perianth rose-red, lobes slightly recurved..... | 14 |
| 13 | Perianth bright red..... | <i>L. radiata</i> |
| – | Perianth deep red with white but faintly pale red filaments..... | <i>L. hubeiensis</i> |
| 14 | Leaves ligulate, ca. 0.8 cm wide | <i>L. rosea</i> |
| – | Leaves narrowly ligulate, ca. 0.5 cm wide..... | <i>L. wulingensis</i> |
| 15 | Perianth white..... | 16 |
| – | Perianth yellow or orange-red | 17 |
| 16 | Perianth white without pink stripes | <i>L. caldwellii</i> |
| – | Perianth white with pink stripes..... | <i>L. shaanxiensis</i> |

- 17 Perianth yellow in bud, becoming orange-red as buds develop
 *L. tsinlingensis*
 – Perianth yellow 18
 18 Perianth lobes without red stripes *L. chinensis*
 – Perianth lobes abaxially with red stripes *L. guangxiensis*

Acknowledgements

All the phylogenomic analyses have been run on the Dell T7920 workstation (Institute of Botany, Chinese Academy of Sciences); this study is also supported by the Bioinformatics Center of Nanjing Agricultural University. National Natural Science Foundation of China (Grant No. 32000163, 32270216, and 31620103902) and Project of National Plant Specimen Resource Center (NPSRC) (E0117G1001) support this study.

References

- Andrews S (2010) FastQC: A quality control tool for high throughput sequence data. <http://www.bioinformatics.babraham.ac.uk/projects/fastqc> [accessed 25 June 2022]
- Bolger AM, Lohse M, Usadel B (2014) Trimmomatic: A flexible trimmer for Illumina sequence data. *Bioinformatics* 30(15): 2114–2120. <https://doi.org/10.1093/bioinformatics/btu170>
- Borowiec ML (2016) AMAS: A fast tool for alignment manipulation and computing of summary statistics. *PeerJ* 4: e1660. <https://doi.org/10.7717/peerj.1660>
- Capella-Gutiérrez S, Silla-Martínez JM, Gabaldón T (2009) trimAl: A tool for automated alignment trimming in large-scale phylogenetic analyses. *Bioinformatics* 25(15): 1972–1973. <https://doi.org/10.1093/bioinformatics/btp348>
- Greiner S, Lehwark P, Bock R (2019) OrganellarGenomeDRAW (OGDRAW) version 1.3.1: Expanded toolkit for the graphical visualization of organellar genomes. *Nucleic Acids Research* 47(W1): W59–W64. <https://doi.org/10.1093/nar/gkz238>
- Hayward W (1957) *Lycoris traubii*, sp. nov. *Plant Life* 13: 40–41.
- Hsu BS, Kurita S, Yu ZZ, Lin JZ (1994) Synopsis of the genus *Lycoris* (Amaryllidaceae). *SIDA, Contributions to Botany* 16: 301–331. <https://doi.org/10.2307/41967120>
- Ji ZH, Meerow AW (2000) Amaryllidaceae. In: Wu ZY, Raven PH, Hong DY (Eds) *Flora of China*. Science Press & St. Louis: Missouri Botanical Garden Press, Beijing, 264–273.
- Kearse M, Moir R, Wilson A, Stones-Havas S, Cheung M, Sturrock S, Buxton S, Cooper A, Markowitz S, Duran C, Thierer T, Ashton B, Meintjes P, Drummond A (2012) Geneious Basic: An integrated and extendable desktop software platform for the organization and analysis of sequence data. *Bioinformatics* 28(12): 1647–1649. <https://doi.org/10.1093/bioinformatics/bts199>
- Kim MY (2004) A taxonomic review of Korean *Lycoris* (Amaryllidaceae). *Korean Journal of Plant Taxonomy* 34(1): 9–26. <https://doi.org/10.11110/kjpt.2004.34.1.009>
- Kurita S (1987) Variation and evolution in the karyotype of *Lycoris*, Amaryllidaceae III. Intraspecific variation in the karyotype of *L. traubii* Hayward. *Cytologia* 52(1): 117–128. <https://doi.org/10.1508/cytologia.52.117>

- Lanfear R, Calcott B, Kainer D, Mayer C, Stamatakis A (2014) Selecting optimal partitioning schemes for phylogenomic datasets. *BMC Evolutionary Biology* 14(1): 82. <https://doi.org/10.1186/1471-2148-14-82>
- Lanfear R, Frandsen PB, Wright AM, Senfeld T, Calcott B (2016) PartitionFinder 2: New methods for selecting partitioned models of evolution for molecular and morphological phylogenetic analyses. *Molecular Biology and Evolution* 34: 772–773. <https://doi.org/10.1093/molbev/msw260>
- Li J, Wang S, Yu J, Wang L, Zhou S (2013) A modified CTAB protocol for plant DNA extraction. *Zhiwu Xuebao* 48(1): 72–78. <https://doi.org/10.3724/SP.J.1259.2013.00072>
- Liu BB, Hong DY, Zhou SL, Xu C, Dong WP, Johnson G, Wen J (2019) Phylogenomic analyses of the *Photinia* complex support the recognition of a new genus *Phippsiomeles* and the resurrection of a redefined *Stranvaesia* in Maleae (Rosaceae). *Journal of Systematics and Evolution* 57(6): 678–694. <https://doi.org/10.1111/jse.12542>
- Liu BB, Campbell CS, Hong DY, Wen J (2020a) Phylogenetic relationships and chloroplast capture in the *Amelanchier-Malacomeles-Peraphyllum* clade (Maleae, Rosaceae): Evidence from chloroplast genome and nuclear ribosomal DNA data using genome skimming. *Molecular Phylogenetics and Evolution* 147: e106784. <https://doi.org/10.1016/j.ympev.2020.106784>
- Liu BB, Liu GN, Hong DY, Wen J (2020b) *Eriobotrya* belongs to *Rhaphiolepis* (Maleae, Rosaceae): Evidence from chloroplast genome and nuclear ribosomal DNA data. *Frontiers in Plant Science* 10: e1731. <https://doi.org/10.3389/fpls.2019.01731>
- Liu BB, Ma ZY, Ren C, Hodel RGJ, Sun M, Liu XQ, Liu GN, Hong DY, Zimmer EA, Wen J (2021) Capturing single-copy nuclear genes, organellar genomes, and nuclear ribosomal DNA from deep genome skimming data for plant phylogenetics: A case study in Vitaceae. *Journal of Systematics and Evolution* 59(5): 1124–1138. <https://doi.org/10.1111/jse.12806>
- Liu BB, Ren C, Kwak M, Hodel RGJ, Xu C, He J, Zhou WB, Huang CH, Ma H, Qian GZ, Hong DY, Wen J (2022) Phylogenomic conflict analyses in the apple genus *Malus* s.l. reveal widespread hybridization and allopolyploidy driving diversification, with insights into the complex biogeographic history in the Northern Hemisphere. *Journal of Integrative Plant Biology* 64(5): 1020–1043. <https://doi.org/10.1111/jipb.13246>
- Lu YJ, Wang T, Wang YC, Zhang PC (2020) *Lycoris tsinlingensis* (Amaryllidaceae), a new species from Shaanxi, China. *Annales Botanici Fennici* 57(4–6): 193–196. <https://doi.org/10.5735/085.057.0424>
- Meng WQ, Zheng L, Shao JW, Zhou SB, Liu K (2018) A new natural allotriploid, *Lycoris* × *hubeiensis* hybr. nov. (Amaryllidaceae), identified by morphological, karyological and molecular data. *Nordic Journal of Botany* 36(6): njb-01780. <https://doi.org/10.1111/njb.01780>
- Minh BQ, Schmidt HA, Chernomor O, Schrempf D, Woodhams MD, Von Haeseler A, Lanfear R (2020) IQ-TREE 2: New models and efficient methods for phylogenetic inference in the genomic era. *Molecular Biology and Evolution* 37(5): 1530–1534. <https://doi.org/10.1093/molbev/msaa015>
- Nakamura T, Yamada KD, Tomii K, Katoh K (2018) Parallelization of MAFFT for large-scale multiple sequence alignments. *Bioinformatics* 34(14): 2490–2492. <https://doi.org/10.1093/bioinformatics/bty121>

- Quan MH, Ou LJ, She CW (2013) A new species of *Lycoris* (Amaryllidaceae) from Hunan, China. *Novon: A Journal for Botanical Nomenclature* 22(3): 307–310. <https://doi.org/10.3417/2011013>
- Ronquist F, Teslenko M, van der Mark P, Ayres DL, Darling A, Höhna S, Larget B, Liu L, Suchard MA, Huelsenbeck JP (2012) MrBayes 3.2: Efficient Bayesian phylogenetic inference and model choice across a large model space. *Systematic Biology* 61(3): 539–542. <https://doi.org/10.1093/sysbio/sys029>
- Stamatakis A (2006) RAxML-VI-HPC: Maximum likelihood-based phylogenetic analyses with thousands of taxa and mixed models. *Bioinformatics* 22(21): 2688–2690. <https://doi.org/10.1093/bioinformatics/btl446>
- Stamatakis A (2014) RAxML version 8: A tool for phylogenetic analysis and post-analysis of large phylogenies. *Bioinformatics* 30(9): 1312–1313. <https://doi.org/10.1093/bioinformatics/btu033>
- Wang YB, Liu BB, Nie ZL, Chen HF, Chen FJ, Figlar RB, Wen J (2020) Major clades and a revised classification of *Magnolia* and Magnoliaceae based on whole plastid genome sequences via genome skimming. *Journal of Systematics and Evolution* 58(5): 673–695. <https://doi.org/10.1111/jse.12588>
- Zhang N, Wen J, Zimmer EA (2015) Congruent deep relationships in the grape family (Vitaceae) based on sequences of chloroplast genomes and mitochondrial genes via genome skimming. *PLoS ONE* 10(12): e0144701. <https://doi.org/10.1371/journal.pone.0144701>
- Zhang C, Rabiee M, Sayyari E, Mirarab S (2018) ASTRAL-III: Polynomial time species tree reconstruction from partially resolved gene trees. *BMC Bioinformatics* 19(S6): 153. <https://doi.org/10.1186/s12859-018-2129-y>
- Zhang SY, Huang Y, Zhang P, Zhu KR, Chen YB, Shao JW (2021) *Lycoris wulingensis*, a dwarf new species of Amaryllidaceae from Hunan, China. *PhytoKeys* 177: 1–9. <https://doi.org/10.3897/phytokeys.177.62741>

Supplementary material I

Figure S1

Authors: Yi-Lei Lou, Dai-Kun Ma, Ze-Tao Jin, Hui Wang, Lu-Huan Lou, Shui-Hu Jin, Kun Liu, Bin-Bin Liu

Data type: Images.

Explanation note: Maximum likelihood phylogeny of *Lycoris* inferred from IQ-TREE2 analysis of the whole plastome data. Numbers above the branches indicate the SH-aLRT support and Ultrafast Bootstrap support.

Copyright notice: This dataset is made available under the Open Database License (<http://opendatacommons.org/licenses/odbl/1.0/>). The Open Database License (ODbL) is a license agreement intended to allow users to freely share, modify, and use this Dataset while maintaining this same freedom for others, provided that the original source and author(s) are credited.

Link: <https://doi.org/10.3897/phytokeys.210.90391.suppl1>

Supplementary material 2

Figure S2

Authors: Yi-Lei Lou, Dai-Kun Ma, Ze-Tao Jin, Hui Wang, Lu-Huan Lou, Shui-Hu Jin, Kun Liu, Bin-Bin Liu

Data type: Images.

Explanation note: Bayesian inference phylogeny of *Lycoris* inferred from MrBayes analysis of the complete chloroplast genome data. Numbers above the branches indicate the posterior probabilities (PP).

Copyright notice: This dataset is made available under the Open Database License (<http://opendatacommons.org/licenses/odbl/1.0/>). The Open Database License (ODbL) is a license agreement intended to allow users to freely share, modify, and use this Dataset while maintaining this same freedom for others, provided that the original source and author(s) are credited.

Link: <https://doi.org/10.3897/phytokeys.210.90391.suppl2>

Supplementary material 3

Figure S3

Authors: Yi-Lei Lou, Dai-Kun Ma, Ze-Tao Jin, Hui Wang, Lu-Huan Lou, Shui-Hu Jin, Kun Liu, Bin-Bin Liu

Data type: Images.

Explanation note: Maximum likelihood phylogeny of *Lycoris* inferred from IQ-TREE2 analysis of the concatenated 78 plastid coding genes. Numbers above the branches indicate the SH-aLRT support and Ultrafast Bootstrap support.

Copyright notice: This dataset is made available under the Open Database License (<http://opendatacommons.org/licenses/odbl/1.0/>). The Open Database License (ODbL) is a license agreement intended to allow users to freely share, modify, and use this Dataset while maintaining this same freedom for others, provided that the original source and author(s) are credited.

Link: <https://doi.org/10.3897/phytokeys.210.90391.suppl3>

Supplementary material 4

Figure S4

Authors: Yi-Lei Lou, Dai-Kun Ma, Ze-Tao Jin, Hui Wang, Lu-Huan Lou, Shui-Hu Jin, Kun Liu, Bin-Bin Liu

Data type: Images.

Explanation note: Maximum likelihood phylogeny of *Lycoris* inferred from RAxML analysis of the concatenated 78 plastid coding genes. Numbers above the branches indicate the bootstrap support.

Copyright notice: This dataset is made available under the Open Database License (<http://opendatacommons.org/licenses/odbl/1.0/>). The Open Database License (ODbL) is a license agreement intended to allow users to freely share, modify, and use this Dataset while maintaining this same freedom for others, provided that the original source and author(s) are credited.

Link: <https://doi.org/10.3897/phytokeys.210.90391.suppl4>

Supplementary material 5

Figure S5

Authors: Yi-Lei Lou, Dai-Kun Ma, Ze-Tao Jin, Hui Wang, Lu-Huan Lou, Shui-Hu Jin, Kun Liu, Bin-Bin Liu

Data type: Images.

Explanation note: Bayesian inference phylogeny of *Lycoris* inferred from MrBayes analysis of the complete chloroplast genome data. Numbers above the branches indicate the posterior probabilities (PP).

Copyright notice: This dataset is made available under the Open Database License (<http://opendatacommons.org/licenses/odbl/1.0/>). The Open Database License (ODbL) is a license agreement intended to allow users to freely share, modify, and use this Dataset while maintaining this same freedom for others, provided that the original source and author(s) are credited.

Link: <https://doi.org/10.3897/phytokeys.210.90391.suppl5>

Supplementary material 6

Figure S6

Authors: Yi-Lei Lou, Dai-Kun Ma, Ze-Tao Jin, Hui Wang, Lu-Huan Lou, Shui-Hu Jin, Kun Liu, Bin-Bin Liu

Data type: Images.

Explanation note: Species tree of *Lycoris* inferred from ASTRAL-III of the 78 plastid coding genes. Numbers above the branches indicate the branch support values measuring the support for a local posterior possibility.

Copyright notice: This dataset is made available under the Open Database License (<http://opendatacommons.org/licenses/odbl/1.0/>). The Open Database License (ODbL) is a license agreement intended to allow users to freely share, modify, and use this Dataset while maintaining this same freedom for others, provided that the original source and author(s) are credited.

Link: <https://doi.org/10.3897/phytokeys.210.90391.suppl6>

Diatoma sinensis: a new diatom species (Bacillariophyta) found in the brackish Lake Qinghai, China

Li Yuan¹, Bing Liu¹, Patrick Rioual^{2,3}, Ji-Yan Long¹, Yu-Mei Peng⁴

1 College of Biology and Environmental Sciences, Jishou University, Jishou 416000, China **2** Key Laboratory of Cenozoic Geology and Environment, Institute of Geology and Geophysics, Chinese Academy of Sciences, P.O. box 9825, Beijing 100029, China **3** CAS Center for Excellence in Life and Paleoenvironment, Beijing 100044, China **4** Shaoyang University, Shaoyang 422000, China

Corresponding author: Bing Liu (jsulb@outlook.com)

Academic editor: Kalina Manoylov | Received 16 July 2022 | Accepted 20 September 2022 | Published 5 October 2022

Citation: Yuan L, Liu B, Rioual P, Long J-Y, Peng Y-M (2022) *Diatoma sinensis*: a new diatom species (Bacillariophyta) found in the brackish Lake Qinghai, China. *PhytoKeys* 210: 93–108. <https://doi.org/10.3897/phytokeys.210.90438>

Abstract

Lake Qinghai is an ancient brackish water lake in which several endemic diatom species have been discovered. In this study, a species of *Diatoma* is observed under light and scanning electron microscopy and described as new, *Diatoma sinensis* **sp. nov.** The living cells of *D. sinensis* always lie in girdle view due to the cell depth being much larger than valve width (3.3–8.8 vs. 2.0–3.0 μm). The valves of *D. sinensis* are characterized by their narrow, linear-lanceolate outline, with capitate to subcapitate apices, the presence of two rimoportulae, one at each apex, embedded in the last rib or located among striae and a 4:2 configuration of girdle bands in normal vegetative cells, with four bands assigned to the epivalve and two to the hypovalve. The new taxon is compared with similar species from the genera *Diatoma* and *Distrionella*.

Keywords

Brackish water, *Diatoma*, *Distrionella*, girdle bands, Lake Qinghai, morphology

Introduction

The araphid diatom genus *Diatoma* Bory (1824) was considered to be a freshwater genus (Round et al. 1990). Later, Snoeijs and Potapova (1998) studied the *Diatoma* taxa in the northern Baltic Sea and proposed two ecotypes for *Diatoma vulgaris* (Bory,

1824) and *D. moniliformis* (Kützing) D.M. Williams (2012) respectively, and described a new species, *D. bottnica* Snoeijs (Snoeijs and Potapova 1998). The genus *Diatoma* can be differentiated from other similar genera because it possesses heavily silicified transapical ribs and a raised central sternum (Williams 1985). In China, Xie and Qi (1997) listed six species and four varieties belonging to *Diatoma*, and Qi and Li (2004) investigated six species and three varieties, of which only six belong to *Diatoma*; the others belong to the genus *Odontidium* Kützing (1844). In addition, Liu et al. (2010) described a new species *Diatoma rupestris* Y. Liu & Q.X. Wang (Liu et al. 2010), which was later transferred into the genus *Odontidium*, as *O. rupestris* (Y. Liu & Q.X. Wang) I. Jüttner & D.M. Williams (Jüttner et al. 2017). More recently, Peng et al. (2017) described *Diatoma kalakulensis* Peng, Rioual and D.M. Williams from a high-altitude lake in western China.

In China, Lake Qinghai is the largest endorheic lake with brackish waters, that was formed 4.63 Ma ago (Fu et al. 2013). The lake has a surface water area of ca. 4294 km² and the lake surface is ca. 3200 m above sea level. Its climate belongs to the plateau continental climate. The average annual temperature is ca. -0.7 °C, the average annual precipitation and the average annual evaporation in the lake region are 319–395 mm and 800–1000 mm, respectively (Luo et al. 2017). More than 50 rivers/streams run into Lake Qinghai but there is no outlet to discharge the lake water, hence it is hydrologically closed. Surface water evaporation is almost the sole source of water loss from the lake. The lake has an 18.3 m average water depth, and the maximum is 26.6 m. The average values for alkalinity and pH are 25.6 mmol L⁻¹ and 9.2 respectively (Peng et al. 2014). There is a three-month ice-covered period (middle November to middle February) in Lake Qinghai so the growth period for diatoms is mainly from May to October.

The Lake Qinghai diatom flora has been under investigation since 1979 (e. g. Lanzhou Institute of Geology and Chinese Academy of Sciences 1979; Yao et al. 2011). These researches have resulted in a list of taxa but lacked useful illustrations (drawings or micrographs) for the taxa recorded from Lake Qinghai. Later, Peng et al. (2013) and Peng (2014) studied diatom assemblages deposited in sediment traps deployed in the center of the lake. From this work, a new species *Hippodonta qinghainensis* Peng & Rioual (Peng et al. 2014), and a new variety, *Gyrosigma peisonis* var. *major* Peng, Rioual & Sterrenburg (Peng et al. 2016) were described. For *Diatoma* species, Peng (2014) listed *D. tenuis* C. Agardh, *D. moniliformis* and *D. vulgaris* and provided a few illustrations. Recently, more new species from Lake Qinghai belonging to the genera *Ctenophora* (Grunow) Williams and Round, *Pinnularia* Ehrenberg and *Entomoneis* (Ehren.) Ehrenberg have been published (Liu et al. 2020; Deng et al. 2021; Long et al. 2022). Thus, there may be numerous endemics yet to be discovered and described from material collected in this ancient lake.

In the summer of 2019, epilithic diatom samples were collected from stones submerged in the littoral waters of Lake Qinghai (Fig. 1). In the current study, we focus on a species of *Diatoma* that was dominant in the community observed in the samples investigated. Thorough examination using light microscopy (LM) and scanning electron microscopy (SEM) supports that it is new to science.



Figure 1. Map of Lake Qinghai showing the three sampling sites located in the lakeshore shallow waters (labeled 1, 2, and 3), on the western side of the lake. Inset map showing Lake Qinghai's location within China and the Qinghai province.

Materials and methods

Three sampling sites were chosen from the lakeshore waters of Lake Qinghai (Fig. 1). Geographically, Lake Qinghai is located between longitudes 99°36'E and 100°47'E, latitudes 36°32'N and 37°15'N in Qinghai Province, China (Fig. 1). At the three sampling sites selected in Lake Qinghai (Fig. 1), there are many submerged stones with yellow-brown surfaces which indicate abundant diatoms growing on them. Each selected stone was placed on a plastic plate, then its surfaces were brushed using a toothbrush, and the brushed-off diatoms were washed into the plate. The diatom samples were transferred to a 100 ml sampling bottles and fixed with 70% ethanol. Two bottles of diatom samples were collected from each sampling site. During sample collection, temperature, pH, and conductivity were measured *in situ* with a portable multimeter (HQ40D, HACH Company). The samples were processed (cleaned of organic material) for microscope examination using 10% HCl and 30% H₂O₂. Permanent LM slides were prepared using the mountant Naphrax (Brunel Microscopes Ltd, UK). These slides were examined and specimens were photographed using a Leica DM3000 light microscope and a Leica MC190 HD digital camera. The holotype slide is deposited in the Herbarium of Jishou University, Hunan, People's Republic of China

(JIU). Samples were also examined using scanning electron microscopy (SEM). Several drops of cleaned diatom material were air-dried onto glass coverslips. Coverslips were attached to aluminum stubs using a double-sided conductive carbon strip and sputter-coated with platinum (Cressington Sputter Coater 108auto, Ted Pella, Inc.). Samples were examined and imaged using a field emission scanning electron microscopy (FE-SEM) Sigma HD (Carl Zeiss Microscopy) available at Huaihua University, China.

The terminology used in the description and discussion of the diatom structures is based on Williams (1985) and Round et al. (1990).

Results

Division: Bacillariophyta Karsten

Class: Bacillariophyceae Haeckel

Order: Rhabdonematales Round & R.M. Crawford

Family: Tabellariaceae Kützing

Genus: *Diatoma* Bory

***Diatoma sinensis* Bing Liu & Rioual, sp. nov.**

Figs 2–7

Holotype. JIU! G202201, specimen circled on slide, illustrated as Fig. 2B.

Registration. Phycobank <http://phycobank.org/103359>.

Type locality. CHINA. Qinghai Province: Lake Qinghai, a sampling point near the lakeshore (Fig. 1, sampling site 1), 36°50'34"N, 99°42'39"E, 3210 m a.s.l., collected by Bing Liu, July 19, 2019.

Description. *LM* (Fig. 2). Living cells always observed in girdle view are rectangular (Fig. 2A, arrows). Cell depth (along the pervalvar axis, $n = 35$) 3.3–8.8 μm , always larger than valve width (2.0–3.0 μm). Valve linear-lanceolate, with subcapitate to capitate apices (Fig. 2B–R). Valve dimensions ($n = 69$): 24–88 μm long, 2.0–3.0 μm wide, transapical ribs unevenly spaced, 8–13 in 10 μm . Striae and sternum not resolved under LM.

SEM (Figs 3–7). Frustule and valvocopula view: Frustule rectangular in girdle view (Fig. 3A); normal vegetative frustule composed of epivalve, hypovalve, and six girdle bands (Fig. 3B–D). Four girdle bands associated with the epivalve (Fig. 3B–D, B1 to B4), two with hypovalve (Fig. 3B–D, B5 and B6), yielding in a 4:2 configuration of girdle bands in non-dividing vegetative cells. Girdle bands open and having a closed-open-closed-open-closed-open arrangement at one apex in a complete cell (Fig. 3C–D). Striae continuing onto deep mantle and no blisters present (Fig. 3B–D). Valvocopula open at one pole, always furnished with two rows of poroids, but sometimes with very short isolated third row of poroids (Fig. 4D, arrow). Valvocopula forming an open ring with the same shape as the valve outline, closely attached to the mantle interior, surrounding the valve margin (Fig. 4B). Advalvar row of valvocopula poroids of each

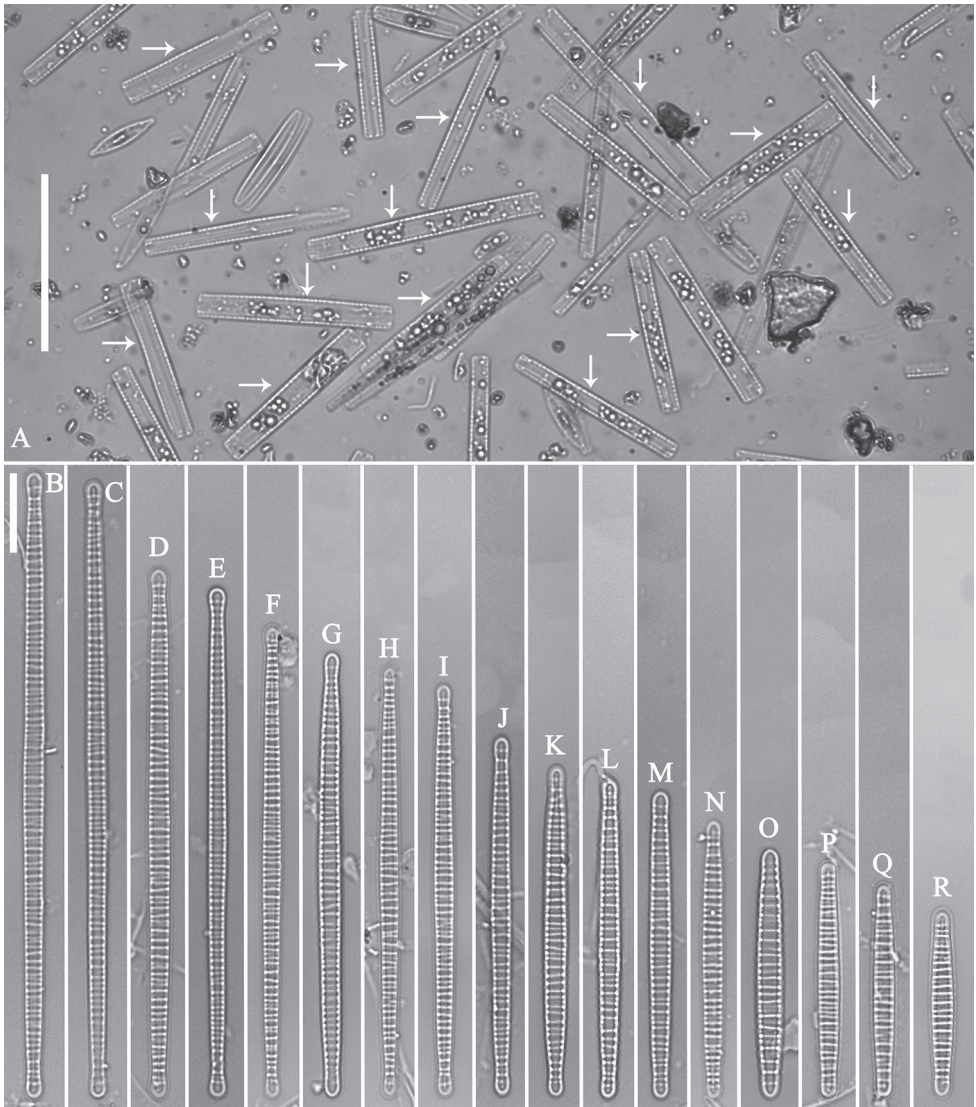


Figure 2. *Diatoma sinensis* sp. nov., LM **A** undigested specimens showing the cells always lying in girdle view with a rectangular shape (arrows) **B–R** seventeen valves showing a valve size diminution series, note the largest specimen (**B**) is three times longer than the smallest one (**R**). **B** illustration of holotype specimen. Scale bars: 50 μm (**A**); 10 μm (**B–R**).

valvocopula bisecting pars interior from exterior, located at mid-line, pars media (Fig. 3C–D), inner row of poroids and the very short isolated third row located on pars exterior (Figs 4D, 5C–E). Valvocopula with crenulated edge attaching to valve, internally visible over virgae (Fig. 4G–H, arrows). Valvocopula open ends hyaline (with no ornamentation) (Figs 4H, 5C, 5F). Poroid density of the valvocopula is 66–70 in 10 μm .

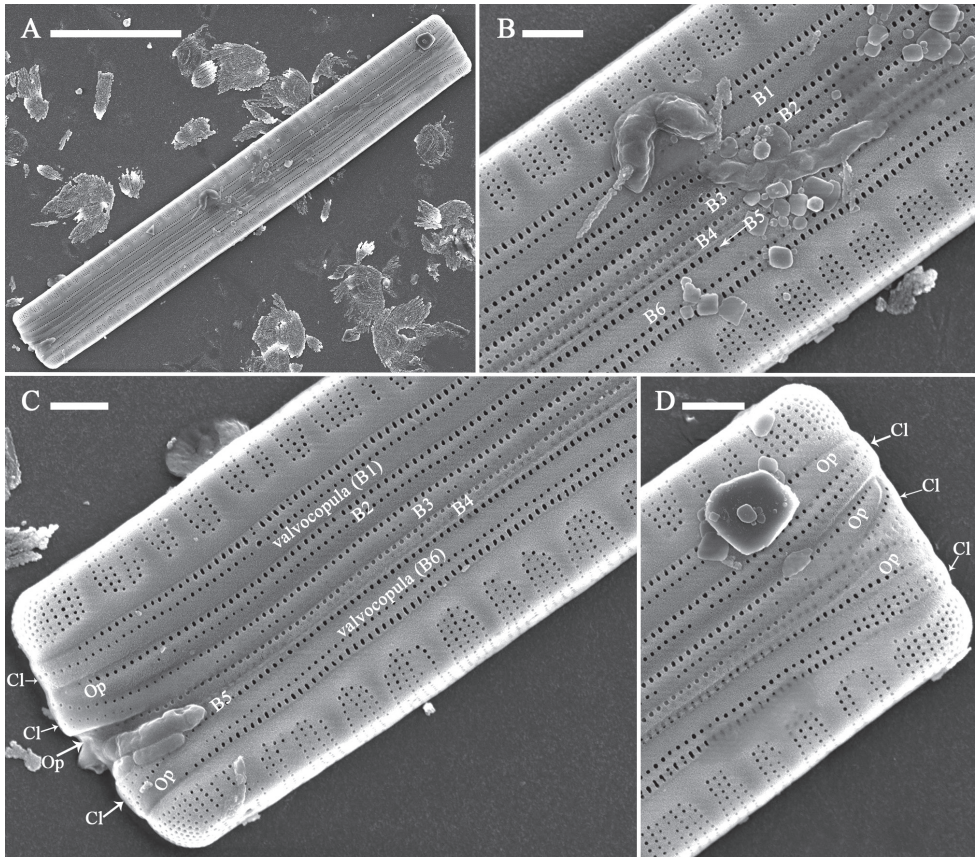


Figure 3. *Diatoma sinensis* sp. nov., SEM, girdle view **A** a complete frustule **B** middle detail of **A**, showing the valve mantle and six bands (labeled B1 to B6) of which B1 to B4 are associated with the epivalve and B5 and B6 are assigned to the hypovalve **C, D** two apical details of **A**, showing the valve mantle, six bands (labeled B1 to B6), and the closed-open-closed-open-closed-open arrangement (labeled Cl = closed and Op = open) of the apices of six bands. Scale bars: 10 μm (**A**); 1 μm (**B–D**).

External view: Valve linear-lanceolate, with subcapitate to capitate apices (Fig. 6A–B). Valve surface smooth, spines absent. Striae uniseriate, perpendicular to a narrow central sternum, 43–54 in 10 μm . Striae in groups of two to six separated by transverse ribs continuing down the vertical mantle (Figs 3A–D, 6C–H). More closely spaced rows of pores occurring at both apices, forming rather distinct apical pore fields (Fig. 6C, E, F, H). Two rimoportulae per valve, one per pole, with slit-like opening externally (Fig. 6C, E, F, H).

Internal view: Valve linear-lanceolate, with subcapitate to capitate apices (Fig. 7A–B). Transapical ribs, mostly primary, part of internal valve surface (Fig. 7A–H). Rimoportula prominent, two per valve ($n = 22$), present at both apices, possessing bilabiate structure (Fig. 7C, E, F, H). Rimoportula positions variable, either embedded in a transapical rib (Fig. 7C, E) or located among striae (Fig. 7E, H).

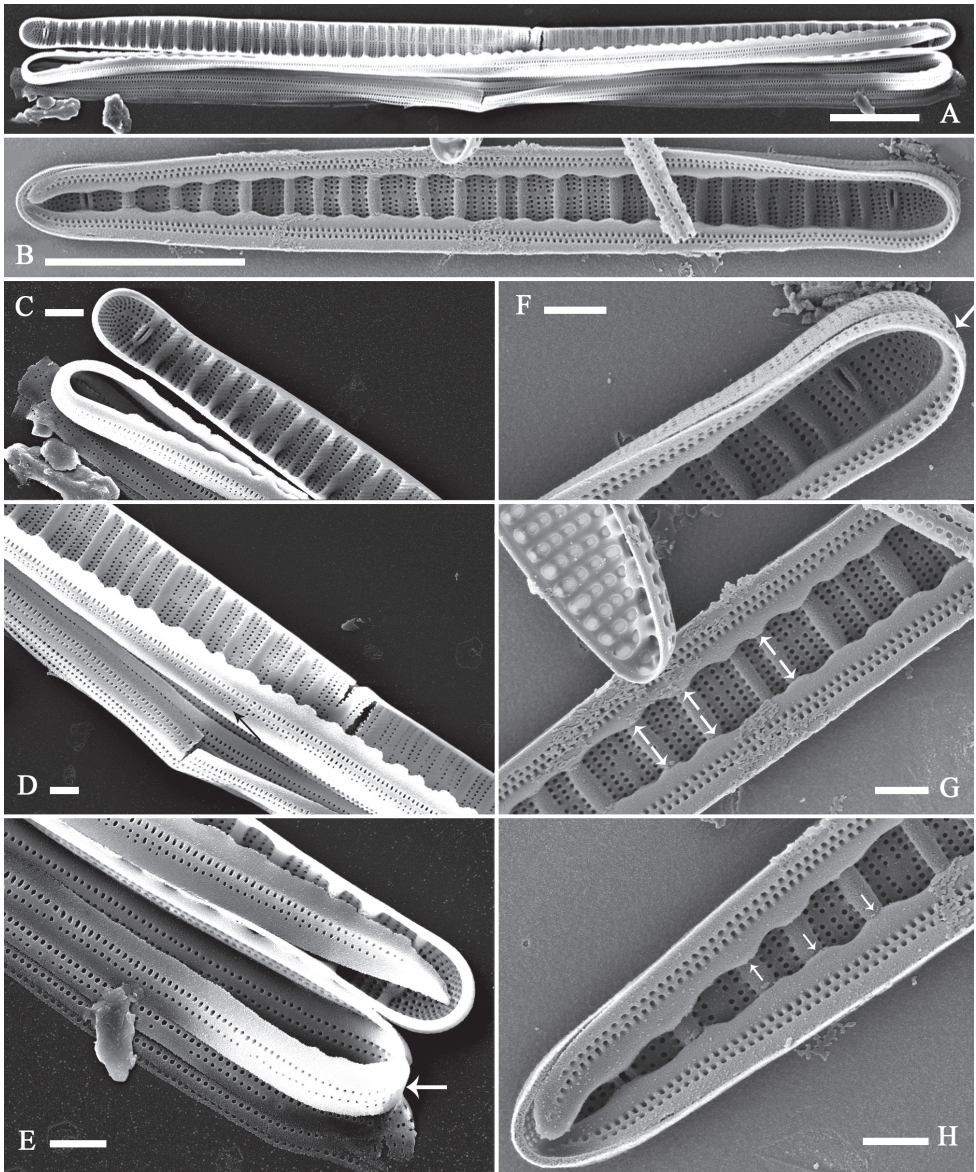


Figure 4. *Diatoma sinensis* sp. nov., SEM **A** a valve with a few girde bands **B** a valve with an attached valvocopula **C–E** details of **A** showing the two rows of poroids in each band, a third very short row of poroids present (**D**, arrow), and the poroids continuing at one closed end (**E**, arrow) **F–G** details of **B** showing the valvocopula, note the two rows of poroids continuing at one closed end (**F**, arrow), silica sawtooth-shaped projections over virgae (**G**, **H**, arrows), and an open end (**H**). Scale bars: 5 μm (**A**, **B**); 1 μm (**C–H**).

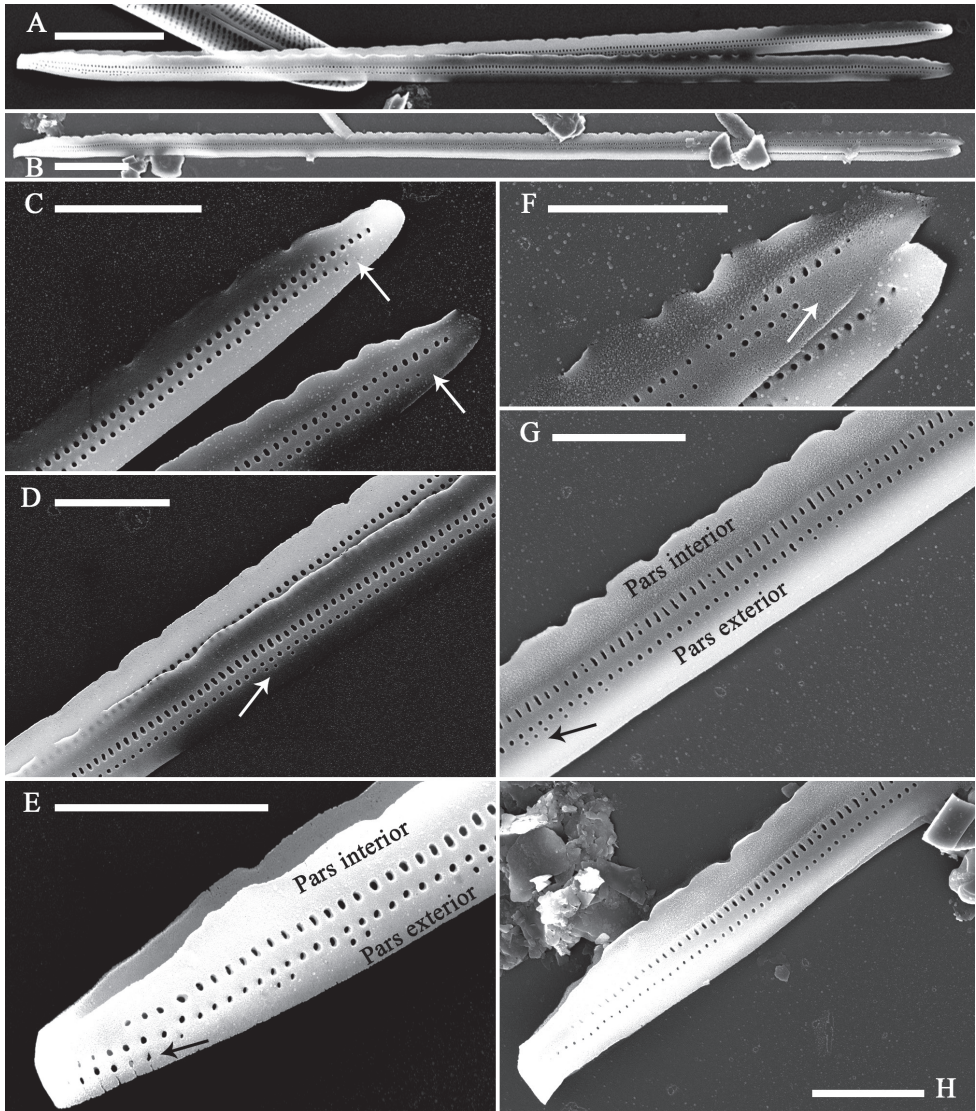


Figure 5. *Diatoma sinensis* sp. nov., SEM, valvocopula **A, B** two valvocopulae showing the sawtooth-shaped projections and the open nature **C–E** details of **A** showing the two rows of poroids, note one open end (**C**, two arrows), a third very short row of poroids present at the middle (**D**, arrow) and one closed end (**E**) **F–H** details of **B** showing the two rows of poroids, note one open end (**F**, arrow), a third very short row of poroids present at the middle (**G**, arrow), and the different poroid shapes of the two rows of poroids. Scale bars: 5 μm (**A, B**); 2 μm (**C–H**).

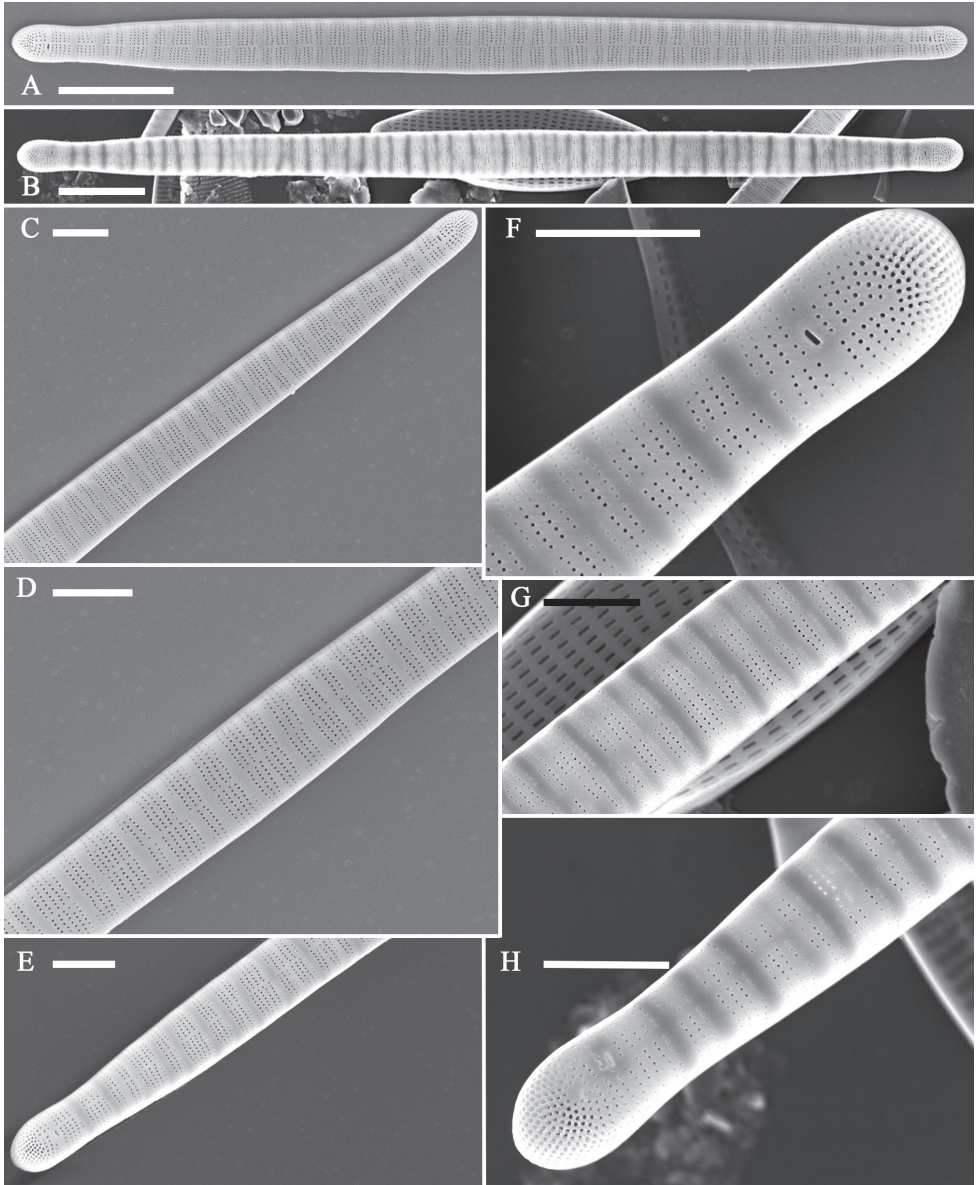


Figure 6. *Diatoma sinensis* sp. nov., SEM, external view **A, B** two complete valves, note two rimoportulae per valve **C–H** details of Figs **A, B** showing the narrow sternum, the striae in groups separated by transverse clear areas, the slit-like external openings of rimoportulae, and the apical pore fields. Scale bars: 5 μm (**A, B**); 2 μm (**C–H**).

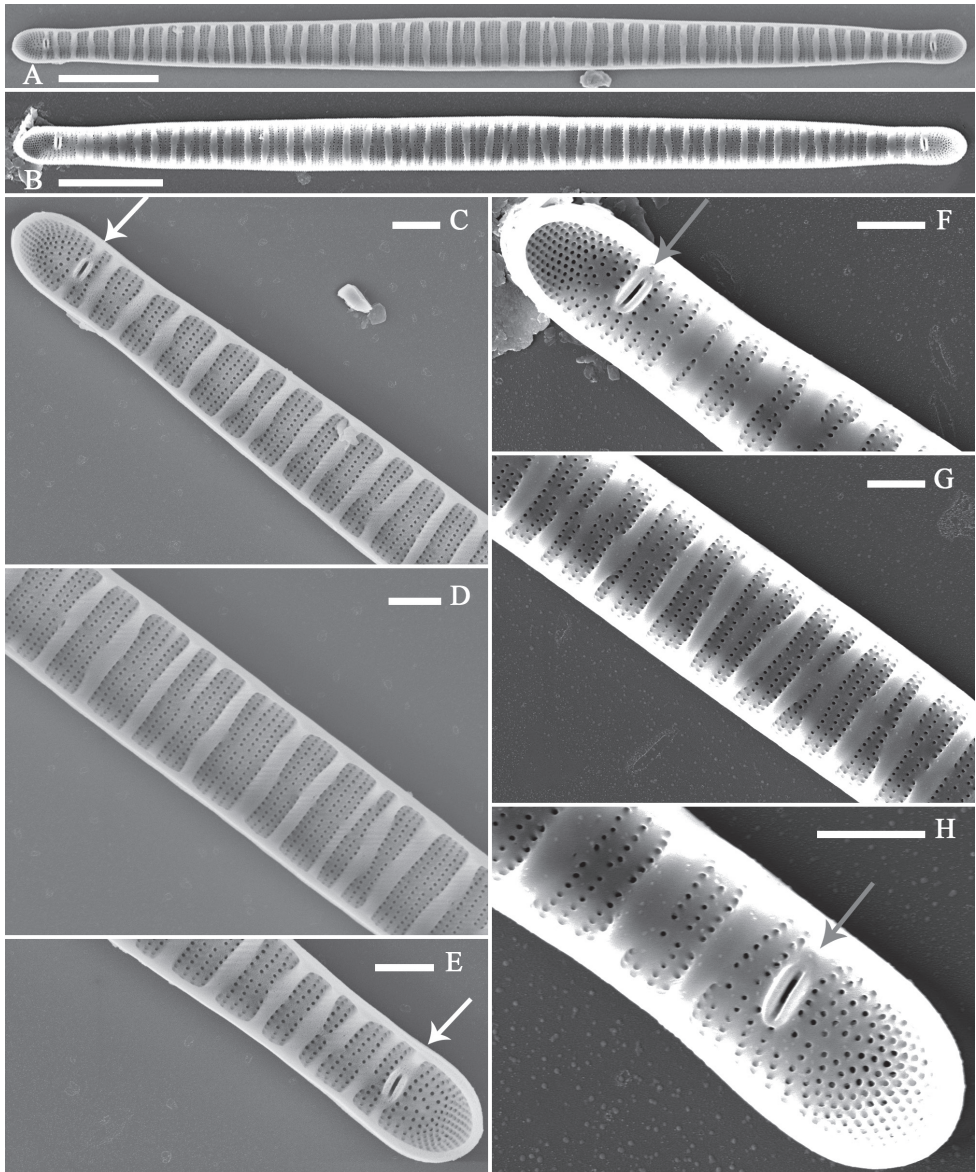


Figure 7. *Diatoma sinensis* sp. nov., SEM, internal view **A, B** two complete valves note the distribution of the ribs and two rimpportulae per valve **C–E** details of **A** showing the distribution of the ribs and the rimpportulae embedded in one rib at each apex (**C, E**, two arrows) **F–H** details of **B** showing the distribution of the ribs and the rimpportulae located among striae (**F, H**, two arrows). Scale bars: 5 μm (**A, B**); 1 μm (**C–H**).

Etymology. Named after China, where the species was found.

Ecology. Measured in situ specific conductivity was $16.30 \pm 0.09 \text{ mS}\cdot\text{cm}^{-1}$, pH was 9.14 ± 0.01 , and the water temperature was $15.5 \pm 0.3 \text{ }^\circ\text{C}$. *Diatoma sinensis* was found on submerged stones with yellow-brown surfaces, occurring with

Berkeleya fennica Juhlin-Dannfelt (1882), *Pinnularia qinghainensis* Bing Liu & S. Blanco (Deng et al. 2021), *Entomoneis sinensis* Bing Liu & D.M. Williams (Long et al. 2022), *E. qinghainensis* Bing Liu and D.M. Williams (Long et al. 2022), *E. paludosa* (W. Smith) Reimer (Long et al. 2022), *Ctenophora sinensis* Bing Liu & D.M. Williams (Liu et al. 2020), and some species of *Navicula* Bory (Bory de Saint-Vincent 1822), *Gyrosigma* Hassall (1845), *Nitzschia* Hassall (1845), and *Surirella* Turpin (1828).

Discussion

Within the Tabellariaceae, assigning some specimens to a particular genus may be problematic, especially between the genera *Diatoma* and *Distrionella* Williams (1990a). Evidence based on five features supports the new species described belonging to the genus *Diatoma* and not to the genus *Distrionella* as described by Williams (1990a) and later amended by Morales et al. (2005). First the thick transapical costae (ribs) are always present and are mainly primary in the new species whereas the costae in *Distrionella* species are either absent, primary or, most commonly, secondary (Morales et al. 2005). Second, the striae are arranged in groups of two to six, which are separated by the thickened costate whereas striae are irregularly arranged in *Distrionella*. Third, a sternum is clearly present, while the central area does not develop into a sternum in *Distrionella* (Williams 1990a). Fourth, the girdle bands always bear two complete rows of poroids whereas in *Distrionella* girdle bands only have one complete row of poroids. Finally, spines are absent while they are often present in *Distrionella* (Casa et al. 2019). Among the *Distrionella* species, the most morphologically similar to *D. sinensis* is *Distrionella incognita* (E. Reichardt) D.M. Williams (Reichardt 1988; Williams 1990b), which differs by its lower stria density (14–38 in 10 µm for *Distrionella incognita* vs. 43–54 in 10 µm for *D. sinensis*) in addition to all the features listed above.

Within the genus *Diatoma*, species can be distinguished by using valve outline, shape of the apices, valve dimensions, stria density, transapical rib density, and number and position of rimoportulae (e.g., Bąk et al. 2014; Peng et al. 2017). The valve outline and dimensions of *D. sinensis* can be usefully compared to those of *D. moniliformis* and *D. tenuis* (Table 1). Other *Diatoma* species cannot be confused with *D. sinensis* because of their different valve outline and/or much larger size.

Diatoma sinensis and *D. tenuis* have similar ranges in valve length, stria and rib densities and both taxa have a linear outline; however *D. sinensis* can be differentiated from *D. tenuis* by its narrower valve breadth (2–3 vs 3–4.5 µm), by having attenuate apices in smaller valves (a feature not observed in *D. tenuis*), by the number of rimoportula per valve (the former has two and the latter one, see Williams 1985), the presence/absence of spines (the former lacks any, but the latter has stub-like spines scattered within the tips of the pore fields, see Williams 1985), and the shape of the frustules in girdle view (rectangular for *D. sinensis*, biconcave for *D. tenuis*, see Snoeijs and Potapova 1998).

Some valves of *D. moniliformis* especially from the Baltic Sea (in Potapova and Snoeijs 1997; Snoeijs and Potapova 1998) and southern Poland (Bąk et al. 2014) also appear very similar in outline to valves of *D. sinensis*, but they are differentiated by

the rimoportulae, striae density, girdle band configuration and poroid occurrence. *D. sinensis* has two rimoportulae with variable positions, but *D. moniliformis* has 1 or 2 rimoportulae embedded in rib (see Snoeijs and Potapova 1998). *D. sinensis* has lower stria density (43–54 in 10 µm) compared to *D. moniliformis* (61–64 in 10 µm, Snoeijs and Potapova 1998). *Diatoma sinensis* has a 4:2 configuration of girdle bands for normal cells while *D. moniliformis* has probably five girdle bands according to Williams (1985). In addition, in *D. sinensis*, a third, very short row of poroids located in the pars exterior of valvocopula is observed (Fig. 5G, arrow), while in *D. moniliformis* the valvocopula only have a double row of poroids on valvocopula.

The configuration of girdle bands (i.e., in a cell, the ratio between the number of girdle bands associated with the epivalve and those associated with the hypovalve, sensu Mann 1982), has rarely been mentioned in studies on the genus *Diatoma*. Williams (1985) mentioned that *D. moniliformis* has five girdle bands, and Peng et al. (2017) only noted that the cingulum of *D. kalakulensis* is composed of 1–3 open bands. As seen above, in a normal cell (i.e., one not dividing), *D. sinensis* has a 4:2 configuration of girdle bands (four bands associated with the epivalve, two with the hypovalve, Fig. 3A–D). Although this is the first time this 4:2 configuration of girdle bands has been reported for a species of the genus *Diatoma*, it has been observed in other araphid genera. For example, it has been observed in the genus *Ctenophora*, e. g. *Ctenophora sinensis*, in the genus *Ulnaria* (Kützing) Compère (2001), e. g. *Ulnaria sinensis* Bing Liu & D.M. Williams (Liu et al. 2017), in the genus *Hannaea* R.M. Patrick (Patrick and Reimer 1966), e. g. *Hannaea inaequidentata* (Lagerstedt) Genkal and Kharitonov (Genkal and Kharitonov 2008) as observed by Liu and Williams (2020).

Another interesting feature of *D. sinensis* is that the two rows of poroids on the valvocopula differ according to the shape of the poroids: the poroids on the row near the pars interior are rectangular but the poroids on the row near the pars exterior are almost rounded (Fig. 5C–H). On some bands, a very short third row of poroids can be observed (Fig. 5D–E, G).

Table 1. Morphological features of *Diatoma sinensis* and similar taxa.

Feature	<i>D. sinensis</i>	<i>D. moniliformis</i>	<i>D. tenuis</i>	<i>Distirionella incognita</i>
Outline	Linear- lanceolate	Elliptical to lanceolate	Linear	Tapering to the poles
Girdle view	Rectangular	Rectangular	Biconcave	Rectangular
Apices	Capitate to subcapitate	Rounded to cuneate	Capitate, subrostrate in small valves	Capitate or rostrate
Valve dimensions (µm)	Length 24–88, breadth 2.0–3.0	Length 3–80, breadth 2.0–7.5	Length 30–62, breadth 3.0–4.5	Length 20–116, breadth 1.4–3.0
Striae in 10 µm	43–54	61–64	50–54	14–38
Ribs in 10 µm	8–13	10–17	9–12	2–14
Rimoportula per valve	2, embedded in one rib or stria area	1 or 2, embedded in a primary rib	1, between ribs	1
Configuration of girdle bands	4: 2	Probably 5 girdle bands	No data	No data
Reference	This paper	Potapova and Snoeijs 1997; Snoeijs and Potapova 1998; Williams 1985; Båk et al. 2014	Snoeijs and Potapova 1998; Williams 1985	Morales et al. 2005; Williams 1990a

Peng (2014) recorded *D. moniliformis*, *D. tenuis* and *D. vulgaris* in 43 trap samples collected from the middle of Lake Qinghai between July 2010 and September 2012. *Diatoma moniliformis* was relatively common but always at low abundance (10 occurrences in 43 samples, maximum abundances of 1.5%) and *D. vulgaris* was extremely rare (only occurred in one sample, representing 0.6% of the assemblages). The LM and SEM illustrations provided in Peng (2014) for the taxon identified as *D. tenuis* show that it was mainly a population of *D. sinensis* although some photographs may suggest that valves of *D. tenuis* were also present in the samples. These *Diatoma* were observed in 14 of the 43 trap samples, at very low abundances except in four trap samples collected between July and September 2012, during which *D. sinensis* became dominant in the assemblages (up to 27%). The ability to compare taxa observed in this study with those observed by Peng (2014) highlights the value in providing illustrations even in ecological or paleoecological studies that do not focus on taxonomy. The usefulness of voucher floras should not be understated (e. g. Bishop et al. 2017).

As discussed by Pavlov et al. (2013), endemism in diatoms is often associated with large, ancient lakes such as Lake Qinghai. However, considering the high possibility that *D. sinensis* has been confused with similar *Diatoma* taxa in previous investigations, it is premature to either claim that this species is endemic to Lake Qinghai or that it is distributed in a wider geographical area.

Acknowledgements

We are grateful to two reviewers and the editor for their careful revisions and helpful comments. This research was supported by the Natural Science Foundation of Hunan (grant number 2022JJ30473).

References

- Bąk M, Lange-Bertalot H, Nosek J, Jakubowska Z, Kielbasa M (2014) *Diatoma polonica* sp. nov. - a new diatom (Bacillariophyceae) species from rivers and streams of southern Poland. *Oceanological and Hydrobiological Studies* 43(2): 114–122. <https://doi.org/10.2478/s13545-014-0123-1>
- Bishop IW, Esposito RM, Tyree M, Spaulding SA (2017) A diatom voucher flora from selected southeast rivers (USA). *Phytotaxa* 332(2): 101–140. <https://doi.org/10.11646/phytotaxa.332.2.1>
- Bory de Saint-Vincent JBG (1822) Bacillariées. *Dictionnaire Classique d'Histoire naturelle* 2: 127–129.
- Casa V, Mataloni G, Van de Vijver B (2019) *Distrionella coxiana*, a new fragilarioid diatom species (Bacillariophyceae) from Tierra del Fuego, Patagonia, Argentina. *Plant Ecology and Evolution* 152(2): 385–391. <https://doi.org/10.5091/plecevo.2019.1587>

- Compère P (2001) *Ulnaria* (Kützinger) Compère, a new genus name for *Fragilaria* subgen. *Alterasynedra* Lange-Bertalot with comments on the typification of *Synedra* Ehrenberg In: Jahn R, Kociolek JP, Witkowski A, Compère P (Eds) Lange-Bertalot-Festschrift: Studies on Diatoms. Dedicated to Prof. Dr. Dr. h.c. Horst Lange-Bertalot on the occasion of his 65th Birthday. A.R.G. Gantner Verlag. K.G., 97–102.
- Deng L-Y, Blanco S, Liu B, Quan S-J, Long J-Y (2021) *Pinnularia qinghainensis*: A new diatom species (Bacillariophyta) found in the brackish Lake Qinghai, China. *Phytotaxa* 483(1): 80–84. <https://doi.org/10.11646/phytotaxa.483.1.5>
- Fu C, An Z, Qiang X, Bloemendal J, Song Y, Chang H (2013) Magnetostratigraphic determination of the age of ancient Lake Qinghai, and record of the East Asian monsoon since 4.63 Ma. *Geology* 41: 875–878. <https://doi.org/10.1130/G34418.1>
- Genkal SI, Kharitonov VG (2008) On the morphology and taxonomy of *Hannaea arcus* (Bacillariophyta). *Novitates Systematicae Plantarum Non Vascularium* 42: 14–23. <https://doi.org/10.31111/nsnr/2008.42.14>
- Hassall AH (1845) A history of the British Freshwater Algae (including descriptions of the Diatomaceae and Desmidiaceae) with upwards of one hundred Plates. Highley, London, 462 pp. <https://doi.org/10.5962/bhl.title.22609>
- Juhlin-Dannfelt H (1882) On the diatoms of the Baltic Sea. *Bihang till Kongliga Svenska Vetenskaps-Akademiens Handlingar* 6(21): 1–52.
- Jüttner I, Williams DM, Gurung S, Van de Vijver B, Levkov Z, Sharma CM, Sharma S, Cox EJ (2017) The genus *Odontidium* (Bacillariophyta) in the Himalaya - a preliminary account of some taxa and their distribution. *Phytotaxa* 332(1): 1–21. <https://doi.org/10.11646/phytotaxa.332.1.1>
- Kützinger FT (1844) Die Kieselschaligen Bacillarien oder Diatomeen. W. Köhne, Nordhausen, 1–152. <https://doi.org/10.5962/bhl.title.64360>
- Lanzhou Institute of Geology, Chinese Academy of Sciences (1979) Qinghai Lake investigation report. Science Press, Beijing, 44–66.
- Liu B, Williams DM (2020) From chaos to order: The life history of *Hannaea inaequidentata* (Lagerstedt) Genkal and Kharitonov (Bacillariophyta), from initial cells to vegetative cells. *PhytoKeys* 162: 81–112. <https://doi.org/10.3897/phytokeys.162.56136>
- Liu Y, Fu C, Wang Q, Stoermer EF (2010) A new species, *Diatoma rupestris*, from the Great Xing'an Mountains, China. *Diatom Research* 25(2): 337–347. <https://doi.org/10.1080/0269249X.2010.9705854>
- Liu B, Williams DM, Tan L (2017) Three new species of *Ulnaria* (Bacillariophyta) from the Wuling Mountains Area, China. *Phytotaxa* 306(4): 241–258. <https://doi.org/10.11646/phytotaxa.306.4.1>
- Liu B, Williams DM, Liu Z-X, Chen J-H (2020) *Ctenophora sinensis*: A new diatom species (Bacillariophyta) from China with comments on its structure, nomenclature and relationships. *Phytotaxa* 460(2): 115–128. <https://doi.org/10.11646/phytotaxa.460.2.1>
- Long J-Y, Williams DM, Liu B, Mo W-H, Quan S-J (2022) Ultrastructure of three species of *Entomoneis* (Bacillariophyta) from Lake Qinghai of China, with reference to the external areola occlusions. *PhytoKeys* 189: 29–50. <https://doi.org/10.3897/phytokeys.189.78149>

- Luo C, Xu C, Cao Y, Tong L (2017) Monitoring of water surface area in Lake Qinghai from 1974 to 2016. *Hupo Kexue* 9: 1245–1253. <https://doi.org/10.18307/2017.0523>
- Mann DG (1982) Structure, life history and systematics of *Rhoicosphenia* (Bacillariophyta). I. The vegetative cell of *Rh. curvata*. *Journal of Phycology* 18(1): 162–176. <https://doi.org/10.1111/j.1529-8817.1982.tb03170.x>
- Morales EA, Bahls LL, Cody WR (2005) Morphological studies of *Distrionella incognita* (Reichardt) Williams (Bacillariophyceae) from North America with comments on the taxonomy of *Distrionella* Williams. *Diatom Research* 20(1): 115–135. <https://doi.org/10.1080/0269249X.2005.9705622>
- Patrick M, Reimer CW (1966) The diatoms of the United States exclusive of Alaska and Hawaii. Volume 1: Fragilariaceae, Eunotiaceae, Achnantheaceae, Naviculaceae. Monographs of the Academy of Natural Sciences of Philadelphia 13: 1–688.
- Pavlov A, Levkov Z, Williams DM, Edlund MB (2013) Observations on *Hippodonta* (Bacillariophyceae) in selected ancient lakes. *Phytotaxa* 90(1): 1–53. <https://doi.org/10.11646/phytotaxa.90.1.1>
- Peng Y (2014) Preliminary study on modern diatoms in Lake Qinghai. Institute of Earth Environment, Chinese Academy of Sciences, Xi'an, Master thesis, 86 pp. [In Chinese with English abstract]
- Peng Y, Rioual P, Jin Z (2013) A brief assessment of diatom assemblages and seasonal dynamics in Lake Qinghai: A time-series sediment trap study. *Journal of Earth Environment* 4: 1338–1345. <https://doi.org/10.7515/JEE201303006>
- Peng Y, Rioual P, Levkov Z, Williams DM, Jin Z (2014) Morphology and ultrastructure of *Hippodonta qinghainensis* sp. nov. (Bacillariophyceae), a new diatom from Lake Qinghai, China. *Phytotaxa* 186(2): 61–74. <https://doi.org/10.11646/phytotaxa.186.2.1>
- Peng Y, Rioual P, Jin Z, Sterrenburg FAS (2016) *Gyrosigma peisonis* var. *major* var. *nov.*, a new variety of *Gyrosigma peisonis* (Bacillariophyta) from Lake Qinghai, China. *Phytotaxa* 245(2): 119–128. <https://doi.org/10.11646/phytotaxa.245.2.3>
- Peng Y, Rioual P, Williams DM, Zhang Z, Zhang F, Jin Z (2017) *Diatoma kalakulensis* sp. nov. – a new diatom (Bacillariophyceae) species from a high-altitude lake in the Pamir Mountains, Western China. *Diatom Research* 32(2): 175–184. <https://doi.org/10.1080/0269249X.2017.1335239>
- Potapova M, Snoeijis P (1997) The natural life cycle in wild populations of *Diatoma moniliformis* (Bacillariophyceae) and its disruption in an aberrant environment. *Journal of Phycology* 33(6): 924–937. <https://doi.org/10.1111/j.0022-3646.1997.00924.x>
- Qi Y, Li J (2004) Flora algarum sinicarum aquae dulcis. Tom X: Bacillariophyta, Pennatae (Araphidiale Raphidionales). Science Press, Beijing, 302 pp. [In Chinese]
- Reichardt E (1988) Neue Diatomeen aus Bayerischen und Nordtiroler Alpenseen. *Diatom Research* 3(2): 237–244. <https://doi.org/10.1080/0269249X.1988.9705036>
- Round FE, Crawford RM, Mann DG (1990) The diatoms: biology and morphology of the genera. Cambridge University Press, Cambridge, 747 pp.
- Snoeijis P, Potapova M (1998) Ecotypes or endemic species? - a hypothesis on the evolution of *Diatoma* taxa (Bacillariophyta) in the northern Baltic Sea. *Nova Hedwigia* 67(3–4): 303–348. <https://doi.org/10.1127/nova.hedwigia/67/1998/303>

- Turpin PJF (1828) Observations sur le nouveau genre *Surirella*. Mémoires du Muséum d'Histoire Naturelle 16: 361–368.
- Williams DM (1985) Morphology, taxonomy and inter-relationships of the ribbed araphid diatoms from the genera *Diatoma* and *Meridion* (Diatomaceae: Bacillariophyta). Bibliotheca Diatomologica 8: 1–227.
- Williams DM (1990a) Cladistic analysis of some freshwater araphid diatoms (Bacillariophyta) with particular reference to *Diatoma* and *Meridion*. Plant Systematics and Evolution 171(1–4): 89–98. <https://doi.org/10.1007/BF00940597>
- Williams DM (1990b) *Distrionella* D.M. Williams, nov. gen., a new araphid diatom (Bacillariophyta) genus closely related to *Diatoma* Bory. Archiv fur Protistenkunde 138(2): 171–177. [https://doi.org/10.1016/S0003-9365\(11\)80159-4](https://doi.org/10.1016/S0003-9365(11)80159-4)
- Williams DM (2012) *Diatoma moniliforme*: Commentary, relationships and an appropriate name. Nova Hedwigia. Beiheft 14: 255–261.
- Xie S, Qi Y (1997) Taxonomic studies on some species of *Diatoma*. Zhiwu Fenlei Xuebao 35: 37–42.
- Yao W, Shi J, Qi H, Yang J, Jia L, Pu J (2011) Study on the phytoplankton in Qinghai Lake during summer of 2006–2010. Freshwater Fisheries 41: 22–28. [In Chinese]

Characterization of the plastome of *Physalis cordata* and comparative analysis of eight species of *Physalis sensu stricto*

Isaac Sandoval-Padilla¹, María del Pilar Zamora-Tavares^{2,3},
Eduardo Ruiz-Sánchez^{2,3}, Jessica Pérez-Alquicira^{2,4}, Ofelia Vargas-Ponce^{2,3}

1 Doctorado en Ciencias en Biosistemática, Ecología y Manejo de Recursos Naturales y Agrícolas, Centro Universitario de Ciencias Biológicas y Agropecuarias, Universidad de Guadalajara, Ramón Padilla Sánchez 2100, 45200 Las Agujas, Zapopan, Jalisco, Mexico **2** Laboratorio Nacional de Identificación y Caracterización Vegetal A(LaniVeg), Consejo Nacional de Ciencia y Tecnología (CONACyT), Universidad de Guadalajara, Ramón Padilla Sánchez 2100, 45200 Las Agujas, Zapopan, Jalisco, Mexico **3** Instituto de Botánica, Departamento de Botánica y Zoología, Centro Universitario de Ciencias Biológicas y Agropecuarias, Universidad de Guadalajara, Ramón Padilla Sánchez 2100, 45200 Las Agujas, Zapopan, Jalisco, Mexico **4** CONACYT, Mexico City, Mexico

Corresponding author: Ofelia Vargas-Ponce (vargasofelia@gmail.com)

Academic editor: Sandy Knapp | Received 21 April 2022 | Accepted 7 September 2022 | Published 5 October 2022

Citation: Sandoval-Padilla I, Zamora-Tavares Mdp, Ruiz-Sánchez E, Pérez-Alquicira J, Vargas-Ponce O (2022) Characterization of the plastome of *Physalis cordata* and comparative analysis of eight species of *Physalis sensu stricto*. *PhytoKeys* 210: 109–134. <https://doi.org/10.3897/phytokeys.210.85668>

Abstract

In this study, we sequenced, assembled, and annotated the plastome of *Physalis cordata* Mill. and compared it with seven species of the genus *Physalis sensu stricto*. Sequencing, annotating, and comparing plastomes allow us to understand the evolutionary mechanisms associated with physiological functions, select possible molecular markers, and identify the types of selection that have acted in different regions of the genome. The plastome of *P. cordata* is 157,000 bp long and presents the typical quadripartite structure with a large single-copy (LSC) region of 87,267 bp and a small single-copy (SSC) region of 18,501 bp, which are separated by two inverted repeat (IRs) regions of 25,616 bp each. These values are similar to those found in the other species, except for *P. angulata* L. and *P. pruinosa* L., which presented an expansion of the LSC region and a contraction of the IR regions. The plastome in all *Physalis* species studied shows variation in the boundary of the regions with three distinct types, the percentage of the sequence identity between coding and non-coding regions, and the number of repetitive regions and microsatellites. Four genes and 10 intergenic regions show promise as molecular markers and eight genes were under positive selection. The maximum likelihood analysis showed that the plastome is a good source of information for phylogenetic inference in the genus, given the high support values and absence of polytomies. In the *Physalis* plastomes analyzed here, the differences found, the positive selection of genes, and the phylogenetic relationships do not show trends that correspond to the biological or ecological characteristics of the species studied.

Keywords

Boundaries, cpDNA, expansion, phylogeny, positive selection

Introduction

Physalis L. (Solanaceae) includes 95 morphologically and ecologically variable species (POWO 2022). The species can be annual herbs, perennial; and shrubs or arborescent perennial rhizomatous geophytes (Martínez 1998). The flowers are usually solitary, only *P. aggregata* Waterf. develops 1–3 flowers closely distributed along a short rachis and two shrub species have 1–5 flowers in axillary fascicles (*P. arborescens* L. and *P. melanocystis* Bitter). The corolla is commonly yellow but can vary to greenish, whitish, orange (*P. campanula* Standl. & Steyerl.) or purple (e.g., *P. purpurea* Wiggins and *P. solanaceus* (Schltdl.) Axelius). The fruits are green, yellow, orange, or purple berries, and are covered by an accrescent fruiting calyx (Vargas-Ponce et al. 2003; Pretz and Deanna 2020). *Physalis* is distributed naturally in the Americas and has been widely introduced in Asia and Europe (Martínez et al. 2017; Feng et al. 2020; Vdovenko et al. 2021). Some species, both annuals and perennials, grow only in restricted areas under particular environmental conditions. In contrast, other species, mostly annuals, have a wide distribution and are found in tropical habitats with varied ecological conditions (Vargas-Ponce et al. 2003; Martínez et al. 2017). *Physalis* inhabits areas from sea level to more than 3,000 m elevation, areas that have high environmental humidity levels through to deserts, with variable temperature and light conditions, in conserved environments, and with anthropocentric disturbances (Martínez and Hernández 1999; Vargas-Ponce et al. 2003, 2016; Toledo 2013). The morphological and ecological diversity of this genus is considered to be the result of different selective pressures and the independent evolutionary dynamics of each species.

Physalis contains species of economic, nutritional, and medicinal importance. The fruits of some species are edible and contain vitamins, minerals, carotenoids, phytosterols, and phenolic compounds that have nutraceutical and antioxidant properties (Puente et al. 2011; Valdivia-Mares et al. 2016; Shenstone et al. 2020). This genus is associated with agroecosystems and monocultures. Only four species are commonly cultivated: *P. grisea* (Waterf.) M. Martínez in the United States, *P. angulata* L. and *P. philadelphica* Lam. in Mexico, and *P. peruviana* L. in South America (Zamora-Tavares et al. 2015; Vargas-Ponce et al. 2016). Some species, such as *P. cordata* Mill., *P. minima* L., *P. pruinosa* L., and *P. pubescens* L., are traditionally used from the wild as food and medicine (Santiaguillo and Blas 2009; Kindscher et al. 2012; Taylor et al. 2012). In addition to nutritional contributions, species of *Physalis* have compounds of pharmacological interest (e.g., flavonoids, physalins, saponins, and withanolides) with antimicrobial, cytotoxic (anticancer and antitumor), neuropsychiatric, and metabolic properties (Rengifo-Salgado and Vargas-Arana 2013; Reyes-Reyes et al. 2013; Shah and Singh-Bora 2019). This diversity of metabolites potentially reflects the variability at the genetic level among species.

Chloroplasts possess photosynthetic machinery for the transformation of solar energy into chemical energy. They present their own genome, the plastome, which in spermatophytes tends to be between 120 and 180 kb long. Its circular structure consists of a large single-copy (LSC) region and a small single-copy (SSC) region separated by two inverted repeat regions (IRa and IRb), and the order and content of genes and introns are overall conserved (Daniell et al. 2016; Shetty et al. 2016; Shen et al. 2020). The proteins encoded by genes in the plastome have photosynthesis as a key function and participate in the synthesis of amino acids, fatty acids, phytohormones, and vitamins and in the assimilation of sulfur and nitrogen. In addition, they intervene in response mechanisms to unfavorable environmental conditions such as extreme temperatures, drought, and high concentrations of light and salinity (Carbonell-Caballero et al. 2015; Shen et al. 2020; Xu and Wang 2021). The plastome has been an important part of the evolutionary and adaptive process of plants.

Comparative plastomic analyses contribute to understanding the evolutionary history of different groups of plants. These comparisons help to identify whether the evolution of a particular group has occurred in parallel, presenting similar evolutionary patterns when homology among genomes is high or has occurred independently showing reticulated evolution (Carbonell-Caballero et al. 2015; D'Agostino et al. 2018; Do et al. 2020; Wu et al. 2021; Yang et al. 2021a). Plastome analysis across all photosynthetic organisms has shown that the size and number of coding DNA sequences (CDSs) are larger in algae and smaller in gymnosperms, relative to angiosperms. However, the loss of regions, genes, and introns is recurrent in all plant lineages (Mohanta et al. 2020). Additionally, pseudogenization and intron loss have been documented at lower taxonomic levels (Saxifragaceae, Liu et al. 2020); translocation, inversion, pseudogenization, or loss of genes (Opuntioideae Burnett, Köhler et al. 2020) and inverted repeat (IR) contractions (*Valeriana* L., Kim and Kim 2021) have also been observed. In contrast, some groups exhibit a high level of structural conservation and gene order and content. The variation is given by InDels (insertions and deletions) and SNPs (single nucleotide polymorphisms), as has been documented in Moraceae (Achakkagari et al. 2020), and *Artocarpus* J.R.Forst. & G.Forst. (Souza et al. 2020). Therefore, there is no single pattern that characterizes the general evolution of the plastome in spermatophytes.

Several comparative plastomic analysis have been conducted on the family Solanaceae, but for *Physalis*, few studies of the chloroplast genome have been undertaken. Feng et al. (2020) analyzed the plastome of five taxa (*P. angulata*, *P. minima*, *P. peruviana*, *P. pubescens*, and *P. alkekengi* L. (= *Alkekengi officinarum* Moench, a genus segregated from *Physalis*). In this study, variation was seen in expansions and contractions in IRs, intergenic spacers, and nucleotide content. Sandoval-Padilla et al. (2022) compared the plastome of two samples of *P. philadelphica*, one representing the wild gene pool and the other the domesticated gene pool and found differences in microsatellite and InDels in coding and non-coding regions, with no apparent trace of changes due to the domestication process. To increase knowledge about the evolution of the plastome in the genus, we selected *P. cordata* – an annual, wild species that grows in tropical areas, and whose fruits are consumed by traditional farmers – to sequence and

annotate its plastome and compare it with those of other species of *Physalis*. Our objectives were (1) to obtain and characterize the plastome of *P. cordata*, (2) to compare its structure and genetic composition with those of seven available *Physalis* plastomes, (3) to identify genes with greater variation as potential markers for genetic studies and genes that are under positive selection, and (4) to obtain a phylogenetic perspective for the genus based on the eight *Physalis* species for which whole plastome sequences exist.

Materials and methods

Plant material, cpDNA extraction, and sequencing

Fresh leaves of *P. cordata* were collected in the field and immediately dried with silica gel for further DNA extraction. The cpDNA was isolated based on Shi et al. (2012) and stored at the Laboratorio Nacional de Identificación y Caracterización Vegetal (LaniVeg) at the University of Guadalajara (voucher JS571, Table 1). DNA quality was assessed by spectrophotometry in a NanoDrop 2000 (Thermo Fisher Scientific). DNA integrity was determined by electrophoresis in a 1% agarose gel, and DNA quantity was analyzed by fluorometry in a Qubit 2.0 (Thermo Fisher Scientific). The sample was sequenced using the Ion Torrent platform following the manufacturer's protocol. The cpDNA was fragmented by sonication and used to prepare the library following the standard Ion Torrent Personal Genome Machine (PGM) protocol (200 bp fragments). The library was quantified by qPCR. The template was amplified in Ion OneTouch2 and enriched in OneTouch2 ES. Sequencing was performed using the Ion PGM Hi Q View Sequencing Kit. Raw data are available under the BioProject number PRJNA870909 in NCBI.

Plastome assembly and annotation

The quality of the raw reads was evaluated in FastQC 0.11.7 (Andrews 2010). Removal of low-quality reads was based on the Phred parameter (> 20) in Trimmomatic (Bolger et al. 2014). Reads were mapped to the plastome of *P. philadelphica* (Table 1) to exclude

Table 1. Data of *Physalis* species and *Alkekengi officinarum* studied.

Species	GenBank accession	Reference	Voucher specimen or DNA number
<i>P. angulata</i>	MH019241	Unpublished	Not available
<i>P. cordata</i>	ON018728	This study	JS571
<i>P. chenopodiifolia</i>	MN508249	Zamora-Tavares et al. 2020	OVP539-5112011
<i>P. minima</i>	MH045577	Feng et al. 2020	PHZ3003
<i>P. peruviana</i>	MH019242	Unpublished	Not available
<i>P. philadelphica</i>	MN192191	Sandoval-Padilla et al. 2019	021118ISP
<i>P. pruinosa</i>	MH019243	Unpublished	Not available
<i>P. pubescens</i>	MH045576	Feng et al. 2020	PHZ2001
<i>A. officinarum</i>	MH045575	Feng et al. 2020	PHZ4001

reads of nuclear and mitochondrial origin in Bowtie2 2.2.3.5 (Langmead and Salzberg 2012). Putative plastome reads were assembled de novo with SPAdes (Bankevich et al. 2012). Plastome coverage and assembly quality were performed in Quast (Gurevich et al. 2013). The complete plastome sequence was manually evaluated and corrected with IGV 2.5.0 (Thorvaldsdóttir et al. 2013). Automated annotation was performed in GeSeq (Tillich et al. 2017). tRNA genes were confirmed with tRNAscan-SE (Chan and Lowe 2019) and the remaining using BLAST in GenBank. The circular representation of the plastome was obtained in OGDRAW 1.3.1 (Greiner et al. 2019).

Comparative plastomic analysis and nucleotide variation

The complete sequence of the plastome of *P. cordata* was compared with the plastomes of seven *Physalis* species: *P. angulata*, *P. chenopodiifolia*, *P. minima*, *P. peruviana*, *P. philadelphica*, *P. pruinosa* L., and *P. pubescens*. The cpDNA of *P. chenopodiifolia* and *P. philadelphica* were stored in the LaniVeg. Accession numbers, references and voucher or DNA number of *Physalis* species are listed in Table 1. The comparison included the genome sequence total and each region's size, gene number and functional classification, nucleotide content, and number and size of introns.

The sequences of the eight plastomes were aligned in MAFFT (Katoh and Standley 2013) for various analysis. Sequence identity between coding and non-coding regions was assessed in mVista (Frazer et al. 2004) using Shuffle-LAGAN mode without modifying the pre-established values of the remaining parameters and using *P. cordata* as a reference. The limits of the LSC/IRs and SSC/IRs regions of the eight *Physalis* plastomes and *A. officinarum* (MH045575) were evaluated in IRSCOPE (Amiryousefi et al. 2018) using the "Manual files" option and default settings. To assess nucleotide differences between coding and intergenic regions, nucleotide diversity (π) was calculated using DnaSP v. 6.12.03 (Rozas et al. 2017).

Characterization of repeat sequences and microsatellites

Forward, reverse, and palindromic repeat sequences in the plastomes were identified in REPuter (Kurtz et al. 2001) under the parameters of repeat unit (RU) length ≥ 21 bp, repeat identity $\geq 90\%$, and a Hamming distance of two. In addition, microsatellites present in each of the eight plastomes were identified with the MICROSATELLITE (MISA) identification tool (Beier et al. 2017). The search parameters were at least 10 RUs for mononucleotides, six for dinucleotides, and five for tri-, tetra-, penta-, and hexanucleotides.

Gene selection analysis

To investigate the type of selection that has acted on *Physalis* plastome genes, we calculated the ratio of non-synonymous (Ka) and synonymous (Ks) substitutions. The Ka/Ks ratios of 51 genes that showed variation were evaluated. The aligned sequences

were analyzed in KaKs_Calculator 2.0 (Wang et al. 2010). The 11th genetic code (-c 11) was used. Ka/Ks ratios > 1, Ka/Ks = 1, and Ka/Ks < 1 suggested positive, neutral, and purifying selection, respectively.

Phylogenetic analysis

To obtain a phylogenetic perspective on the relationships of *P. cordata* and the other seven species of *Physalis sensu stricto* we used *A. officinarum* as outgroup. The sequences of nine plastomes were aligned in MAFFT (Katoh and Standley 2013). The evolutionary model of the whole plastome dataset without partitions was estimated in jModelTest 2.1.10 (Darriba et al. 2012). GTR + I + G was the best evolutionary model. Finally, a maximum likelihood (ML) analysis was conducted in Garli 2.01 (Bazin et al. 2014) with 1,000 bootstrap replicates.

Results

Characteristics of the plastome of *Physalis cordata*

The *Physalis cordata* plastome is 157,000 bp long and presents a quadripartite structure, with an LSC region of 87,267 bp, an SSC region of 18,501 bp, and two IRs of 25,616 bp (Fig. 1). The GC content was 37.52%, with a higher content in IRs (43.08%) than in the LSC (35.57%) and SSC (31.26%) regions (Table 2). There were 115 genes and five pseudogenes, including 80 genes coding for proteins, 31 for tRNA, and four for rRNA. Twenty-two duplicate genes were identified in IRs. Nineteen introns were present in 17 genes, two genes with two introns (*clpP* and *ycf3*) and the remainder with one (*atpF*, *ndhA*, *ndhB*, *petB*, *rpl16*, *rpl2*, *rps12*, *rpoC1*, *rps16*, *trnA-UGC*, *trnG-GCC*, *trnI-GAU*, *trnK-UUU*, *trnL-UAA*, and *trnV-UAC*). The *rps12* gene (small ribosomal protein 12) was the only gene that was trans-spliced. This result implies that it has an intron, the first exon (5' end) is in the LSC region, and the second (3' end) is in IRb; therefore, it is duplicated in IRa (Table 3).

Comparison of the plastome of *P. cordata* with those of seven other species of *Physalis*

The comparison of the plastome of *P. cordata* with those of *P. angulata*, *P. chenopodiifolia*, *P. minima*, *P. peruviana*, *P. philadelphica*, *P. pruinosa*, and *P. pubescens* showed that all plastomes presented the typical quadripartite structure and genetic organization (Table 2). The sizes of the plastomes were variable, ranging from 156,692 bp in *P. minima* to 157,007 bp in *P. pubescens*. The regions also varied in size; the LSC region was 86,845 bp in *P. minima* and 90,977 bp in *P. angulata*, the SSC region was 18,393 bp in *P. peruviana* and 18,503 bp in *P. minima*, and the IRs were 23,667 bp in *P. angulata* and 25,695 bp in *P. peruviana*. The total GC content was similar in all species (37.51% in *P. philadelphica* and up to 37.56% in *P. pruinosa*), and by region, the total

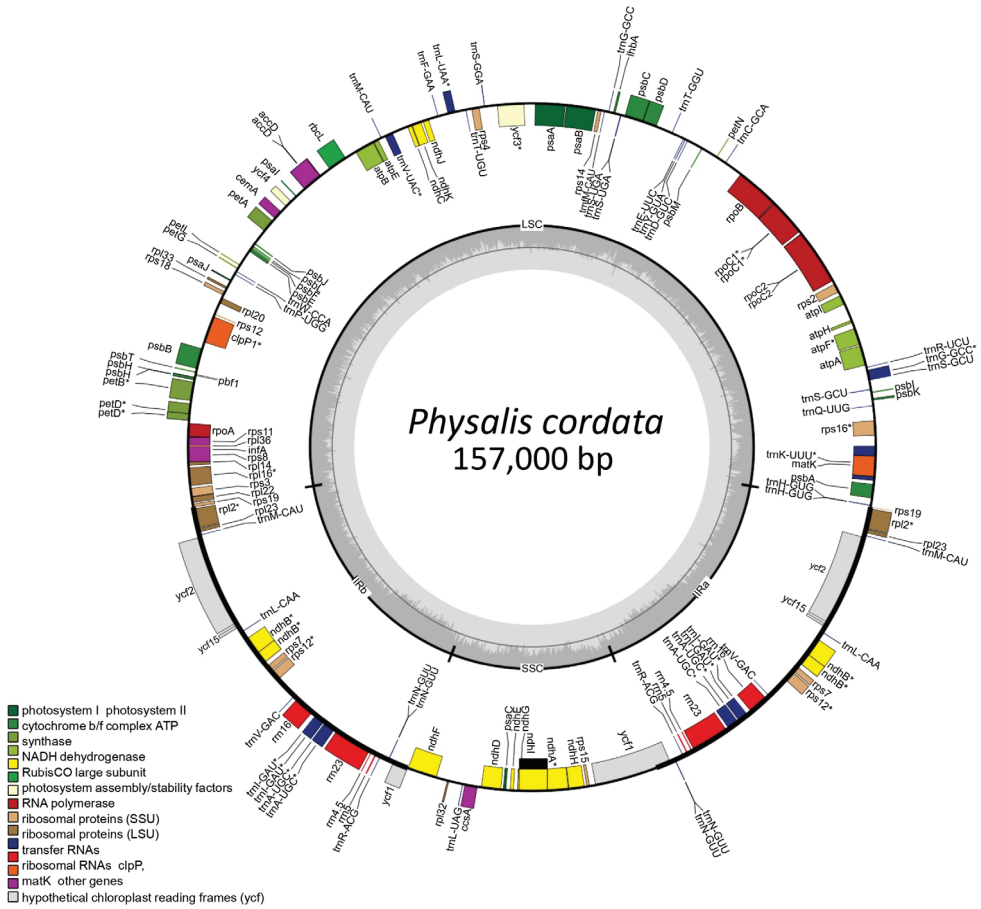


Figure 1. Plastome map of *Physalis cordata*. Genes located outside the outer circle are transcribed in the clockwise direction, whereas genes within the circle are transcribed in the counterclockwise direction. Genes with introns were marked with (*). Genes belonging to different functional groups are color-coded. Darker gray dashed area in the inner circle indicates GC content while lighter gray corresponds to the AT content of the plastome.

GC content was higher in the IRs (43.03% in *P. minim* up to 43.19% in *P. pruinosa*), intermediate in the LSC region (35.57% in *P. cordata*, *P. chenopodiifolia*, *P. peruviana*, and *P. pubescens* and up to 35.7% in *P. pruinosa*), and lower in the SSC region (31.26% in *P. cordata* and up to 31.4% in *P. angulata* and *P. minima*).

The plastome of *P. cordata* presented 115 genes. This number is only shared with *P. philadelphica* since *P. angulata*, *P. minima*, *P. peruviana*, *P. pruinosa*, and *P. pubescens* have 114 genes and *P. chenopodiifolia* 113 genes. Of the species sharing 113 genes, *P. cordata* and *P. philadelphica* differed in the presence of the *trnP-GGG* gene, and *P. chenopodiifolia* was lacking *orf188*. All species presented 22 genes in IRs and the *rps12* gene was trans-spliced (Table 3). Of the shared genes, 103 were the same size, and 10 showed variation between species (*accD*, *petB*, *psbB*, *psbC*, *psbH*, *rpl16*,

Table 2. Summaries of plastomes of eight *Physalis* species and *Alkekengi officinarum*.

Characteristics	<i>P. angulata</i>	<i>P. cordata</i>	<i>P. chenopodiifolia</i>	<i>P. minima</i>	<i>P. peruviana</i>	<i>P. philadelphica</i>	<i>P. pruinosa</i>	<i>P. pubescens</i>	<i>A. officinarum</i>
Size (bp)	156,706	157,000	15,6888	15,6692	15,6706	156,804	156,706	15,7007	156,578
LSC length (bp)	90,977	87,267	87,117	86,845	86,995	87,131	88,758	87,137	88,309
SSC length (bp)	18,395	18,501	18,451	18,503	18,393	18,483	18,394	18,500	18,363
IR length (bp)	23,667	25,616	25,660	25,672	25,695	25,595	24,777	25,685	24,953
Number of genes	114	115	113	114	114	115	114	114	115
Protein-coding genes	79	80	79	80	79	80	79	80	80
tRNA genes	31	31	30	30	31	31	31	30	31
rRNA genes	4	4	4	4	4	4	4	4	4
Genes in IR	22	22	22	22	22	22	22	22	22
Genes with introns	19	19	19	19	19	19	19	19	19
Genes in IR with introns	5	5	5	5	5	5	5	5	5
Nucleotide content									
A	30.81	30.84	30.83	30.82	30.81	30.87	30.81	30.83	30.78
C	19.1	19.07	19.08	19.09	19.08	19.06	19.1	19.09	19.14
G	18.45	18.45	18.44	18.45	18.46	18.45	18.46	18.45	18.52
T	31.63	31.64	31.65	31.64	31.64	31.66	31.63	31.63	31.56
GC content (%)									
Total	37.55	37.52	37.52	37.54	37.54	37.51	37.56	37.54	37.65
LSC	35.58	35.57	35.57	35.6	35.57	35.63	35.7	35.57	35.75
SSC	31.4	31.26	31.36	31.4	31.36	31.32	31.37	31.36	31.88
IR	43.06	43.08	43.06	43.03	43.08	43.1	43.19	43.08	42.88

bp = base pairs, LSC = large single-copy, SSC = small single-copy, IR = inverted repeat regions.

rpoC2, $\psi ycf1$, *ycf1*, *ycf2*, and *ycf5*). The number and distribution of introns were identical, 19 in 17 genes; however, 12 introns ranged from three to 99 bp (Suppl. material 1: Table S1).

Expansion and contraction of IRs

The comparison of the limits of the LSC/IR and SSC/IR regions of the eight *Physalis* plastomes and *A. officinarum* showed some variations (Fig. 2). At the LSC/IRb boundary, the *rps19* gene can be located at the end of the LSC region and continue at the beginning of the IRb (*P. chenopodiifolia*, *P. cordata*, *P. minima*, *P. philadelphica*, *P. pubescens*, and *A. officinarum*), presenting the second exon of *rpl2* in the LSC region and the first in the IRb (*P. peruviana* and *P. pruinosa*) or the *rpl23* gene in the LSC region and the *trnM*-CAU in the IRb (*P. angulata*). At the limit of IRb and the SSC region, two variations were observed: $\psi ycf1$ was in the IRb and ended at the beginning of the SSC region (*P. angulata*, *P. chenopodiifolia*, *P. cordata*, *P. peruviana*, *P. philadelphica*, *P. pruinosa*, and *A. officinarum*), followed by the *ndhF* gene or the final sequence of $\psi ycf1$, which ended at the limit of the IRb, and in the SSC region, the *ndhF* gene (*P. minima* and *P. pubescens*). In the SSC/IRa limit, the eight *Physalis* species and *A. officinarum* presented the *ycf1* gene. Finally, the IRa/LSC limit showed three variations: the IRa

Table 3. Plastome gene content and functional classification in *Physalis* species.

Gene group	Gene name	
Photosynthesis	Photosystem I	<i>psaA, psaB, psaC, psaI, psaJ, ycf3^{uv}, ycf4</i>
	Photosystem II	<i>psbA, psbB, psbC, psbD, psbE, psbF, psbH, psbI, psbJ, psbK, psbL, psbM, psbN, psbT, lhbA</i>
	ATP synthase	<i>atpA, atpB, atpE, atpF, atpH, atpI</i>
	NADH dehydrogenase	<i>ndbA^w, ndbB^{*w}, ndbC, ndbD, ndbE, ndbF, ndbG, ndbH, ndbI, ndbJ, ndbK</i>
	Cytochrome b/f complex	<i>petA, petB^w, petD, petG, petL, petN</i>
	Large subunit of RuBisCO	<i>rbcL</i>
	Large subunit of ribosome	<i>rpl2^{*w}, rpl14, rpl16^w, rpl20, rpl22, rpl23*, rpl32, rpl33, rpl36</i>
Self-replication	RNA polymerase subunits	<i>rpoA, rpoB, rpoC1^w, rpoC2</i>
	Small subunit of ribosome	<i>rps3, rps4, rps7*, rps8, rps11, rps12^{*w}, rps12_3end, rps14, rps15, rps18, rps19</i>
	Ribosomal RNA genes	<i>rrn16*, rrn23*, rrn4.5*, rrn5*</i>
	Transfer RNA genes	<i>trnA-UGC^{*w}, trnC-GCA, trnD-GUC, trnE-UUC, trnF-GAA, trnM-CAU, trnG-GCC^w, trnG-UCC, trnH-GUG, trnI-CAU*, trnI-GAU^{*w}, trnK-UUU^w, trnL-CAA*, trnL-UAA^w, trnL-UAG, trnM-CAU, trnN-GUU*, trnP-GGG†, trnP-UGG, trnQ-UUG, trnR-ACG*, trnR-UCU, trnS-GCU, trnS-GGA, trnS-UGA, trnT-GGU, trnT-UGU, trnV-GAC*, trnV-UAC^w, trnW-CCA, trnY-GUA</i>
	Other genes	
Hypothetical chloroplast reading frames	<i>orf42*, orf56*, ycf2*, ycf68*, orf188‡</i>	
Subunit of acetyl-CoA carboxylase	<i>accD</i>	
c-type cytochrome synthesis	<i>ccsA</i>	
Envelope membrane protein	<i>cemA</i>	
Protease	<i>clpP^{uv}</i>	
Maturase	<i>matK</i>	
Pseudogenes	<i>infA, rps2, rps16^w, ycf1*, ycf15*</i>	

* Genes in IRs, ^w genes with introns, ^{uv} genes with two introns. † only present in *P. cordata* and *P. philadelphica*, ‡ absent in *P. chenopodiifolia*.

may have the *trnM-CAU* gene and *rpl23* (*P. angulata*) in the LSC region; the IRa may have the second exon of *rpl2* and the *trnH-GUG* in the LSC region (*P. chenopodiifolia*, *P. cordata*, *P. minima*, *P. philadelphica*, *P. pruinosa*, and *A. officinarum*); or the IRa may have the first exon *rpl2* and the second exon in the LSC region (*P. peruviana* and *P. pruinosa*) present. In addition, an extension of the LSC region and contraction in IRs were identified in *P. angulata* and *P. pruinosa*.

Divergence in plastome sequences

The identity between the plastome of *P. cordata* and those of the other seven *Physalis* species was high. Identical sequences were mainly found in coding regions, and the greatest divergence was in the intergenic regions. The comparison between regions showed that the LSC and SSC regions were more divergent than were IRs. Introns also exhibited greater variation than the exons. The most divergent genes were *ycf1* and *ycf2*, as well as the intergenic regions *trnH-GUG-psbA* and *trnL-UAA-trnF-GAA* (Fig. 3).

The sequences of 51 genes and 75 intergenic regions showed variation. The lowest variation in genes was one change in 14 genes, and the highest variation was 173 changes in *ycf1*. The lowest variation in intergenic regions was one change in 16 of them, and the highest was in *trnL-UAA-trnF-GAA* with 42. The average value of π was lower in the genes than in the intergenic regions (Suppl. material 1: Fig. S1). The nucleotide diversity in the genes varied from $\pi = 0.00016$ in *ndhB* to $\pi = 0.01038$ in *ycf1* and in the intergenic regions from $\pi = 0.0003$ in *rps7-trnV-GAC* to $\pi = 0.02671$ in *trnL-UAA-trnF-GAA*. In general, 14 regions presented π values > 0.005 , which included four genes (*trnD-GUC*, *trnW-CCA*, *ndhE*, and *ycf1*) and 10 intergenic regions (*trnH-GUG-psbA*, *trnfM-CAU-rps14*, *trnL-UAA-trnF-GAA*, *petA-psbJ*, *rps18-rpl20*, *infA-rps8*, *rpl16-rps3*, *rpl32-trnL-UAG*, *trnL-UAG-ccsA*, and *ndhG-ndhI*).

Characterization of repeat sequences and microsatellites

The repeated sequences in the plastome ranged from 35 in *P. philadelphica* to 49 in *P. cordata* (Suppl. material 1: Fig. S2). The most abundant type of repetition was forward (19 in *P. philadelphica* up to 29 in *P. cordata*), followed by palindromic (five in *P. philadelphica* up to 23 in *P. angulata*) and finally reverse (one in *P. philadelphica* up to three in *P. angulata*, *P. minima*, *P. peruviana*, and *P. pruinosa*). The number of microsatellites fluctuated from 52 in *P. peruviana* to 62 in *P. angulata* (Suppl. material 1: Fig. S3). Mono-, di-, and trinucleotide URs (repeat units) were present in all eight species; tetranucleotides were absent in *P. peruviana*, and pentanucleotides and hexanucleotides were only present in *P. angulata* and *P. pruinosa*. The types of UR with the highest number were T and A mononucleotides. In contrast, the mononucleotide C is present in a single region in five species (*P. chenopodiifolia*, *P. cordata*, *P. minima*, *P. philadelphica* and *P. pubescens*), and G was not found in any regions. In turn, the region with the highest number of microsatellites was the LSC region, followed by the SSC region, and then IRs.

Gene selection analysis

In 51 genes, eight showed values of $Ka/Ks > 1$, indicating that they are under positive selection (*cemA*, *ndhB*, *ndhJ*, *ndhK*, *psaC*, *rbcL*, *rpoA*, and *ycf1*, Fig. 4). Six genes -*cemA*, *ndhB*, *ndhJ*, *ndhK*, *rbcL*, and *rpoA*- are under positive selection in all eight species, *psaC* in five (*P. chenopodiifolia*, *P. cordata*, *P. peruviana*, *P. philadelphica*, and *P. pruinosa*), and *ycf1* in four (*P. angulata*, *P. peruviana*, *P. philadelphica*, and *P. pruinosa*). The values in *ndhB*, *ndhJ*, *ndhK*, and *psaC* were slightly higher than 1, compared to those in *cemA*, *rbcL*, *rpoA*, and *ycf1*, which presented higher values ($Ka/Ks = 1.516$ to $Ka/Ks = 6.029$). The other 43 genes showed Ka/Ks values < 1 , which indicates they are under purifying selection.

Phylogenetic analysis

The ML phylogeny recovers *P. minima* as a sister to the seven other *Physalis* species included in this study (BS = 100; see Fig. 5). We recovered *P. philadelphica* as sister to

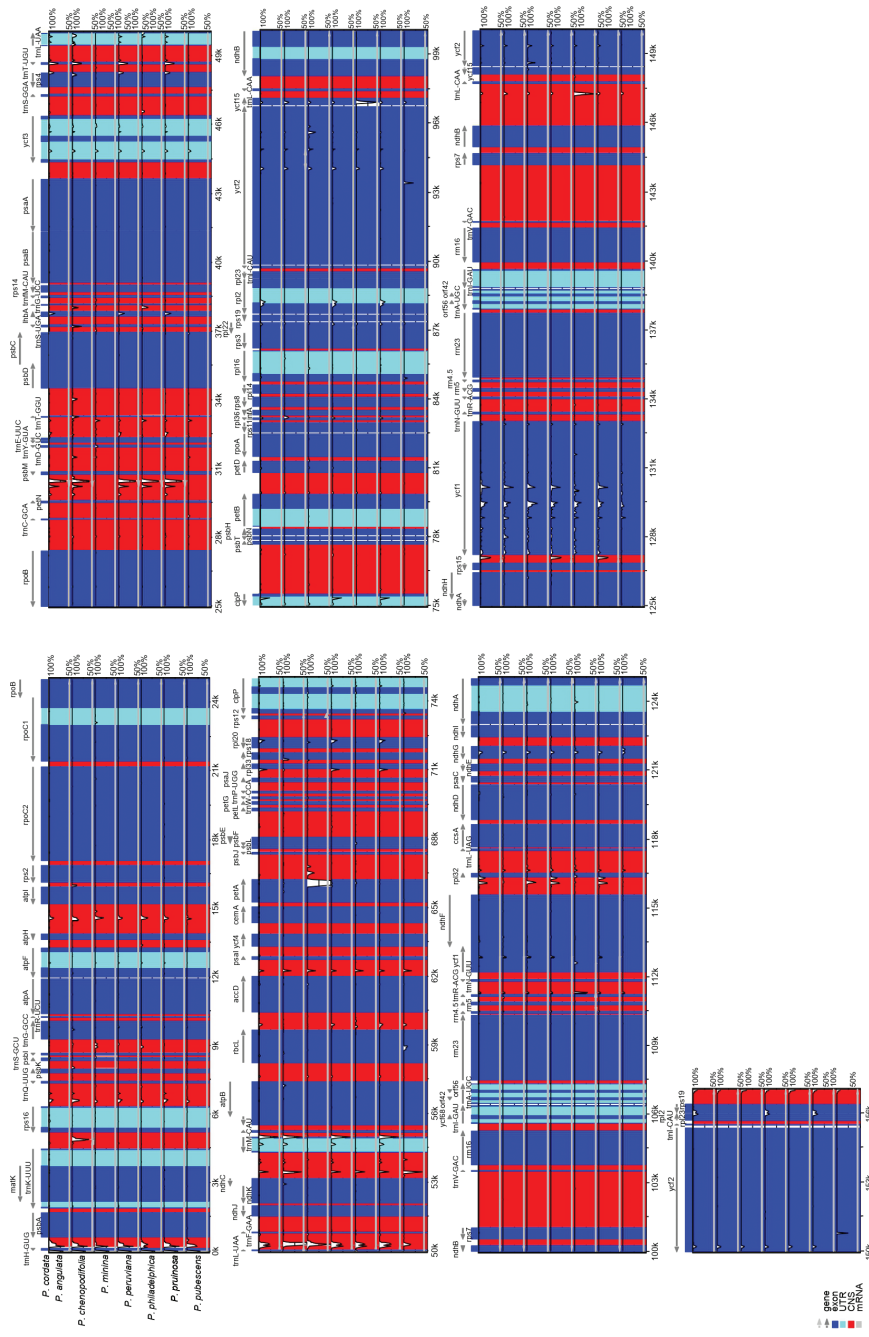


Figure 3. Comparative plots of identity among *Physalis* species. The percentage of identity ranges from 50 to 100% and is shown in the vertical axis. Gray arrows indicate genes with their orientation and position of their transcription in the reference plastome (*P. cordata*). Plastome regions are color coded as blue blocks for the conserved coding genes (exon), turquoise for introns and red blocks for non-coding regions in intergenic regions (CNS).



Figure 4. Non-synonymous substitution (Ka), synonymous substitution (Ks) and Ka/Ks values of genes of eight *Physalis* species. Blue bars indicate Ka values, orange bars indicate Ks values, and gray bars indicate Ka/Ks ratios. Genes with Ka or Ks values equal to 0 are not shown.

the clade containing *P. pruinosa*, *P. angulata*, *P. peruviana*, and *P. chenopodiifolia* (BS = 91). This group was in turn sister to the clade formed by *P. pubescens* and *P. cordata* (BS = 91).

Discussion

Structure and organization of *Physalis* plastomes

The plastome of *P. cordata* analyzed here presents the typical quadripartite structure and the same order of genes as has been found for other species of the genus. However, the species vary in the total size and the size of the regions. In general, the average size of plastomes in *Physalis* is 156,814 bp, and the difference between the largest (*P. pubescens*,

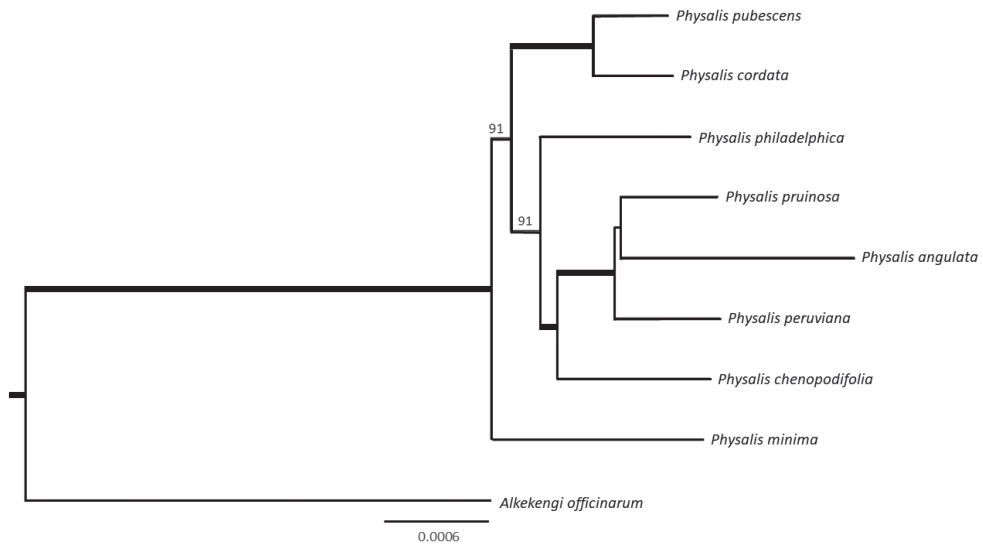


Figure 5. Phylogenetic tree based on Maximum Likelihood (ML) using the plastome sequence of *Physalis* species. Bold lines indicate bootstrap support values (BS) = 100, values < 100 are shown above the branches.

157,007 bp) and the smallest plastome (*P. minima*, 156,692 bp) was 315 bp. Phylogenetically, closely related species tend to be homogeneous in size and their regions (Daniell et al. 2016; Mohanta et al. 2020). In the studied *Physalis*, however, this is true in terms of the size of the plastome but not with regions. The expansion of the LSC regions and contraction of IRs found in *P. angulata* and *P. pruinosa* is not an isolated evolutionary event; it has characterized the evolutionary history of other groups of angiosperms such as *Indigofera* L. (Fabaceae, Oyebanji et al. 2020), *Passiflora* L. (Passifloraceae, Pacheco et al. 2020), and *Corydalis* DC. (Papaveraceae, Xu and Wang 2021). Expansions and contractions in regions have occurred multiple times and in different lineages; there are models that indicate this may be due to single or double-strand breaks or be promoted by multiple inversions along with several rounds of expansions and/or contractions (Zhu et al. 2016). In *Physalis* the total GC content shows a minimal variation range of only 0.05%, ranging from 37.51% (*P. philadelphica*) to 37.56% (*P. pruinosa*). These values are similar to those documented in other genera of Solanaceae, such as *Atropa* L., *Capsicum* L., *Nicotiana* L., and *Solanum* L. (Kaur et al. 2014; Magdy et al. 2019), and families such as Asteraceae and Saxifragaceae (Zhong et al. 2019; Liu et al. 2020).

The *Physalis* species studied have between 113 to 115 genes; 113 of these are completely shared, with the same distribution and number of introns. The difference in the number of genes is based on the presence of *trnP-GGG* in *P. cordata* and *P. philadelphica* and the absence of *orf188* in *P. chenopodiifolia*. We suggest that the genes that are not shared are the product of loss events during the evolutionary process. In addition, the size of 10 genes was different in at least one of the eight species. For example, in *P. philadelphica*, the second exon of the *petB* gene differs by three bp with respect to those of

the other species. Additionally, gene sizes are variable among the eight species, as occurs for *ycf1*, which varies from six to 114 bp. In the eight species, there were 17 genes with 19 introns, 15 genes with one intron, and two genes with two introns (*clpP* and *ycf3*). *Physalis* does not have an intron in the *petD* gene (gene of the cytochrome b6-f subunit 4 complex), unlike that which occurs in other genera of Solanaceae such as *Atropa*, *Capsicum*, *Datura* L., *Nicotiana*, *Solanum*, and *Withania* Pauquy (Kaur et al. 2014; Mehmood et al. 2020a) and in families belonging to other orders such as Oxalidaceae (Li et al. 2021) and Lamiaceae (Zhao et al. 2020). Similarly, 12 introns presented differences ranging from three bp in *atpF* and *petB* to 99 bp in *trnI*-GAU. In *Physalis*, the difference in the sizes of exons and introns does not impact the total size or the regions; however, changes in intergenic regions could contribute to the unequal sizes.

Variation in the boundaries of plastome regions is a relatively common evolutionary process that occurs in different plant groups (Huang et al. 2020). In the *Physalis* species studied, this variation is present in three types, distinguished by the presence of different genes at the IRs/LSC boundaries (Fig. 2). The first type is most common and it is found in *P. chenopodiifolia*, *P. cordata*, *P. minima*, *P. philadelphica*, *P. pubescens*, and *A. officinarum*. In these species the *rps19* gene starts at LSC and ends at IRb at LSC/IRb boundary; furthermore, at IRa/LSC boundary, the second exon of the gene *rpl2* is at IRa and the *trnH*-GUG gene at LSC. The second type is found in *P. peruviana* and *P. pruinosa*, which had the intron of the *rpl2* gene at both of the IR/LSC boundaries. The third and most distinctive type is present in *P. angulata*, here there is change in the order of the genes, with *rpl23* located at LSC and *trnM*-CAU at IRs (Fig. 2). The changes in *P. angulata* and *P. pruinosa* may be a product of the expansion of LSC and contraction of IRs about 2 kb (Table 2) which contrasts with the rest of the *Physalis* species analyzed, other Solanaceae genera, and several land plant families with average sizes of 25 kb in IRs (Kaur et al. 2014; Ruhlman and Jansen 2014; D'Agostino et al. 2018; Zhao et al. 2020; Yang et al. 2021a). Our results are somewhat similar to those reported by Feng et al. (2020), where the boundaries of the four regions reported in *P. angulata*, *P. minima*, *P. peruviana*, and *P. pubescens* are the same as those observed in the first type identified by us for *P. chenopodiifolia*, *P. cordata*, *P. minima*, *P. philadelphica*, and *P. pubescens*. In contrast, *A. officinarum* differs in the IRs/LSC boundaries by the presence and position of *rpl2* gene (Fig. 2). Furthermore, this species exhibits an expansion of LSC (ca. 1.2 kb) and a contraction of IRs (ca. 0.7 kb) like that in *P. pruinosa*. Boundary variations are heritable and provide information on evolutionary and speciation processes. These mutations can be traced throughout the evolutionary process and used as evidence of shared ancestry (Stettler et al. 2021). In the *Physalis* species analyzed here there appears to be no evolutionary pattern that characterizes the boundaries of the four regions; future studies are necessary to identify a particular pattern in the genus.

Microsatellite and repetitive regions

The variation between plastomes, in some cases, is limited due to their low rate of evolution, so repetitive regions and microsatellites can reveal interspecific variation

(D'Agostino et al. 2018). In the case of repetitive regions, their divergence has been correlated to a precursor of inversions and rearrangements, so their analysis allows for different types of studies (Weng et al. 2014). In *Physalis*, repetitive regions mostly have sizes of 30–39 bp. This result coincides with those found in other genera of Solanaceae (*Nicotiana*, Mehmood et al. 2020b; and *Withania*, Mehmood et al. 2020a) and even in phylogenetically distant families such as Moraceae (Souza et al. 2020) and Poaceae (Wang et al. 2021). In turn, microsatellites have been used for the identification of plants and in analysis of population genetics and relationships between cultivars of the same species (Bassil et al. 2020). In *Physalis*, the most abundant URs are mononucleotides T and A, this may be the result of the high content of T and A in the plastome in relation to G and C. Most microsatellites are in the LSC region, which is probably because this region is longer than the SSC region and IRs. Additionally, microsatellites occur mainly in non-coding regions rather than in coding regions. The microsatellites identified in *Physalis* plastomes could be useful as potential molecular markers.

Selection pressures

The evolutionary history of species is shaped by two main factors: mutation, which generates new genotypes, and selection, which determines the probability that new genotypes will be fixed or eliminated (Marcos and Echave 2020). If selection fixes the mutations, then the patterns of polymorphism, divergence, and gene expression are modified (Johri et al. 2020). Mutations, based on the effect of amino acid coding, are classified as Ka and Ks. Their relationship (Ka/Ks) allows us to understand the independent evolutionary history of each gene and determine if it is under positive selection (Ka/Ks > 1), purifying/stabilizing (Ka/Ks < 1), or neutral selection (Ka/Ks = 1) (Menezes et al. 2018; Yang et al. 2020a). In *Physalis*, most of the genes analyzed were under purifying selection. This implies that these regions of the plastome are maintained in terms of size and nucleotide content and that the variants that could modify the functions of the encoded proteins are eliminated (Cho et al. 2021; Yang et al. 2021a). However, eight genes were under positive selection, either in the eight species or in some of them. This result implies that certain allelic variants are fixed and benefit the optimization of physiological processes and adaptive advantages to the environment (Cho et al. 2021). Under this condition, the genes *cemA*, *ndhB*, *ndhJ*, *ndhK*, *rbcL*, and *rpoA* occurred in the eight species; *psaC* occurred in five species (*P. chenopodiifolia*, *P. cordata*, *P. peruviana*, *P. philadelphica*, and *P. pruinosa*), and *ycfI* occurred in four species (*P. angulata*, *P. peruviana*, *P. philadelphica*, and *P. pruinosa*).

Throughout the evolutionary history of the plastome, most genes have been under purifying selection due to functional limitations (Yang et al. 2020b). However, positive selection can act on those that encode proteins involved in environmental adaptive processes or during the domestication process (D'Agostino et al. 2018; Li et al. 2020b; Yang et al. 2020b). In *Physalis*, the eight genes that are under positive selection can confer certain advantages. The genes *ndhB*, *ndhJ*, and *ndhK* (NADH-dehydrogenase subunits B, J, and K) protect against stress caused by high concentrations of light,

stabilizing the NADH complex and adjusting the photosynthetic rate, in addition to delaying plant growth because of drought (Yang et al. 2021a). The *cemA* gene (protein that envelops the chloroplast membrane) contributes to the absorption of more CO₂ by chloroplasts (Chen et al. 2020). The *rbcL* gene (large subunit of RuBisCO) increases the transfer of electrons during the process of photosynthesis, as well as the catalytic activity on CO₂ (Piot et al. 2018; Gui et al. 2020). The *psaC* gene (subunit of photosystem I), which occurred in the six species that are under positive selection, increases the photosynthetic rate when plants are exposed to high concentrations of ambient light (Fischer et al. 1998). The *rpoA* gene (alpha subunit of RNA polymerase) increases the transcription and expression of plastomic photosynthetic genes so that a plant develops correctly (Mehmood et al. 2020b). Finally, the *ycf1* gene (membrane protein) is essential for cell survival and improves the construction of the cell membrane and the importation of photosynthetic proteins that contribute to the environmental adaptation process (Ye et al. 2018; Wang et al. 2020). This gene is differentially expressed in *P. angulata*, *P. cordata*, *P. philadelphica*, and *P. pruinosa*. In contrast to that which occurs in other genera, such as in *Citrus* L. (Carbonell-Caballero et al. 2015), in *Physalis*, it is not possible to associate the differential expression of genes with biological and ecological characteristics shared between the species analyzed (Suppl. material 1: Table S2). This can be the result of the historical evolutionary process of the species, such as in the case of *ycf1* (Carbonell-Caballero et al. 2015; Jiang et al. 2018; Yang et al. 2021b).

Divergent regions and phylogenetic analysis

Coding and non-coding regions of plastomes both tend to have a high degree of conservation (Daniell et al. 2016; Tonti-Filippini et al. 2017). But some variable regions are routinely used in the construction of phylogenetic hypotheses, phylogeographic analysis, and population genetics (Kim et al. 2020; Li et al. 2020a; Zhang et al. 2020; Zhao et al. 2021). Our results show that the π values in the coding and non-coding regions in *Physalis* are lower than those documented in other genera of Solanaceae, such as *Nicotiana* (Mehmood et al. 2020b) and *Capsicum* (D'Agostino et al. 2018). In *Physalis*, previous phylogenetic analyses have not resolved the relationships between species due to the presence of polytomies or low support values. These studies have only included one to five of the following regions: *matK*, *rbcL*, *ndhF*, *psbA-trnH*, *rpl32-trnL*, *trnL-trnF*, *trnS-trnG*, and *ycf1* (Olmstead et al. 2008; Särkinen et al. 2013; Zamora-Tavares et al. 2016; Feng et al. 2018; Deanna et al. 2019). Use of more plastome regions in phylogenetic analyses has the potential to help clarify species level relationships. We recommend using regions of the plastome with values of $\pi > 0.005$ (*trnD-GUC*, *trnW-CCA*, *ndhE*, and *ycf1* and the intergenes *trnH-psbA*, *trnfM-rps14*, *trnL-trnF*, *petA-psbJ*, *rps18-rpl20*, *infA-rps8*, *rpl16-rps3*, *rpl32-trnL*, *trnL-ccsA*, and *ndhG-ndhI*).

The phylogenetic perspective we obtained confirms the usefulness of the plastome as a source of information for conducting phylogenetic studies in *Physalis*, despite the limited number of species studied. In comparison with other studies that include partial nucleus and chloroplast sequences (Whitson and Manos 2005; Zamora-Tavares et al.

2016; Deanna et al. 2019), our analysis had high support values and polytomies are not present. In this study, *P. minima* is rescued as a sister species to the remaining seven. This partially agrees with Deanna et al. (2019) where *P. minima* is recovered as sister to the great majority of *Physalis* species. In contrast, in the study of Whitson and Manos (2005) *P. minima* forms a clade with *P. angulata*, *P. cordata*, and *P. pubescens*. Similar to Deanna et al. (2019), in our work *P. angulata* and *P. pruinosa* maintain a sister species relationship, while in Zamora-Tavares et al. (2016) *P. pubescens* is sister to *P. angulata*. Furthermore, the phylogenetic relationship of the *Physalis* species studied based on the plastome does not reflect groupings according to the chromosome number, as *P. angulata*, *P. minima*, *P. peruviana*, and *P. pubescens* have $n = 24$, while the other species have $n = 12$. This agrees with the results of Rodríguez et al. (2021), who showed that the genera *Physalis*, *Quincula* Raf. and *Chamaesaracha* (A.Gray) Benth. & Hook comprise a lineage with asymmetric karyotypes. For its part, *A. officinarum* has a symmetric karyotype (Rodríguez et al. 2021) and is an independent lineage. Moreover, since *Physalis* includes 95 species, the inclusion of a large number of species is needed to elucidate its evolutionary history and to analyze if it has a correlation with their ecological affinities and the life history of the species.

Conclusions

The plastome of *Physalis cordata* has the typical quadripartite structure, total size, and GC content similar with other *Physalis* species for which full plastome sequences are available. *Physalis* plastomes have 113 to 115 genes with the same distribution and number of introns. Comparative analysis among eight *Physalis* species showed differences in the boundary of the LSC/IR and SSC/IR regions and three distinct types were identified, given by the variation in genes present. The high percentage of conservation of the sequences and the variation observed at the boundaries of the plastome regions, in the *ycf1* and *ycf2* genes, and in some coding and intergenic regions are relatively common evolutionary processes, and is seen here in all the *Physalis* species studied. Likewise, the presence of genes under positive selection, in some or all of the *Physalis* species analyzed, suggest that they are differentially expressed, and could favor the photosynthetic process and environmental adaptation, which needs to be verified. We have shown that the plastome is potentially useful for further phylogenetic studies if key highly variable genes are used. Finally, we identified that despite the level of conservation in the plastome of *Physalis*, variation in sequence does exist and probably reflects independent evolutionary processes. Future studies should include a larger number of species representing the variation in biological and ecological characteristics to understand the evolution of the plastome in *Physalis*.

Acknowledgements

This work was supported by UDG and CONACyT-Laboratorio Nacional de Identificación y Caracterización Vegetal (LaniVeg) [Grant No. 293833], Universidad de

Guadalajara [Grant Prosní-2018 to OVP] and CONACyT-México through a Doctor scholarship for graduate studies in Doctorado en Biosistemática, Ecología y Manejo de Recursos Naturales y Agrícolas (BEMARENA) [Grant No. 928518 awarded to ISP].

References

- Achakkagari SR, Kyriakidou M, Tai HH, Anglin NL, Ellis D, Strömvik MV (2020) Complete plastome assemblies from a panel of 13 diverse potato taxa. *PLoS ONE* 15(8): e0240124. <https://doi.org/10.1371/journal.pone.0240124>
- Amiryousefi A, Hyvönen J, Poczai P (2018) IRscope: An online program to visualize the junction sites of chloroplast genomes. *Bioinformatics (Oxford, England)* 34(17): 3030–3031. <https://doi.org/10.1093/bioinformatics/bty220>
- Andrews S (2010) Babraham bioinformatics-FastQC a quality control tool for high throughput sequence data. <https://www.bioinformatics.babraham.ac.uk/projects/fastqc/>
- Bankevich A, Nurk S, Antipov D, Gurevich AA, Dvorkin M, Kulikov AS, Lesin VM, Nikolenko SI, Pham S, Pribelski AD, Pyshkin AV, Sirotkin AV, Vyahhi N, Tesler G, Alekseyev MA, Pevzner PA (2012[, May]) SPAdes: A new genome assembly algorithm and its applications to single-cell sequencing. *Journal of Computational Biology* 19(5): 455–477. <https://doi.org/10.1089/cmb.2012.0021>
- Bassil N, Bidani A, Nyberg A, Hummer K, Rowland LJ (2020) Microsatellite markers confirm identity of blueberry (*Vaccinium* spp.) plants in the USDA-ARS National Clonal Germplasm Repository collection. *Genetic Resources and Crop Evolution* 67(2): 393–409. <https://doi.org/10.1007/s10722-019-00873-8>
- Bazin AL, Zwickl DJ, Cummings MP (2014) A gateway for phylogenetic analysis powered by grid computing featuring GARLI 2.0. *Systematic Biology* 63(5): 812–818. <https://doi.org/10.1093/sysbio/syu031>
- Beier S, Thiel T, Münch T, Scholz U, Mascher M (2017) MISA-web: A web server for microsatellite prediction. *Bioinformatics (Oxford, England)* 33(16): 2583–2585. <https://doi.org/10.1093/bioinformatics/btx198>
- Bolger AM, Lohse M, Usadel B (2014) Trimmomatic: A flexible trimmer for Illumina sequence data. *Bioinformatics (Oxford, England)* 30(15): 2114–2120. <https://doi.org/10.1093/bioinformatics/btu170>
- Carbonell-Caballero J, Alonso R, Ibañez V, Terol J, Talon M, Dopazo J (2015) A phylogenetic analysis of 34 chloroplast genomes elucidates the relationships between wild and domestic species within the genus *Citrus*. *Molecular Biology and Evolution* 32(8): 2015–2035. <https://doi.org/10.1093/molbev/msv082>
- Chan PP, Lowe TM (2019) tRNAscan-SE: Searching for tRNA genes in genomic sequences. *Methods in Molecular Biology (Clifton, N.J.)* 1962: 1–14. https://doi.org/10.1007/978-1-4939-9173-0_1
- Chen Y, Zhong H, Zhu Y, Huang Y, Wu S, Liu Z, Lan S, Zhai J (2020) Plastome structure and adaptive evolution of *Calanthe* s.l. species. *PeerJ* 8: e10051. <https://doi.org/10.7717/peerj.10051>

- Cho M-S, Kim JH, Yamada T, Maki M, Kim S-C (2021) Plastome characterization and comparative analysis of wild crabapples (*Malus baccata* and *M. toringo*): Insights into infraspecific plastome variation and phylogenetic relationships. *Tree Genetics & Genomes* 17(5): e41. <https://doi.org/10.1007/s11295-021-01520-z>
- D'Agostino N, Tamburino R, Cantarella C, De Carluccio V, Sannino L, Cozzolino S, Cardi T, Scotti N (2018) The complete plastome sequences of eleven *Capsicum* genotypes: Insights into DNA variation and molecular evolution. *Genes* 9(10): e503. <https://doi.org/10.3390/genes9100503>
- Daniell H, Lin C-S, Yu M, Chang W-J (2016) Chloroplast genomes: Diversity, evolution, and applications in genetic engineering. *Genome Biology* 17(1): e134. <https://doi.org/10.1186/s13059-016-1004-2>
- Darriba D, Taboada GL, Doallo R, Posada D (2012) jModelTest 2: More models, new heuristics, and parallel computing. *Nature Methods* 9(8): 772–772. <https://doi.org/10.1038/nmeth.2109>
- Deanna R, Larter MD, Barboza GE, Smith SD (2019) Repeated evolution of a morphological novelty: A phylogenetic analysis of the inflated fruiting calyx in the Physalideae tribe (Solanaceae). *American Journal of Botany* 106(2): 270–279. <https://doi.org/10.1002/ajb2.1242>
- Do HDK, Kim C, Chase MW, Kim JH (2020) Implications of plastome evolution in the true lilies (monocot order Liliales). *Molecular Phylogenetics and Evolution* 148: 106818. <https://doi.org/10.1016/j.ympev.2020.106818>
- Feng S, Jiao K, Zhu Y, Wang H, Jiang M, Wang H (2018) Molecular identification of species of *Physalis* (Solanaceae) using a candidate DNA barcode: The chloroplast *psbA-trnH* intergenic region. *Genome* 61(1): 15–20. <https://doi.org/10.1139/gen-2017-0115>
- Feng S, Zheng K, Jiao K, Cai Y, Chen C, Mao Y, Wang L, Zhan X, Ying Q, Wang H (2020) Complete chloroplast genomes of four *Physalis* species (Solanaceae): Lights into genome structure, comparative analysis, and phylogenetic relationships. *BMC Plant Biology* 20(1): 1–14. <https://doi.org/10.1186/s12870-020-02429-w>
- Fischer N, Hippler M, Sétif P, Jacquot JP, Rochaix JD (1998) The PsaC subunit of photosystem I provides an essential lysine residue for fast electron transfer to ferredoxin. *The EMBO Journal* 17(4): 849–858. <https://doi.org/10.1093/emboj/17.4.849>
- Frazer KA, Pachter L, Poliakov A, Rubin EM, Dubchak I (2004) VISTA: Computational tools for comparative genomics. *Nucleic Acids Research* 32(Web Server): W273–W279. <https://doi.org/10.1093/nar/gkh458>
- Greiner S, Lehwark P, Bock R (2019) Organellar Genome DRAW (OGDRAW) version 1.3.1, expanded toolkit for the graphical visualization of organellar genomes. *Nucleic Acids Research* 47(W1): W59–W64. <https://doi.org/10.1093/nar/gkz238>
- Gui L, Jiang S, Xie D, Yu L, Huang Y, Zhang Z, Liu Y (2020) Analysis of complete chloroplast genomes of *Curcuma* and the contribution to phylogeny and adaptive evolution. *Gene* 732: 144355. <https://doi.org/10.1016/j.gene.2020.144355>
- Gurevich A, Saveliev V, Vyahhi N, Tesler G (2013) QUAST: Quality assessment tool for genome assemblies. *Bioinformatics (Oxford, England)* 29(8): 1072–1075. <https://doi.org/10.1093/bioinformatics/btt086>

- Huang J, Yu Y, Liu YM, Xie DF, He XJ, Zhou SD (2020) Comparative chloroplast genomics of *Fritillaria* (Liliaceae), inferences for phylogenetic relationships between *Fritillaria* and *Lilium* and plastome evolution. *Plants* 9(2): e133. <https://doi.org/10.3390/plants9020133>
- Jiang P, Shi FX, Li MR, Liu B, Wen J, Xiao HX, Li LF (2018) Positive selection driving cytoplasmic genome evolution of the medicinally important ginseng plant genus *Panax*. *Frontiers in Plant Science* 9: e359. <https://doi.org/10.3389/fpls.2018.00359>
- Johri P, Charlesworth B, Jensen JD (2020) Toward an evolutionarily appropriate null model: Jointly inferring demography and purifying selection. *Genetics* 215(1): 173–192. <https://doi.org/10.1534/genetics.119.303002>
- Katoh K, Standley DM (2013) MAFFT Multiple Sequence Alignment Software Version 7: Improvements in Performance and Usability. *Molecular Biology and Evolution* 30(4): 772–780. <https://doi.org/10.1093/molbev/mst010>
- Kaur H, Singh BP, Singh H, Nagpal AK (2014) Comparative genomics of ten solanaceous plastomes. *Advances in Bioinformatics 2014*: e424873. <https://doi.org/10.1155/2014/424873>
- Kim HT, Kim JS (2021) Structural mutations in the organellar genomes of *Valeriana sambucifolia* f. *dageletiana* (Nakai. Ex Maekawa) Hara show dynamic gene. *International Journal of Molecular Sciences* 22(7): e3770. <https://doi.org/10.3390/ijms22073770>
- Kim YK, Jo S, Cheon SH, Joo MJ, Hong JR, Kwak M, Kim KJ (2020) Plastome evolution and phylogeny of Orchidaceae, with 24 new sequences. *Frontiers in Plant Science* 11: e22. <https://doi.org/10.3389/fpls.2020.00022>
- Kindscher K, Long Q, Corbett S, Bosnak K, Loring H, Cohen M, Timmermann BN (2012) The ethnobotany and ethnopharmacology of wild tomatillos, *Physalis longifolia* Nutt., and related *Physalis* species: A review. *Economic Botany* 66(3): 298–310. <https://doi.org/10.1007/s12231-012-9210-7>
- Köhler M, Reginato M, Souza-Chies TT, Majure LC (2020) Insights into chloroplast genome evolution across Opuntioideae (Cactaceae) reveals robust yet sometimes conflicting phylogenetic topologies. *Frontiers in Plant Science* 11: e729. <https://doi.org/10.3389/fpls.2020.00729>
- Kurtz S, Choudhuri JV, Ohlebusch E, Schleiermacher C, Stoye J, Giegerich R (2001) REPuter: The manifold applications of repeat analysis on a genomic scale. *Nucleic Acids Research* 29(22): 4633–4642. <https://doi.org/10.1093/nar/29.22.4633>
- Langmead B, Salzberg S (2012) Fast gapped-read alignment with Bowtie 2. *Nature Methods* 9(4): 357–359. <https://doi.org/10.1038/nmeth.1923>
- Li Q, Guo X, Niu J, Duoje D, Li X, Opgenoorth L, Zou J (2020a) Molecular phylogeography and evolutionary history of the endemic species *Corydalis hendersonii* (Papaveraceae) on the Tibetan Plateau inferred from chloroplast DNA and ITS sequence variation. *Frontiers in Plant Science* 11: e436. <https://doi.org/10.3389/fpls.2020.00436>
- Li P, Lou G, Cai X, Zhang B, Cheng Y, Wang H (2020b) Comparison of the complete plastomes and the phylogenetic analysis of *Paulownia* species. *Scientific Reports* 10(1): e2225. <https://doi.org/10.1038/s41598-020-59204-y>
- Li X, Zhao Y, Tu X, Li C, Zhu Y, Zhong H, Liu ZJ, Wu S, Zhai J (2021) Comparative analysis of plastomes in Oxalidaceae: Phylogenetic relationships and potential molecular markers. *Plant Diversity* 43(4): 281–291. <https://doi.org/10.1016/j.pld.2021.04.004>

- Liu LX, Du YX, Folk RA, Wang SY, Soltis DE, Shang FD, Li P (2020) Plastome evolution in Saxifragaceae and multiple plastid capture events involving *Heuchera* and *Tiarella*. *Frontiers in Plant Science* 11: e361. <https://doi.org/10.3389/fpls.2020.00361>
- Magdy M, Ou L, Yu H, Chen R, Zhou Y, Hassan H, Feng B, Taitano N, van der Knaap E, Zou X, Li F, Ouyang B (2019) Pan-plastome approach empowers the assessment of genetic variation in cultivated *Capsicum* species. *Horticulture Research* 6(1): e108. <https://doi.org/10.1038/s41438-019-0191-x>
- Marcos ML, Echave J (2020) The variation among sites of protein structure divergence is shaped by mutation and scaled by selection. *Current Research in Structural Biology* 2: 156–163. <https://doi.org/10.1016/j.crstbi.2020.08.002>
- Martínez M (1998) Revisión de *Physalis* section Epeteiorhiza (Solanaceae). *Anales del Instituto de Biología de la Universidad Nacional Autónoma de México* 69(2): 71–117.
- Martínez M, Hernández L (1999) Una nueva especie de *Physalis* (Solanaceae) de Querétaro, México. *Acta Botánica Mexicana* 46(46): 73–76. <https://doi.org/10.21829/abm46.1999.817>
- Martínez M, Vargas-Ponce O, Rodríguez A, Chiang F, Ocegueda S (2017) Solanaceae family in Mexico. *Botanical Sciences* 95(1): 1–15. <https://doi.org/10.17129/botsci.658>
- Mehmood F, Abdullah, Ubaid Z, Bao Y, Poczai P, Mirza B (2020a) Comparative plastomics of ashwagandha (*Withania*, Solanaceae) and identification of mutational hotspots for barcoding medicinal plants. *Plants* 9(6): e752. <https://doi.org/10.3390/plants9060752>
- Mehmood F, Abdullah, Ubaid Z, Shahzadi I, Ahmed I, Waheed MT, Poczai P, Mirza B (2020b) Plastid genomics of *Nicotiana* (Solanaceae): Insights into molecular evolution, positive selection, and the origin of the maternal genome of Aztec tobacco (*Nicotiana rustica*). *PeerJ* 8: e9552. <https://doi.org/10.7717/peerj.9552>
- Menezes APA, Resende-Moreira LC, Buzatti RSO, Nazareno AG, Carlsen M, Lobo FB, Kalapothakis E, Lovato MB (2018) Chloroplast genomes of *Byrsonima* species (Malpighiaceae): Comparative analysis and screening of high divergence sequences. *Scientific Reports* 8(1): e2210. <https://doi.org/10.1038/s41598-018-20189-4>
- Mohanta TK, Mishra AK, Khan A, Hashem A, Abdullah EF, Al-Harrasi A (2020) Gene loss and evolution of the plastome. *Genes* 11(10): e1133. <https://doi.org/10.3390/genes11101133>
- Olmstead RG, Bohs L, Migid HA, Santiago-Valentin E, Garcia VF, Collier SM (2008) A molecular phylogeny of the Solanaceae. *Taxon* 57(4): 1159–1181. <https://doi.org/10.1002/tax.574010>
- Oyebanji O, Zhang R, Chen SY, Yi TS (2020) New insights into the plastome evolution of the Millettioideae/Phaseoloid clade (Papilionoideae, Leguminosae). *Frontiers in Plant Science* 11: e151. <https://doi.org/10.3389/fpls.2020.00151>
- Pacheco T, de Santana A, de Oliveira JD, Campos W, Balsanelli E, Oliveira F, Maltempi E, Rogalski M (2020) The complete plastome of *Passiflora cirrhiiflora* A. Juss.: Structural features, RNA editing sites, hotspots of nucleotide diversity and molecular markers within the subgenus *Deidamioides*. *Revista Brasileira de Botânica. Brazilian Journal of Botany* 43(4): 839–853. <https://doi.org/10.1007/s40415-020-00655-y>
- Piot A, Hackel J, Christin PA, Besnard G (2018) One-third of the plastid genes evolved under positive selection in PACMAD grasses. *Planta* 247(1): 255–266. <https://doi.org/10.1007/s00425-017-2781-x>

- POWO (2022) Plants of the World Online. Facilitated by the Royal Botanic Gardens, Kew. <http://www.plantsoftheworldonline.org/> [accessed 31 July 2022]
- Pretz C, Deanna R (2020) Typifications and nomenclatural notes in *Physalis* (Solanaceae) from the United States. *Taxon* 69(1): 170–192. <https://doi.org/10.1002/tax.12159>
- Puente LA, Pinto-Muñoz CA, Castro ES, Cortés M (2011) *Physalis peruviana* Linnaeus, the multiple properties of a highly functional fruit: A review. *Food Research International* 44(7): 1733–1740. <https://doi.org/10.1016/j.foodres.2010.09.034>
- Rengifo-Salgado E, Vargas-Arana G (2013) *Physalis angulata* L. (Bolsa Mullaca): A review of its traditional uses, chemistry and pharmacology. *Boletín Latinoamericano y del Caribe de Plantas Medicinales y Aromáticas* 12(5): 431–445.
- Reyes-Reyes EM, Jin Z, Vaisberg AJ, Hammond GB, Bates PJ (2013) Physangulidine A, a withanolide from *Physalis angulata*, perturbs the cell cycle and induces cell death by apoptosis in prostate cancer cells. *Journal of Natural Products* 76(1): 2–7. <https://doi.org/10.1021/np300457g>
- Rodríguez J, Deanna R, Chiarini F (2021) Karyotype asymmetry shapes diversity within the physaloids (Physalidinae, Physalideae, Solanaceae). *Systematics and Biodiversity* 19(2): 168–185. <https://doi.org/10.1080/14772000.2020.1832156>
- Rozas J, Ferrer-Mata A, Sánchez-DelBarrio JC, Guirao-Rico S, Librado P, Ramos-Onsins SE, Sánchez-Gracia A (2017) DnaSP 6: DNA sequence polymorphism analysis of large data sets. *Molecular Biology and Evolution* 34(12): 3299–3302. <https://doi.org/10.1093/molbev/msx248>
- Ruhlman TA, Jansen RK (2014) The plastid genomes of flowering plants. In: Maliga P (Ed.) *Chloroplast biotechnology*. USA. Humana Press, 3–38. https://doi.org/10.1007/978-1-62703-995-6_1
- Sandoval-Padilla I, Pérez-Alquicira J, Zamora-Tavares MP, Rodríguez A, Cortés-Cruz M, Alcalá-Gómez G, Vargas-Ponce O (2019) Complete sequence of wild *Physalis philadelphica* chloroplast genome. *Mitochondrial DNA. Part B, Resources* 4(2): 3295–3297. <https://doi.org/10.1080/23802359.2019.1673231>
- Sandoval-Padilla I, Pérez-Alquicira J, Rodríguez A, Zamora-Tavares MP, Vargas-Ponce O (2022) The plastome of the husk tomato (*Physalis philadelphica* Lam., Solanaceae): A comparative analysis between wild and cultivated pools. *Genetic Resources and Crop Evolution* 69(3): 1391–1405. <https://doi.org/10.1007/s10722-021-01334-x>
- Santiaguillo JF, Blas S (2009) Aprovechamiento tradicional de las especies de *Physalis* en México. *Revista de Geografía Agrícola* 43: 81–86.
- Särkinen T, Bohs L, Olmstead RG, Knapp S (2013) A phylogenetic framework for evolutionary study of the nightshades (Solanaceae): A dated 1000-tip tree. *BMC Ecology and Evolution* 13: e214. <https://doi.org/10.1186/1471-2148-13-214>
- Shah P, Singh-Bora K (2019) Phytochemical and therapeutic potential of *Physalis* species: A review. *IOSR Journal of Pharmacy and Biological Sciences* 14(4): 34–51.
- Shen J, Zhang X, Landis JB, Zhang H, Deng T, Sun H, Wang H (2020) Plastome evolution in *Dolomiaea* (Asteraceae, Cardueae) using phylogenomic and comparative analysis. *Frontiers in Plant Science* 11: e376. <https://doi.org/10.3389/fpls.2020.00376>

- Shenstone E, Lippman Z, Van Eck J (2020) A review of nutritional properties and health benefits of *Physalis* species. *Plant Foods for Human Nutrition* (Dordrecht, Netherlands) 75(3): 316–325. <https://doi.org/10.1007/s11130-020-00821-3>
- Shetty SM, Md Shah MU, Makale K, Mohd-Yusuf Y, Khalid N, Othman RY (2016) Complete chloroplast genome sequence of *Musa balbisiana* corroborates structural heterogeneity of inverted repeats in wild progenitors of cultivated bananas and plantains. *The Plant Genome* 9(2): 1–14. <https://doi.org/10.3835/plantgenome2015.09.0089>
- Shi C, Hu N, Huang H, Gao J, Zhao YJ, Gao LZ (2012) An improved chloroplast DNA extraction procedure for whole plastid genome sequencing. *PLoS ONE* 7(2): e31468. <https://doi.org/10.1371/journal.pone.0031468>
- Souza UJB, Vitorino LC, Bessa LA, Silva FG, Souza UJBd (2020) The complete plastid genome of *Artocarpus camansi*: A high degree of conservation of the plastome structure in the family Moraceae. *Forests* 11(11): e1179. <https://doi.org/10.3390/f11111179>
- Stettler JM, Stevens MR, Meservey LM, Crump WW, Grow JD, Porter SJ, Love LS, Maughan PJ, Jellen EN (2021) Improving phylogenetic resolution of the Lamiales using the complete plastome sequences of six *Penstemon* species. *PLoS ONE* 16(12): e0261143. <https://doi.org/10.1371/journal.pone.0261143>
- Taylor P, Arsenak M, Abad MJ, Fernández A, Milano B, Gonto R, Ruiz M-C, Fraile S, Taylor S, Estrada O, Michelangeli F (2012) Screening of Venezuelan medicinal plant extracts for cytostatic and cytotoxic activity against tumor cell lines. *Phytotherapy Research* 27(4): 530–539. <https://doi.org/10.1002/ptr.4752>
- Thorvaldsdóttir H, Robinson JT, Mesirov JP (2013) Integrative Genomics Viewer (IGV): High-performance genomics data visualization and exploration. *Briefings in Bioinformatics* 14(2): 178–192. <https://doi.org/10.1093/bib/bbs017>
- Tillich M, Lehwark P, Pellizzer T, Ulbricht-Jones ES, Fischer A, Bock R, Greiner S (2017) GeSeq - versatile and accurate annotation of organelle genomes. *Nucleic Acids Research* 45(W1): W6–W11. <https://doi.org/10.1093/nar/gkx391>
- Toledo JM (2013) *Physalis victoriana* (Solanaceae) a new species from northern Argentina. *Phytotaxa* 124(1): 60–64. <https://doi.org/10.11646/phytotaxa.124.1.8>
- Tonti-Filippini J, Nevill PG, Dixon K, Small I (2017) What can we do with 1000 plastid genomes? *The Plant Journal* 90(4): 808–818. <https://doi.org/10.1111/tpj.13491>
- Valdivia-Mares LE, Rodríguez FA, Sánchez JJ, Vargas-Ponce O (2016) Phenology agronomic and nutritional potential of three wild husk tomato species (*Physalis*, Solanaceae) from Mexico. *Scientia Horticulturae* 200: 83–94. <https://doi.org/10.1016/j.scienta.2016.01.005>
- Vargas-Ponce O, Martínez M, Dávila P (2003) La familia Solanaceae en Jalisco -El género *Physalis*-. Universidad de Guadalajara, Guadalajara, Mexico, 126 pp.
- Vargas-Ponce O, Sánchez-Martínez J, Zamora-Tavares MP, Valdivia-Mares LE (2016) Traditional management of a small-scale crop of *Physalis angulata* in western Mexico. *Genetic Resources and Crop Evolution* 63(8): 1383–1395. <https://doi.org/10.1007/s10722-015-0326-3>
- Vdovenko SA, Polutin OO, Muliarchuk OI, Hareba OV, Havryls IL (2021) Peculiarities of tomatillo (*Physalis philadelphica*) field production in Ukraine with the use of different elements of technology. *Research on Crops* 22(1): 116–128. <https://doi.org/10.31830/2348-7542.2021.044>

- Wang D, Zhang Y, Zhang Z, Zhu J, Yu J (2010) KaKs_Calculator 2.0: A toolkit incorporating gamma-series methods and sliding window strategies. *Genomics, Proteomics & Bioinformatics* 8(1): 77–80. [https://doi.org/10.1016/S1672-0229\(10\)60008-3](https://doi.org/10.1016/S1672-0229(10)60008-3)
- Wang RN, Milne RI, Du XY, Liu J, Wu ZY (2020) Characteristics and mutational hotspots of plastomes in *Debregeasia* (Urticaceae). *Frontiers in Genetics* 11: e729. <https://doi.org/10.3389/fgene.2020.00729>
- Wang R, Liu K, Zhang XJ, Chen WL, Qu XJ, Fan SJ (2021) Comparative plastomes and phylogenetic analysis of *Cleistogenes* and closely related genera (Poaceae). *Frontiers in Plant Science* 12: e638597. <https://doi.org/10.3389/fpls.2021.638597>
- Weng ML, Blazier JC, Govindu M, Jansen RK (2014) Reconstruction of the ancestral plastid genome in Geraniaceae reveals a correlation between genome rearrangements, repeats, and nucleotide substitution rates. *Molecular Biology and Evolution* 31(3): 645–659. <https://doi.org/10.1093/molbev/mst257>
- Whitson M, Manos PS (2005) Untangling *Physalis* (Solanaceae) from the physaloids: A two-gene phylogeny of the Physalinae. *Systematic Botany* 30(1): 216–230. <https://doi.org/10.1600/0363644053661841>
- Wu CS, Sudianto E, Chaw SM (2021) Tight association of genome rearrangements with gene expression in conifer plastomes. *BMC Plant Biology* 21(1): e33. <https://doi.org/10.1186/s12870-020-02809-2>
- Xu X, Wang D (2021) Comparative chloroplast genomics of *Corydalis* Species (Papaveraceae): Evolutionary perspectives on their unusual large scale rearrangements. *Frontiers in Plant Science* 11: e600354. <https://doi.org/10.3389/fpls.2020.600354>
- Yang X, Xie DF, Chen JP, Zhou SD, Yu Y, He XJ (2020a) Comparative analysis of the complete chloroplast genomes in *Allium* subgenus *Cyathophora* (Amaryllidaceae): Phylogenetic relationship and adaptive evolution. *BioMed Research International* 1732586: 1–17. <https://doi.org/10.1155/2020/1732586>
- Yang J, Takayama K, Youn JS, Pak JH, Kim SC (2020b) Plastome characterization and phylogenomics of east asian beeches with a special emphasis on *Fagus multinervis* on Ulleung Island, Korea. *Genes* 11(11): e1338. <https://doi.org/10.3390/genes11111338>
- Yang J, Chiang YC, Hsu TW, Kim SH, Pak JH, Kim SC (2021a) Characterization and comparative analysis among plastome sequences of eight endemic *Rubus* (Rosaceae) species in Taiwan. *Scientific Reports* 11(1): e1152. <https://doi.org/10.1038/s41598-020-80143-1>
- Yang H, Wang L, Chen H, Jiang M, Wu W, Liu S, Wang J, Liu C (2021b) Phylogenetic analysis and development of molecular markers for five medicinal *Alpinia* species based on complete plastome sequences. *BMC Plant Biology* 21(1): e431. <https://doi.org/10.1186/s12870-021-03204-1>
- Ye WQ, Yap ZY, Li P, Comes HP, Qiu YX (2018) Plastome organization, genome-based phylogeny and evolution of plastid genes in Podophylloideae (Berberidaceae). *Molecular Phylogenetics and Evolution* 127: 978–987. <https://doi.org/10.1016/j.ympev.2018.07.001>
- Zamora-Tavares P, Vargas-Ponce O, Sánchez-Martínez J, Cabrera-Toledo D (2015) Diversity and genetic structure of the husk tomato (*Physalis philadelphica* Lam.) in Western Mexico. *Genetic Resources and Crop Evolution* 62(1): 141–153. <https://doi.org/10.1007/s10722-014-0163-9>

- Zamora-Tavares MP, Martínez M, Magallón S, Guzmán-Dávalos L, Vargas-Ponce O (2016) *Physalis* and physaloids: A recent and complex evolutionary history. *Molecular Phylogenetics and Evolution* 100: 41–50. <https://doi.org/10.1016/j.ympev.2016.03.032>
- Zamora-Tavares MP, Sandoval-Padilla I, Chávez Zendejas A, Pérez-Alquicira J, Vargas-Ponce O (2020) Complete chloroplast genome of *Physalis chenopodiifolia* Lam. (Solanaceae). *Mitochondrial DNA, Part B, Resources* 5(1): 162–163. <https://doi.org/10.1080/23802359.2019.1698364>
- Zhang X, Liu YH, Wang YH, Shen SK (2020) Genetic diversity and population structure of *Rhododendron rex* subsp. *rex* inferred from microsatellite markers and chloroplast DNA sequences. *Plants* 9(3): e338. <https://doi.org/10.3390/plants9030338>
- Zhao F, Li B, Drew BT, Chen YP, Wang Q, Yu WB, Liu ED, Salmaki Y, Peng H, Xiang CL (2020) Leveraging plastomes for comparative analysis and phylogenomic inference within Scutellarioideae (Lamiaceae). *PLoS ONE* 15(5): e0232602. <https://doi.org/10.1371/journal.pone.0232602>
- Zhao K, Li L, Quan H, Yang J, Zhang Z, Liao Z, Lan X (2021) Comparative analysis of chloroplast genomes from 14 *Zanthoxylum* species: Identification of variable DNA markers and phylogenetic relationships within the genus. *Frontiers in Plant Science* 11: e605793. <https://doi.org/10.3389/fpls.2020.605793>
- Zhong Q, Yang S, Sun X, Wang L, Li Y (2019) The complete chloroplast genome of the Jerusalem artichoke (*Helianthus tuberosus* L.) and an adaptive evolutionary analysis of the *ycf2* gene. *PeerJ* 7: e7596. <https://doi.org/10.7717/peerj.7596>
- Zhu A, Guo W, Gupta S, Fan W, Mower JP (2016) Evolutionary dynamics of the plastid inverted repeat: The effects of expansion, contraction, and loss on substitution rates. *The New Phytologist* 209(4): 1747–1756. <https://doi.org/10.1111/nph.13743>

Supplementary material I

Tables S1, S2 and Figures S1–S3

Authors: Isaac Sandoval-Padilla, María del Pilar Zamora-Tavares, Eduardo Ruiz-Sánchez, Jessica Pérez-Alquicira, Ofelia Vargas-Ponce

Data type: Tables and images of plastome data and attributes (MS Word file)

Explanation note: The tables contains data about introns in chloroplast genes and biological and ecological traits of *Physalis* species included in the study. Graphs show data about type of microsatellites and frequency.

Copyright notice: This dataset is made available under the Open Database License (<http://opendatacommons.org/licenses/odbl/1.0/>). The Open Database License (ODbL) is a license agreement intended to allow users to freely share, modify, and use this Dataset while maintaining this same freedom for others, provided that the original source and author(s) are credited.

Link: <https://doi.org/10.3897/phytokeys.210.85668.suppl1>

Schiedea haakoensis, a new facultatively autogamous species of *Schiedea* sect. *Mononeura* (Caryophyllaceae) from the Hawaiian Islands

Warren L. Wagner¹, Stephen G. Weller², Ann K. Sakai²,
Tom DeMent³, Josh VanDeMark³

1 Department of Botany, MRC-166, National Museum of Natural History, Smithsonian Institution, P.O. Box 37012, Washington, DC 20013-7012, USA **2** Department of Ecology and Evolutionary Biology, University of California, Irvine, CA 92697, USA **3** DLNR/Division of Forestry & Wildlife, 19 E. Kawili St., Hilo, HI 96720, USA

Corresponding author: Warren L. Wagner (wagnerw@si.edu)

Academic editor: G. P. Giusso del Galdo | Received 3 August 2022 | Accepted 12 September 2022 | Published 10 October 2022

Citation: Wagner WL, Weller SG, Sakai AK, DeMent T, VanDeMark J (2022) *Schiedea haakoensis*, a new facultatively autogamous species of *Schiedea* sect. *Mononeura* (Caryophyllaceae) from the Hawaiian Islands. *PhytoKeys* 210: 135–141. <https://doi.org/10.3897/phytokeys.210.91226>

Abstract

In 2016 during a survey for potential fencing of the Ha'akoa unit on windward Mauna Kea, Hawai'i Island (Hawaiian Islands) a single plant of the genus *Schiedea* was discovered. No species of the genus had ever been known to occur in this area, and only three species of *Schiedea* were known previously from Hawai'i Island. Two are vining species and the third is a coastal subshrub. The single plant obviously represented an interesting find, and because the plant was vegetative another visit was scheduled to collect a flowering specimen, but by then the plant had died. Soil taken from the site with seeds in the soil produced two plants, one of which flowered in cultivation in 2021. A study of this individual indicated it was a member of *Schiedea* sect. *Mononeura*, characterized by erect to ascending habit, quadrangular stems, seeds not persistent on the placenta and readily dispersing from the dehisced capsule, and flowers facultatively autogamous. With the discovery of this new species there are 35 species in this Hawaiian endemic genus.

Keywords

Caryophyllaceae, conservation, Hawaiian Islands, Hawai'i Island, *Schiedea*

Introduction and discussion

An unusual *Schiedea* was discovered by Tom DeMent in September 2016 while scouting the area for a future fence line for the Ha'akoa Unit. Photos and a leaf sample were taken that day for a second opinion and possible identification. A second visit to the site of the plant was made in July 2017. At that time, only the desiccated remains of the non-reproductive plant were found. The stem was still turgid, the leaves were brown and dry, but still attached. A branch cutting was taken with the hope there was still enough life in the stem to root and resprout. It was unsuccessful. A soil sample was also taken during the 2017 visit, but nothing germinated from it. A third visit took place in 2018 by Tom DeMent, Josh VanDeMark and Reid Loo. The dead individual was completely gone, and the area was surveyed for any new individuals without success. A new soil sample was also taken. Jaime Enoka at the Volcano Rare Plant Facility (VRPF) propagated two plants from this soil collection in 2019. One of the plants flowered in 2021, a portion of which was used to make a partial specimen (type), which together with a number of photographic images of the plant in cultivation as well as some of images of the original plant in the field, were used to write the following description.

In our long-term study of the diversification of *Schiedea* Cham. & Schltld. to distinguish species, especially those clusters of closely related species, we have emphasized changes in breeding systems correlated with discrete floral and vegetative characters (Wagner et al. 2005). Changes in breeding system are usually correlated with habitat and geographical discontinuities. Many species of *Schiedea*, especially those from older islands where extinction of intermediate forms may have occurred, are readily distinguished from all other species (e.g., *S. apokremnos* H. St. John, *S. helleri* Sherff, *S. spergulina* A. Gray, *S. stellarioides* H. Mann, and *S. verticillata* F. Br.). Other species, especially those on younger islands, are less readily separated from their congeners. For example, in sect. *Mononeura*, *S. laui* W. L. Wagner & Weller was initially viewed as a rediscovery of *S. nuttallii* Hook. on Moloka'i, albeit in a wetter habitat at higher elevations than is typical for *S. nuttallii* on O'ahu. Plants grown in the greenhouse, however, showed several morphological differences from *S. nuttallii*. Flowers of all plants of *S. laui* are completely cleistogamous, whereas *S. nuttallii* on O'ahu has protandrous flowers and is primarily outcrossing (Wagner et al. 2005). Initially, we planned to recognize *S. laui* as a subspecies of *S. nuttallii*, but it failed to group with *S. nuttallii* in phylogenetic analyses using Sanger sequences of several plastid and nuclear loci and morphology (Nepokroeff et al. 2005; Willyard et al. 2011), and therefore we described *S. laui* as a distinct species. In a parallel contrast, *S. jacobii* W. L. Wagner, Weller & Medeiros (Wagner et al. 1999) superficially resembles *S. nuttallii* but occurs allopatrically at higher elevations in very wet forests. Moreover, *S. jacobii* is autogamous and produces seeds that are retained in capsules, a characteristic feature of *Schiedea* species occurring in very wet habitats. Similarly, the new species described here at first seemed very similar to *S. nuttallii* as well as to *S. jacobii* and *S. laui*, but after careful study of all available characters, it possesses a suite of features distinguishing it from these other very similar species, including the erect to ascending habit, quadrangular stems,

seeds not persistent on the placenta, readily dispersing from the dehisced capsule, and flowers facultatively autogamous. The molecular studies published so far indicate that *S. nuttallii*, *S. jacobii*, *S. laui*, and *S. kaalae* Wawra are all in the same subclade of sect. *Mononeura* (Nepokroeff et al. 2005; Willyard et al. 2011). Ongoing analyses using Hyb-Seq target enrichment will include *S. haakoensis* to resolve more fully the relationships among this group of closely related species of sect. *Mononeura* that have diversified across all of the main Hawaiian Islands. The morphological, breeding system and geographical/ecological characteristics of the new species and its close relatives are compared in Table 1.

Table 1. Comparison of morphological, breeding system, and geographical/ecological characters of the subclade of species of *Schiedea* sect. *Mononeura*.

Character	<i>S. nuttallii</i>	<i>S. kaalae</i>	<i>S. jacobii</i>	<i>S. laui</i>	<i>S. haakoensis</i>
Stem texture and shape	Weakly fleshy, flattened	Thick and fleshy, rounded, but pedicels flattened	Fleshy, quadrangular, winged	Weakly fleshy, flattened, or upper weakly quadrangular	Fleshy, quadrangular, not winged
Leaf shape	Narrowly ovate or lanceolate to narrowly or broadly elliptic	Elliptic-oblanccolate to nearly spatulate	Lanceolate to oblong-elliptic	Narrowly ovate or lanceolate to narrowly or broadly elliptic	Narrowly or broadly elliptic, sometimes lanceolate to oblanccolate
Leaf length and width (cm)	5–13 × 1.4–3.5	(8–) 14–24 × (1.5–) 2–5 (–6)	4.5–10.5 × 1.4–2.6	6.5–13 × 1.5–2.8	3–18 × 1.2–4.5
Inflorescence length (cm)	Inflorescence with 50–240 flowers, 20–25 (–32) cm long	Inflorescence with 20–300 flowers, 20–40 (–60) cm long	Inflorescence with 10–70 flowers, 40–50 cm long	Inflorescence with 10–18 flowers, 17–26 cm long	Inflorescence with up to 80 or more flowers, 40–50 cm long
Pedicel length (mm) at anthesis	6–12 mm	7–10 mm	3–8 mm	3–11 mm	4–6 mm
Inflorescence pubescence	Bracts ciliate, internodes with scattered hairs	Bracts ciliate	Glabrous	Bracts ciliate, internodes with scattered hairs	Bracts ciliate, internodes with scattered hairs
Pollination	Chasmogamous	Chasmogamous	Facultatively autogamous	Cleistogamous	Apparently facultatively autogamous
Sepal orientation from pedicel	5° to 30° angle	ca. 5° to 10° angle	90° to 135° angle	175° to 180° angle	ca. 30° to 60° angle
Sepal pubescence	Sparsely ciliate	Sparsely ciliate	Glabrous	Sparsely ciliate	Ciliate
Seeds persistent on placenta	No	No	Yes	No	Apparently not
Seed length (mm)	0.9–1	1.0–1.1	0.7–0.9	1.0–1.1	0.8–1.0
Distribution	O'ahu (Wai'anae Mts.); previously from Moloka'i (E end), West Maui	O'ahu (Wai'anae and Ko'olau Mts.)	East Maui (Hanawi)	Moloka'i (Waikolu)	Hawai'i (Ha'akoa unit on windward Mauna Kea)

Taxonomic treatment

Schiedea haakoensis W. L. Wagner, Weller & A. K. Sakai, sp. nov.

urn:lsid:ipni.org:names:77306319-1

Fig. 1

Type. Hawaiian Islands: Hawai'i: Hawai'i County, North Hilo District, Laupāhoehoe Section of Hilo Forest Reserve, windward Mauna Kea, Mauka of Ha'akoa and Pāhale Streams, 5020 ft (1530 m), Cult. material harvested July 2021, *Tom DeMent & Josh VanDeMark s.n.* (holotype: US-3742219!).



Figure 1. *Schiedea haakoaensis* W. L. Wagner, Weller & A. K. Sakai **A** habit, stem with leaves and inflorescence **B** habit of plant in habitat **C** stem internode, showing sparse hairs **D** stem internode with leaf bases **E** branch of inflorescence with developing fruit and flower **F** bract **G** flower at full anthesis **H** branch of inflorescence, post anthesis **I** capsule **J** seed. Drawn from photograph of cultivated individual from which holotype was taken (**A**), drawn from field photograph and cropped to fit plate (**B**), drawn from holotype (**C, D, H, I, J**), and from the holotype and photographs (**E, F, G**). Coloration added to plate figures from photographs. Illustration by Alice Tangerini.

Description. Erect to strongly ascending subshrubs 7–10 dm tall or in wild perhaps more; stem single or sometimes with few short side branches, conspicuously quadrangular, pale green, but distal internodes often purple-tinged, glabrous except internodes of inflorescence, bracts and sepals. Leaves opposite; blades 3–18 cm long, 1.2–4.5 cm wide, narrowly or broadly elliptic, sometimes lanceolate to oblanceolate, pale green to yellowish green, sometimes younger ones purple-tinged, slightly thickened and rubbery, chartaceous when dry, with only the midvein evident, the midvein \pm slightly excentric, margin entire, slightly thickened becoming weakly involute toward the apex, apex acute to acuminate; petioles 0.5–1 cm long, weakly grooved. Inflorescence terminal, 40–50 cm long, with up to 80 or more flowers, diffuse, erect, the lateral branches 11–18 cm long, ascending, each with 6–20 flowers, the tertiary and higher level internodes, usually ascending or appressed, with pedicels usually spreading at anthesis, sometimes with a few minute curved hairs along the inflorescence internodes; bracts usually yellowish green, foliaceous, and nearly as large as the leaves in the lowest portions of the central axis, those in the upper part of the inflorescence and subtending the flowers, subulate, purple and usually yellowish green near base, margins ciliate; pedicels 4–6 mm long at anthesis, elongating slightly in fruit, conspicuously asymmetrically flattened and weakly quadrangular, sometimes with a few hairs toward the base. Flowers hermaphroditic, facultatively autogamous. Sepals 3–4.1 mm long, lanceolate, purple, and sometimes greenish toward the base, concave to shallowly navicular toward the apex, oriented at ca. 30° to 60° angle to the pedicel, abaxial side smooth and rounded, glabrous, margins weakly scariou, ciliate, apex attenuate. Nectary shaft 1.5–2.1 mm long, gently recurved, apex weakly bifid. Stamens 10; filaments weakly dimorphic, the antisepalous whorl 2.5–3.1 mm long, the alternate whorl 1.5–2.6 mm long; anthers ca. 0.3 mm long, yellow, apparently dehiscent after flower opens. Styles 3, stigmas elongated and apparently receptive when flower opens, and anthers are dehiscent. Capsules 4.3–5 mm long, ovoid. Seeds 0.8–1.0 mm long, suborbicular, slightly asymmetrical, compressed, brown, the surface rugose. Chromosome number unknown.

Distribution. *Schiedea haakoaensis* was known from only a single plant from Hawaiian Islands, on the northeastern side of Hawai'i Island, in the Laupāhoehoe Section of Hilo Forest Reserve. No individuals are currently known from the wild but progeny from one of the two individuals grown from seed collected at the type locality are in cultivation at locations in Hilo and Irvine, California, with outplantings anticipated soon.

Habitat. The only known plant of *Schiedea haakoaensis* was discovered in 2016 in the montane wet forests of windward Mauna Kea and died of natural causes shortly thereafter. Montane wet forests in this area are dominated by closed canopies of *Metrosideros polymorpha* Gaudich. and *Acacia koa* A. Gray with a sub-canopy comprised of *Cheirodendron trigynum* (Gaudich.) A. Heller subsp. *trigynum*, *Melicope* sp., *Myrsine lessertiana* A. DC., *Myrsine sandwicensis* A. DC., *Ilex anomola* Hook. & Arn., *Coprosma* sp., *Phytolacca sandwicensis* Endl., and *Vaccinium calycinum* Sm. The thick and dense vegetation of the understory host *Rubus hawaiiensis* A. Gray, *Hydrangea arguta* (Gaudich.) Y. De Smet & Granados, *Cibotium glaucum* (Sm.) Hook. & Arn.,

Cibotium menziesii Hook., *Cibotium chamissoi* Kaulf., and a rich diversity of additional ferns including *Adenophorus tamariscinus* (Kaulf.) Hook. & Grev. var. *tamariscinus*, *Asplenium polyodon* G. Forst., *Asplenium aethiopicum* (Burm. f.) Bech., *Athyrium microphyllum* (Sm.) Alston, *Diplazium sandwichianum* (C. Presl) Diels, *Dryopteris wallichiana* (Spreng.) Hyl., *Microlepia strigosa* (Thunb.) C. Presl, *Polypodium pellucidum* Kaulf. var. *pellucidum*, *Sadleria* sp., and the uncommon *Asplenium schizophyllum* C. Chr. The forests of this area have a low number of non-native species, most of which occur in the understory and consist of non-native grasses and shrubs including *Cenchrus clandestinus* (Hochst. ex Chiov.) Morrone, *Ehrharta stipoides* Labill., *Rubus argutus* Link, *Passiflora tarminiana* Coppens & Barney and *Juncus* sp. The terrain and topography of the region are carved by seasonal and perennial streams with gulches varying in depth from a few meters to very large river gulches at lower elevations. The area of the previously known individual, ~5000 ft (1525 m) elevation, lies uphill from the dominant streams of Ha'akoa and Pāhale with a mean annual rainfall of ~115 inches (292 cm; Rainfall Atlas of Hawaii).

Threats. Habitat degradation by feral pigs continues to threaten species that grow at ground level in the understory of these forests, which remain unprotected by ungulate-proof exclusionary fences. Currently, a ~1200-acre fenced unit is being constructed in the area and once completed will encompass the area where *Schiedea haakoensis* was discovered. The sole individual of *S. haakoensis* was naturally protected from feral pig damage due to its location on a log elevated 3–4 ft (0.9–1.2 m) above the ground. Although ungulate damage was not the cause of death other threats to extremely rare species exist. The only individual of *S. haakoensis* was probably affected by a prolonged period of drought and its particular location on the log.

Breeding system. Facultative autogamy is indicated by the occurrence of abundant seed production of the one plant that has so far flowered at the VRPF. The plant is growing in an enclosed facility, but some pollinator access is possible. Most species in the VRPF that have floral adaptations for pollinator attraction do not produce fruits unless pollinated, suggesting that the abundant fruit production of *S. haakoensis* is likely to result from self-pollination. Nearly all wet forest species of *Schiedea* are facultatively or obligately autogamous with self-pollination and subsequent self-fertilization facilitated by synchrony between stigma receptivity and release of pollen from anthers.

Conservation assessment. IUCN Red List Category. When evaluated using the IUCN criteria for endangerment, *Schiedea haakoensis* falls into the Extinct in the Wild (EW) category. Surveys of the surrounding area and habitat have failed to locate additional individuals although it is possible more exist in the vast and remote landscape of the windward Mauna Kea wet forests. Future surveys of the area should concentrate on the adjacent US Fish & Wildlife Maulua Tract, the Laupāhoehoe Section of Hilo Forest Reserve, and the Laupāhoehoe Natural Area Reserve. Future protection and feral ungulate exclusion in these areas will help preserve habitat for this species should it be rediscovered, and for individuals of *S. haakoensis* restored to the area.

Acknowledgements

We are grateful to Alice Tangerini for her excellent illustrations of this new species to reconstruct its characteristics from limited collection and photographs. This work was supported by National Science Foundation grants DEB-1753659, DEB-1753664, DEB-1750373, and DEB-1752785: Collaborative Research: Unlocking the evolutionary history of *Schiedea* (carnation family, Caryophyllaceae): Rapid radiation of an endemic plant genus in the Hawaiian Islands. PIs: A. Sakai, S. Weller, N. Wickett, M. Moore, W. Wagner. The authors appreciate the useful reviews by Dave Lorence and Rich Rabeler.

References

- Nepokroeff M, Wagner WL, Soltis PS, Weller SG, Soltis DE, Sakai AK, Zimmer EA (2005) Phylogeny. In: Wagner WL, Weller SG, Sakai AK (Eds) Monograph of *Schiedea* (Caryophyllaceae subfam. Alsinoideae). Systematic Botany Monographs 72: 13–20 [pl 2].
- Wagner WL, Weller SG, Sakai AK (2005) Monograph of *Schiedea* (Caryophyllaceae–Alsinoideae). Systematic Botany Monographs 72: 1–169.
- Wagner WL, Weller SG, Sakai AK, Medeiros AC (1999) An autogamous rain forest species of *Schiedea* (Caryophyllaceae) from East Maui, Hawaiian Islands. *Novon* 9(2): 284–287. <https://doi.org/10.2307/3391816>
- Willyard A, Wallace LE, Wagner WL, Weller SG, Sakai AK, Nepokroeff M (2011) Estimating the species tree for Hawaiian *Schiedea* (Caryophyllaceae) from multiple loci in the presence of reticulate evolution. *Molecular Phylogenetics and Evolution* 60(1): 29–48. <https://doi.org/10.1016/j.ympev.2011.04.001>

